

FINAL REPORT

Predicting the Fate and Effects of Resuspended Metal Contaminated Sediments

SERDP Project ER-1746

DECEMBER 2015

Dr. G. Allen Burton
University of Michigan

Dr. Kevin Farley
Manhattan College

Dr. Richard Carbonaro
Dr. Kevin Rader
Mutch Associates

Dr. Joe Gailani
United States Army Corps of Engineer Research and Development Center

Distribution Statement A

This document has been cleared for public release



Page Intentionally Left Blank

This report was prepared under contract to the Department of Defense Strategic Environmental Research and Development Program (SERDP). The publication of this report does not indicate endorsement by the Department of Defense, nor should the contents be construed as reflecting the official policy or position of the Department of Defense. Reference herein to any specific commercial product, process, or service by trade name, trademark, manufacturer, or otherwise, does not necessarily constitute or imply its endorsement, recommendation, or favoring by the Department of Defense.

Page Intentionally Left Blank

REPORT DOCUMENTATION PAGE			Form Approved OMB No. 0704-0188		
Public reporting burden for this collection of information is estimated to average 1 hour per response, including the time for reviewing instructions, searching existing data sources, gathering and maintaining the data needed, and completing and reviewing this collection of information. Send comments regarding this burden estimate or any other aspect of this collection of information, including suggestions for reducing this burden to Department of Defense, Washington Headquarters Services, Directorate for Information Operations and Reports (0704-0188), 1215 Jefferson Davis Highway, Suite 1204, Arlington, VA 22202-4302. Respondents should be aware that notwithstanding any other provision of law, no person shall be subject to any penalty for failing to comply with a collection of information if it does not display a currently valid OMB control number. PLEASE DO NOT RETURN YOUR FORM TO THE ABOVE ADDRESS.					
1. REPORT DATE (DD-MM-YYYY) 23-12-2015		2. REPORT TYPE Final		3. DATES COVERED (From - To) April 2012 – October 2015	
4. TITLE AND SUBTITLE Predicting the Fate and Effects of Resuspended Metal Contaminated Sediments (ER-1746)			5a. CONTRACT NUMBER		
			5b. GRANT NUMBER ER-1746		
			5c. PROGRAM ELEMENT NUMBER		
6. AUTHOR(S) Burton, G.A. Fairley, K.J. Rader, K. Carbonaro, R.F. Gailani, J.			5d. PROJECT NUMBER		
			5e. TASK NUMBER		
			5f. WORK UNIT NUMBER		
7. PERFORMING ORGANIZATION NAME(S) AND ADDRESS(ES) University of Michigan, 400 Church, Ann Arbor, MI 48109 Manhattan College, 4513 Manhattan College Pkwy, Bronx, NY 10471 Mutch Associates, LLC, 360 Darlington Ave, RSamsey NJ 07446 United States Army Corps of Engineers Engineer Research and Development Center, 3909 Halls Ferry Road, Vicksburg, MS 39180			8. PERFORMING ORGANIZATION REPORT NUMBER Environmental Restoration Project #ER-1746		
9. SPONSORING / MONITORING AGENCY NAME(S) AND ADDRESS(ES)			10. SPONSOR/MONITOR'S ACRONYM(S) N/A		
			11. SPONSOR/MONITOR'S REPORT NUMBER(S) N/A		
12. DISTRIBUTION / AVAILABILITY STATEMENT					
13. SUPPLEMENTARY NOTES					
14. ABSTRACT The over-arching objective of this project was to determine the environmental significance of resuspended metal contaminated sediments, considering spatial and temporal issues as they relate to exposure, fate and real-time vs. ecological effects. The focus was on strong resuspension events, such as those caused by propeller wash, which prevail in harbors and navigation systems. Physical-chemical models were developed that predict metal contaminant speciation, partitioning and transport and the resulting exposures linked to biological effects in these dynamic ecosystems. It appears that most resuspension events, whether conducted in the laboratory or field, are non-toxic events due to the short duration of the exposures. Metals released from sediments are quickly scavenged by Fe and Mn oxyhydroxides becoming non-bioavailable and then settle out onto the surficial sediments. Model results showed that during short-term resuspension events metal bioavailability is limited due to the slow oxidation of metal sulfides, and the binding of released metal to NOM and HFO. The TICKET-PTM was applied to a pilot field test of a propeller-wash event in San Diego Bay as a proof of concept evaluation of the model capabilities. Model results demonstrated the importance of transport, oxidation kinetics and metal partitioning behavior in assessing the effects of propeller-wash events on copper bioavailability in the overlying water.					
15. SUBJECT TERMS resuspension, metals, sediment, model, bioavailability, toxicity					
16. SECURITY CLASSIFICATION OF:			17. LIMITATION OF ABSTRACT SAR	18. NUMBER OF PAGES 181	19a. NAME OF RESPONSIBLE PERSON Allen Burton
a. REPORT U	b. ABSTRACT U	c. THIS PAGE U			19b. TELEPHONE NUMBER (include area code) 734-763-3601

Page Intentionally Left Blank

Table of Contents

List of Tables	ii
List of Figures	ii
Appendices.....	iv
Abstract.....	5
ER-1746: Predicting the Fate and Effects of Resuspended Metal Contaminated Sediments	9
Objective	9
Task 1a: Measure Metal Partitioning in Bedded Sediments	11
Materials and Methods.....	11
SeFEC Sediment Exposure Scenarios	16
SeFEC Organism Exposures.....	17
Task 1a: Results and Discussion.....	18
SeFEC Sediment Exposure Scenarios	18
Gust Chamber Sediment Exposure Scenario	21
Task 1b and 2b: Assess the Ability of Equilibrium Models to Accurately Predict Speciation in Sediments.....	27
Task 1b and 2b: Materials and Methods	29
Task 3b: Integrated TICKET-PTM.....	52
Task 3b: Materials and Methods.....	53
Task 3b: Results and Discussion.....	57
Task 3a and 3c: Verification Testing	85
Conclusions and Implications for Future Research/Implementation.....	102
Literature Cited	104

List of Tables

Table 1. Total metals (mg kg ⁻¹ dry weight) for all bedded sediments used in experiments.	13
Table 2: Experimental conditions using Lake DePue sediments in Gust erosion chambers.	15
Table 3. Analysis of total organic carbon (TOC) (%), acid volatile sulfides (AVS) (μmol/g), and simultaneously extracted metals (SEM) (μmol/g) for all bedded sediments.	18
Table 4. Percent of total metal (mg/L) dissolved during 4-hour continuous and 16-hour multiple (hourly and total) resuspension events, adjusted for sediment loss during water exchange.	21
Table 5. Day 7 and 14 survival and maximum/average (n=19) zinc concentrations for each Gust experiment with Lake DePue sediment.	26
Table 6: Kinetically-controlled Redox Reactions in the Chemical Model	30
Table 7: Solubility Products for Precipitation/Dissolution Reactions Considered in Chemical Equilibrium Calculations for Initial Conditions.	32
Table 8: Second-order Oxidation Rate Coefficients (M ⁻¹ hr ⁻¹) from Previous Modeling Studies.	32
Table 9: Initial Conditions for Time-variable Model Simulations for Oxidation of the Clarence River, Tweed River and Anacostia River Sediment Samples.	36
Table 10: Initial Conditions for Time-variable Model Simulations for Oxidation of the Portsmouth Naval Station Sediment Samples (MS03, MS04).	44
Table 11: Second-order Oxidation Rate Coefficients (M ⁻¹ hr ⁻¹) Determined from Chemical Model Evaluations in This Study.	50
Table 12: Mass Balance Equations and Analytical Solutions for Time-Variable Concentrations of FeS(s), MS(s), HFO, “Labile” Metal and Elemental Sulfur in the Simplified Chemical Model	54
Table 13: Initial Conditions and Water Chemistry Parameters for Time-variable Simulations Using the Simplified Model. ^a	56
Table 14: Apparent First-order Oxidation Rate Coefficients (hr ⁻¹) for Time-variable Simulations Using the Simplified Model. ^a	57
Table 15: Copper and Zinc Suspended Matter/Water log K _D Summaries from Literature Data as Compiled by Allison and Allison (2005).	65
Table 16: Water Quality Parameters for San Diego Bay	70
Table 17: Water Quality Parameters for Pearl Harbor.	71
Table 18: List of Symbols	74
Table 19: List of Acronyms	76
Table 20: Model Input and Output.	82

List of Figures

Figure 1. SeFEC modified from Hammerschmidt and Fitzgerald, 2008.	12
Figure 2 . Gust-type benthic flux chamber	13
Figure 3. Gust chamber laboratory set-up.	16
Figure 4. Metal concentrations of each sediment type throughout the 4 hour resuspension in the SeFEC chambers.	19
Figure 5. 16-hour multiple resuspensions of Duck Lake, Lake DePue and Idaho sediments.	20
Figure 6. Dissolved Zn (μg L ⁻¹) for the bioturbation only experiment	22
Figure 7. Dissolved Zn (μg L ⁻¹) for the resuspension experiment.	22
Figure 8. Dissolved Zn and particulate Mn (μg L ⁻¹) for the bioturbation only experiment.	23

Figure 9. Dissolved Zn and particulate Fe ($\mu\text{g L}^{-1}$) for the resuspension experiment .	23
Figure 10. Survival of <i>H. azteca</i> and <i>D. magna</i> during exposures bedded sediments and to 4-hour resuspensions.	24
Figure 11. Qwik-lite toxicity values of elutriates compared to controls for each sediment type.	25
Figure 12. Qwik-lite toxicity of the dinoflagellate from exposure to the 16-hour multiple resuspension event.	25
Figure 13. Survival data (%) of <i>H. azteca</i> calculated from two replicates..	26
Figure 14. Laboratory results.	28
Figure 15: Model-data comparisons for the Clarence River sediment oxidation study.	37
Figure 16: Model-data comparisons for the Tweed River sediment oxidation study.	39
Figure 17: Model-data comparisons for the Anacostia River sediment oxidation study.	41
Figure 18: Model-data comparisons for the Portsmouth Naval Station MS03 sediment oxidation study.	45
Figure 19: Model-data comparisons for the Portsmouth Naval Station MS04 sediment oxidation study	46
Figure 20: Model-data comparisons for the Portsmouth Naval Station MS03 sediment oxidation study.	47
Figure 21: Model-data comparisons for the Portsmouth Naval Station MS04 sediment oxidation study.	48
Figure 22: Comparisons of simplified model and detailed model results for the Tweed River sediment oxidation study.	58
Figure 23: Comparisons of simplified model with and without metal binding to natural organic matter (NOM) for the Tweed River sediment oxidation study	59
Figure 24: Comparisons of simplified model with and without metal binding to natural organic matter (NOM) for the Portsmouth Naval Station MS03 sediment oxidation study.	59
Figure 25: Performance assessment plot for nickel (Ni), copper (Cu), zinc (Zn), cobalt (Co), and lead (Pb) and (b) log KD prediction residual plot using default WHAM parameters.	62
Figure 26: (a) Performance assessment plot for nickel (Ni), copper (Cu), zinc (Zn), cobalt (Co), and lead (Pb) and (b) log KD prediction residual plot for WHAM simulation.	63
Figure 27: San Diego Bay sample locations.	64
Figure 28: Summary of observed log K_D data from Chadwick et al. (2005) and the SPAWAR propeller wash sampling events at San Diego Bay	65
Figure 29: San Diego Bay performance assessment plot.	66
Figure 30: Propeller wash study sample locations.	66
Figure 31: Summary of sampling events at Pearl Harbor.	67
Figure 32: Pearl Harbor performance assessment plot.	68
Figure 33: Schematics of contaminant partitioning.	73
Figure 34: San Diego Bay	86
Figure 35: Schematic of tug plume monitoring	87
Figure 36: Tug, sampling boat, and plume in San Diego Bay	87
Figure 37: Flowchart of laboratory processing and analysis of the field samples.	88
Figure 39: The location of the prop wash source.	91
Figure 40: Tides during the simulation.	92
Figure 41: Parcel positions at 4/4 2pm, 4/4 4pm, 4/5 12am, 4/6 12am, 4/7 12am and 4/8 12am.	94
Figure 42: Time series of total sediment mass.	95
Figure 43: Maximum TSS	95

Figure 44: Time series of particulate and dissolved Cu mass.....	98
Figure 45: Time series of particulate mass and dissolved mass for Tier 3 with two different decay rates.	99
Figure 46: Time series of maximum concentration for dissolved phase contaminant	100

Appendices

Appendix A: Supporting Data.....	98
Appendix B: List of Scientific/Technical Publications.....	174
Appendix C: Draft summary report “Biological Effects Associated with Resuspension from Propeller Wash at Navy Facilities.	182

Abstract

Objectives

The over-arching objective of this project was to determine the environmental significance of resuspended metal contaminated sediments, considering spatial and temporal issues as they relate to exposure, fate and real-time vs. ecological effects. The focus was on strong resuspension events, such as those caused by propeller wash, which prevail in harbors and navigation systems. The metals that will be studied are Cd, Cu, Pb, and Zn. A physical-chemical models was developed that predicts metal contaminant speciation, partitioning and transport and the resulting exposures linked to biological effects in these dynamic ecosystems.

Technical Approach

A wide range of sediment types were used as their physicochemical characteristics greatly influence metal release dynamics. Sediments known to have metals related issues were obtained from five locations and transported to the University of Michigan for analysis. Three sites were freshwater: a reference sediment from Duck Lake (Muskegon, MI), Idaho river bank (Blackbird Mine, IN), and Lake DePue (DePue, IL). Freshwater sediments were used initially due to difficulty and delays in obtaining marine sediments. Two sediments were eventually collected at marine harbors: San Diego Bay (San Diego, CA), and Portsmouth Naval Shipyard (Portsmouth, NH).

Initial stages of this research involved developing the SeFEC, which was modified from a previous design (Hammerschmidt and Fitzgerald, 2008). These chambers are useful in laboratory experiments, as they are inexpensive to construct and easily allowed for multiple replications. In our experiment, the SeFEC was used to assess sediment-water exchange of metal bioavailability and toxicity.

Benthic flux chambers were also constructed based on the Gust erosion chamber design involving the combination of a plate stirrer with a center port for outflow. The flux chambers were modified so that pore water flow could be superimposed in addition to the turbulent shear applied to the sediment surface. This also allowed testing of various combinations of pore water motion induced by boundary shear, direct inflow and outflow of pore water (which is induced in the field by larger-scale boundary exchange processes), and sediment resuspension.

Resuspension events were simulated in the Gust chamber by increasing the rate of disc rotation in the Gust erosion head and by increase water flow through the chamber. For those studies simulating resuspension, full bed erosion was generated and maintained for four hours. After the resuspension event, samples for dissolved and particulate metal concentration were collected approximately every hour to capture temporal dynamics of metal flux. Various sediment characteristics were analyzed including total metals, AVS, SEM, and total organic carbon (TOC).

Propeller wash resuspension events in San Diego Bay and Pearl Harbor were simulated in April and August 2012, respectively. The objective of the field work component is the collection of

discrete seawater samples, representative of background and conditions within the resuspended sediment plume generated by a tug boat propeller. These samples were manipulated in the laboratory for quantification of the load of metal and organic CoCs associated with a suite of sediment-size fractions, information that will be used for parameterization of predictive hydrodynamic models.

The TICKET chemical model was subsequently developed for incorporation into the Particle Tracking Model (PTM) to assess metal release and bioavailability in field setting. The combined TICKET-PTM effectively simulates the movement of a large number of dissolved and particulate parcels through complex open water flow fields using a Lagrangian framework. Along with transport, a simplified version of the TICKET chemical model is used to track the oxidation of metal sulfide [MS(s)] to “labile” metal concentrations, and to determine the partitioning of “labile” metal between dissolved and particulate phases. The TICKET-PTM was applied to a pilot field test of a propeller-wash event in San Diego Bay as a proof of concept evaluation of the model capabilities. Model results demonstrated the importance of transport, oxidation kinetics and metal partitioning behavior in assessing the effects of propeller-wash events on copper bioavailability in the overlying water.

Results

In SeFEC exposures, three sediment types (Idaho, San Diego, and Lake DePue) had a total SEM > AVS, indicating that the amount of metals present exceeded the sulfide binding capacity in the sediment, indicating these sediments may cause toxicity in organisms. Across all sediment types an average decrease in pH (0.14) and DO (0.24 mg/L) was observed. The drops in pH and DO indicate potential oxidation of metal sulfides, resulting in dissolved metals released into the water. Increased dissolved metal concentrations were slight, and increased metals could be a product of easily exchangeable sediment particles, rather than metal sulfide release, or potentially a combination of both. Survival of *H. azteca* varied across sediment types in SeFEC exposures. The most striking result was the zero survival in the Lake DePue bedded sediments. The toxicity was not observed immediately following the resuspension event, but in later tests of the bedded sediments. This is the only occurrence in which bedded sediments were more toxic than resuspended and suggested that redeposited sediment at this site had greater toxicity than sediments not resuspended.

Gust chamber exposures utilized Lake DePue sediment which yielded decreased zinc concentrations during bioturbation studies. Copper, nickel, and zinc levels all exceeded probable effect levels (PELs). Additionally, bioturbation increased abundance of particulate Mn binding ligands. Resuspension of metals also increased both particulate Fe and Mn ligands in Gust chambers. Based on Gust chamber exposure data, there was variable *H. azteca* survival outcomes depending on treatment. High and low density *L. variegatus* exposures showed acute toxicity only during the combined bioturbation and resuspension events. The most acute toxic effects were observed when no worms were present, which is counter-intuitive.

It appears that most resuspension events, whether conducted in the laboratory or field, are non-toxic events due to the short duration of the exposures. Metals released from sediments are quickly scavenged by Fe and Mn oxyhydroxides becoming non-bioavailable and then settle out onto the surficial sediments. If there are metal sensitive epibenthic species, such as *Hyaella*

azteca, in the area where these resuspension events occur then they may be chronically exposed feeding subsequent feeding on the metal elevated particles. The laboratory studies with the SEFEC and Gust chambers confirmed a lack of effects and the chemical and particle exposure dynamics supported those findings.

Model results showed that during short-term resuspension events metal bioavailability is limited due to the slow oxidation of metal sulfides, and the binding of released metal to NOM and HFO. This latter effect is enhanced by: (i) the production of additional HFO binding sites during the oxidation of reduced iron phases (e.g., FeS(s) , $\text{FeCO}_3\text{(s)}$); and (ii) minimal decreases in pH due to pH buffering and negligible acid production during FeS(s) and $\text{FeCO}_3\text{(s)}$ oxidation and precipitation to HFO and elemental sulfur (an intermediate sulfur oxidation state). The TICKET-PTM was applied to a pilot field test of a propeller-wash event in San Diego Bay as a proof of concept evaluation of the model capabilities. Model results demonstrated the importance of transport, oxidation kinetics and metal partitioning behavior in assessing the effects of propeller-wash events on copper bioavailability in the overlying water.

Benefits

The laboratory and modeling work that was performed as part of this project has provided a much clearer understanding of the critical processes that control metal bioavailability and ultimately toxicity effects associated with propeller-wash events. Additional research would be beneficial in assessing differences in metal sulfide oxidation rates in freshwater and marine systems. The development of protocols is also needed for characterizing sediment chemistry prior to resuspension. Further model development should be considered for cases where subsequent oxidation of elemental sulfur to sulfate (and an associated release of acid) may occur. Finally, additional testing of the TICKET-PTM should be performed be a variety of field conditions that are likely to be encountered at DoD sites.

This work has helped improve fundamental understanding of the behavior and ecological impacts of resuspended sediments that contain elevated levels of priority metals (zinc, copper, and lead) and oxy-anions (arsenic). This advances DOD's ability to manage these priority contaminants by contributing detailed, fundamental, and general knowledge of the processes that control their stability, mobility, and bioavailability in sediments. Additionally, this work has been performed in cooperation with the USACE who are primarily responsible for national guidance on dredging operations and is actively involved in sediment and contaminant management in harbors and waterways. Results will be transitioned through publication of peer-reviewed journal articles, technical reports, technical symposia, and short course training. It is anticipated that this work will lay the foundation for technical guidance for use in dredging, site risk assessments and feasibility studies for possible remediation efforts.

1.0 ER-1746: Predicting the Fate and Effects of Resuspended Metal Contaminated Sediments

1.1 Objective

The primary objective of this research was to determine the environmental significance of resuspended metal contaminated sediments and better understand the temporal and spatial effects of metal transport and fate. This project addressed three objectives of the SERDP Statement of Need. (1) Protocols were developed in which naturally contaminated sediments from the field could be resuspended in laboratory experiments to simulate propeller wash in harbors and navigation systems. The Sediment Flux Exposure Chamber (SeFEC) was developed as the tool to resuspend sediments. It allows researchers to assess site-specific bioavailability of metals. (2) To better understand the uptake, assimilation, and efflux of metals in benthic organisms, organisms (*Daphnia magna* and *Hyalella azteca*) were exposed to resuspended sediments. Gust erosion chambers were also utilized in resuspension studies. (3) The data collected from these chambers and organism exposures allowed researchers to model the impacts of sediment resuspension, thus improving modeling methods to predict metal availability and sediment toxicity.

Our hypotheses were based on current chemical speciation models, which may not be adequate for predicting metal speciation and bioavailability in sediments. Existing equilibrium models for chemical speciation do not take into account solid phases that are expected to control pore water metal concentrations in oxic sediments. Our understanding of the chemical speciation of metals in sediments with high metal loadings (where $SEM > AVS$) is limited. As the sediments are resuspended and come into contact with oxic conditions, it was expected that dissolved metals will be released from the total metals pool in the sediments. It was also expected that sediments with high acid volatile sulfide (AVS) bound metals will release more metal than oxic-bound metals.

Bedded sediments of five sediment types were analyzed, varying in physical and chemical characteristics (Task 1a) at the University of Michigan. Four of the five sediments were analyzed for biotic toxic effects during a 10-day bedded sediment exposure to two freshwater species *Daphnia magna* and *Hyalella azteca*. Each sediment type has also been resuspended using the SeFEC and Gust erosion chambers, and analyzed for the chemical parameters listed in Task 1a. Test organisms were also exposed to sediments during resuspensions. Chemical speciation modeling of the data produced at the University of Michigan was performed by Manhattan College and ESACE ERDC.

A reactive-transport model was therefore developed using the Tableau Input Coupled Kinetic Equilibrium Transport (TICKET) framework to evaluate the detailed effects of sediment resuspension on metal bioavailability. The TICKET chemical model was successfully applied in evaluating metal release during resuspension in four laboratory chamber studies. The TICKET chemical model was subsequently developed for incorporation into the Particle Tracking Model (PTM) to assess metal release and bioavailability in field setting. The combined TICKET-PTM effectively simulates the movement of a large number of dissolved and particulate parcels

through complex open water flow fields using a Lagrangian framework. Along with transport, a simplified version of the TICKET chemical model is used to track the oxidation of metal sulfide [MS(s)] to “labile” metal concentrations, and to determine the partitioning of “labile” metal between dissolved and particulate phases. The TICKET-PTM was applied to a pilot field test of a propeller-wash event in San Diego Bay as a proof of concept evaluation of the model capabilities.

1.2 Background

The proposed work addresses SERDP ERSON-10-04 by improving fundamental understanding of the behavior of priority metals (zinc, copper, and lead) and oxy-anions (arsenic). We proposed to make multiple, tangible advances in DOD’s ability to manage these priority contaminants by contributing detailed, fundamental, and general knowledge of the processes that control their stability, mobility, and bioavailability in sediments. This was accomplished through highly controlled laboratory experimentation using both amended sediments and field-contaminated materials. The unique benefit of the laboratory studies proposed here is that they will include realistic sediment structure and internal chemical gradients generated by the combined action of benthic organisms and pore fluid flow under realistic hydrodynamic and geochemical conditions. Further, use of laboratory mesocosms allowed pore fluid flow, biological activity, development of redox gradients, chemical speciation, contaminant efflux, and contaminant bioavailability and toxicity to be characterized in detail using state-of-the-art methods. This high-quality information is needed in order to assess the complex suite of processes that regulate overall contaminant behavior and effects. While many of these processes have been studied individually, complex interactions control contaminant bioavailability. For example, bioturbation and chemical precipitation/dissolution processes alter sediment structure, which strongly influences transport in pore water, which in turn regulates redox conditions, contaminant efflux, and exposure of organisms to contaminants. These sorts of interactions have generally confounded site characterization, and so detailed investigations under controlled conditions are needed to improve understanding of key governing processes, as well as to develop improved methods for evaluating these interactions at contaminated sites.

The need for this type of work was specifically articulated in the Report of the SERDP and ESTCP Expert Panel Workshop on Research and Development Needs for Understanding and Assessing the Bioavailability of Contaminants in Soils and Sediments (SERDP and ESTCP, 2008). The proposed work meets several specific research priorities identified by the panel. First the work contributes to the Critical Priority Need “Improved Understanding of Metal Bioavailability in Sediments” by advancing fundamental understanding of not only governing physical, chemical, and biological processes (e.g., contaminant fluxes in pore waters, role of bioturbation and bioirrigation in structuring contaminated sediments, and role of all these processes in controlling contaminant speciation), but also how their coupling affects overall system structure (physical heterogeneity and chemical gradients in sediments). Second, the work addresses the Critical Priority Need for “Improved Approaches for Biological Assessments of Bioavailability” by developing new methods to evaluate the combined effects of pore water flows, chemical diagenesis, and biological activity (bioturbation and bioirrigation) on contaminant bioavailability. Third, the work substantially contributes to the High-Priority Need “Better Understanding of Bioavailability across Small-Scale Gradients and Interfaces” by

characterizing how pore structure, pore fluid flow, and biological activity combine to generate these gradients, and by explicitly linking the resulting chemical gradients to bioavailability and toxicity. We focus particularly on the processes that generate redox gradients in sediments, starting with delivery of oxygen from the overlying water column. This meets the Critical Priority Need to “Improve modeling methods for predicting metal availability and benthic toxicity in oxic sediments.” Further, by using newly developed methods to probe the distribution of arsenic in sediments in relation to biological activity and bioavailability, the Critical Priority Need to “Complete basic research on the bioavailability of oxy-anions (As and Cr)...to improve basic understanding of the mobility and bioavailability of these metals” was also met. Finally, with regard to assessing contaminant transmission and biomagnification to higher trophic level organisms, and thence to humans, the Critical Priority Need to “Develop understanding of key parameters that influence both in situ and ex situ sediment contaminant partitioning and bioavailability” was also met. In particular, the need to “A better understanding [of] flux from sediments into the water column and into the food chain” by assessing net outcomes in terms of contaminant efflux from sediments, sequestration into sediments by precipitation and sorption mechanisms, and entry into the food chain via bioavailability to benthic organisms was met.

Disclaimers: For simplification, Task 1b and Task 2b are combined in one cohesive section for the purposes of this report. Task 1c appears after 1b and 2b, for cohesiveness of model development.

Task 1a: Measure Metal Partitioning in Bedded Sediments: Materials and Methods

SeFEC Exposures

Initial stages of this research (Task 1a) produced the SeFEC (Figure 1), which was modified from a previous design (Hammerschmidt and Fitzgerald, 2008). These chambers are useful in laboratory experiments, as they are inexpensive to construct and allow for multiple measured replications of the same sediment sample. In our experiment, the SeFEC was used to assess sediment-water exchange of metal bioavailability and toxicity.

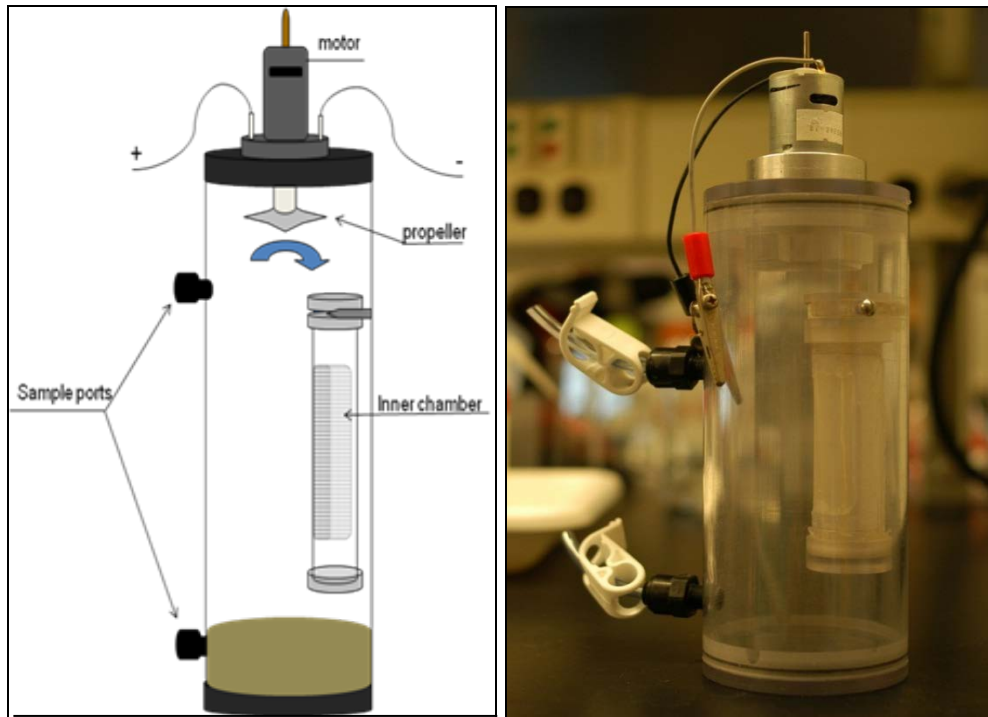


Figure 1. SeFEC modified from Hammerschmidt and Fitzgerald, 2008.

Benthic flux chambers were also constructed based on the Gust erosion chamber design (see below) involving the combination of a plate stirrer with a center port for outflow. The flux chamber is a cylindrical design having ~10 cm inner diameter, with emplaced sediments at the bottom and an overlying water column agitated by a stirrer at the top, as shown in Figure 2. The advantage of the Gust-type design is that this is known to produce a more realistic hydrodynamic shear over the surface of the sediments than simpler batch systems (Tengberg et al., 2004ab). The flux chambers were modified so that pore water flow could be superimposed in addition to the turbulent shear applied to the sediment surface. This was accomplished by adding an inflow/outflow port on the bottom to allow pressurized flow-through in order to impose desired rates of vertical pore water advection in a manner similar to a permeameter. This also allowed testing of various combinations of pore water motion induced by boundary shear, direct inflow and outflow of pore water (which is induced in the field by larger-scale boundary exchange processes), and sediment resuspension.

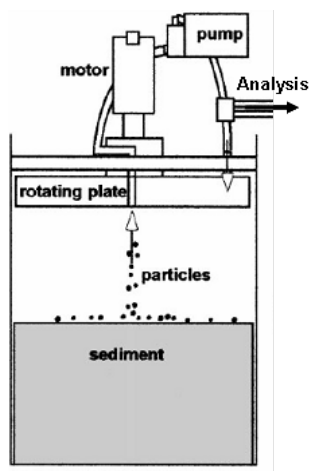


Figure 2 . Gust-type benthic flux chamber, shown here with analysis of sediment resuspension (Thomsen and Gust, 2000).

Sediments were obtained from five locations and transported to the University of Michigan for analysis. Three sites were freshwater: a reference sediment from Duck Lake (Muskegon, MI), Idaho river bank (Blackbird Mine, IN), and Lake DePue (DePue, IL). Two sediment types were collected at marine harbors: San Diego Bay (San Diego, CA), and Portsmouth Naval Shipyard (Portsmouth, NH). At the beginning of the research naval harbor sediments were not available, and other sediments with known metal contamination and variable chemical characteristics were obtained as illustrated in Table 1. As the majority of sediments were not marine, culture water (dechlorinated municipal water from Ann Arbor, MI) was used in the initial SeFEC experiments.

Table 1. Total metals (mg kg⁻¹ dry weight) for all bedded sediments used in experiments. Bold values are levels above NOAA Threshold Effect Level (TEL) for *H. azteca* (Buchman 1999). * Values reported were below detection limit of instrument. Detection limits reported in table.

Site	Cu	Ni	Zn	Pb	Cd	Co	Fe	Mn
Duck Lake	49	0.1-1*	116	1-10*	< 0.1*	73	15025	668
Idaho	323	0.1-1*	56	1-10*	< 0.1*	257	90	41197
San Diego	290	16	290	35	6	180	67600	342
DePue	1458	54	29791	1-10*	108	37	41340	1738
Portsmouth	599	72	366	113	5	33	27300	172

After several initial trials of the SeFEC, it was discovered that only a small amount of sediment (3-5 grams) was required to obtain realistic concentrations of total suspended solids (TSS), due to the small volume of the chamber (580 ml). Thus, sampling of porewater and bedded sediments from the chamber was unable to occur because there was not sufficient sediment present. Bedded sediment was instead sampled from beakers during a 10-day sediment exposure of each sediment type. Overlying water was sampled at regular intervals during two types of sediment resuspensions (4-hour and 16-hour) and daily in the 10-day bedded sediment exposures.

Gust Erosion Chamber Exposures

Several experiments were also conducted using Gust erosion chambers (Figure 3). These experiments used Lake DePue (Zn-contaminated) sediments to compare the effect of resuspension versus bioturbation on Cd-Cu-Fe-Mn-Ni and Zn bioavailability under laboratory conditions. Gust erosion chambers have been used in other studies to characterize erodibility of surface sediments. The Gust chamber consists of a large (check diameter) polycarbonate tube with water input and output connections. A rotating stirring disk can be fastened to the tube. The rotation rate of the disk can be varied to generate a uniform shear stress across the sediment surface. Depending on sediment characteristics, a certain shear stress can result in resuspension of sediments. Tubing was added to the water outlet that drained into 4-L borosilicate beakers to minimize sediment disruption. For each experiment there were two beakers: one with control water and the other with water that was siphoned from, and recirculated through, the Gust erosion chamber. Exposure chambers were placed in these beakers that housed test organisms (in this case, the freshwater amphipod *H. azteca*). There were 4 chambers with 10 amphipods each in the exposure beakers and 4 chambers with 10 amphipods each in the control beaker.

Prior to starting the experiment, Lake DePue sediment was homogenized and measurements of sediment pH, AVS-SEM, along with sediment dry weight were taken. Sediments were added to the chamber to create a maximum depth of 10 cm. Once the sediment was loaded, the Gust column was filled with reconstituted freshwater (Smith et al. 1997) using filtered Ann Arbor (MI) city water. The column was then allowed to settle for 8 to 16 hours. To begin the experiment, the erosion head and peristaltic pump were started to generate a shear force on the sediment. Over the course of the experiment, dissolved and particulate metal concentrations, dissolved oxygen, temperature, turbidity, pH, conductivity, and ammonia were measured.

Eight different experimental conditions were simulated (Table 2) to compare the effects of short-term (4-hr) resuspension events with the effects of bioturbation of the oligochaete *Lumbriculus variegatus*. Varying density (or biomass) of oligochaetes was assessed by using a low density condition. To assess the effects of bioturbation on water concentration of metals, the oligochaete *L. variegatus* was added to the Gust chambers. Two different densities of bioturbators were used to test for a potential effective on metal fluxes: a low-density condition (5,000 individuals/m² or approximately 1 g of organisms per chamber) and a high-density condition (10,000 individuals/m², or approximately 2 g of organisms per chamber).

Resuspension events were simulated in the Gust chamber by increasing the rate of disc rotation in the Gust erosion head and by increase water flow through the chamber. For those studies simulating resuspension, full bed erosion was generated and maintained for four hours. After the

resuspension event, dissolved and particulate metal concentration were sampled approximately every hour to capture temporal dynamics of metal flux.

At the end of the experiment, core sediment samples were taken from the Gust chambers, using 140-mL plastic syringes. Layers of sediments were collected as from the surface as follows: 0.5 cm, 1.0 cm, 1.5 cm, 2.0 cm, 3.0 cm, 4.0 cm, and 5.0 cm. These samples were dried to assess dry weight and analyzed with SEM/AVS.

The toxicological endpoints of this study were mortality rates and metal concentrations in body tissues. To evaluate temporal effects on these two endpoints, test organisms (*H. azteca*) were removed and assessed their conditions on d7 and d14. To measure body burden, a modification of Borgmann's method (as described in Norwood et al. 2006) was utilized. After removing the amphipods and evaluating condition, individuals were placed in a container with 50 uM EDTA, a small piece of unbleached paper towel, and a small amount of Tetramin™. After 24 h, the individuals would be rinsed with culturing water and transferred to aluminum weigh dishes and placed in a dessicater for at least 48 hours. Dried individuals would be weighed and digested with 70% nitric acid for 6 days at room temperature, then add 30% hydrogen peroxide, sit for an additional 24 hours. Finally, Mili-Q water was added to dilute to 2.5% nitric acid. Digestates were then analyzed on an ICP-MS.

Table 2: Experimental conditions using Lake DePue sediments in Gust erosion chambers. Note that *Lumbriculus* are not usually used as a test organism to measure toxicity with since they can reproduce in short periods of time. They were only used as bioturbators in these experiments.

Experiment type	Bioturbator	Bioturbator density (ind/m ²)	Sheer Stress	Toxicological endpoint
No resuspension, no bioturbators	None	None	0%	<i>H. azteca</i> survival and body burden data
Resuspension only	None	None	3%	<i>H. azteca</i> survival and body burden data
Bioturbation only – low density	<i>L. variegatus</i>	5,000	0%	<i>H. azteca</i> survival and body burden data
Both: bioturbation low and resuspension	<i>L. variegatus</i>	5,000	3%	<i>H. azteca</i> survival and body burden data
Bioturbation only – high density	<i>L. variegatus</i>	10,000	3%	<i>H. azteca</i> survival and body burden data
Both: bioturbation high and resuspension	<i>L. variegatus</i>	10,000	3%	<i>H. azteca</i> survival and body burden data

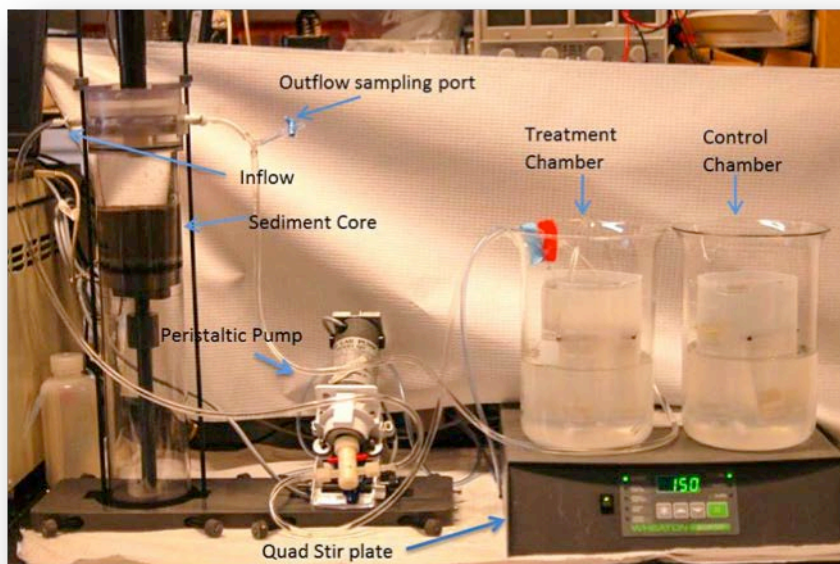


Figure 3. Gust chamber laboratory set-up.

SeFEC Sediment Exposure Scenarios

Various parameters were measured to analyze chemical characteristics in the 10-day bedded sediment exposures. The bedded sediment samples were analyzed for total metals, acid volatile sulfides (AVS), simultaneously extracted metals (SEM), and total organic carbon (TOC). Total metal concentrations were obtained by microwave acid digestion (3:1 ratio of nitric:hydrochloric acid) followed by ICP-OES analysis. The USEPA protocol (1991) for measuring AVS-SEM was used and SEM metals were analyzed on the ICP-OES. SEM metals of interest included copper, zinc and nickel (USEPA 2005). TOC was measured as the loss-on-ignition (samples placed in an ashing oven at 450°C for 6 hours) multiplied by the Redfield ratio, 0.36. Overlying water was also sampled above the bedded sediments in the 10-day beaker exposure. Dissolved metal samples were filtered through a 0.2 μm polycarbonate membrane filter, acidified with 10% nitric acid solution, and analyzed on the ICP-OES.

A 4-hour continuous resuspension was used to replicate a single, intensive dredging event. All five sediments were exposed to the 4-hour continuous resuspension (three replicate sediment chambers and one control chamber). For a total volume removal of less than 10% per chamber, only 10 mL of water was removed once an hour for a total of 50 ml water removal throughout the 4-hour continuous resuspension. Any water removed for analysis was replaced before re-sealing the chamber top and all air was removed throughout the resuspensions. Overlying water was sampled hourly during the resuspension and was analyzed for dissolved metals, pH, dissolved oxygen, and temperature.

A 16-hour multiple resuspension was also implemented in the SeFEC, intended to replicate intermittent ship traffic in a harbor. Three of the five sediments were selected for the 16-hour pulsed resuspensions, Duck Lake, Lake DePue, and Idaho. At the time of the experiments, the

Portsmouth sediments were not available. The chambers were suspended during hour 1, stopped and settled for hours 2-4, sampled for chemistry after hour 4, and repeated for a 16 hour time period (four total 1-hour resuspensions over a 16-hour time period). Overlying water was sampled at the end of hours 4, 8, 12, and 16. Samples were analyzed for: dissolved metals, pH, dissolved oxygen, and temperature (three replicate treatment chambers, one control chamber). After the overlying water was sampled, a complete water change was done for each chamber to simulate a natural flow-through system. All air was removed from the chambers before re-sealing. Each water change reduced the TSS in the SeFEC, as not all sediments settled out completely during the 3 hour settling time. A new TSS value was calculated after each complete water exchange. Water exchanges took place after measuring for dissolved metals and physiochemical parameters (once every four hours).

SeFEC Organism Exposures

Test organisms, *D. magna* and *H. azteca*, were exposed to bedded sediments during the 10-day bedded sediment exposure for 7 and 10 days (respectively). Beakers were filled with 50 ml of sediment and 200 ml of culture water. After one day of equilibration, 10 *D. magna* or *H. azteca* were added to each beaker. A full water exchange was performed every other day.

Hyalella azteca and *D. magna* were also exposed to overlying water during the 4-hour and 16-hour sediment resuspension events. A small inner chamber was installed within the SeFEC to expose test organisms to the overlying water (Figure 1). The mesh lining of the inner chamber protected the organisms within from excessive propeller turbulence. There were three organism exposure scenarios within the SeFEC, in which 10 *H. azteca* neonates (<2 weeks of age), 10 *D. magna* neonates (<24 hours age), or 10 *D. magna* adults (2 weeks of age) were placed in the inner chamber during the resuspension. Following the resuspension, organisms were placed in clean culture water and survival was determined by the number of living organisms present. Long-term survival of *D. magna* and *H. azteca* neonates was measured at 7 to 10 days (respectively) after the resuspension. *D. magna* adults of reproducing age were present only in the 4-hour continuous resuspension. Afterward they were placed in culture water and monitored for reproduction for seven days (counted number of neonates produced each day). San Diego and Portsmouth sediments were omitted from these tests, as they are marine sediments and both species are freshwater organisms.

Additional organism exposures were performed on the bioluminescence of the marine dinoflagellate, *Pyrocystis lunula*, using Qwik-lite toxicity tests. The dinoflagellate was exposed to a sediment aliquot sample (to observe basic whole sediment toxicity) and the overlying water from both the 4-hour and 16-hour sediment resuspensions. In the sediment aliquots, a ratio of sediment to artificial sea water (1:4) was mixed for one hour, and settled to produce the aliquot elutriate. The aliquot elutriate and resuspension samples were all filtered prior to *P. lunula* exposure. Salinity and pH of the resuspension chamber water were adjusted to create optimal conditions for the marine species (salinity increased to 32-34‰ and pH increased to 8.0-8.2) prior to exposure. The dinoflagellate was exposed to the water for 24 hours on a 12-12 light-dark cycle in a cuvette. Bioluminescence was measured in the Qwik-lite testing chamber while the sample was agitated with bubbling air.

Task 1a: Results and Discussion

SeFEC Sediment Exposure Scenarios

Bedded sediments used in SeFEC chambers were analyzed for AVS and SEM (

Table 33). Idaho, San Diego, and Lake DePue sediments had a total SEM > AVS, indicating that the amount of metals present exceeded the sulfide binding capacity in the sediment and these sediments may cause toxicity in organisms. Duck Lake and Portsmouth sediments had an AVS > SEM, indicating that all metals were bound by sulfides in the sediment and not toxic to organisms. Metals in bedded sediments tend to accumulate in the porewater, due to reductive dissolution of Fe and Mn oxyhydroxides in anoxic conditions (Saulnier, 2000). Unfortunately, due to the small volume of the chamber and our attempts to obtain realistic values of TSS, there was no porewater present prior to or during resuspension events. A larger resuspension chamber, similar to the Gust-type flux chamber (Thomsen 2000) is currently being used to better sample porewater of the sediments during resuspension events.

Table 3. Analysis of total organic carbon (TOC) (%), acid volatile sulfides (AVS) ($\mu\text{mol/g}$), and simultaneously extracted metals (SEM) ($\mu\text{mol/g}$) for all bedded sediments.

Sites	Cu	Ni	Zn	AVS	Total SEM*	SEM:AVS	TOC
Duck Lake	0.71	0.23	1.50	51.00	2.44	0.05	0.23
Idaho	4.10	0.22	0.26	0.63	4.58	7.27	0.96
San Diego	4.17	0.05	4.13	0.29	8.35	29.82	3.47
Lake DePue	10.47	0.24	443.16	14.21	453.87	31.94	2.59
Portsmouth	1.20	0.87	4.88	40.96	6.94	0.17	2.04

*Lead and Cadmium are two of the five SEM metals that have not yet been analyzed at each site.

The 4-hour continuous resuspension was monitored for physicochemical parameters and sampled for dissolved metals hourly. Across all sediment types an average decrease in pH (0.14) and DO (0.24 mg/L) was observed. The drops in pH and DO indicate potential oxidation of metal sulfides, resulting in dissolved metals released into the water. Increased dissolved metal concentrations were slight, and increased metals could be a product of easily exchangeable sediment particles, rather than metal sulfide release, or potentially a combination of both. Metal

concentrations varied across time and sediment type (Figure 4, Figure 5), but overall, less than 2% of total metal was released into the water column for the majority of sediment types.

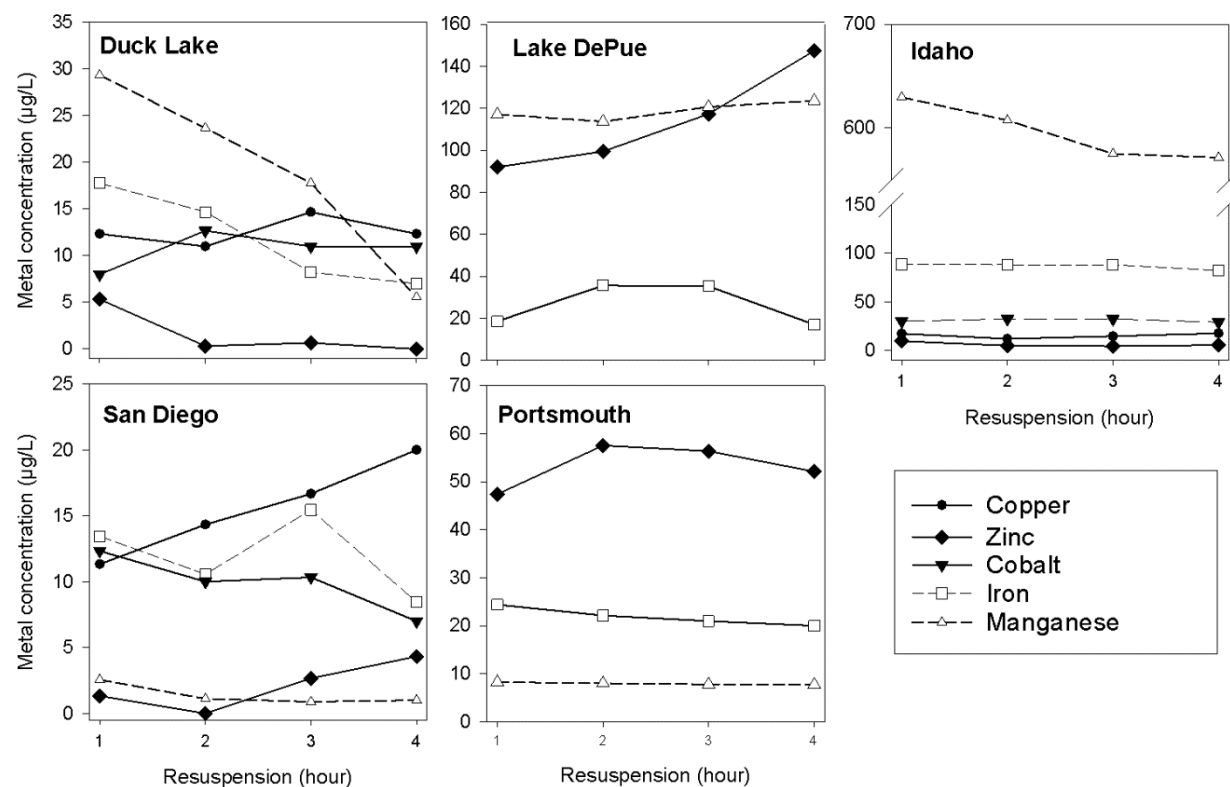


Figure 4. Metal concentrations of each sediment type throughout the 4 hour resuspension in the SeFEC chambers. These values are means of three replicate SeFEC chambers, standard deviations were omitted from graphs, but are present in Appendix A.

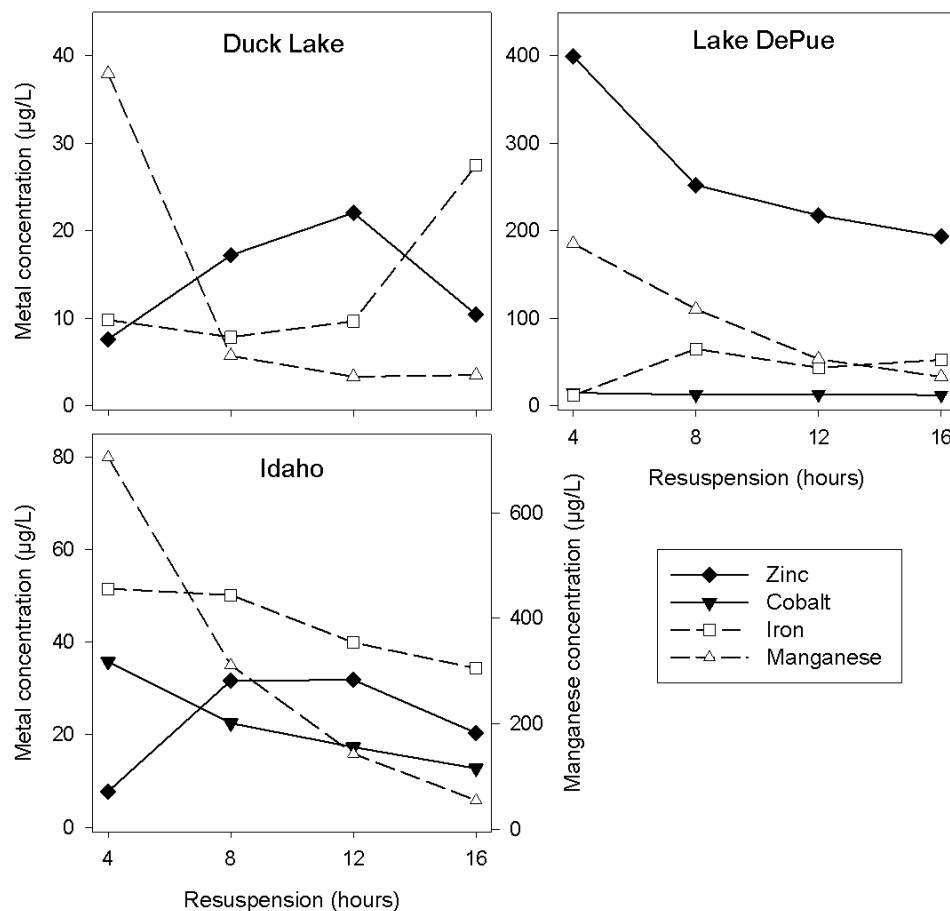


Figure 5. 16-hour multiple resuspensions of Duck Lake, Lake DePue and Idaho sediments. Idaho Mn concentrations were sufficiently higher than other metals and placed on a secondary y-axis.

Part of the SeFEC project aim was to determine if different types of resuspension events release different amounts of metals into the water column. The percent of each metal released during the summed 16-hour multiple resuspensions, on average, was significantly greater than the 4-hour continuous resuspensions across all sediment types ($p < 0.05$). The only exception was the amount of Cu released from Duck Lake, which was similar for the 4-hour and 16-hour resuspension event. Multiple resuspension events release more percent metal over time than one short-term continuous event. In both resuspension events the sediment was resuspended for the same amount of time (4 hours total), but the multiple one-hour resuspensions resulted in greater percent metal release. Intermittent resuspension events, like ship traffic, may then release greater percent of available metals into the water column.

The percent of metals released was also analyzed for the 16-hour multiple resuspension events. In the Duck Lake sediment, the percent of Cu, Zn and cobalt released increased with each resuspension event. The Idaho sediment observed an increase in percent Zn, but a decrease in percent Co and Mn with each subsequent resuspension. Lake DePue sediments had an increase in percent Co and a decrease in percent Mn released over time. Sediment type may be important to the trends in percent metal released. Idaho and Lake DePue sediments were low in organic matter, had fine grain sediment particles. Duck Lake, however, had high amounts of organic

matter, which along with sulfides, binds to metals to make them less available to organisms. This indicates that multiple resuspension events have a continued release of metal overtime, and are also potentially more bioavailable overtime than continuously resuspended sediments.

In the 16-hour multiple resuspensions both Idaho and Lake DePue sediments exhibited a decrease in Mn concentrations over time. Lake DePue additionally showed a decrease in Zn over with each successive resuspension event. These trends suggest that multiple resuspensions may ‘wash’ the sediment, decreasing its toxicity more than a continuous single resuspension. There is still metal release with each successive resuspension event, even though sediment metal release is decreasing. This may indicate that not all metals that can be released from sediment particles will actually be released in a single resuspension, and multiple resuspensions may be the only way in which the maximum amount of metals are released.

Table 4. Percent of total metal (mg/L) dissolved during 4-hour continuous and 16-hour multiple (hourly and total) resuspension events, adjusted for sediment loss during water exchange. Each hourly percent is determined from total sediment present at start of resuspension. The arrows (↑↓) display an increasing or decreasing trend in percent metal released through time.

Sediment	Resuspension	Cu	Zn	Co	Fe	Mn
			↑	0.76	↑	
Duck Lake	Multiple hour 4	0.01	0.39		---	0.34
Duck Lake	Multiple hour 8	0.14	1.35	0.92	---	0.08
Duck Lake	Multiple hour 12	0.24	2.47	1.68	0.01	0.06
Duck Lake	Multiple hour 16	1.08	2.07	2.60	0.04	0.12
Duck Lake	Multiple Total	1.47	6.28*	5.96*	0.05	0.60
Duck Lake	4-hour Continuous	1.53	0.08	0.87	---	0.17
Idaho	Multiple hour 4	0.12	1.22	1.23	0.01	14.23
Idaho	Multiple hour 8	0.25	5.37	0.83	0.01	6.78
Idaho	Multiple hour 12	0.38	6.32	0.75	0.01	3.65
Idaho	Multiple hour 16	0.27	6.24	0.85	0.01	2.16
Idaho	Multiple Total	1.02*	19.15*	3.66*	0.04	26.82*
Idaho	4-hour Continuous	0.42	0.97	1.06	0.02	12.01
Lake DePue	Multiple hour 4	0.10	0.22	15.92	0.01	4.18
Lake DePue	Multiple hour 8	0.15	0.36	14.52	0.07	2.68
Lake DePue	Multiple hour 12	0.11	0.33	16.24	0.05	1.41
Lake DePue	Multiple hour 16	0.17	0.34	17.94	0.07	1.01
Lake DePue	Multiple Total	0.53*	1.25*	64.62*	0.20	9.28*
Lake DePue	4-hour Continuous	0.05	0.15	14.38	0.03	2.68
San Diego	4-hour Continuous	0.77	0.10	0.87	---	0.07

*Significant difference between 4-hour continuous and 16-hour multiple resuspension.

Gust Chamber Sediment Exposure Scenario

Gust chamber exposures utilized Lake DePue sediment, which was characterized by anoxic, fine grained, depositional sediments and low porewater metals.

Decreased zinc concentrations in water were attributed to bioturbation, which begs several questions. First, by what mechanism do worms decrease zinc concentrations? And second, what is influencing dissolved zinc during resuspension? Figures 6 and 7 illustrate dissolved zinc concentrations over time during bioturbation and resuspension experiments.

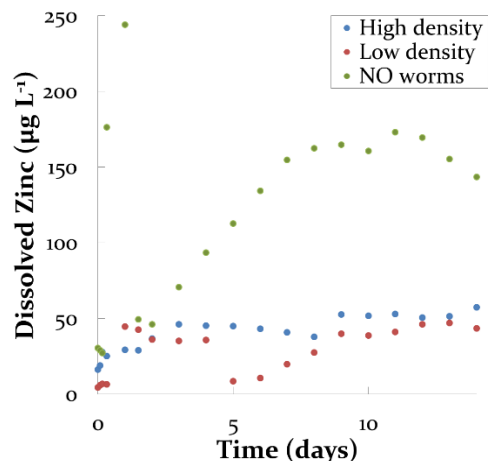


Figure 6. Dissolved Zn ($\mu\text{g L}^{-1}$) for the bioturbation only experiment \pm standard error ($n = 2; 3$).

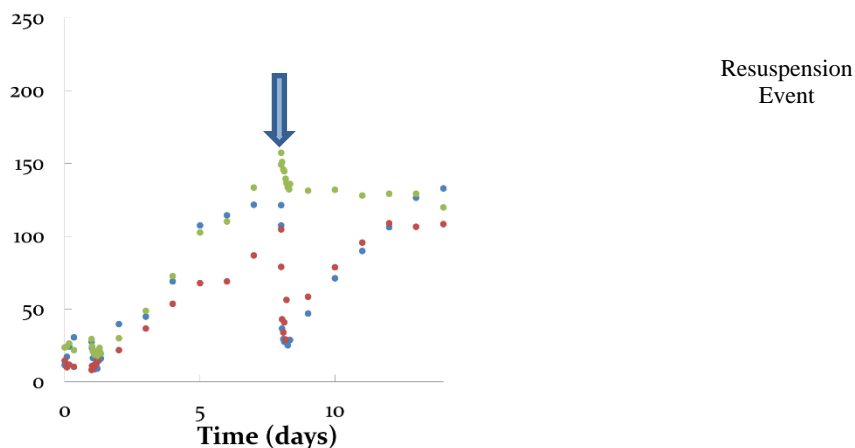


Figure 7. Dissolved Zn ($\mu\text{g L}^{-1}$) for the resuspension experiment \pm standard error ($n = 2; 3$).

bioturbation increased abundance of particulate Mn binding ligands as shown in Figure 7. Resuspension of metals increased both particulate Fe and Mn ligands in Gust chambers illustrated by Figure 8.

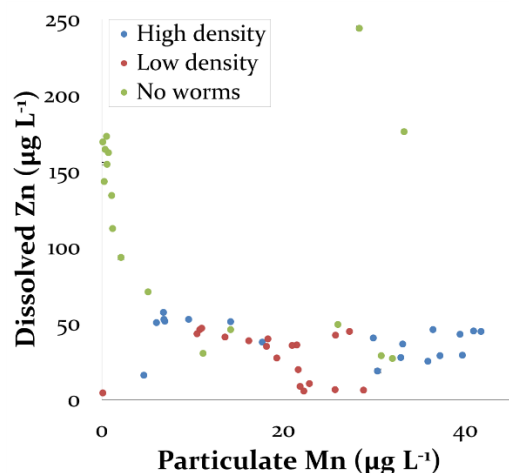


Figure 8. Dissolved Zn and particulate Mn ($\mu\text{g L}^{-1}$) for the bioturbation only experiment +/- standard error (n = 2; 3).

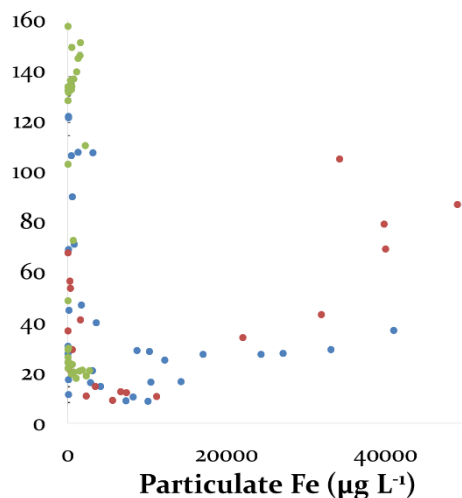


Figure 9. Dissolved Zn and particulate Fe ($\mu\text{g L}^{-1}$) for the resuspension experiment +/- standard error (n = 2; 3).

SeFEC Organism Exposures

Survival of *H. azteca* and *D. magna* was measured following bedded sediment exposures in SeFEC chambers, 4-hour continuous, and 16-hour multiple resuspensions. All organism exposure scenarios contained control SeFECs and control bedded sediment exposures without sediment, in order to show that water turbulence from the SeFEC was not inhibiting survival of either species. Generally, bedded sediments observed higher overall survival of both species, though not statistically higher. Duck Lake sediments had greater survival than Idaho or Lake DePue, which was expected, as Duck Lake was the reference sediment and had the lowest metal concentrations of the three sediments.

The near 50% survival of *D. magna* in the resuspended Lake DePue sediments may be indicative of the high dissolved Zn concentrations present in the water column. These values were closest of all sediments to the acute toxicity value for Zn (Buchman 1999). Additionally increased turbidity could be a possible cause for decreased survival (Robinson 2010), as *D. magna* inhabit the water column and sediment particles can clog their gills.

Survival of *H. azteca* varied across sediment types. The most striking result was the zero survival in the Lake DePue bedded sediments. This is the only occurrence in which bedded sediments were more toxic than resuspended. The bedded sediment is potentially higher in metal concentrations and lower in DO than the resuspension conditions of the SeFEC chamber. *H. azteca* primarily reside in the sediment, unlike *D. magna*, who inhabit that water column primarily. This would explain the approximate 70% survival of *D. magna* in the water column of the DePue bedded sediment.

Reproduction of *D. magna* was also quantified after resuspensions exposures. No differences were observed in reproduction (number of neonates produced per adult) between sediment types.

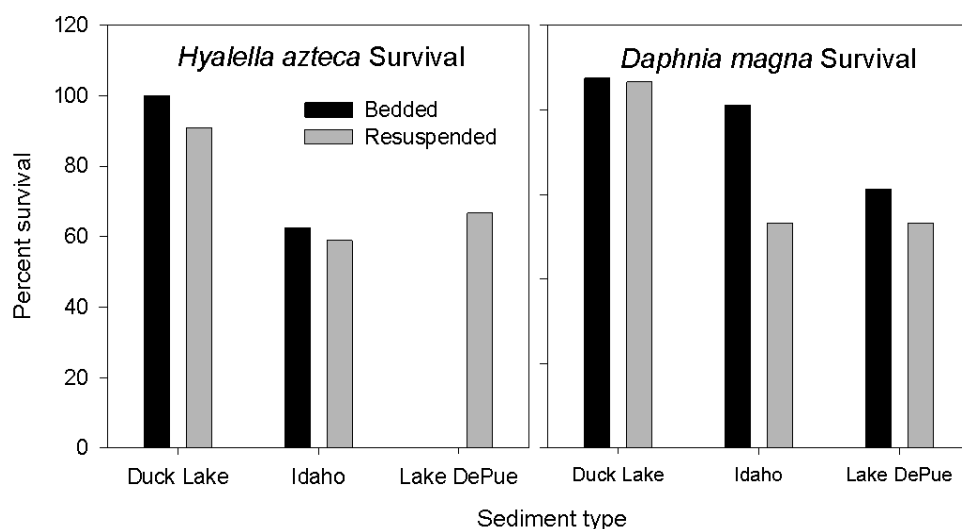


Figure 10. Survival of *H. azteca* and *D. magna* during exposures bedded sediments and to 4-hour resuspensions.

Qwik-lite testing revealed differences over time and among sediment types. Toxicity can range from one to ten, less than three is considered low toxicity and greater than seven is high toxicity. Lake DePue and Idaho sediments had relatively high elutriate toxicity values, while Duck Lake and San Diego had very low non-toxic values (Figure 11). The control was zero, as expected. Idaho sediment had the highest toxicity in both 4-hour continuous resuspensions and the 16-hour multiple resuspension scenarios (Figure 12). Both Idaho and Lake DePue sediments decreased in toxicity with each successive resuspension event. Duck Lake values were low and non-toxic in both 4-hour and 16-hour resuspensions, as was Lake DePue's 4-hour resuspension event. Both Lake DePue and Idaho sediments had the highest levels of Mn, and Lake DePue had near toxic concentration of Zn during the 4-hour resuspensions. These values may explain the higher toxicity observed in the Qwik-lite experiments.

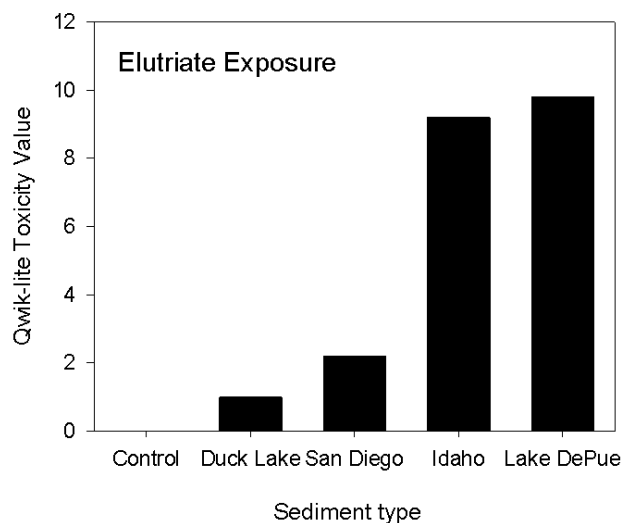


Figure 11. Qwik-lite toxicity values of elutriates compared to controls for each sediment type.

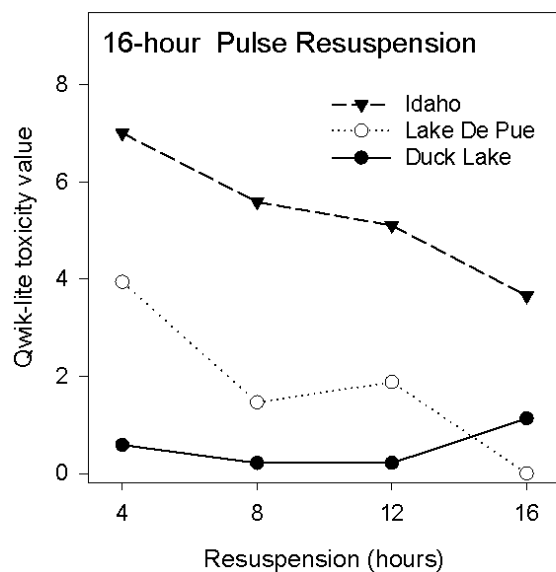


Figure 12. Qwik-lite toxicity of the dinoflagellate from exposure to the 16-hour multiple resuspension event.

Gust Chamber Organism Exposures

Based on Gust chamber exposure data with Lake DePue sediment, there was variable *H. azteca* survival outcomes dependent on treatment. High and low density *L. variegatus* exposures showed acute toxicity only during the combined bioturbation and resuspension events. The most acute toxic effects were observed when no worms were present. On day 14 in the “no worm” exposure, there was no *H. azteca* survival. In all experiments, control organism survival remained about 80% (Figure 13). Resuspension increased toxicity in all experiments. *H. azteca* survival and dissolved zinc were negatively correlated as the lowest survival rates in experiments

were where highest zinc concentrations were observed. Zinc concentrations in the bioturbation only no worms experiment were significantly higher than in the no worms resuspension experiment, yet resuspension survival rates are lowest as shown in Table 5. Other possible influences on toxicity may include other metals present, such as copper or nickel, particulate zinc concentrations, or bioturbation only experimental outliers. In general, decreased *H. azteca* survival was observed with resuspension events.

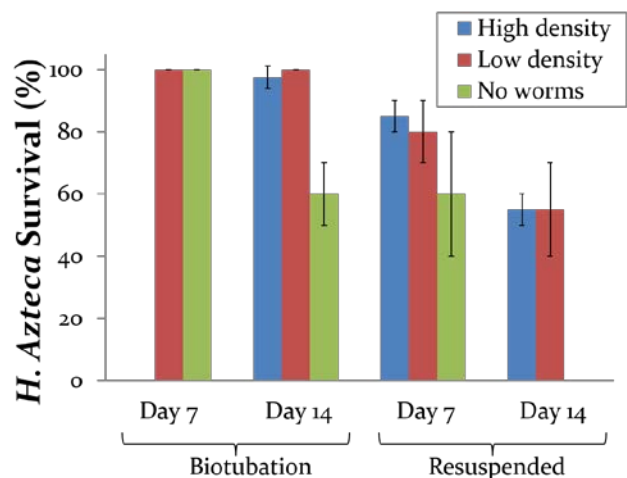


Figure 13. Survival data (%) of *H. azteca* calculated from two replicates (\pm calculated standard deviation) of Lake DePue sediment. No data collected for *high density* bioturbation experiment on day 7. *No worm* survival on day 14 of the resuspended experiment was 0%. Control remained above 80% survival in all experiments.

Table 5. Day 7 and 14 survival and maximum/average (n=19) zinc concentrations for each Gust experiment with Lake DePue sediment.

Experiment		Survival		Zinc ($\mu\text{g L}^{-1}$)	
		Day 7	Day 14	Maximum	Average
Resuspension	High density	85	55	133	69 ± 10
	Low density	80	55	109	57 ± 9
	No worms	60	0	157	83 ± 12
Bioturbation only	High density	NA	97.5	58	40 ± 3
	Low density	100	100	47	28 ± 4
	No worms	100	60	244	121 ± 14

Task 1b and 2b*: Develop and test Chemical Models for Metal Partitioning in Bedded and Resuspended Sediments

Chemical Model Development: Application to Laboratory Oxidation Studies

Kevin J. Farley, Richard F. Carbonaro, Paul M. McMahon and Patricia T. Heegle

Background

Bioavailability of metals in anoxic sediments has been shown to be limited by metal-sulfide precipitation and metal binding to organic matter and other sorbent phases (Di Toro et al. 1990, 1992, 1996). Resuspension of anoxic sediments by dredging and propeller-wash events however can result in rapid changes in redox chemistry with metals potentially being released in the overlying water (Eggleton and Thomas 2004). The effects of sediment resuspension on metal releases to the water column have largely been examined in laboratory oxidation studies (see Table A-8 for a summary of studies identified in our review of the literature). In general, these studies have been conducted by suspending 10-100 g L⁻¹ of sediments in oxygenated water and monitoring changes in dissolved metal concentrations and other water chemistry parameters over time.

Typical laboratory results are shown in Figure 14A-B for the oxidation of Clarence River sediment (Burton et al. 2009) and in Figure 14C-E for the oxidation of Tweed River sediment (Burton et al. 2006). For both sediments, Acid Volatile Sulfide (AVS) was rapidly oxidized abiotically within the first few hours to elemental sulfur, S₈(s), which remained stable for 20-30 hours (panels A and C). During this initial time period, pH remained relatively constant (panels B and D) and releases of Ni and Zn to the aqueous phase were small, possibly due to slow oxidation of NiS(s) and ZnS(s) and/or sorption of Ni and Zn on freshly-precipitated iron and manganese oxyhydroxides (panel E). After 20-30 hours, S₈(s) was oxidized to SO₄²⁻ via a microbially-mediated reaction. This resulted in severe acidification (pH < 4) and significant releases of Ni and Zn to the aqueous phase.

In order to better understand chemical responses during oxidation, a chemical equilibrium model was first developed to examine the initial speciation of metals in bedded sediments (Task 1b). Chemical equilibrium reactions that were included in the model include acid-base and complexation reactions in pore water, precipitation / dissolution of oxide and carbonate and sulfide solids, and sorption of major cations, anions and metals to hydrous ferric oxide (HFO). Results of this modeling effort were subsequently used in defining initial conditions for a time-

** This section includes the results for Task 1b (“Assess the Ability of Equilibrium Models to Accurately Predict Speciation in Sediments”) and Task 2b (“Develop a Chemical Equilibrium / Kinetic Model for Metal Partitioning During Resuspension”).*

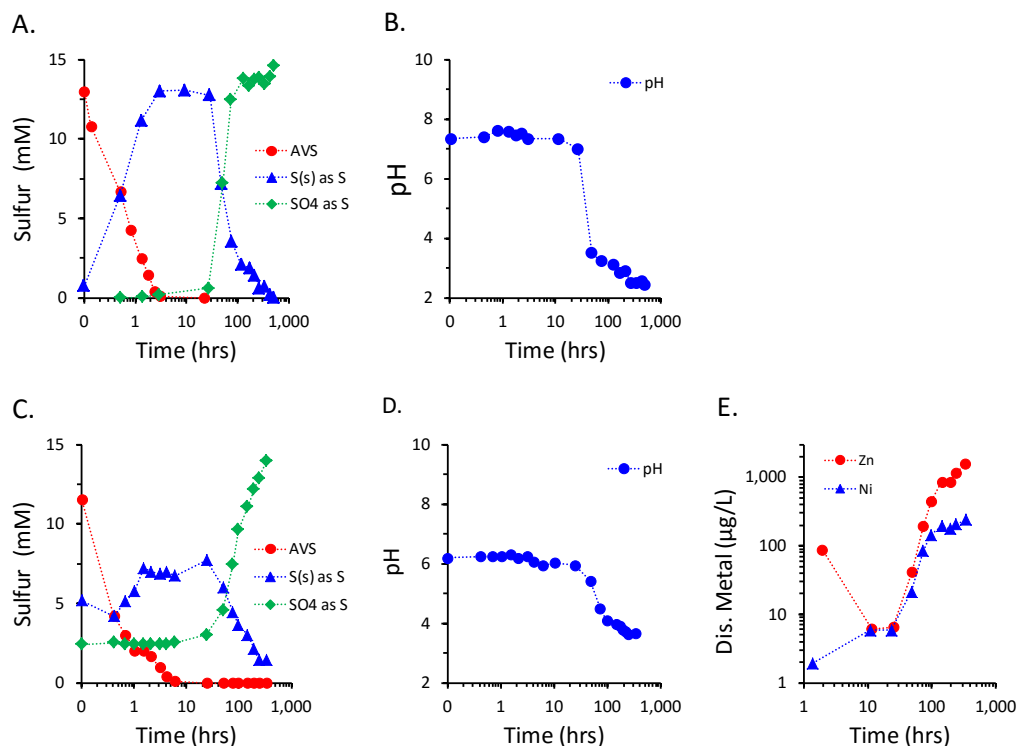


Figure 14. Laboratory results for (A) acid volatile sulfide (AVS), elemental sulfur [$S_8(s)$] as sulfur and sulfate (SO_4^{2-}) as sulfur, and (B) pH from the Clarence River sediment oxidation study (Burton et al. 2009), and (C) AVS, $S_8(s)$ as sulfur and SO_4 as sulfur, (D) pH and (E) dissolved Ni and dissolved Zn from the Tweed River sediment oxidation study (Burton et al. 2006).

variable, chemical equilibrium / kinetic model of chemical responses during the oxidation of sediment suspensions (Task 2b). Because sediment suspensions from propeller-wash events are expected to remain in the overlying water for periods of hours, development of the time-variable model focused on short-term chemical responses (e.g., 6-12 hours). Chemical processes that were considered to be important during this time period include abiotic oxidation of sulfide to elemental sulfur, oxidation of reduced iron and precipitation of hydrous iron oxyhydroxides (HFO), sorption of metals to freshly-precipitated HFO, acid-base and complexation reactions in the solution phase, and precipitation / dissolution of non-sulfide solids.

Description of the chemical equilibrium model for bedded sediments and the time-variable, chemical equilibrium / kinetic model for oxidation during sediment resuspension are presented below. This is followed by calibration and initial testing of the model using datasets that were previously reported in the literature. Datasets used in these evaluations included laboratory oxidation studies with sediments from the Clarence River (Burton et al. 2009), the Tweed River (Burton et al. 2006) and the Anacostia River (Hong et al. 2011). It is important to note that datasets used for model calibration and initial testing were all performed with sediment suspensions of 10-100 g L^{-1} , which are in excess of the suspended sediment concentrations of approximately 1 g L^{-1} that are typically observed during propeller wash.

Laboratory oxidation datasets that were conducted as part of this project with sediment suspensions of approximately 1 g L⁻¹ (see Task 1a) were subsequently considered as possible candidates for model validation. The Portsmouth Naval Station (PNS) sediment oxidation studies were ultimately selected for model validation based on the following: (i) the PNS dataset provided a relatively complete description of sediment geochemistry, (ii) metal concentrations in the PNS sediments were representative of contamination levels at DoD sites, and (iii) laboratory oxidation studies on the PNS sediments were performed with sediment suspensions that are typical of propeller wash events. Other laboratory studies that were reported under Task 1a were not used for model validation for the following reasons. First, the initial toxicity studies that were conducted for Duck Lake (Muskegon, MI), Idaho River bank (Blackbird Mine, IN) and San Diego Bay (San Diego, CA) did not contain sufficient geochemical information to define chemical model inputs (e.g., for pore water pH, alkalinity, sediment moisture content). Second, the Lake DePue laboratory studies, which did contain sufficient geochemical information to define chemical model inputs, were not used because the zinc contamination in the Lake DePue sediments was exceedingly high (and not representative of contamination levels at DoD sites).

Task 1b and 2b: Materials and Methods

Model Descriptions

Chemical Equilibrium Model for Bedded Sediment: The chemical equilibrium model for both bedded sediment was developed using the Tableau Input Coupled Kinetic Equilibrium Transport (TICKET) computational framework (Farley et al. 2008). All model calculations were performed in Microsoft Excel with the TICKET program code included as a Visual Basic for Applications (VBA) enabled macro. Model calculations for bedded sediment included acid-base chemistry and complexation reactions in pore water, precipitation / dissolution of oxide and carbonate and sulfide solids, and sorption of major cations, anions and metals to hydrous ferric oxide (HFO). Results of the chemical equilibrium modeling for bedded sediment were subsequently used in defining initial conditions for the time-variable chemical equilibrium / kinetic model simulations for chemical responses during the oxidation of resuspended sediment.

Time-Variable Model for Oxidation of Resuspended Sediment: The time-variable chemical equilibrium / kinetic model was also developed in the TICKET computational framework. The time-variable model was used to simulate the short-term (i.e., 6-12 hour) chemical responses that would occur during resuspension of anoxic sediments into oxygenated waters. Model computations were performed in Microsoft Excel with the TICKET program code included as a VBA embedded macro. In the model, FeS(s) is oxidized to Fe²⁺ and S₈(s) following second-order kinetics where the FeS(s) oxidation rate is a function of FeS(s) and dissolved oxygen concentrations (Di Toro et al. 1996) (see Eq. 1, Table 6). Other metal sulfides [MS(s)] are assumed to oxidize to M²⁺ and S₈(s) in similar fashion (see Eq. 2, Table 6).

In the oxidation reactions described above, Fe^{II} that is produced during the oxidation of FeS(s) can subsequently be oxidized to Fe³⁺. The rate of this reaction has been shown to be highly dependent on pH (Stumm and Lee 1961; Singer and Stumm 1970; Milero 1985; Milero et al. 1987), and has been described by three species-dependent oxidation reactions for Fe²⁺, FeOH⁺ and Fe(OH)₂^o (Stumm 1992). The Fe^{II} oxidation rate has also been shown to be enhanced when

Fe^{2+} is bound to hydroxo surface groups on HFO (e.g., as $\equiv FeO-Fe^{II}$) (Wehrli et al. 1989; Wehrli 1990; Luther 1990). A total of four reactions are therefore used in the model to describe Fe^{2+} oxidation (see Eq. 3-6, Table 6).

Table 6: Kinetically-controlled Redox Reactions in the Chemical Model

<u>FeS(s) and MeS(s) Oxidation Reactions based on Di Toro (1996)</u>	
$FeS(s) + \frac{1}{2}O_2 + 2H^+ \rightarrow Fe^{2+} + \frac{1}{8}S_8^o(s) + H_2O \quad (1)$ $rate = k_{FeS} [FeS(s)][O_2]$	
$MS(s) + \frac{1}{2}O_2 + 2H^+ \rightarrow M^{2+} + \frac{1}{8}S_8^o(s) + H_2O \quad (2)$ $rate = k_{MeS} [MeS(s)][O_2]$	
Rate coefficients (k_{FeS} , k_{MS}) are determined from model calibration.	
<u>Species-dependent Reactions for Fe^{II} Oxidation (Stumm 1992)</u>	
$Fe^{2+} + H^+ + \frac{1}{4}O_2 \rightarrow Fe^{3+} + \frac{1}{2}H_2O \quad (3)$ $rate = k_o [Fe^{2+}][O_2]$	
$FeOH^+ + 2H^+ + \frac{1}{4}O_2 \rightarrow Fe^{3+} + \frac{3}{2}H_2O \quad (4)$ $rate = k_1 [FeOH^+][O_2]$	
$Fe(OH)_2^o + 3H^+ + \frac{1}{4}O_2 \rightarrow Fe^{3+} + \frac{5}{2}H_2O \quad (5)$ $rate = k_2 [Fe(OH)_2^o][O_2]$	
$\equiv FeO-Fe^{II} + 2H^+ + \frac{1}{4}O_2 \rightarrow \equiv FeOH^o + Fe^{3+} + \frac{1}{2}H_2O \quad (6)$ $rate = k_3 [\equiv FeO-Fe^{II}][O_2]$	
Rate coefficients (k_o , k_1 , k_2 , k_3) are taken directly from Stumm (1992) and are given as: $\log k_o = -5.1$, $\log k_1 = 1.4$, $\log k_2 = 6.9$, and $\log k_3 = 0.7$.	

The kinetic reactions described above for FeS(s), MS(s) and Fe^{II} oxidation are linked to the pH, dissolved O_2 , Fe^{3+} , HFO and other chemical constituents in the sediment-water mixture. To account for these factors, acid-base chemistry, solution complexation, dissolution/precipitation of non-sulfur solids and sorption of major cations, anions and metals to HFO are also included in the time-variable model. All of these reactions are considered to be fast (relative to the oxidation reactions) and are therefore described by chemical equilibrium relationships. For laboratory

evaluations, the model is applied to a single well-mixed cell. Transport of chemicals into or out of the cell is limited to kinetically-controlled gas transfer of O₂, CO₂ and H₂S at the air-water interface.

The final time-variable model considers approximately 40 chemical components, approximately 150 chemical species and 8-10 non-linear kinetic reactions in a single model cell. This requires the solution of approximately 40 mole balance equations and 110 chemical equilibrium relationships. These equations are solved in TICKET using a fully-implicit time solution with simultaneous solution of the mole balance and equilibrium relationships at each time step using a Newton-Raphson iteration technique (see Farley et al. 2008 for details). Additional reactions for metal binding to natural organic matter (NOM) are not included in TICKET model applications because the inclusion of metal binding to NOM using reactions specified in the Windermere Humic Aqueous Model Version 7 (WHAM7) would have added an additional 100 chemical components and approximately 400 chemical species to time-variable model calculations. This exclusion of NOM from the model is justified in most cases because HFO appeared to be the dominant sorbing phase for the laboratory oxidation studies. However, the effects of metal binding to NOM will be considered later under Task 3b as part of our development of a simplified chemical sub-model for incorporation in multi-dimensional contaminant transport models.

Model Parameterization

Chemical equilibrium constants are well-documented in the literature and in several databases. For acid-base and solution complexation reactions, equilibrium constants were taken from the MINTEQA2 database (Allison et al. 1991). Solubility products (K_{sp} values) for equilibrium solid phases that are considered in model calculations were obtained from several sources and are given in Table 7. Equilibrium sorption of major cations, anions and metals to HFO were described using the surface complexation model and binding coefficients of Dzombak and Morel (1990). These equilibrium constants were used both in the chemical equilibrium model for bedded sediment and in the time-variable chemical equilibrium / kinetic model for the oxidation of resuspended sediment.

In addition to chemical equilibrium constants, the time-variable chemical equilibrium / kinetic model for resuspended sediment also required the specification of kinetic rate coefficients and transport processes. A compilation of second-order rate coefficients for FeS(s) and MS(s) oxidation were obtained from the literature (see Table 8). Based on this compilation, FeS(s) is expected to be oxidized rapidly with second-order rate coefficient on the order of 1000 M⁻¹ hr⁻¹. In comparison, MS(s) oxidation rate coefficients are typically one to two orders of magnitude slower than the FeS(s) oxidation rates. Variations in the reported FeS(s) and MS(s) oxidation rate coefficients however are noted. In particular, Vanthuyne and Maes (2006) reported MS(s) oxidation rates that are an order of magnitude higher than other reported values. Because of reported variations in oxidation rates, second-order oxidation rate coefficients for FeS(s) and MS(s) were considered as calibration parameters in fitting the laboratory oxidation datasets.

Table 7: Solubility Products for Precipitation/Dissolution Reactions Considered in Chemical Equilibrium Calculations for Initial Conditions.

Reaction	log K _{sp}	Reference
FeS(mackinawite) + H ⁺ → Fe ²⁺ + HS ⁻ + H ⁺	-3.6	MINTEQA2 ^a
FeCO ₃ (siderite) + 2H ⁺ → Fe ²⁺ + H ₂ CO ₃	6.44	MINTEQA2 ^a
FeOOH(ferrihydrite) + 3H ⁺ → Fe ³⁺ + 2H ₂ O	3.19	MINTEQA2 ^a
Al(OH) ₃ (amorphous) + 3H ⁺ → Al ³⁺ + 3H ₂ O	10.8	MINTEQA2 ^a
CaCO ₃ (calcite) + 2H ⁺ → Ca ²⁺ + H ₂ CO ₃	8.20	MINTEQA2 ^a
CaMg(CO ₃) ₂ (dolomite) + 2H ⁺ → Ca ²⁺ + Mg ²⁺ + 2H ₂ CO ₃	16.27	MINTEQA2 ^a
MnCO ₃ (rhodochrosite) + 2H ⁺ → Mn ²⁺ + H ₂ CO ₃	4.17	Jensen et al. (2002)
NiS(hexagonal) + H ⁺ → Ni ²⁺ + HS ⁻	-9.68	Wilken and Rogers (2010)
MnS(green) + H ⁺ → Mn ²⁺ + HS ⁻	0.17	MINTEQA2 ^a
ZnS(amorphous) + H ⁺ → Ni ²⁺ + HS ⁻	-9.05	MINTEQA2 ^a
S ₈ (rhombic) → 8S ⁰ (aq)	-6.68	Wang and Tessier (2009)
^a For information on MINTEQA2 database, see Allison et al. (1991).		

Table 8: Second-order Oxidation Rate Coefficients (M⁻¹ hr⁻¹) from Previous Modeling Studies.

		Fe	Cd	Cu	Ni	Pb	Zn
Carbonaro et al. (2005)	spiked sediment core	4133	11		133	40	13
Choi et al. (2006)	in-place sediment	34					34
Vanthuyne and Maes (2006) ^a	sediment suspension	148		180		597	195
Canavan et al. (2007)	sediment core						11
Hong et al. (2011)	sediment suspension	4125					25
^a Second-order oxidation rate coefficients were calculated using average rates from corrected oxidation rates for four sediment and assuming saturated dissolved oxygen concentrations of 9.09 mg/L (corresponding to the reported temperature of 20°C).							

In addition to the FeS(s) and MS(s) oxidation reactions, the species-dependent reactions for Fe^{II} oxidation were described by second-order kinetics (see Eqs. 3-6, Table 6). The second-order rate coefficients for the oxidation of Fe²⁺, FeOH⁺, and Fe(OH)₂⁰ were taken directly from the literature and are as given as: $k_0 = 7.9 \times 10^{-6} \text{ M}^{-1} \text{ s}^{-1}$; $k_1 = 25 \text{ M}^{-1} \text{ s}^{-1}$; $k_2 = 7.9 \times 10^6 \text{ M}^{-1} \text{ s}^{-1}$; $k_3 = 5.0 \text{ M}^{-1} \text{ s}^{-1}$ (Stumm 1992). The second-order rate coefficient for the oxidation of Fe²⁺ bound to HFO ($\equiv\text{FeO-Fe}^{\text{II}}$) was also taken from the literature and is as given as: $k_3 = 5.0 \text{ M}^{-1} \text{ s}^{-1}$ (Wehrli 1990; Stumm 1992).

The interfacial gas transfer rate coefficient for O₂, CO₂ and H₂S was also required for evaluating the laboratory oxidation studies. For the Clarence River (Burton et al. 2009) and the Tweed River (Burton et al. 2006), the gas transfer rate coefficient was set to a high value to simulate the continuous bubbling of air and near saturated oxygen concentrations in the laboratory oxidation chambers. This approach was also used in setting the gas transfer rate coefficient for the Portsmouth Naval Station (Fetters 2013) model validation studies. For the Anacostia River study (Hong et al. 2011), the gas transfer rate coefficient was adjusted downward to match model results to observed concentrations of dissolved oxygen that were measured during the laboratory oxidation study.

Chemical Equilibrium Model Calculations for Bedded Sediments

The chemical equilibrium model calculations for bedded sediment were performed as follows. For the Clarence River (Burton et al. 2009), the Tweed River (Burton et al. 2006) and the Portsmouth Naval Station (Fetters 2013) studies, chemical model calculations were performed for the bedded sediment and porewater system assuming that all chemical phases including FeS(s) and MS(s) were in equilibrium with the porewater. For this calculation, total concentrations of metals (including iron), major cations and major anions were determined from measured sediment and porewater concentrations. pH was set based on the measured pH of the porewater. An initial Fe^{II}:Fe^{III} distribution in the sediment was assumed, subject to the constraint that a sufficient amount of Fe^{II} would be available for the formation of siderite, FeCO₃(s), in the sediment. The partial pressure of CO₂ in the porewater was then adjusted to match measured porewater Fe^{II} concentration (based on equilibrium with siderite). Results from this model calculation provided an accounting of concentrations of FeS(s), MS(s), non-sulfidic Fe^{II} [total Fe^{II} minus FeS(s)], non-sulfidic metal [total M minus MS(s)], total (dissolved plus particulate) carbonate, HFO surface sites, and total alkalinity or acid neutralizing capacity for the bedded sediment–porewater.

Time-Variable Model Calculations for Oxidation of Resuspended Sediments

Time-variable chemical equilibrium / kinetic model simulations for the oxidation of resuspended sediments required a complete characterization of initial chemical conditions in the laboratory oxidation chamber. This includes initial concentrations of FeS(s) and MS(s), as well as total (dissolved plus particulate) concentrations of Fe^{II} in non-sulfidic forms, Fe^{III} (which is present primarily in oxyhydroxides), other metals (e.g., Al, Mn), major cations (e.g., Ca²⁺, Mg²⁺, Na⁺), major anions (e.g., Cl⁻, SO₄²⁻), carbonate and total alkalinity. Since a complete characterization of initial chemical conditions is difficult to determine from measurements alone, the following methods were used in specifying initial conditions for time-variable simulations.

For the Clarence River (Burton et al. 2009), the Tweed River (Burton et al. 2006) and the Portsmouth Naval Station (Fetters 2013) studies, bedded sediment – porewater model results and the reported chemistry of the resuspension water were used in a conservative mixing calculation to determine the initial chemical characterization of the resuspension mixture. As a check of the assumed $\text{Fe}^{\text{II}}:\text{Fe}^{\text{III}}$ distribution given above, a chemical equilibrium model calculation was performed for the resuspension mixture by assuming that only the non-sulfidic phases would be in equilibrium with the resuspension water at the beginning of the oxidation study. The computed pH of the mixture was then compared to the initial pH measurement of the mixture. If the computed pH do not match the initial pH measurement of the mixture, the initial $\text{Fe}^{\text{II}}:\text{Fe}^{\text{III}}$ distribution in the sediment was adjusted and the calculation was repeated.

For the Anacostia River study (Hong et al. 2011), porewater pH was not reported. Initial chemical conditions were therefore determined as follows. First, total (dissolved plus particulate) concentrations of iron, metals, major cations and major anions in the resuspension mixture were determined from a conservative mixing calculation using measured chemical concentrations of the sediment, porewater and resuspension water. Since the reported AVS was greater than the simultaneously extracted metal (SEM), concentrations of low solubility metal sulfides, MS(s) , were set equal to their total metal concentrations. This approach avoided complications of incomplete extraction of metal sulfides in the standard AVS extraction. Following the approach of Carbonaro et al. (2005), the FeS(s) concentration was set equal to the AVS minus the MS(s) concentrations. The total concentration of the non-sulfidic Fe^{II} was determined by subtracting FeS(s) from the total iron concentration. A chemical equilibrium model calculation was then performed for a fixed pH of 6.1 based on an initial measurement of pH in the resuspended sediment mixture. The partial pressure of CO_2 and the initial $\text{Fe}^{\text{II}} : \text{Fe}^{\text{III}}$ distribution in the resuspended sediment mixture were adjusted to match measured concentrations of initial HCO_3^- and dissolved Fe^{II} concentration. Results of the chemical equilibrium model calculations for the non-sulfidic phases were then used to determine the total (dissolved plus particulate) carbonate, total alkalinity or acid neutralizing capacity, and HFO surface site concentrations for the resuspended sediment mixture.

Using chemical equilibrium constants, kinetic rate coefficients and initial conditions described above, time-variable chemical equilibrium / kinetic model simulations were performed in TICKET for time simulations of 4-12 hours using a time step of 0.001 hours. Model simulations for the Clarence River (Burton et al. 2009) were used in calibrating the second-order oxidation rate coefficient for FeS(s) (k_{FeS}). Model simulations for the Anacostia River (Hong et al. 2011) were used in calibrating the gas transfer rate coefficient for oxygen and the second-order oxidation rates for ZnS(s) (k_{ZnS}). Finally, model simulations for the PNS sediments (Fetters et al. 2006) were used for model validation.

Task 1b and 2b: Results and Discussion

Model Calibration and Initial Testing

As described above, the chemical equilibrium model for bedded sediment utilizes information from the MINTEQA2 database (Allison et al. 1991) and the literature (see Table 7) in specifying

chemical equilibrium constants for acid-base, solution complexation and precipitation/dissolution reactions. In addition to the chemical equilibrium constants that were obtained from the MINTEQA2 database and the literature (see Table 7), the time-variable chemical equilibrium / kinetic model for oxidation of resuspended sediment required specification of several kinetic and transport rate coefficients. For this purpose, the second-order reaction rate coefficients for Fe^{II} oxidation were taken directly from the literature (Stumm 1992). The remaining coefficients for the oxidation of FeS(s) , the oxidation of MS(s) and the gas transfer coefficient (which describes the transfer of O_2 , CO_2 and H_2S across the air-water interface) were determined through model calibration and testing using laboratory oxidation datasets for the Clarence River (Burton et al. 2009), the Tweed River (Burton et al. 2006), and the Anacostia River (Hong et al. 2011). Chemical equilibrium model results for bedded sediments and time-variable chemical equilibrium / kinetic model results for the oxidation of resuspended sediments are described for the three datasets below.

Clarence River: Initial calibration of the model was performed using laboratory data for the oxidation of 12.6 g L^{-1} of Clarence River floodplain sediment in 0.1 M NaCl (Burton et al. 2009). Measured chemical concentrations for the bedded sediment and the pore water are given in Table A-9. These values were first used in a chemical equilibrium model calculation to determine a more complete chemical characterization of the bedded sediment and pore water. This was accomplished by assuming an 80:20 distribution of $\text{Fe}^{\text{II}}:\text{Fe}^{\text{III}}$ in the sediment and setting the partial pressure of CO_2 in the pore water to $1.11 \times 10^{-3} \text{ atm}$ to match the measured dissolved Fe^{II} concentration of 0.55 mM in the pore water. The chemical equilibrium model results for bedded sediment were consistent with powder x-ray diffraction (XRD) results indicating the presence of siderite in the sediment (Table A-10).

Chemical equilibrium results from the bedded sediments were then used in determining the initial chemical composition of the resuspended sediment mixture. In this calculation, mackinawite [FeS(s)] and elemental sulfur [$\text{S}_8\text{(s)}$] were considered to be present as non-equilibrium (i.e. kinetically-controlled) solid phases. Total H^+ , Total Fe(2+) and Total HS(-) concentrations were apportioned accordingly between phases considered to be in equilibrium (e.g., $\text{FeCO}_3\text{(s)}$) and non-equilibrium phases (e.g., FeS(s) , $\text{S}_8\text{(s)}$). Total concentrations of equilibrium and non-equilibrium phases in the initial resuspension mixture were then determined from a conservative mixing calculation of the sediment-pore water and 0.1 NaCl resuspension water (Table A-11). As a check of the assumed $\text{Fe}^{\text{II}}:\text{Fe}^{\text{III}}$ distribution given above, total concentrations for equilibrium phases in the initial resuspension mixture were used in a chemical equilibrium calculation. The computed pH of the mixture was determined to be 7.65. Although the assumed $\text{Fe}^{\text{II}}:\text{Fe}^{\text{III}}$ distribution could be adjusted downward (e.g., to a 40:60 distribution) to obtain closer agreement of the computed pH and the initial pH measurement of 7.39, this would have resulted in a lower concentration of siderite in the computed mixture. Since siderite ultimately provided acid buffering capacity in maintaining pH at approximately 7.5 throughout the first 3-4 hours in the time-variable model simulation (see below), the 80:20 $\text{Fe}^{\text{II}}:\text{Fe}^{\text{III}}$ distribution was retained in model calculations.

Total concentrations of equilibrium phases and non-equilibrium solid phases (e.g. FeS(s) and $\text{S}_8\text{(s)}$) that were calculated above were used as initial chemical conditions for the time-variable model simulation (see Table 9). Since air was bubbled through the laboratory reactor at a high

Table 9: Initial Conditions for Time-variable Model Simulations for Oxidation of the Clarence River, Tweed River and Anacostia River Sediment Samples

Time-Variable Model Input ^a			
	<u>Clarence River</u>	<u>Tweed River</u>	<u>Anacostia River</u>
<u>Equilibrium Phases</u>			
Total H(+)	-8.10E-02	-4.15E-01	-3.09E-01
Total Al(3+)	--	6.17E-02	3.47E-02
Total Ca(2+)	--	5.74E-04	2.13E-02
Total Cl(-)	1.00E-01	1.53E-02	2.52E-03
Total H ₂ CO ₃	2.52E-02	2.11E-03	2.15E-03
Total Cu(2+)	--	--	--
Total Fe(2+)	2.63E-02	5.27E-03	2.04E-04
Total Fe(3+)	9.82E-03	7.64E-02	6.92E-02
Total K(+)	--	3.01E-04	5.12E-05
Total Mg(2+)	--	2.07E-03	6.36E-03
Total Mn(2+)	--	1.96E-04	3.32E-04
Total Na(+)	1.00E-01	1.39E-02	2.30E-03
Total Ni(2+)	--	6.14E-07	--
Total SO ₄ (2-)	3.19E-04	5.98E-03	1.03E-03
Total HS(-)	1.07E-08	3.47E-07	1.00E-10
Total Zn(2+)	--	2.37E-06	1.00E-10
<u>Non-equilibrium Phases</u>			
FeS(s)	1.30E-02	1.15E-02	3.29E-03
CuS(s)	--	--	--
NiS(s)	--	1.36E-05	--
ZnS(s)	--	6.20E-05	8.13E-04
S ₈ (0) as S	7.55E-04	5.95E-03	--
<u>Boundary Concentrations</u>			
O ₂ (sat) ^b	2.84E-04	2.84E-04	2.49E-04
H ₂ CO ₃ (sat)	1.00E-05	1.00E-05	1.00E-05
^a All concentrations are given in moles L ⁻¹ . See text and tables in the appendix for determination of initial conditions. ^b Initial O ₂ concentration was set equal to the O ₂ saturation values for the Clarence River and Tweed River model simulations. Initial O ₂ concentration for the Anacostia River model simulation was set equal to 9.5E-06 M based on the reported measurement.			

rate of 200 L hr^{-1} , a high gas exchange rate coefficient of 20 m hr^{-1} was specified to maintain dissolved oxygen concentrations in the laboratory chamber at saturated or near saturated concentrations of $2.84 \times 10^{-4} \text{ M}$ (corresponding to freshwater with a temperature of 20°C). The remaining coefficient for the second-order oxidation of FeS(s) was initially set to $4100 \text{ M}^{-1} \text{ hr}^{-1}$ (based on Carbonaro et al. 2005). This value was subsequently adjusted to $5000 \text{ M}^{-1} \text{ hr}^{-1}$ (an increase of approximately 20%) to obtain a better fit to the measured AVS and $\text{S}_8\text{(s)}$ -S data.

Time-variable model responses for AVS and $\text{S}_8\text{(s)}$ agreed very well with experimental observations and showed AVS [as represented by FeS(s)] being oxidized to $\text{S}_8\text{(s)}$ within 1-2 hours (Figure 15A). The pH model response was also consistent with experimental measurements and showed an immediate small increase followed by a slight decrease in pH during the simulation period (Figure 15B). The lack of a large change in pH is attributed to two factors. First, H^+ consumption during the FeS(s) oxidation reaction and the subsequent oxidation of Fe^{II} to Fe^{III} (see Reactions 1 and 3 in Table 6) was largely offset by the acid production during the hydrolysis of Fe^{III} and subsequent precipitation of FeOOH(s) . Second, smaller amounts of H^+ that was generated as Fe^{II} initially present in the dissolved and sorbed phases was oxidized to Fe^{III} and precipitated as FeOOH(s) were neutralized by the dissolution of $\text{FeCO}_3\text{(s)}$ during the first few hours.

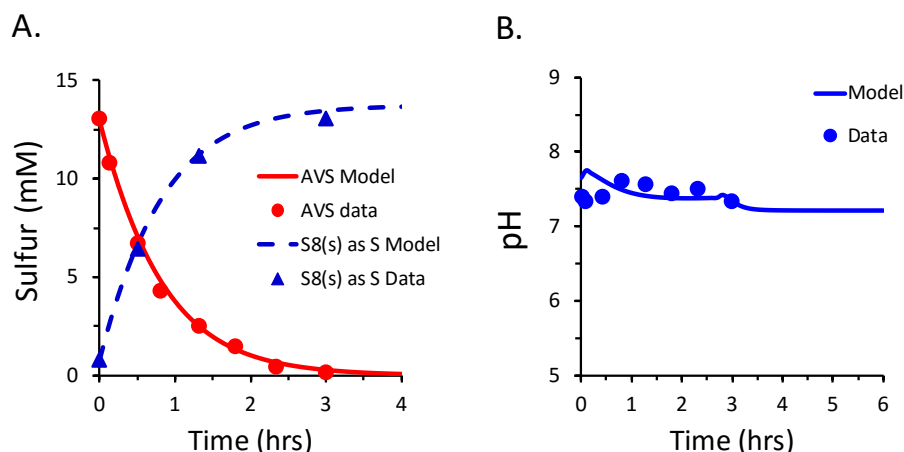


Figure 15: Model-data comparisons for the Clarence River sediment oxidation study: (A) acid volatile sulfide (AVS) and elemental sulfur [$\text{S}_8\text{(s)}$] as sulfur, and (B) pH as a function of time. Data from Burton et al. (2009).

Tweed River: Model calibration and testing for the oxidation of approximately 50 g L^{-1} of Tweed River floodplain sediment in acid-sulfate drainwater from the site (Burton et al. 2006) followed a similar procedure. Measured chemical concentrations for the bedded sediment and the pore water (Table A-12) were again used in a chemical equilibrium model calculation to determine a more complete chemical characterization of the bedded sediment. This was accomplished by assuming a 18:82 $\text{Fe}^{\text{II}}:\text{Fe}^{\text{III}}$ distribution in the sediment and adjusting the partial pressure of CO_2 in the pore water to 0.075 atm to match measured pore water Fe concentration of 1.47 mM (Table A-13). Based on the computed chemical equilibrium model results, solid phases in the sediment included mackinawite [FeS(s)], nickel sulfide [NiS(s)], amorphous zinc sulfide

[ZnS(s)], elemental sulfur [S₈(s)], amorphous aluminum hydroxide [Al(OH)₃(s)], ferrihydrite [FeOOH(s)], and rhodochrosite [MnCO₃(s)]). In addition to the dissolved Fe²⁺ concentration, the model computed dissolved Mn²⁺ concentration was very close to the measured pore water Mn concentration. Measured pore water concentrations for Ni and Zn were under-predicted by the model. A possible explanation for this discrepancy is the presence of colloidal HFO or DOC-bound metal in the pore water. Since the measured pore water Ni and Zn concentrations were very low and represented less than 0.2% of the total Ni and Zn in the sediment, this discrepancy did not appear to have any effect on the time-variable model calculations as described below.

The chemical equilibrium model results from bedded sediments were used in determining the initial chemical composition of the resuspended sediment mixture. In this calculation, FeS(s), NiS(s), ZnS(s) and S₈(s) were considered as non-equilibrium solid phases. Based on this assumption, concentrations of Total H⁺, Total Fe(2+), Total Ni(2+), Total Zn(2+) and Total HS(-) from the sediment-pore water calculation were apportioned into equilibrium phases and non-equilibrium phases. Total concentrations of equilibrium and non-equilibrium phases in the initial resuspension mixture were then determined from a conservative mixing calculation of the sediment-pore water and acid-sulfate drainwater (Table A-14). As a check on the assumed Fe^{II}:Fe^{III} distribution given above, total concentrations for equilibrium phases in the initial resuspension mixture were used as input in a chemical equilibrium calculation. This resulted in a computed pH of 6.21 which was equal to the measured value. The computed H₂CO₃ activity was 10^{-2.98} M which indicates that the mixture was supersaturated with respect to CO₂. In addition to the non-equilibrium solid phases, amorphous aluminum hydroxide [Al(OH)₃(s)], ferrihydrite [FeOOH(s)] and rhodochrosite [MnCO₃(s)] were determined to be present as equilibrium solid phases in the resuspension mixture. Finally, the computed dissolved Mn²⁺, Ni²⁺ and Zn²⁺ were all within a factor of two of measured pore water concentrations. However, the dissolved Fe²⁺ concentration was four times higher than the measured pore water Fe concentration, which may indicate some oxidation of Fe²⁺ during the laboratory preparation of the resuspension mixture.

Total concentrations of equilibrium phases and non-equilibrium solid phases [FeS(s), NiS(s), ZnS(s) and S₈(s)] in the computed resuspension mixture were used as initial conditions in a time-variable model simulation (see Table 9). A high gas exchange rate coefficient of 20 m hr⁻¹ was again specified to maintain dissolved oxygen concentrations in the laboratory chamber at saturated or near saturated concentrations of 2.84 × 10⁻⁴ M (corresponding to freshwater with a temperature of 20°C). The second-order oxidation rate coefficient for FeS(s) was specified as 5000 M⁻¹ hr⁻¹ based on the previous model calibration for the Clarence River sediment oxidation study. The remaining coefficients for the second-order oxidation of NiS(s) and ZnS(s) were initially set to 133 M⁻¹ hr⁻¹ and 13 M⁻¹ hr⁻¹ respectively (based on Carbonaro et al. 2005). The second-order oxidation coefficients were subsequently adjusted to 20 M⁻¹ hr⁻¹ for NiS(s) and 16 M⁻¹ hr⁻¹ ZnS(s) to obtain a better fit to the limited measurements for dissolved Ni and Zn concentrations.

The time-variable model results, which again described a rapid decrease in FeS(s) concentration, are consistent with measured AVS concentrations (Figure 16A). The computed results for elemental sulfur [S₈(s) as S] showed a corresponding increase in concentration with the oxidation of FeS(s). The computed S₈(s)-S results however were not consistent with the S₈(s)-S measurements. The S₈(s)-S measurements for this dataset, which were obtained using a

modified chromium-reducible sulfur method for reduced inorganic sulfur (Sullivan et al. 2000), were considered questionable because they did not provide a closed mass balance for total sulfur in the oxidation chamber. The computed pH corresponded closely with measured values and remained relatively constant at a pH of approximately 6.1 during oxidation (Figure 16B). This was in large part attributed to acid consumption during the oxidation of FeS(s) and the subsequent oxidation of the released Fe^{II} to Fe^{III} being offset by acid generation during the precipitation of Fe^{III} to FeOOH(s) . In addition, some acid buffering capacity was also provided by the protonation of $-\text{OH}$ surface groups on HFO.

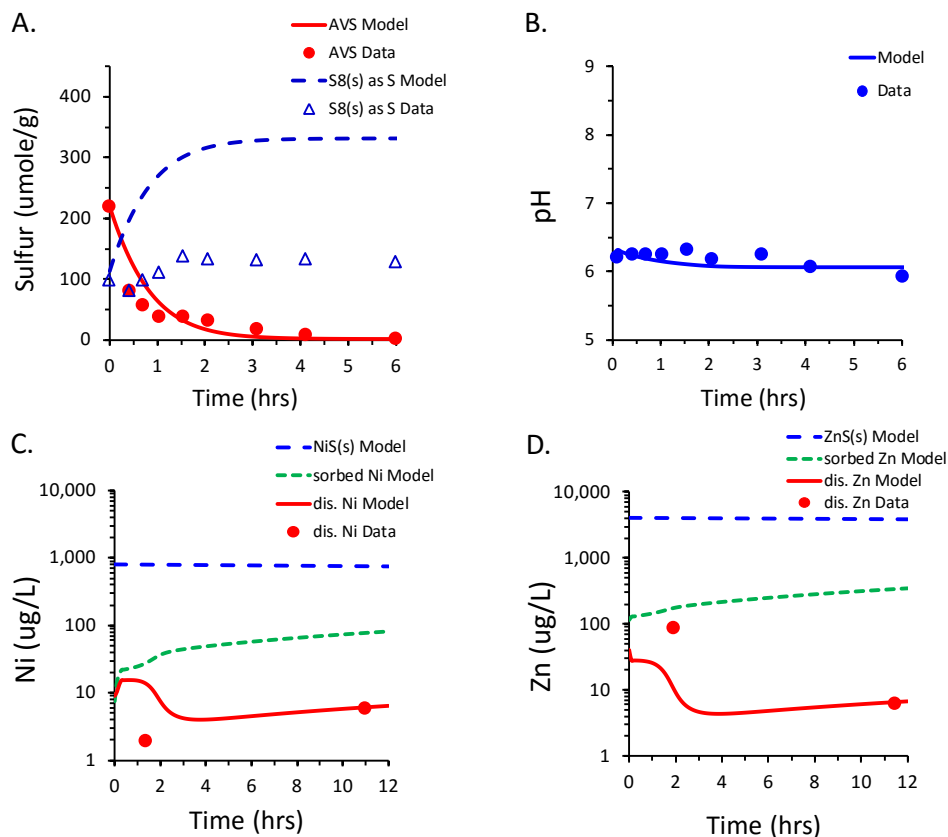


Figure 16: Model-data comparisons for the Tweed River sediment oxidation study: (A) acid volatile sulfide (AVS) and elemental sulfur [$\text{S}_8(\text{s})$] as sulfur, (B) pH, (C) NiS(s) , sorbed Ni and dissolved Ni, and (D) ZnS(s) , sorbed Zn and dissolved Zn as a function of time. Open triangles in panel B represent questionable elemental sulfur [$\text{S}_8(\text{s})$] data (see text). Data from Burton et al. (2006).

The time-variable model results for Ni and Zn showed that $52 \mu\text{g L}^{-1}$ of NiS(s) and $212 \mu\text{g L}^{-1}$ ZnS(s) were oxidized and released into solution during the first twelve hours of the study (Figure 16C-D). However, a large portion of the released Ni and Zn was adsorbed onto freshly precipitated ferrihydrite (which formed after the rapid oxidation of FeS(s) and the subsequent oxidation of Fe^{2+} to Fe^{3+}). As a result, concentrations of released metal that remained in the dissolved phase was relatively low (i.e., $5\text{--}10 \mu\text{g L}^{-1}$) after twelve hours of oxidation.

Anacostia River: Model calibration and testing were also performed for laboratory oxidation results with approximately 75 g L⁻¹ of Anacostia River sediment in artificial river water (Hong et al. 2011). Measured chemical concentrations for the Anacostia River bedded sediment and pore water are given in Table A-15. Since the porewater pH was not reported, a chemical equilibrium model calculation for the bedded sediment was not performed. Instead, total chemical concentrations in the resuspension mixture were determined directly from a conservative mixing calculation of measured concentrations of total (dissolved plus particulate) iron, metals, major cations and major anions in the bedded sediment, pore water and resuspension water (Table A-16). In this calculation, all of the Zn and a portion of the Fe^{II} in the bedded sediment was considered to be present in a non-equilibrium phase as ZnS(s) and FeS(s), where the sum of ZnS(s) and FeS(s) was equated to the measured AVS concentration.

The computed chemical concentrations in the resuspension mixture were then used in a chemical equilibrium calculation to determine the total acidity/alkalinity, total carbonate and equilibrium solid phases that were initially present in the resuspension mixture (Table A-16). For the calculation, the pH was set at 6.1 (based on an initial measurement of pH in the resuspension mixture); the partial pressure of CO₂ was set to 0.032 atm (to match the measured HCO₃⁻ concentration in the mixture); and the initial Fe^{II} : Fe^{III} distribution of the mixture was set to 4.8:95.2 (to match the measured dissolved Fe^{II} concentration of 0.0138 mM). The results show a computed H₂CO₃ activity of 10^{-2.99} M which indicates that the mixture was supersaturated with respect to CO₂. In addition to the non-equilibrium solid phases, amorphous aluminum hydroxide [Al(OH)₃(s)], ferrihydrite [FeOOH(s)] and rhodochrosite [MnCO₃(s)] were also determined to be present as equilibrium solid phases in the resuspension mixture.

Computed concentrations of equilibrium phases and non-equilibrium solid phases [FeS(s) and ZnS(s)] in the resuspension mixture were used as initial conditions in a time-variable model simulation (see Table 10). A gas exchange rate coefficient of 1.2 m hr⁻¹ and a dissolved oxygen saturation concentration of 2.49 × 10⁻⁴ M (corresponding to freshwater with a temperature of 27°C) were determined by calibrating the model to measured dissolved oxygen concentrations in the laboratory chamber (Figure 17A). The second-order oxidation rate coefficient for FeS(s) was specified as 5000 M⁻¹ hr⁻¹ based on the previous model calibration for the Clarence River and Tweed River sediment oxidation studies. The rate coefficient for ZnS(s) oxidation was initially set to 16 M⁻¹ hr⁻¹ based on the previous result for the Tweed River. Since no zinc was measured in the dissolved phase, the second-order rate coefficient for ZnS(s) was adjusted downward to a value of 5 M⁻¹ hr⁻¹ to match the dissolved Zn detection limit at 6 hours. Therefore, this value represents an upper bound on the rate coefficient for Anacostia River sediment.

The time-variable model results for the AVS concentration (represented by the sum of the FeS(s) and ZnS(s) concentrations) compared very well to the AVS measurements (Figure 17B). For the Anacostia River sediment oxidation study, the decrease in AVS was computed to be somewhat slower than AVS decreases for the Clarence and Tweed River studies. This was due to the slower gas exchange rate (which resulted in dissolved oxygen concentrations that were significantly below saturation during the first few hours in the Anacostia study). The corresponding results for pH showed only a slight increase followed by a leveling-off of pH during the simulation period (Figure 17C). The initial rise in pH was attributed to the outgassing of excess CO₂ and the concomitant dissolution of MnCO₃(s) that occurred during the first hour.

The subsequent leveling-off of pH at approximately 6.4 was again largely attributed to acid consumption during the oxidation of FeS(s) and the subsequent oxidation of the released Fe^{II} to Fe^{III} being largely offset by acid generation during the precipitation of Fe^{III} as FeOOH(s). In addition, acid buffering in the mixture was provided by the dissolution of rhodochrosite [MnCO₃(s)] and the protonation of –OH surface groups on HFO.

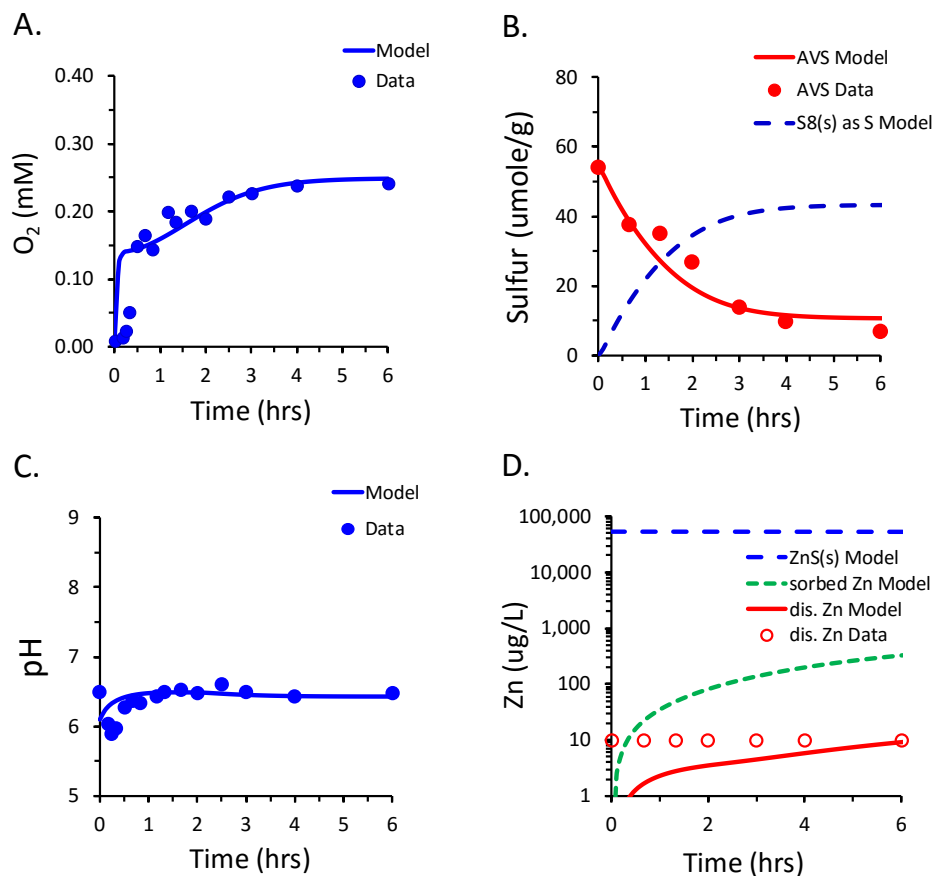


Figure 17: Model-data comparisons for the Anacostia River sediment oxidation study: (A) dissolved oxygen, (B) acid volatile sulfide (AVS) and elemental sulfur [$S_8(s)$] as sulfur, (C) pH, and (D) $ZnS(s)$, sorbed Zn and dissolved Zn as a function of time. Open circles in panel D represent the detection limit for non-detectable measurements. Data from Hong et al. (2011).

Finally, model results for Zn showed that 335 $\mu\text{g L}^{-1}$ of $ZnS(s)$ was oxidized and released into solution during the first six hours of the study (Figure 17D). As in the case of the Tweed River sediment study, a large portion of the released Zn was adsorbed onto freshly precipitated ferrihydrite (which was formed after FeS(s) oxidation and the subsequent oxidation of Fe^{II} to Fe^{III}). In addition to Zn sorption to freshly-precipitated ferrihydrite, a significant amount of Zn may have also sorbed onto particulate organic carbon (POC) which was present at high concentration in the Anacostia River sediment. Neglecting Zn sorption to POC in the chemical model may have resulted in an underestimation in the second-order rate coefficient of $ZnS(s)$ oxidation. Although we were not able to include a full WHAM calculation for metal binding to POC in the detailed chemical model, the effects of metal sorption to particulate

organic carbon will be addressed in developing a simplified version of the chemical submodel (see Task 3b of the report).

Model Validation

Up to this point, model calculations have been performed using laboratory oxidation studies with 10 - 100 g L⁻¹ of sediment suspended in freshwater. Suspended sediment concentrations associated with propeller-wash events however are expected to be 1 g L⁻¹ or less. As part of this project, detailed geochemical laboratory oxidation studies were conducted with suspended sediment concentration of approximately 0.5 g L⁻¹ with a freshwater sediment sample from Lake DePue, IL and a two marine sediment samples from the Portsmouth Naval Station (PNS), NH (see Task 1a and Fetters 2013). The Lake DePue sediment oxidation study was not considered for model validation because the sediment contained extremely high concentrations of Zn that were not representative of metal contamination at DoD sites. Model validation of the PNS sediment samples is provided below.

Portsmouth Naval Station: Measured chemical concentrations for the bedded sediment and the pore water for the two sediment samples (MS03 and MS04) from the PNS are given in Tables A-17 and A-18, respectively. Chemical equilibrium model calculations for bedded sediments were performed for both sediment samples to test the bedded sediment model and to provide a more complete chemical characterization of the sediments. This was accomplished by adjusting the partial pressure of CO₂ in the pore water to 1.20 × 10⁻² atm for the MS03 sediment and 1.06 × 10⁻² atm for the MS04 sediment to match measured pore water concentrations of dissolved Fe^{II}. Since the measured data were not sufficient to determine the distribution of Fe^{II} and Fe^{III} in the sediments, a 50:50 Fe^{II}:Fe^{III} distribution was assumed for both sediment samples.

Chemical equilibrium model results for the bedded PNS sediments showed that computed dissolved concentrations of Mn²⁺, Ni²⁺ and Zn²⁺ for the MS03 sample (Table A-19) were less than the measured pore water Mn, Ni and Zn concentrations. Based on previous results for the Tweed River, this is an expected result due to the possible presence of colloidal HFO or DOC-bound metal in the pore water. The MS-03 modeling results is in contrast with computed dissolved Ni²⁺ and Zn²⁺ concentrations for the MS04 sample (Table A-20) which showed computed dissolved metal concentrations that were greater than the measured pore water concentrations. Since the MS04 sample contained more total recoverable metal (given as the summation of Cu, Ni and Zn) than AVS, this result is likely due to the use of the more rigorous total recoverable extraction procedure for metals with the less rigorous AVS extraction procedure that was used in determining the sulfide concentration. (Sensitivity model calculations using the less rigorous Simultaneously Extracted Metal measurements will be presented below.) Finally, solid phases that were computed to be present in both sediment included copper sulfide [CuS(s)], nickel sulfide [NiS(s)], and amorphous zinc sulfide [ZnS(s)], siderite [FeCO₃(s)], ferrihydrite [FeOOH(s)] and rhodochrosite [MnCO₃(s)] (see Tables A-19 for the MS03 and A-20 for the MS04 bedded sediment-porewater results). Due to the lower AVS concentration in the MS04 sample, mackinawite [FeS(s)] was only determined to be present in the MS03 sediment sample.

Computed results from the bedded sediments were used in determining the initial chemical composition of the resuspended sediment mixture. In this calculation, FeS(s), CuS(s), NiS(s), and ZnS(s) were considered as non-equilibrium solid phases. Based on this assumption, concentrations of Total H⁺, Total Fe(2+), Total Cu(2+), Total Ni(2+), Total Zn(2+) and Total HS(-) from the sediment-pore water calculation were apportioned into equilibrium phases and non-equilibrium phases. Total concentrations of equilibrium and non-equilibrium phases in the initial resuspension mixture were then determined from a conservative mixing calculation of the sediment-pore water and 31 ppt of artificial seawater (see Table A-21 for MS03 sediment and Table A-22 for the MS04 sediment samples). As a check, total concentrations for equilibrium phases in the initial resuspension mixture were used in a chemical equilibrium calculation. This resulted in a computed pH of 7.46 and a computed H₂CO₃ activity was 10^{-4.07} M for both the MS03 and MS04 resuspension mixtures. In addition to the non-equilibrium solid phases, ferrihydrite [FeOOH(s)], calcite [CaCO₃(s)] and rhodochrosite [MnCO₃(s)] were also present as equilibrium solid phases in the resuspension mixture.

Total concentrations of equilibrium phases and non-equilibrium solid phases [FeS(s), CuS(s), NiS(s) and ZnS(s)] in the resuspension mixture were used as initial conditions in the time-variable model simulations (see Table 11). A high gas exchange rate coefficient of 20 m hr⁻¹ was again specified to maintain dissolved oxygen concentrations in the laboratory chamber at saturated or near saturated concentrations of 2.16 × 10⁻⁴ M (corresponding to measured salinity of 31 ppt and a measured temperature of 24°C). The second-order oxidation rate coefficient for FeS(s) was again specified as 5000 M⁻¹ hr⁻¹ based on the previous model results for the Clarence River, Tweed River and Anacostia River sediment oxidation studies. The remaining coefficients for the second-order oxidation of CuS(s), NiS(s) and ZnS(s) were initially set to approximately 20 M⁻¹ hr⁻¹ (based on previous results for the Tweed River sediment oxidation study).

In the time-variable model simulation for the MS03 sediment sample, it was necessary to adjust the second-order oxidation rate coefficient for NiS(s) to 700 M⁻¹ hr⁻¹ to match measurements of the dissolved nickel concentration. Because dissolved copper and zinc were typically reported below detection limits, the second-order oxidation rate coefficient for CuS(s) was set at 700 M⁻¹ hr⁻¹ [based on the calibrated rate coefficient for NiS(s)] and the ZnS(s) rate coefficient was set to a maximum rate of 75 M⁻¹ hr⁻¹ (to match the dissolved Zn detection limit at four hours). In the time-variable model simulation for the M04 sediment sample, it was necessary to adjust the second-order oxidation rate coefficient for NiS(s) to 250 M⁻¹ hr⁻¹ to match measurements of the dissolved nickel concentration. The second-order oxidation rate coefficient for CuS(s) was again set equal to the calibrated rate coefficient for NiS(s). The ZnS(s) rate coefficient was set at 15 M⁻¹ hr⁻¹ based on previous results for the Tweed River oxidation study.

Final model results for the MS03 and MS04 sediment samples are shown in Figures 18 and 19, respectively. For both sediment samples, dissolved oxygen concentrations were computed to remain at or near saturation throughout the model simulations (Figure 18A, 19A). Measured dissolved oxygen concentrations showed small decreases (ca. 1 mg L⁻¹) during the four hours of oxidation. Since AVS concentrations (as expressed on a mole L⁻¹ basis) were low in both suspended sediment mixtures, the observed decreases in dissolved oxygen (ca. 1 mg L⁻¹) were likely the result of microbial oxidation of sediment organic matter (Figure 18B, 19B). Computed pH values also remained relatively constant after an initial increase in pH that was associated

Table 10: Initial Conditions for Time-variable Model Simulations for Oxidation of the Portsmouth Naval Station Sediment Samples (MS03, MS04).

Time-Variable Model Input ^a				
	<u>Using Total Recoverable Metal</u>		<u>Using SEM Measurements</u>	
	<u>PNS: MS03</u>	<u>PNS: MS04</u>	<u>PNS: MS03</u>	<u>PNS: MS04</u>
<u>Equilibrium Phases</u>				
Total H(+)	-2.88E-03	-2.57E-03	-2.18E-03	-2.13E-03
Total Al(3+)	--	--	--	--
Total Ca(2+)	9.04E-03	9.04E-03	9.04E-03	9.04E-03
Total Cl(-)	4.83E-01	4.83E-01	4.83E-01	4.83E-01
Total H ₂ CO ₃	2.23E-03	2.17E-03	2.09E-03	2.09E-03
Total Cu(2+)	5.83E-20	8.41E-18	5.74E-20	4.71E-20
Total Fe(2+)	1.64E-04	1.00E-04	1.77E-05	1.06E-05
Total Fe(3+)	1.65E-04	1.00E-04	2.48E-05	1.34E-05
Total K(+)	9.04E-03	9.04E-03	9.04E-03	9.04E-03
Total Mg(2+)	4.70E-02	4.70E-02	4.70E-02	4.70E-02
Total Mn(2+)	3.03E-06	2.63E-06	3.68E-07	2.91E-07
Total Na(+)	4.15E-01	4.15E-01	4.15E-01	4.15E-01
Total Ni(2+)	3.46E-12	3.19E-08	6.99E-13	4.81E-13
Total SO ₄ (2-)	2.50E-02	2.50E-02	2.50E-02	2.50E-02
Total HS(-)	7.25E-10	4.45E-14	7.25E-10	6.61E-10
Total Zn(2+)	5.26E-11	4.49E-07	1.12E-11	7.74E-12
<u>Non-equilibrium Phases</u>				
FeS(s)	8.08E-07	5.43E-28	7.18E-06	2.85E-06
CuS(s)	4.53E-06	2.87E-06	4.07E-07	4.30E-07
NiS(s)	5.88E-07	3.77E-07	1.71E-07	1.07E-07
ZnS(s)	4.08E-06	1.26E-06	2.24E-06	1.11E-06
S ₈ (0) as S	--	--	--	--
<u>Boundary Concentrations</u>				
O ₂ (sat) ^b	2.16E-04	2.16E-04	2.16E-04	2.16E-04
H ₂ CO ₃ (sat)	1.23E-05	1.23E-05	1.23E-05	1.23E-05
^a All concentrations are given in moles L ⁻¹ . See text and tables in the appendix for determination of initial conditions. ^b Initial O ₂ concentration was set equal to the O ₂ saturation values for all Portsmouth Naval Station model simulations.				

with the outgassing of excess CO₂ from the resuspension mixtures (Figure 18C, 19C). Although CuS(s), NiS(s), and to a lesser extent, ZnS(s) were oxidized during the study, metal sorption onto freshly-precipitated ferrihydrite was effective in minimizing Cu, Ni and Zn concentrations the dissolved phase (Figure 18D,E,F, 19D,E,F).

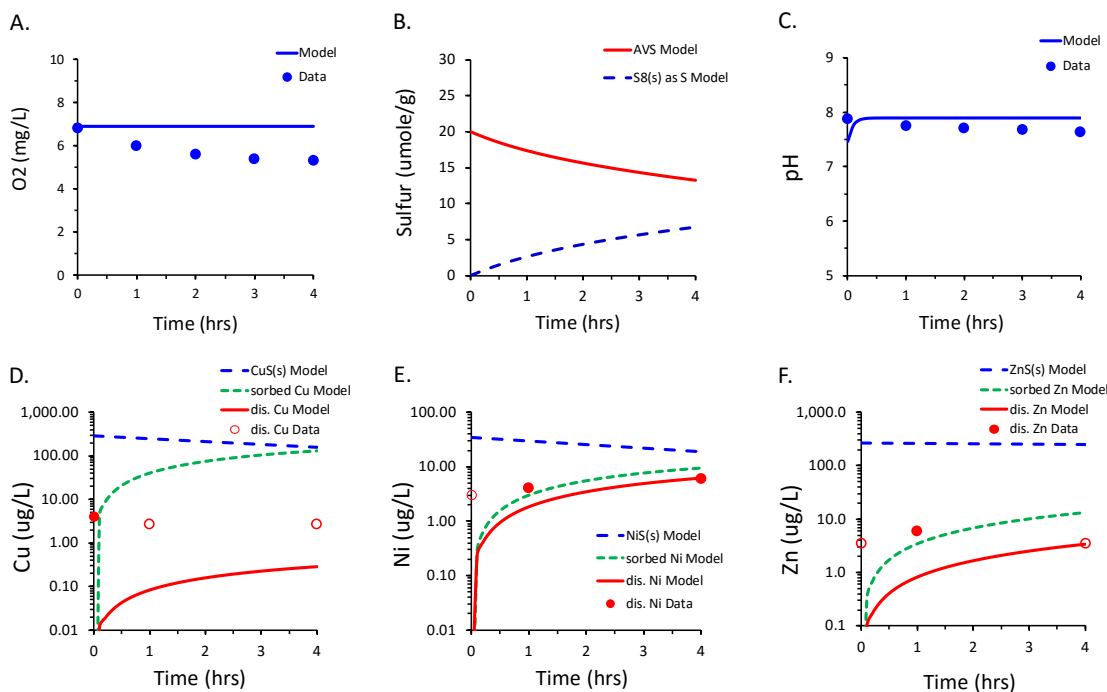


Figure 18: Model-data comparisons for the Portsmouth Naval Station MS03 sediment oxidation study based on total recoverable iron and total recoverable metal: (A) dissolved oxygen, (B) acid volatile sulfide (AVS) and elemental sulfur [S₈(s)] as sulfur, (C) pH, (D) CuS(s), sorbed Cu and dissolved Cu, (E) NiS(s), sorbed Ni and dissolved Ni, and (F) ZnS(s), sorbed Zn and dissolved Zn as a function of time. Open circles in panels D, E and F represent the detection limit for non-detectable measurements. Data from Fetters (2013).

Model Sensitivity Calculations

All model validation calculations presented above for the PNS sediments were performed using total recoverable iron and total recoverable metal concentrations. For the PNS oxidation study, simultaneously extracted metal (SEM) concentrations for iron and other metals were also reported (see Tables A-17 and A-18). Model sensitivity calculations were therefore performed for the PNS sediment samples using SEM concentrations in place of the total recoverable iron/metal concentrations. Chemical equilibrium model calculations for the bedded sediments were performed to again test the bedded sediment model and to determine a complete chemical characterization of the bedded sediments (Tables A-23 and A-24). Overall results for the SEM sensitivity model calculations for bedded sediments were similar to results previously presented with three exceptions. First, concentrations of Fe, Cu, Ni and Zn were 10% to 60% lower for the SEM sensitivity model calculations. Second, model-computed dissolved Mn²⁺, Ni²⁺ and Zn²⁺ were less than the measured pore water metal concentrations for both the MS03 and MS04 sediment samples. Third, since SEM was greater than AVS for the MS03 and MS04 samples,

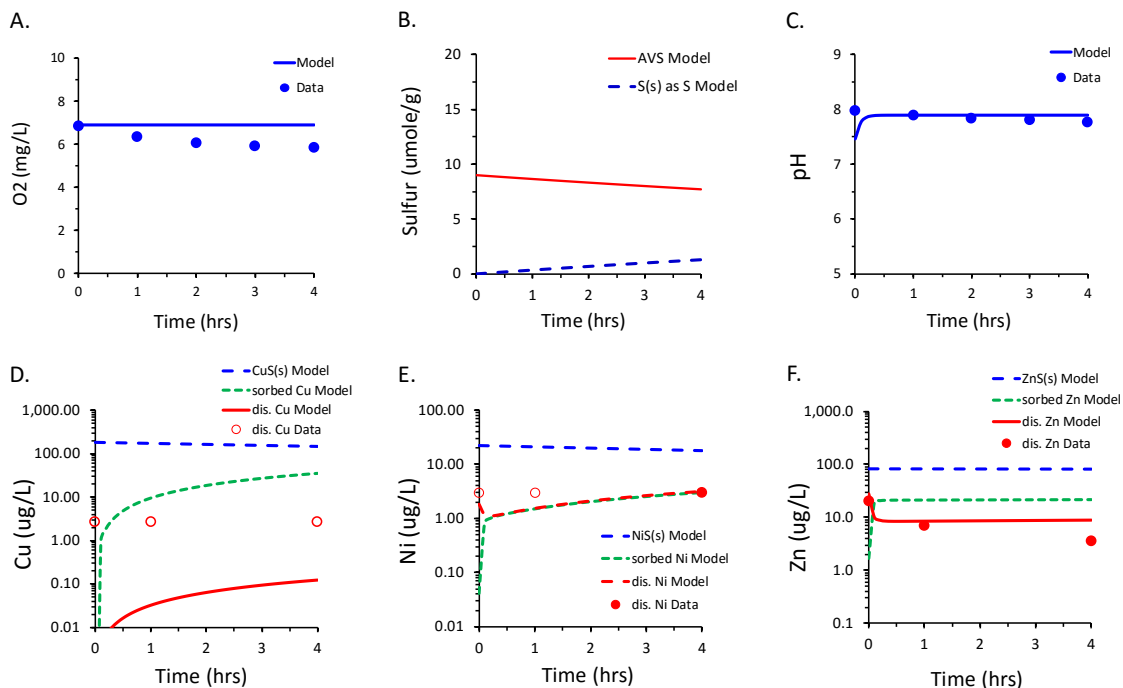


Figure 19: Model-data comparisons for the Portsmouth Naval Station MS04 sediment oxidation study based on total recoverable iron and total recoverable metal: (A) dissolved oxygen, (B) acid volatile sulfide (AVS) and elemental sulfur [$S_8(s)$] as sulfur, (C) pH, (D) $CuS(s)$, sorbed Cu and dissolved Cu, (E) $NiS(s)$, sorbed Ni and dissolved Ni, and (F) $ZnS(s)$, sorbed Zn and dissolved Zn as a function of time. Open circles in panels D and E represent the detection limit for non-detectable measurements. Data from Fetters (2013).

mackinawite [$FeS(s)$] was computed to be present in both sediments. Computed dissolved metal concentrations in the initial resuspension mixtures (Tables A-25 and A-26) were also approximately equal to or less than the initial measured dissolved concentrations.

Total concentrations of equilibrium phases and non-equilibrium solid phases [$FeS(s)$, $CuS(s)$, $NiS(s)$ and $ZnS(s)$] that were computed for bedded sediments were used as initial conditions for the time-variable model simulation and are listed in Table 10. The gas exchange rate coefficient was again set at 20 m hr^{-1} , and the dissolved oxygen saturation concentration was again set at $2.16 \times 10^{-4} \text{ M}$ (corresponding to a measured salinity of 31 ppt and a measured temperature of 24°C). The second-order oxidation rate coefficient for $FeS(s)$ was again specified as $5000 \text{ M}^{-1} \text{ hr}^{-1}$ and the remaining oxidation rate coefficients were determined through model calibration. For the MS03 sediment sample, it was necessary to adjust the second-order oxidation rate coefficient for $NiS(s)$ to $1400 \text{ M}^{-1} \text{ hr}^{-1}$ to match measurements of the dissolved nickel concentration. Because dissolved copper and zinc were typically reported below detection limits, the second-order oxidation rate coefficient for $CuS(s)$ was set at $1400 \text{ M}^{-1} \text{ hr}^{-1}$ [based on the calibrated rate coefficient for $NiS(s)$] and the $ZnS(s)$ rate coefficient was set to a maximum rate of $45 \text{ M}^{-1} \text{ hr}^{-1}$ (to match the dissolved Zn detection limit at four hours). For the MS04 sediment sample, it was necessary to adjust the second-order oxidation rate coefficient for $NiS(s)$ to $1000 \text{ M}^{-1} \text{ hr}^{-1}$ to match measurements of the dissolved nickel concentration. The second-order

oxidation rate coefficient for CuS(s) was again set equal to the calibrated rate coefficient for NiS(s). The ZnS(s) rate coefficient was set to a maximum of 80 M⁻¹ hr⁻¹ (to match the dissolved Zn detection limit at four hours).

Final model results for the SEM model sensitivity results are shown for the M03 and M04 sediment samples in Figures 20 and 21, respectively. Computed concentrations of dissolved Cu, Ni and Zn were again consistent with measurements. However, the calibrated oxidation rate coefficients for the SEM model sensitivity calculations were 2-4 times greater than the rate coefficients that were previously determined using total recoverable metal concentrations to specify initial conditions. These differences may be attributed to the fact that the total recoverable metal extraction provides an over-estimation of the reactive metal concentrations and this overestimation is compensated for by the use of lower oxidation rate coefficients in the model simulations.

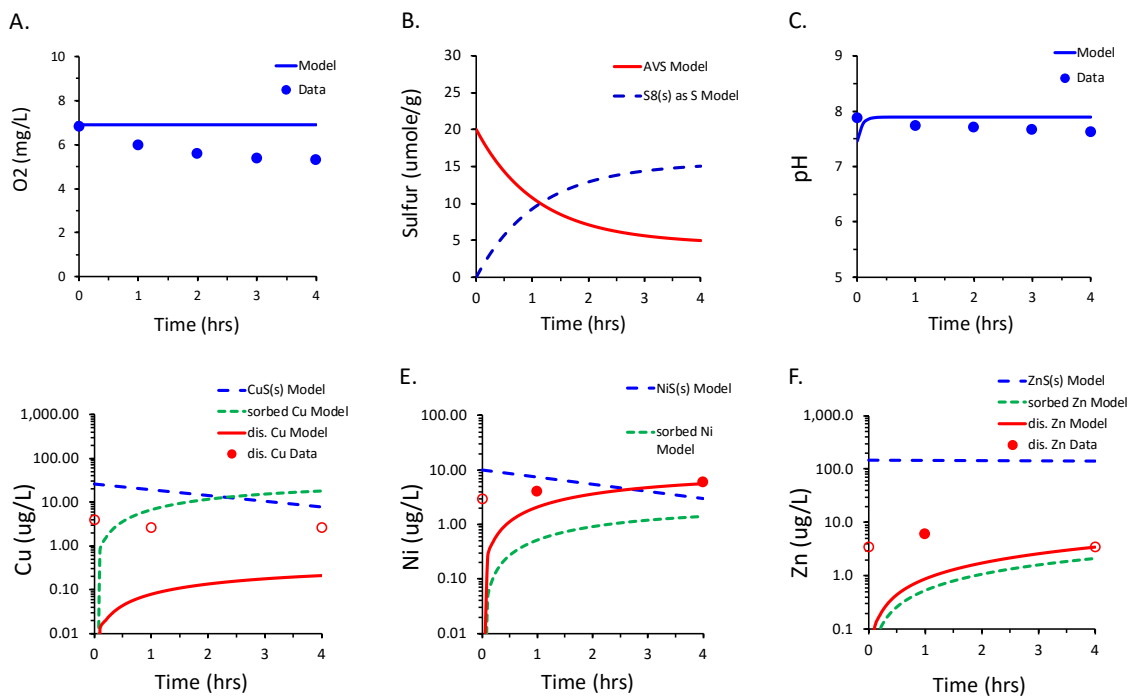


Figure 20: Model-data comparisons for the Portsmouth Naval Station MS03 sediment oxidation study based on simultaneously extracted iron and simultaneously extracted metal (SEM): (A) dissolved oxygen, (B) acid volatile sulfide (AVS) and elemental sulfur [S₈(s)] as sulfur, (C) pH, (D) CuS(s), sorbed Cu and dissolved Cu, (E) NiS(s), sorbed Ni and dissolved Ni, and (F) ZnS(s), sorbed Zn and dissolved Zn as a function of time. Open circles in panels D, E and F represent the detection limit for non-detectable measurements. Data from Fetters (2013).

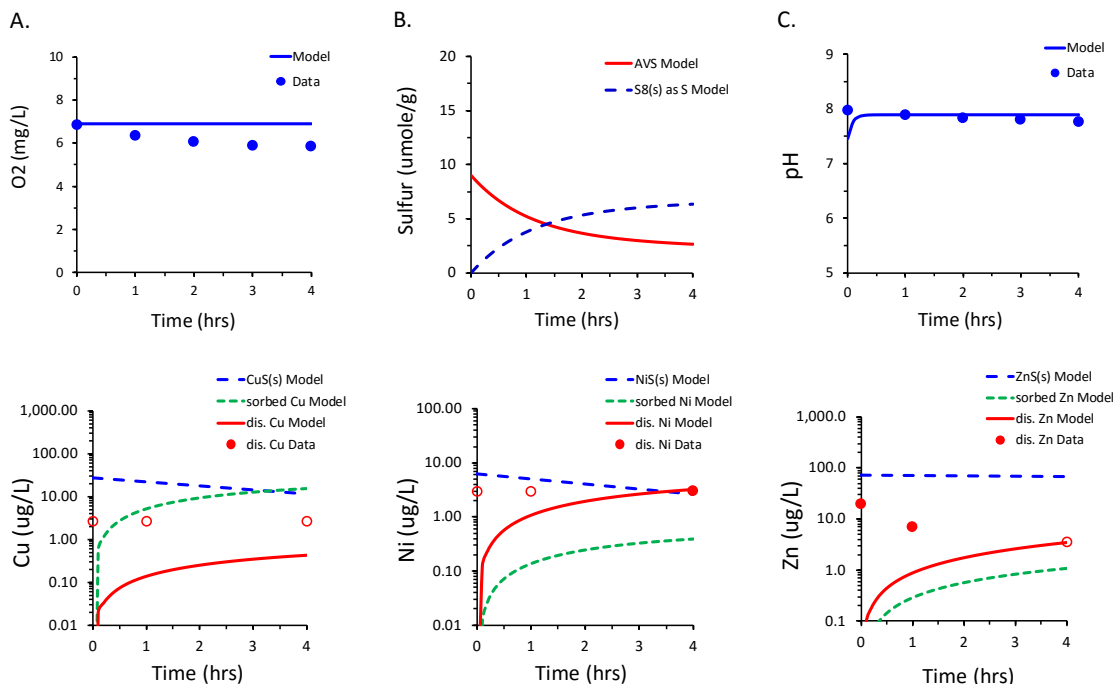


Figure 21: Model-data comparisons for the Portsmouth Naval Station MS04 sediment oxidation study based on simultaneously extracted iron and simultaneously extracted metal (SEM): (A) dissolved oxygen, (B) acid volatile sulfide (AVS) and elemental sulfur [$S_8(s)$] as sulfur, (C) pH, (D) $CuS(s)$, sorbed Cu and dissolved Cu, (E) $NiS(s)$, sorbed Ni and dissolved Ni, and (F) $ZnS(s)$, sorbed Zn and dissolved Zn as a function of time. Open circles in panels D, E and F represent the detection limit for non-detectable measurements. Data from Fetters (2013).

Summary

Chemical equilibrium model calculations for bedded sediments from the Clarence River and the Tweed River sediments provided a consistent description of iron and sulfur chemistry of anoxic sediments. Model coefficients that were used in the evaluations came in large part from the literature and included the chemical equilibrium constants for acid-base, solution complexation, precipitation and surface complexation reactions. For both the Clarence River and Tweed River sediment, Fe was present primarily in the solid phase as mackinawite [$FeS(s)$], siderite [$FeCO_3(s)$] and ferrihydrite [$FeOOH(s)$] with lower concentrations present as Fe sorbed to HFO and dissolved Fe^{2+} in the pore water. Measured porewater Ni and Zn concentrations were less than 0.2% of the total Ni and Zn sediment concentrations in the Tweed River sediment sample. Although model-computed dissolved concentrations of Ni^{2+} and Zn^{2+} concentrations were less than the measured porewater Ni and Zn concentrations, these underpredictions were likely due to the presence of metal bound to colloidal HFO or DOC in the porewater. Similar findings were also obtained to PNS MS03 sediment sample. However, in chemical equilibrium model calculations for PNS MS04, model-computed dissolved Ni^{2+} and Zn^{2+} concentrations were calculated to be higher than the measured porewater Ni and Zn concentrations when model calculations were based on total recoverable metal measurements. This issue (i.e., the overprediction of measured porewater metal concentrations) resolved itself when model

calculations were based on the less rigorous simultaneously extractable metal (SEM) measurements. It is therefore recommended to measure SEM concentrations in sediment characterizations.

Time-variable model simulations for the oxidation of resuspended sediments from the Clarence River, Tweed River and Anacostia River demonstrated the ability of the model to describe time responses for AVS, elemental sulfur [$S_8(s)$], pH and dissolved oxygen in laboratory oxidation studies. Model coefficients that were used in the evaluations came in large part from the literature. These included the chemical equilibrium constants for acid-base, solution complexation, precipitation and surface complexation reactions, as well as the four kinetic rate coefficients that were used to describe Fe^{II} oxidation. The remaining kinetic coefficient for $FeS(s)$ oxidation were determined through model calibration and was determined to be $5000\text{ M}^{-1}\text{ hr}^{-1}$ for the Clarence River, Tweed River and Anacostia River sediment oxidation studies. Based on the consistency of the $FeS(s)$ oxidation rate coefficient in three studies, a rate coefficient of $5000\text{ M}^{-1}\text{ hr}^{-1}$ was assumed for the PNS sediment samples. An independent check on the $FeS(s)$ oxidation rate coefficient for the PNS samples however could not be made because AVS measurements were not taken over the time course of the laboratory studies.

In contrast to the $FeS(s)$ oxidation rate coefficient, the $MeS(s)$ oxidation rate coefficients were found to vary from site to site (Table 11). This was most noticeable for $NiS(s)$ oxidation rate coefficients which varied from $20\text{ M}^{-1}\text{ hr}^{-1}$ for the Tweed River sediment, to $250\text{--}700\text{ M}^{-1}\text{ hr}^{-1}$ for the PNS sediments (based on total recoverable metal) to $1000\text{--}1400\text{ M}^{-1}\text{ hr}^{-1}$ for the PNS sediments (based on simultaneously extracted metal). Although it is not possible to fully explain these differences at this time, several factors may have played a role including: (i) differences in freshwater (Tweed River) and marine (PNS) water chemistry, (ii) differences in resuspended sediment concentrations in the Tweed River (50 g L^{-1}) and PNS (0.5 g L^{-1}) sediment oxidation studies, and (iii) differences in the initial $NiS:FeS$ ratio of approximately 0.1% (Tweed River) versus greater than 70% (PNS sediments). Finally, it was not possible to determine $MS(s)$ oxidation rate coefficients with the same certainty as the $FeS(s)$ oxidation rates. This was because of the limited measurements of dissolved metal concentrations in several of the oxidation studies and the prevalence of metal measurements that were reported as being below the laboratory detection limit. The issue of metal measurements below detection limits was most noticeable for Cu. Although low levels of dissolved Cu could be indicative of very slow $CuS(s)$ oxidation rate, it is also likely that most of the Cu that was released during $CuS(s)$ oxidation was bound to freshly precipitated HFO (or other sorbent phases) and was not measured in the dissolved phase.

At this time, it is recommended that the $MS(s)$ oxidation rate coefficients obtained in these studies be used on a site-specific basis, or be used in establishing upper and lower bound estimates for $MS(s)$ oxidation rates in model simulations. In many cases, it is likely that the selection of the $MS(s)$ oxidation rate coefficient will not have a large effect on dissolved metal concentrations during propeller-wash events because most of the metal released during $MS(s)$ oxidation will bind to freshly precipitated HFO (or other binding phases). Additional laboratory and modeling studies for the oxidation of resuspended sediment however should be considered to better understand the reasons for variations in $MS(s)$ oxidation rates.

Table 11: Second-order Oxidation Rate Coefficients ($M^{-1} \text{ hr}^{-1}$) Determined from Chemical Model Evaluations in This Study.

		Fe	Cu	Ni	Zn
Clarence River (Burton et al. 2009)	total recoverable Fe	5000			
Tweed River Sediment (Burton et al. 2006)	total recoverable Fe, Ni, Zn	5000		20	15
Anacostia River Sediment (Hong et al. 2011)	total recoverable Fe, Mn, Ni, Zn	5000			< 5 ^a
PNS: MS03 (This Study; Fetters 2013)	total recoverable Fe, Cu, Mn, Ni, Zn	5000 ^b	<700 ^c	700	< 75 ^d
PNS: MS04 (This Study; Fetters 2013)	total recoverable Fe, Cu, Mn, Ni, Zn	5000 ^b	<250 ^c	250	15 ^e
PNS: MS03 (This Study; Fetters 2013)	SEM Fe, Cu, Mn, Ni, Zn	5000 ^b	<1400 ^c	1400	< 45 ^d
PNS: MS04 (This Study; Fetters 2013)	SEM Fe, Cu, Mn, Ni, Zn	5000 ^b	<1000 ^c	1000	< 75 ^d
^a Dissolved Zn concentrations were often below detection limits. A maximum oxidation rate coefficient for Zn was therefore determined by calibrating the model to the detection limit. ^b Second-order oxidation rate coefficient for Fe was taken from previous results from the Clarence River, Tweed River and Anacostia River sediment oxidation studies. ^c Dissolved Cu concentrations were below detection limits. Second-order oxidation rate coefficient for Cu was therefore assumed to be equal the oxidation rate coefficient for Ni. ^d Dissolved Zn concentrations were often below detection limits. A maximum oxidation rate coefficient for Zn was therefore determined by calibrating the model to the detection limit.					

Finally, the chemical equilibrium model for bedded sediment and the time-variable model for the oxidation of resuspended sediment that were presented in this section of the report were developed specifically to provide a more detailed understanding of the chemical processes affecting metal partitioning in bedded and resuspended sediments. Although the models were found to be extremely useful in evaluating laboratory datasets, the models as presented are too complex for direct incorporation into a multi-dimensional contaminant transport model. A simplified version of the time-variable model for oxidation of resuspended sediments was therefore developed to describe metal partitioning during sediment resuspension and is presented under Task 3b of the report. As part of this development, the simplified chemical model was tested using laboratory oxidation datasets for the Tweed River (Burton et al. 2006) and the PNS sediments (Fetters 2013). Incorporation of the simplified chemical model into a three-

dimensional contaminant transport model (i.e., the Particle Tracking Model) is addressed in the final section of the report.

Task 3b: Develop Integrated TICKET-PTM Background

Simplified Chemical Model: For Incorporation to Multi-Dimensional Transport Models

Kevin J. Farley, Kevin J. Rader and Richard F. Carbonaro

Background

A detailed model describing changes in water chemistry and metal bioavailability that would occur during the early stages (e.g., 6-12 hours) of sediment oxidation was described in the previous section. Processes that were considered in the model included the abiotic oxidation of sulfide to elemental sulfur, the oxidation of reduced iron and precipitation of hydrous ferric oxides (HFO), sorption of metals to freshly-precipitated HFO, acid-base and complexation in the solution phase, precipitation / dissolution of non-sulfide solids, and gas exchange of oxygen and carbon dioxide across the air-water interface. The model was successfully applied in evaluating laboratory oxidation datasets for the Clarence River (Burton et al. 2009), Tweed River (Burton et al. 2006), Anacostia River (Hong et al. 2011) and Portsmouth Naval Station sediments (Fetters 2013).

Because of the complexities and computational burden of the detailed model, it was not feasible to incorporate the detailed chemical calculation directly into a multi-dimensional transport model such as the Particle Tracking Model (PTM). A simplified version of the chemical model was therefore developed and is described in the first part of this section. The model includes a simple time-variable calculation to determine changes in key chemical variables (e.g., metal sulfide [MeS(s)], “labile” metal concentrations) and a chemical equilibrium model calculation to determine the partitioning of “labile” metal between dissolved and particulate phases. As part of this work, the simplified model was tested by comparing results to previous detailed chemical model calculations for the Tweed River (Burton et al. 2006) and the Portsmouth Naval Station (Fetters 2013) oxidation studies. The simplified model was also used in sensitivity calculations to evaluate the role of dissolved (DOC) and particulate organic carbon (POC) on metal partitioning behavior.

Although it is possible to interface the simplified chemical model and the PTM by running the models in tandem, it was determined to be more expeditious to incorporate the time-variable portion of the simplified chemical model into the PTM and to use a look-up table at each time step to determine partitioning of “labile” metal between the dissolved and particulate phases. For this purpose, a series of metal partitioning look-up tables were generated from a large array of chemical equilibrium model calculations that considered the effects of pH, hardness (or salinity), HFO, DOC, POC and “labile” metal concentrations on metal partitioning behavior. As part of the development of partitioning look-up tables, performance testing of the Windermere Humic Aqueous Model version 7 (WHAM7) (Tipping et al. 2011) was conducted using metal partitioning datasets from Delaware Bay, San Diego Bay and Pearl Harbor. Final results for the

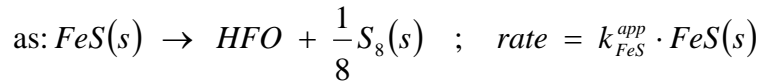
incorporation of the simplified time-variable chemical calculations and the use of metal partitioning look-up tables into PTM calculations are presented in the final section of the report.

Task 3b: Materials and Methods

Model Description

Results from detailed model evaluations of laboratory oxidation studies were used in developing a simplified chemical model. Simplifying assumptions that were considered are as follows. First, dissolved oxygen concentrations and pH were considered to remain relatively constant during the early stages (e.g., 6-12 hours) of sediment oxidation. Second, carbonic acid (H_2CO_3) concentrations were considered to be in equilibrium with the overlying atmosphere. Third, the oxidation of reduced iron (that was either initially present in the solution or was subsequently released during the oxidation of $FeS(s)$) was considered to occur instantaneously in the presence of oxygen.

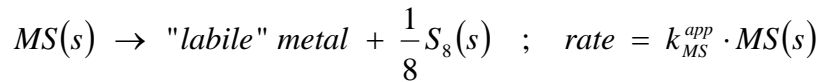
Based on the simplifying assumptions, the oxidation of iron sulfide [$FeS(s)$] can be described



where $FeS(s)$ is kinetically oxidized producing Fe^{II} (which is considered to rapidly oxidize to Fe^{III} and precipitate as HFO) and elemental sulfur. The rate of the reaction is considered to be first order with respect to $FeS(s)$ with an apparent first-order reaction rate coefficient (k_{FeS}^{app}) equal to the second-order $FeS(s)$ oxidation rate coefficient multiplied by the dissolved oxygen concentration (given in moles L^{-1}). For example, using the second-order $FeS(s)$ oxidation rate coefficient of $5000 \text{ M}^{-1} \text{ hr}^{-1}$ (see Table 11) and a dissolved oxygen concentration of $8 \text{ mg } L^{-1}$, k_{FeS}^{app} is calculated as follows:

$$k_{FeS}^{app} = 5000 \text{ M}^{-1} \text{ hr}^{-1} \times \left(\frac{8 \text{ mg } L^{-1}}{10^3 \text{ mg } g^{-1} \times 32 \text{ g } mole^{-1}} \right) = 1.25 \text{ hr}^{-1}$$

In similar fashion, the oxidation of metal sulfide [$MS(s)$] can be described as:



where $MS(s)$ is kinetically oxidized producing “labile” metal (which represents metal that is not present as metal sulfide) and elemental sulfur. The rate of the reaction is considered to be first order with respect to $MS(s)$ with an apparent first-order reaction rate coefficient (k_{MS}^{app}) equal to the second-order $MS(s)$ oxidation rate coefficient (see Table 12) multiplied by the dissolved oxygen concentration (given in moles L^{-1}).

Based on the $FeS(s)$ and $MS(s)$ oxidation reactions given above, concentrations of $FeS(s)$, $MS(s)$, HFO, “labile” metal and elemental sulfur can be determined as a function of time. Solutions for $FeS(s)$, $MS(s)$, HFO, “labile” metal and elemental sulfur can be obtained numerically (e.g., for an Eulerian contaminant transport model) or analytically (e.g., for a well-mixed laboratory chamber, or for a Lagrangian transport model such as the PTM). The analytical solutions for

FeS(s), MS(s), HFO, “labile” metal and elemental sulfur are given in Table 12 and will be used subsequently in testing the simplified model using the Tweed River and Portsmouth Naval Station laboratory oxidation studies.

Table 12: Mass Balance Equations and Analytical Solutions for Time-Variable Concentrations of FeS(s), MS(s), HFO, “Labile” Metal and Elemental Sulfur in the Simplified Chemical Model

<u>Simplified FeS(s) and MeS(s) Oxidation Reactions</u>	
$FeS(s) \rightarrow HFO + \frac{1}{8}S_8(s)$	$; \text{ rate } = k_{FeS}^{app} \cdot FeS(s)$
$MS(s) \rightarrow \text{"labile" metal} + \frac{1}{8}S_8(s)$	$; \text{ rate } = k_{MS}^{app} \cdot MS(s)$
<u>Mass Balance Equations (Batch Systems)</u>	
$\frac{d FeS}{dt} = -k_{FeS}^{app} \cdot FeS$	$; \quad \frac{d MS}{dt} = -k_{MS}^{app} \cdot MS$
$\frac{d HFO}{dt} = +k_{FeS}^{app} \cdot FeS$	$; \quad \frac{d \text{"labile" metal}}{dt} = +k_{MS}^{app} \cdot MS$
$\frac{d S_8(s)}{dt} = +\frac{1}{8} \cdot k_{FeS}^{app} \cdot FeS + \frac{1}{8} \cdot k_{MS}^{app} \cdot MS$	
<u>Time-Variable (Analytical) Solutions</u>	
$FeS = (FeS)_o \cdot \exp\{-k_{FeS}^{app} \cdot t\}$	
$MS = (MS)_o \cdot \exp\{-k_{MS}^{app} \cdot t\}$	
$HFO = (HFO)_o + (FeS)_o \cdot [1 - \exp\{-k_{FeS}^{app} \cdot t\}]$	
$\text{"labile" metal} = (\text{"labile" metal})_o + (MS)_o \cdot [1 - \exp\{-k_{MS}^{app} \cdot t\}]$	
$S_8(s) = (S_8(s))_o + \frac{1}{8} \cdot (FeS)_o \cdot [1 - \exp\{-k_{FeS}^{app} \cdot t\}] + \frac{1}{8} \cdot (MS)_o \cdot [1 - \exp\{-k_{MS}^{app} \cdot t\}]$	

Time-varying concentrations of HFO and “labile” metal along with the specified pH, major cations (Na⁺, K⁺, Ca²⁺, Mg²⁺) and anions (Cl⁻, SO₄²⁻), and possibly other binding phases (e.g., DOC, POC) are then used in a chemical equilibrium model calculation to determine the distribution of “labile” metal between dissolved and particulate phases. For model testing presented below, chemical equilibrium model calculations are performed using the TICKET (Farley et al, 2008, 2011) with the MINTEQA2 database (Allison et al. 1991) and metal binding

to HFO described by the surface complexation model of Dzombak and Morel (1990). In subsequent sensitivity calculations, metal binding to DOC and POC were also included in TICKET chemical equilibrium calculations using reactions from WHAM 7 (Tipping et al. 2011).

Model Testing

The simplified model was tested by comparing computed results for acid volatile sulfides (AVS), elemental sulfur [$S_8(s)$ as S], MS(s), sorbed metal and dissolved metal concentrations to results that were determined from the detailed time-variable model for the oxidation of resuspended sediment previously presented in Section 2. The Tweed River (Burton et al. 2006) and the Portsmouth Naval Station MS03 sediment sample (Fetters 2013) were considered in this evaluation. Simplified model calculations were performed as follows. Initial concentrations of FeS(s), MS(s), HFO, elemental sulfur and “labile” metal were taken from previously-defined initial conditions and are given in Table 13. Apparent first-order oxidation rate coefficients were calculated from the previously-determined second-order rate coefficients and the dissolved oxygen concentration, and are summarized in Table 14. Concentrations of FeS(s), MS(s), HFO, elemental sulfur and “labile” metal were then determined as a function of time using the analytical solutions given in Table 12.

Subsequent chemical equilibrium model calculations were performed at selected time increments to determine partitioning of “labile” metal between dissolved and particulate phases. For the equilibrium model calculations, major cation and anion concentrations were taken from previously-defined values for the resuspension mixture (see Table 13). pH was set equal to the final computed value in the detailed time-variable model calculations.

Model Sensitivity

In the development of the detailed time-variable model for the oxidation of resuspended sediment (Section 2), metal binding to natural organic matter (NOM) was assumed to be small compared to metal binding to HFO. The applicability of this assumption was tested for the Tweed River and Portsmouth Naval Station MS03 laboratory oxidation studies using the simplified chemical model. The procedure was similar to the simplified model calculations described above. Chemical concentrations and apparent first-order oxidation rate coefficients were previously defined (see Tables 13 and 14). Time-variable concentrations of FeS(s), MS(s), HFO and elemental sulfur were again calculated using the analytical solutions in Table 12, and subsequent chemical equilibrium model calculations were performed at selected time increments to determine partitioning of “labile” metal between dissolved and particulate phases. However, metal binding to dissolved and particulate NOM was also considered in the chemical equilibrium model calculations by including metal binding reactions from WHAM 7. For this calculation, DOC and POC concentrations in the resuspension mixture were determined from measured values and conservative mixing calculations (see Table 13 for details). The dissolved and particulate NOM was assumed to be equal to 2 times the DOC and 2 times the POC concentrations. Finally, half of the dissolved NOM and half of the particulate NOM were assumed to be active.

Table 13: Initial Conditions and Water Chemistry Parameters for Time-variable Simulations Using the Simplified Model. ^a

	<u>Tweed River</u>	<u>PNS MS03</u> (Total Extractable Metal)	<u>PNS MS03</u> (Simultaneously Extracted Metal)
<u>Initial Concentrations</u>			
FeS(s) ^b	1.15E-02	8.08E-07	7.18E-06
CuS(s) ^b	--	4.53E-06	4.07E-07
NiS(s) ^b	1.36E-05	5.88E-07	1.71E-07
ZnS(s) ^b	6.20E-05	4.08E-06	2.24E-06
S8(0) as S ^b	5.95E-03	--	--
HFO ^c	8.17E-02	3.30E-04	4.25E-05
“labile” Cu ^d	--	--	--
“labile” Ni ^d	6.14E-07	--	--
“labile” Zn ^d	2.37E-06	--	--
<u>Water Chemistry Parameters ^a</u>			
Total Al(3+)	6.17E-02	--	--
Total Ca(2+)	5.74E-04	9.04E-03	9.04E-03
Total Cl(-)	1.53E-02	4.83E-01	4.83E-01
Total K(+)	3.01E-04	9.04E-03	9.04E-03
Total Mg(2+)	2.07E-03	4.70E-02	4.70E-02
Total Mn(2+)	1.96E-04	3.03E-06	3.68E-07
Total Na(+)	1.39E-02	4.15E-01	4.15E-01
Total SO4(2-)	5.98E-03	2.50E-02	2.50E-02
pH ^d	6.06	7.90	7.89
DOC ^e	6.14	0.08	0.08
POC ^e	2470	8.0	8.0

^a All concentrations are given in moles L⁻¹, except where noted.

^b Initial concentrations for sulfidic solids are from non-equilibrium concentrations (Tables 9 and 10, Section 2).

^c Initial HFO concentrations are equal to the summation of Total Fe(2+) and Total Fe(3+) concentrations in the equilibrium phase (Tables 9 and 10, Section 2).

^d Initial concentrations of “labile” metal are equal to Total metal concentrations in the equilibrium phase (Tables 19 and 10, Section 2).

^c Water chemistry concentrations are from Total chemical concentrations in the equilibrium phase (Tables 9 and 10, Section 2).

^d pH is set to final pH obtained in the detailed, time-variable chemical model simulations in Section 2.

^e DOC and POC concentrations are determined from conservative mixing calculations. See Table A-12 (Tweed River) and Table A-17 (Portsmouth Naval Station MS03) for measured porewater DOC, sediment organic carbon, sediment solids and mixing volumes. Concentrations are given in mg L⁻¹.

Table 14: Apparent First-order Oxidation Rate Coefficients (hr⁻¹) for Time-variable Simulations Using the Simplified Model. ^a

	<u>Tweed River</u> ^b	<u>PNS MS03</u> ^c (Total Extractable Metal)	<u>PNS MS03</u> ^c (Simultaneously Extracted Metal)
k_{FeS}^{app}	1.42	1.08	1.08
k_{CuS}^{app}	--	1.51E-01	3.02E-01
k_{NiS}^{app}	5.68E-03	1.51E-01	3.02E-01
k_{ZnS}^{app}	4.26E-03	1.62E-02	9.70E-03
^a Apparent first-order rate coefficients were multiplying the second-order oxidation rate coefficients in M ⁻¹ hr ⁻¹ (Table 11) by the dissolved oxygen concentration in M. ^b Dissolved oxygen concentration for the Tweed River oxidation study was set at 2.84×10^{-4} M (or 9.09 mg L ⁻¹) which corresponds to dissolved oxygen saturation in freshwater at 20°C. ^c Dissolved oxygen concentration for the Portsmouth Naval Station MS03 oxidation study was set at 2.16×10^{-4} M (or 6.9 mg L ⁻¹) which corresponds to dissolved oxygen saturation in marine waters with a salinity of 31 ppt and a temperature of 24°C.			

Task 3b: Results and Discussion

Model Testing

Calculated results for AVS and S₈(s) as S in the Tweed River laboratory oxidation study are presented in Figure 22A for both the simplified chemical model (thicker lines) and the detailed chemical model (thinner lines). As shown, results for the two models are nearly indistinguishable. Calculated results for NiS(s), sorbed Ni and dissolved Ni concentrations are given in Figure 22B following a similar format. As shown, results are again largely indistinguishable except for dissolved and sorbed Ni concentrations during the first 1-2 hours of oxidation. Differences in computed results for dissolved and sorbed Ni concentration during the first 1-2 hours is due to competition of Fe²⁺ and M²⁺ for binding to HFO. This effect, which is considered in the detailed chemical model, causes less M²⁺ to bind to HFO and more of the “labile” metal in the dissolved phase. Within 1-2 hours, Fe²⁺ oxidation is nearly complete and the effects of competition for binding to HFO are diminished. Because Fe²⁺ is assumed to oxidize instantaneously in the simplified chemical model, Fe²⁺ is not present and Fe²⁺ competition for HFO binding sites does not occur.

Comparable results for the Portsmouth Naval Station MS03 oxidation study are shown in Figure 22C, D. For this study, computed results for the simplified model and the detailed model are indistinguishable throughout the entire simulation period. Results for Cu and Zn (not shown) show similar behavior. Based on these findings, the simplified model appears to provide a good

description of metal release and metal bioavailability during early stages (e.g., 6-12 hours) of sediment oxidation.

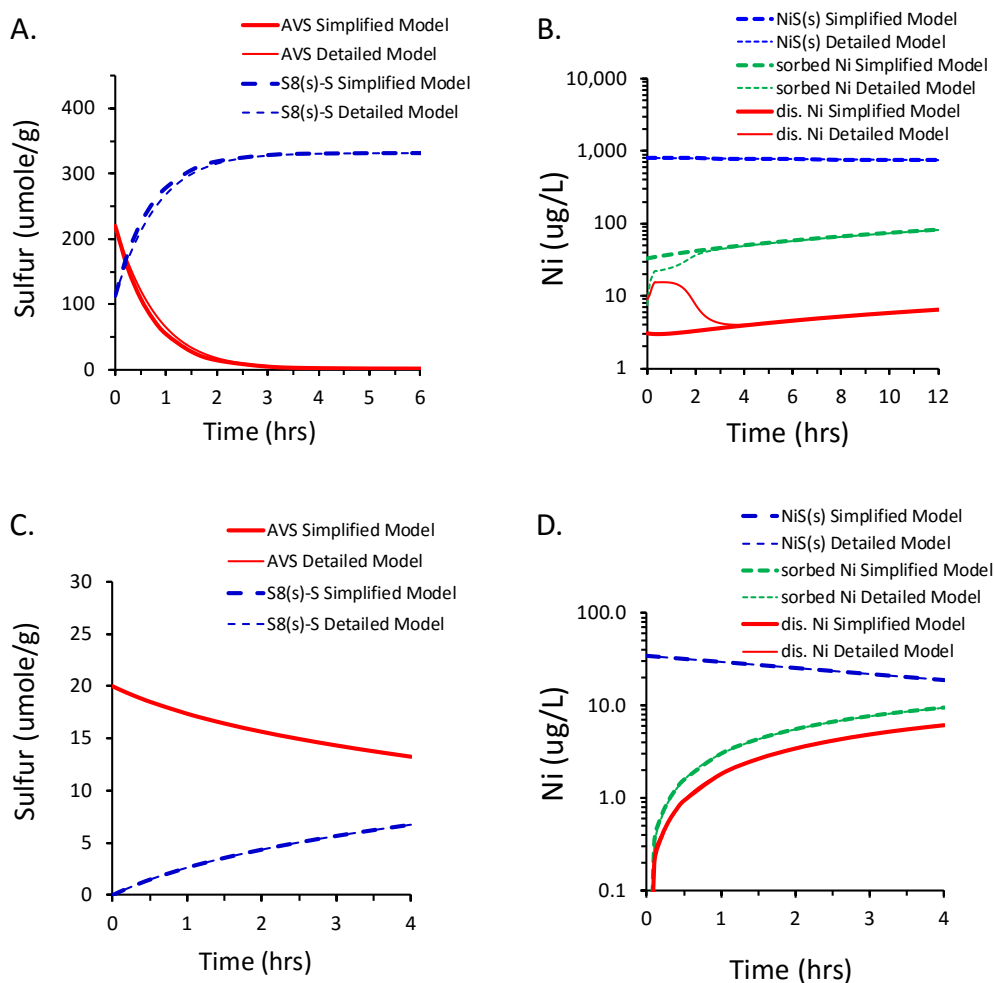


Figure 22: Comparisons of simplified model and detailed model results for the Tweed River sediment oxidation study: (A) acid volatile sulfide (AVS) and elemental sulfur [S₈(s)] as sulfur, and (B) NiS(s), sorbed Ni and dissolved Ni concentrations; and for the Portsmouth Naval Station MS03 sediment oxidation study: (C) AVS and S₈(s) as S, and (D) NiS(s), sorbed Ni and dissolved Ni concentrations.

Model Sensitivity

The simplified chemical model was also used in sensitivity calculations to evaluate the role of NOM in controlling partitioning of “labile” metal between the dissolved and particulate phases. Simplified model results for the Tweed River oxidation study are presented in Figure 23 without metal binding to NOM (thicker lines) and with metal binding to NOM (thinner lines). As shown, sorbed metal results were nearly indistinguishable for both Ni and Zn. The binding of metal to dissolved NOM was found to be negligible for both metals. However, Ni and Zn binding to

particulate NOM did result in dissolved concentrations that were 10-20% lower when metal binding to particulate NOM was included in the model calculations.

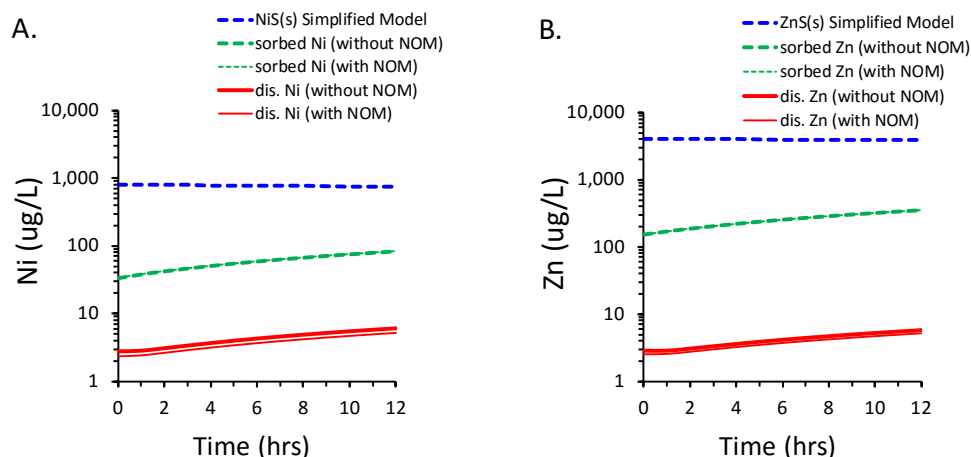


Figure 23: Comparisons of simplified model with and without metal binding to natural organic matter (NOM) for the Tweed River sediment oxidation study: (A) Ni, (B) Zn.

Similar calculations were performed for the Portsmouth Naval Station MS03 sediment using total recoverable iron and total recoverable metal concentrations. Results without metal binding to NOM (thicker lines) and with metal binding to NOM (thinner lines) were found to be largely indistinguishable for Cu, Ni and Zn (Figure 24). However, Cu bound to dissolved NOM did account for approximately 5% of Cu in the dissolved phase and Cu bound to particulate NOM was approximately 1.5% of Cu in the particulate phase. Effects of NOM on metal binding were smaller for both Ni and Zn.

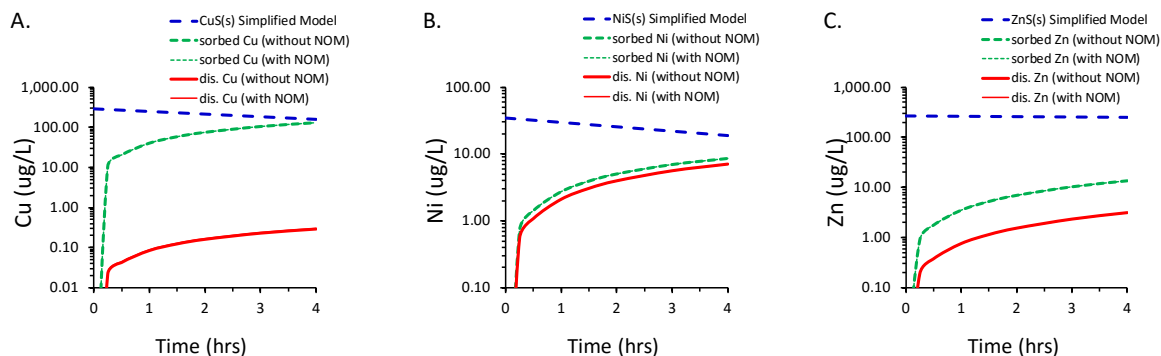


Figure 24: Comparisons of simplified model with and without metal binding to natural organic matter (NOM) for the Portsmouth Naval Station MS03 sediment oxidation study: (A) Cu, (B) Ni, and (C) Zn.

Finally, model calculations for the Portsmouth Naval Station MS03 sediment using simultaneously extracted iron and simultaneously extracted metal concentrations. For this case,

metal binding to NOM was expected to play a larger role because HFO concentrations were computed to be approximately seven times smaller than HFO concentrations based on total recoverable iron (Table 13). However, model results for Cu, Ni and Zn were again found to be largely indistinguishable when metal binding to NOM was and was not considered. A closer look at model results showed that approximately 5% of the dissolved Cu was again bound to dissolved NOM and that nearly 9% of the Cu in the particulate phase was now bound to particulate NOM. Although concentrations bound to NOM became more important, their effect of Cu partitioning remain relatively small because Cu binding to particulate NOM (which would cause a decrease in dissolved Cu concentrations) was in part offset by Cu binding to dissolved NOM (which kept more of the “labile” Cu in the dissolved phase). For Ni and Zn, approximately 3% of the metal in the particulate phase was bound to particulate NOM and negligible concentrations of the two metals were bound to dissolved NOM.

Based on results presented above, metal binding to NOM did not have a large effect in determining metal partitioning behavior in the Tweed River and Portsmouth Naval Station laboratory oxidation studies. However, since NOM concentration may be higher at field sites, metal partitioning look-up tables were generated from chemical equilibrium model calculations based on expected ranges in pH, hardness (or salinity), HFO, “labile” metal, and dissolved and particulate NOM concentrations.

Metal Partitioning Look-up Tables

Metal partitioning look-up tables offer a rapid and computationally efficient means of determining a distribution coefficient (K_D)¹ within a transport model simulation. In this approach, potentially time- and cpu-intensive chemical speciation calculations are performed separate from the transport simulation using the range of key chemical parameters for a given site. Interpolation is used to select an appropriate K_D value from the table.

Assemblage chemical equilibrium speciation models quantify partitioning of metals to suspended solids by modeling the binding of metals to various constituents that make up suspended particulate matter (e.g., HFO, POC). These models predict metal partitioning based on water chemistry and therefore can be used to generate the look-up tables described above. One such model, WHAM7 (Tipping et al., 2011), can be used to simulate simultaneously the chemical speciation of a number of metals in the dissolved and particulate (i.e., adsorbed phases) and generate modeled K_D values based on a specified water chemistry. Typical input for the calculation includes pH, temperature, concentrations of dissolved/particulate organic carbon (i.e., DOC and POC), major cations (Na^+ , K^+ , Ca^{2+} , Mg^{2+}) and anions (Cl^- , SO_4^{2-} , CO_3^{2-}), amounts of hydrous ferric oxide (HFO) and hydrous manganese oxide (HMO). The particulate species POC, HFO, HMO, etc. are associated with the suspended solids (TSS).

¹ The distribution coefficient, K_D , defined as

$$K_D = \frac{v_M}{[M]_{\text{diss}}} = \frac{[M]_{\text{part}}}{[M]_{\text{diss}} \text{ TSS}}$$

where v_M is the solids-normalized particulate metal concentration [$\text{mol} \cdot \text{kg}^{-1}$], TSS is the total suspended solids concentration [$\text{kg} \cdot \text{L}^{-1}$], and $[M]_{\text{diss}}$ and $[M]_{\text{part}}$ are the molar dissolved and particulate metal concentrations [$\text{mol} \cdot \text{L}^{-1}$], respectively.

Preliminary Speciation Model Performance Testing

Prior to the development of look-up tables, preliminary model performance testing was conducted to assess the ability of the model to predict metal binding to suspended solids. This analysis entails collecting water quality data with sufficient detail to (a) calculate an “observed” distribution coefficient value based on measured dissolved and particulate metal concentrations and (b) specify WHAM input values and generate “predicted” distribution coefficient values.

Rader (2009) assessed the performance of the immediate predecessor of the WHAM7 model, WHAM6, in predicting metal partitioning to suspended solids in rivers and estuaries. The results of the WHAM6 performance assessment indicated that the model, using a generalized set of typical binding phases, could predict solid-solution partitioning reasonably well in certain cases. For example, WHAM6 estimates for Ni and Cu $\log K'_D$ ² in the Trinity River fell within a factor of 4 of observed values. Sensitivity analyses indicated that hardness cation (Mg and Ca) competition had a significant impact on the calculated solid-solution distribution coefficient particularly when manganese oxides are involved and at salinities approaching that of seawater. Excluding cation competition effects generally improved model fits in certain cases.

In the present research, the Delaware Bay partitioning dataset from (Rader, 2009) was selected to provide an initial performance test for WHAM7. This dataset was selected because it contains a relatively complete set of water quality parameters required for input in WHAM7. It also has metal partitioning data across a salinity gradient. Model performance was also evaluated using metal partitioning data from San Diego Bay and Pearl Harbor including data from propeller wash studies conducted by SPAWAR.

Delaware Bay Dataset

Water quality and trace metal data for the Delaware Estuary were taken from the Delaware Bay Database (Church and Scudlark, 1998; Culberson, 1988). Thirty-four surface samples (1 meter depth) taken from transects along a salinity gradient from four cruises were selected for analysis. These samples had measurements for all parameters necessary to make a speciation calculation in WHAM7. Details of analytical methods are provided in references in Culberson (1988). Details of the calculation procedure can be found in Rader (2009) (note: the procedure for WHAM6 and 7 are almost identical). DOC, POC, HFO and HMO were included as metal binding phases in the WHAM7 calculations.

Comparison of measured and model-predicted logarithmic distribution coefficient ($\log K_D$) values is shown in Figure 25a. As shown, WHAM7-calculated $\log K_D$ values generally underestimated the distribution coefficient for nickel, zinc and cobalt (data points fell below the 1:1 line). The extent of $\log K_D$ underestimation exceeded two orders of magnitude in some cases (e.g., for cobalt). In contrast to $\log K_D$ results for nickel, zinc and cobalt, WHAM7 results for copper typically overestimated the observed $\log K_D$ values. Possible reasons for these

²The dimensionless distribution coefficient, K'_D , defined as

$$K'_D = K_D \times TSS = \frac{[M]_{\text{part}}}{[M]_{\text{diss}}}$$

where v_M is the solids-normalized particulate metal concentration [$\text{mol} \cdot \text{kg}^{-1}$], TSS is the total suspended solids concentration [$\text{kg} \cdot \text{L}^{-1}$], and $[M]_{\text{diss}}$ and $[M]_{\text{part}}$ are the molar dissolved and particulate metal concentrations [$\text{mol} \cdot \text{L}^{-1}$], respectively.

discrepancies include overestimation of DOC binding, presence of additional binding phases not considered in the WHAM7 calculation, overestimation of hardness cation competition for particulate binding sites, and non-surface complexed particulate metals (e.g. precipitated metal). Since discrepancies tended to be more pronounced at higher salinities (Figure 25b), the overestimate of hardness cation competition was considered to be the most likely explanation.

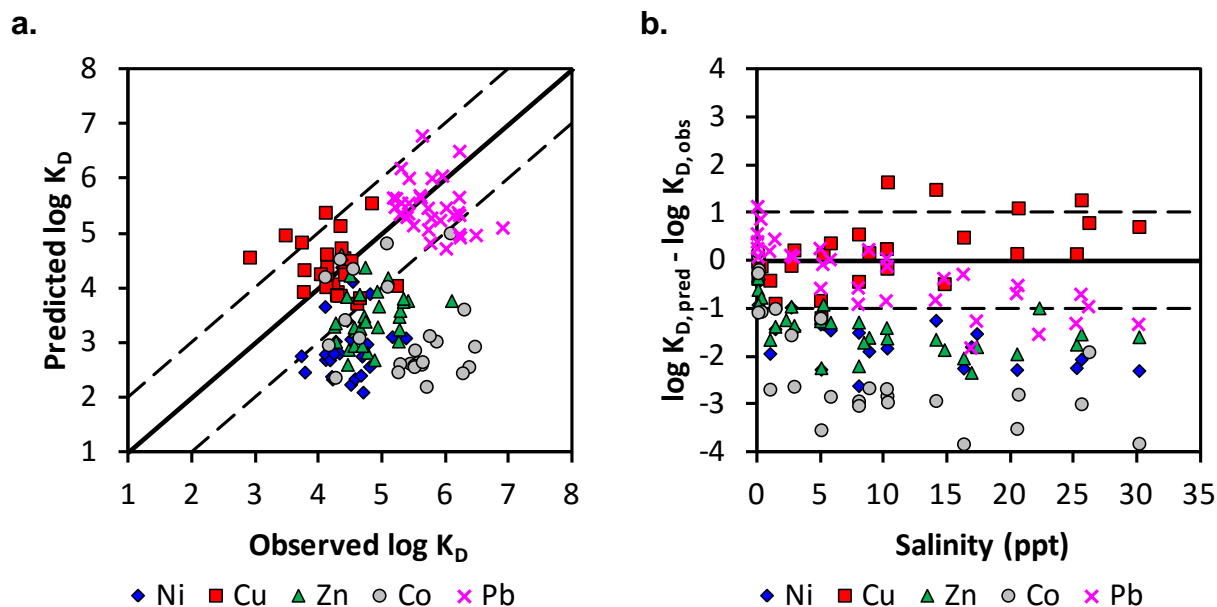


Figure 25: (a) Delaware Bay performance assessment plot for nickel (Ni), copper (Cu), zinc (Zn), cobalt (Co), and lead (Pb) and (b) $\log K_D$ prediction residual plot using default WHAM parameters. Binding phases considered in the calculation included DOC, POC, HFO and HMO. The solid black line in (a) is the 1:1 line indicating perfect agreement between the observed and model-predicted $\log K_D$ values. The dashed values in the plot indicate a factor of 10 about the 1:1 line. The solid black line in (b) indicates a residual of zero (i.e., no discrepancy between observed and modeled $\log K_D$ values). The dashed lines in this plot indicate residuals of one log unit.

A sensitivity analysis was therefore conducted in which the WHAM7 speciation calculations were rerun with hardness cation binding to DOC, POC, HFO, and HMO turned off. Exclusion of this competitive effect improved the agreement between the model and observed $\log K_D$ values for nickel, copper, and zinc in Delaware Estuary (Figure 26). The improvements were most pronounced for nickel, zinc and cobalt. In comparison, model-predicted copper $\log K_D$ values are not very sensitive to cation competitive effects.

San Diego Bay Dataset

Two water column datasets from San Diego Bay were available for model testing: data from six sampling campaigns in the early 2000s (Chadwick et al., 2005) and data from an April 2012 propeller wash sampling event collected by the Space and Naval Warfare Systems Command (SPAWAR). Data from the early 2000s (Chadwick et al. 2005) included measurements of temperature, salinity, pH, TSS, DOC, alkalinity, and dissolved/total copper and zinc. Samples

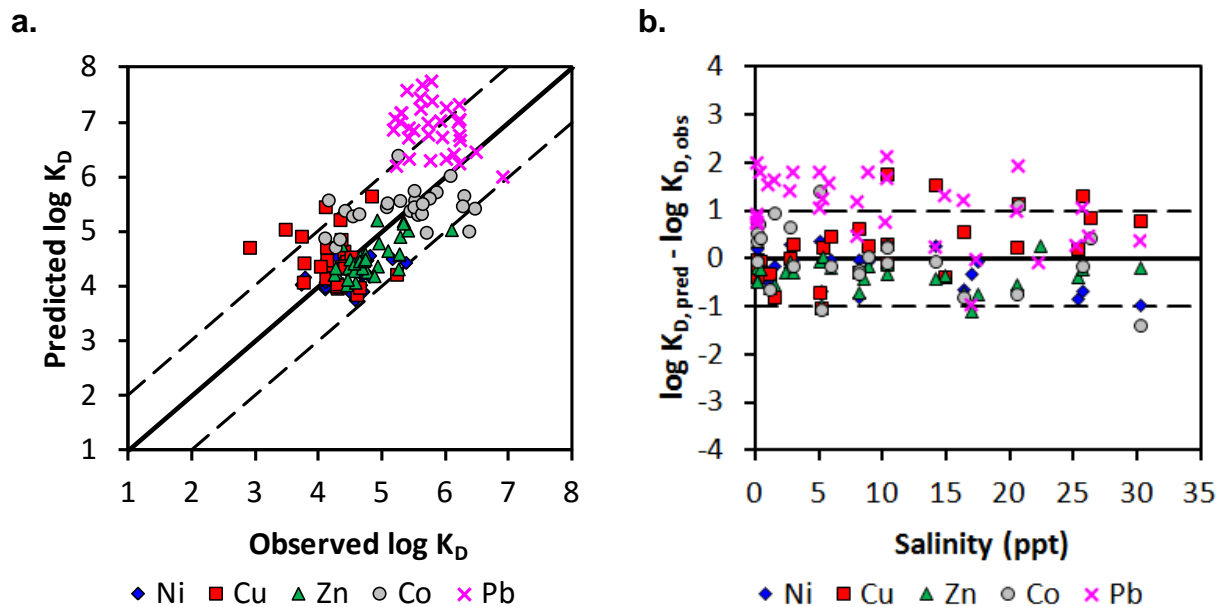


Figure 26: (a) Delaware Bay performance assessment plot for nickel (Ni), copper (Cu), zinc (Zn), cobalt (Co), and lead (Pb) and (b) log K_D prediction residual plot for WHAM simulation with hardness cation (calcium and magnesium) binding to DOC, POC, HFO and HMO turned off. See caption in Figure 25 for additional plot details.

were collected along transects extending throughout the bay (Figure 27 inset), but only samples collected closest to the prop wash event were selected for this analysis. For the propeller wash sampling event, surface (3 feet) and mid-depth (15 feet) samples were collected from behind a tug boat as it traveled around piers at the eastern side of the Bay (Figure 27). The data included measurements of total suspended solids, dissolved and particulate metals (associated with various size fractions).

Except for pH, DOC and POC, input parameters for the WHAM7 calculations for the propeller wash sampling event were specified based on concurrent field measurements. The pH, DOC and POC input values were estimated using data from other studies conducted in San Diego Bay including Peng (2004), Chadwick et al. (1999), and Burton Jr et al. (2012). For POC, input values were calculated as the product of the TSS and the fractional organic carbon content of the solids (f_{oc}). The quantities f_{oc} and POC were estimate using an approach based on the work of Turner (1996)³. Both San Diego Bay datasets utilize this relationship to obtain POC from TSS.

³TSS was assumed to be comprised of (a) a permanently suspended fraction, TSS_{PS} with an $f_{oc,PS}$ and (b) a temporarily resuspended fraction, TSS_{TS} where ($TSS_{TS} = TSS_{Measured} - TSS_{PS}$) with an $f_{oc,TS}$ value of 0.02 mg/mg based on San Diego Bay sediment (Chadwick et al., 1999). The values of TSS_{PS} and $f_{oc,PS}$ were optimized using POC and TSS data from Peng, J., 2004. Integrated geochemical and hydrodynamic modeling of San Diego Bay, California. University of Southern California, Ann Arbor, pp. 230-230 p. The f_{oc} varies with the measured TSS as the weighted average of the $f_{oc,TS}$ and $f_{oc,PS}$:

$$f_{oc} = [TSS_{PS} \times f_{oc,PS} + TSS_{TS} \times f_{oc,TS}] / TSS_{Measured} \quad (1)$$

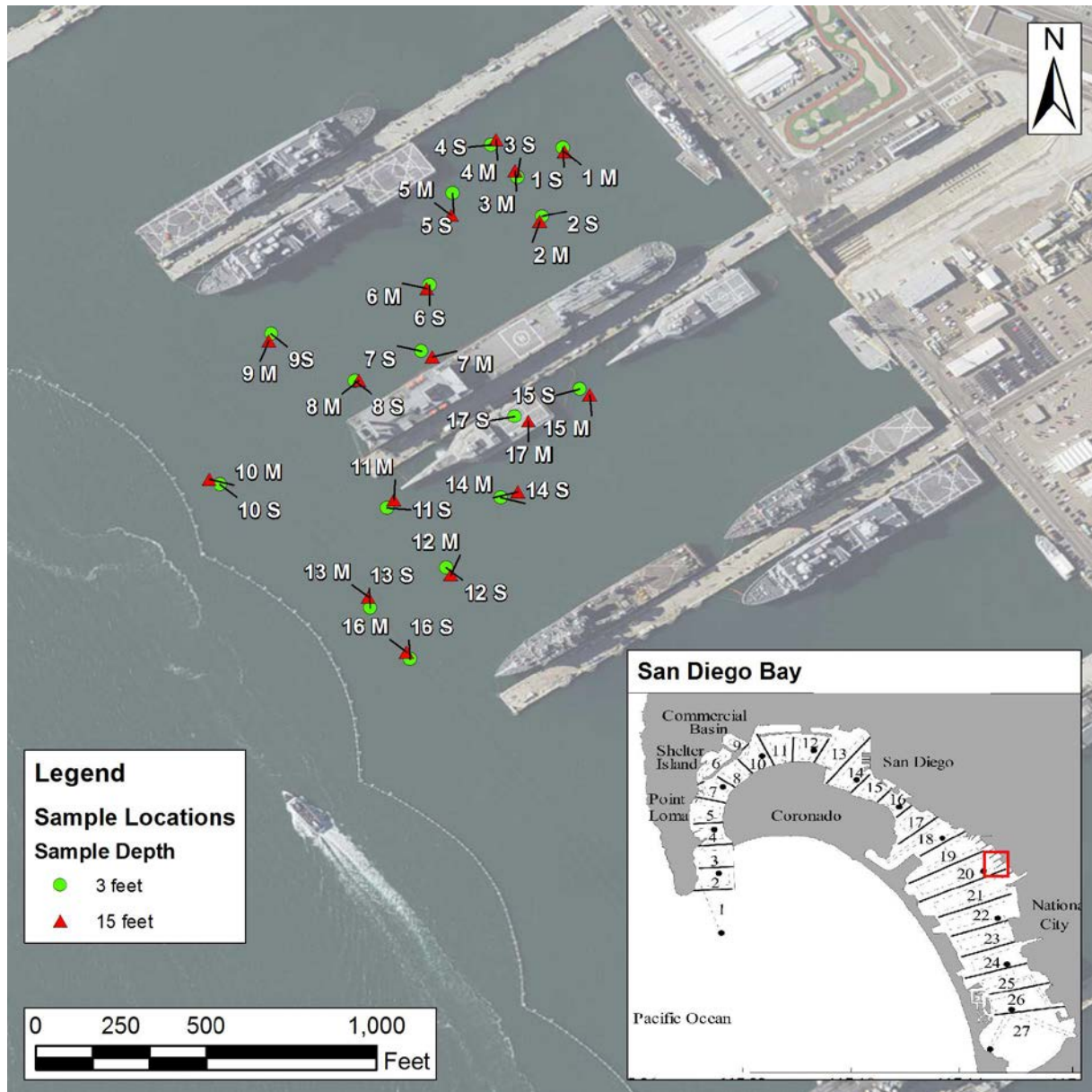


Figure 27: San Diego Bay sample locations. Main map shows locations of SPAWAR propeller wash samples. The inset map shows the transects and boxes from the Chadwick et al. (2005) sampling events. The prop wash area is highlighted in red in the inset map. Source: Esri, DigitalGlobe, GeoEye, earthstar Geographics, CNES/Airbus DS, USDA, USGS, AeroGRID, IGN, and the GIS User Community.

where TSS_{PS} is 0.246 mg/L, $TSS_{TS} = TSS_{Measured} - TSS_{PS}$, $f_{oc,PS} = 0.256$ mg/mg, $f_{oc,TS} = 0.02$ mg/mg. Since $POC = TSS_{Measured} \times f_{oc}$, the above equation can be expressed:

$$POC = [0.063 + (TSS_{Measured} - 0.246) \times 0.02] \quad (2)$$

where both TSS and POC are in mg/L.

A summary of the observed (i.e., measured) copper and zinc log K_D values from the studies is provided in Figure 28. The median and mean log K_D values for both the Chadwick et al. (2005) and SPAWAR prop-wash event are similar to observed log K_D values of 4.7 ± 0.4 for copper and 5.0 ± 0.5 that were reported for other sites (Table 15). It is important to note however that log K_D values for copper and zinc observed in the Chadwick et al. (2005) study are higher than those from the SPAWAR study. This result is likely the result of lower organic carbon content in bedded sediments that were resuspended during the SPAWAR prop-wash study.

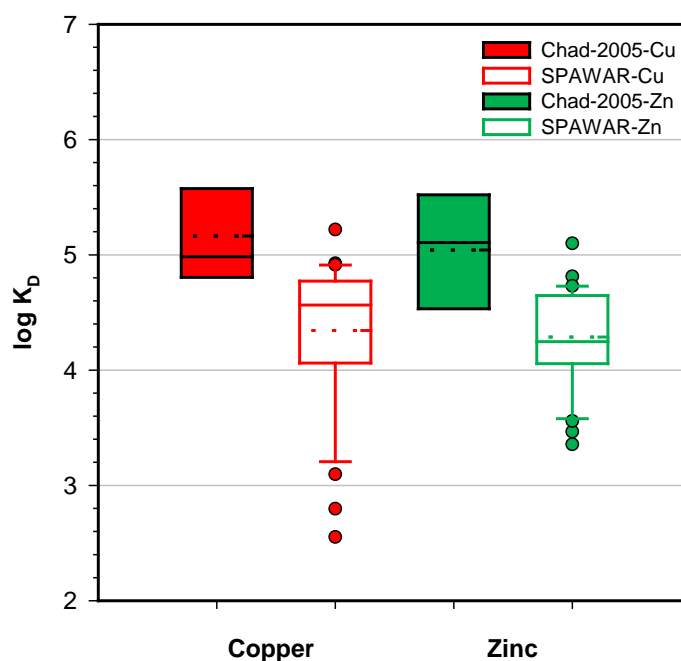


Figure 28: Summary of observed log K_D data from Chadwick et al. (2005) and the SPAWAR propeller wash sampling events at San Diego Bay. The boundary of the box closest to zero indicates the 25th percentile, the solid line within the box marks the median, the dashed line within the box indicates the mean, and the boundary of the box farthest from zero indicates the 75th percentile. The error bars above and below the box indicate the 95th and 5th percentile values, respectively. Points represent values outside of the 5th and 95th percentile (i.e. outliers), respectively. Error bars and outliers are only calculated if a minimum number of data points exist.

Table 15: Copper and Zinc Suspended Matter/Water log K_D Summaries from Literature Data as Compiled by Allison and Allison (2005)

Metal	Median	Mean	Std. Dev.	Min	Max	Comments
Cu(II)	4.7	4.7	0.4	3.1	6.1	From literature data (edited, n=42); log-normal; CL=1
Zn(II)	5.1	5.0	0.5	3.5	6.9	From literature data (edited, n=47); log-normal; CL=1

A comparison of model-predicted and observed $\log K_D$ values is provided for copper and zinc (Figure 29a). As shown, the model-predicted $\log K_D$ values are generally within an order of magnitude of the observed $\log K_D$ values for copper. WHAM7 calculations however underestimated the observed $\log K_D$ values for zinc (i.e., values fell below the 1:1 line). Following the approach presented previously for Delaware Bay, cation competition to the WHAM7 binding sites was excluded in subsequent WHAM7 calculations (Figure 29b). As in the case of the Delaware Bay study, the exclusion of cation competition for DOC, POC, HFO and HMO binding sites greatly improved the performance of WHAM7 in predicting $\log K_D$ values for zinc and had minimal effect on the $\log K_D$ calculations for copper. Based on these findings, the metal partitioning look-up tables for saline waters were developed using WHAM7 with Ca and Mg binding to DOC, POC, HFO and HMO excluded from the calculations.

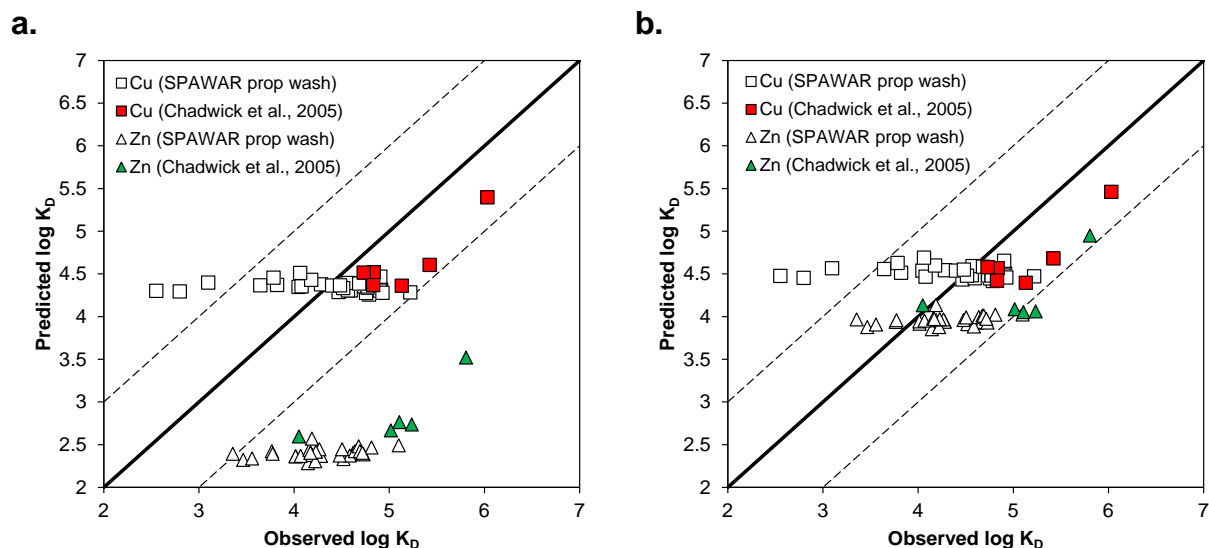


Figure 29: San Diego Bay performance assessment plot for copper (Cu, squares) and zinc (Zn, triangles) for the Chadwick et al. (2005) dataset (hollow symbols) and the SPAWAR prop wash dataset (filled symbols appended). The analysis was made using (a) default model parameters and (b) with hardness cation (calcium and magnesium) binding to DOC, POC, HFO and HMO turned off.

Pearl Harbor Dataset

Two water column datasets from Pearl Harbor were available for model testing: (1) samples collected from eight ambient stations throughout the harbor (Figure 30) over a 16-month period in 2005 and 2006 (Earley et al., 2007) and (2) data from an August 2012 propeller wash sampling event collected by the Space and Naval Warfare Systems Command (SPAWAR). Data from the Earley et al. (2007) sampling events included measurements of salinity, pH, TSS, TOC, DOC, and dissolved/total copper from the water column. For the propeller wash sampling event, surface (3 feet) and mid-depth (15 feet) samples were collected from behind a tug boat (Figure

30). The data included measurements of total suspended solids, dissolved and particulate metals (associated with various size fractions).

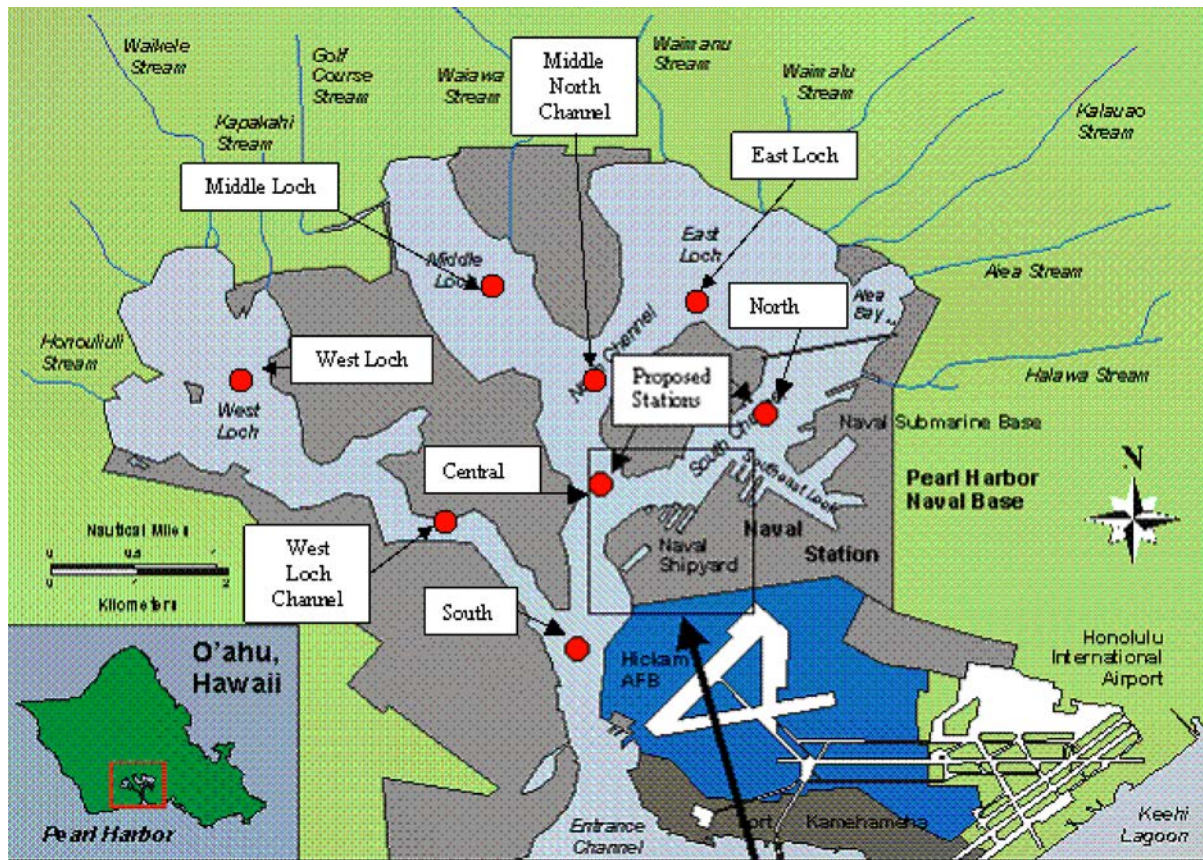


Figure 30. Upper Panel – Location of eight ambient stations from Earley et al. (2007) study. Reproduced from Earley et al. (2007) report. Lower Panel – Pearl Harbor propeller wash study sample locations. Basemap Source: Esri, DigitalGlobe, GeoEye, Earthstar Geographics, CNES/Airbus DS, USDA, USGS, AeroGRID, IGN, and the GIS User Community

Except for pH, DOC and POC, input parameters for the WHAM7 calculations for the propeller wash sampling event were specified based on concurrent field measurements. For temperature, pH and DOC, input values were specified at the average values from the eight ambient stations (Earley et al., 2007). The quantities f_{oc} and POC were estimated using an approach similar to that used for the San Diego Bay the propeller wash datasets. Since sediment organic carbon content was not available in Earley et al. (2007) or a related study, $f_{oc,TS}$ was estimated during optimization process with an upper bound of 0.05 (see footnote above for details on this optimization process).

A summary of the observed (i.e., measured) copper and zinc $\log K_D$ values from the studies is provided in Figure 31. The median and mean copper $\log K_D$ values from Earley et al. (2007) samples are similar to those from Chadwick et al. (2005). Similar to the San Diego Bay data, the propeller wash study K_D values are generally lower than ambient samples from the same water body. The propeller wash study K_D values for Pearl Harbor are generally high than those from San Diego Bay (compare Figure 31 to Figure 28).

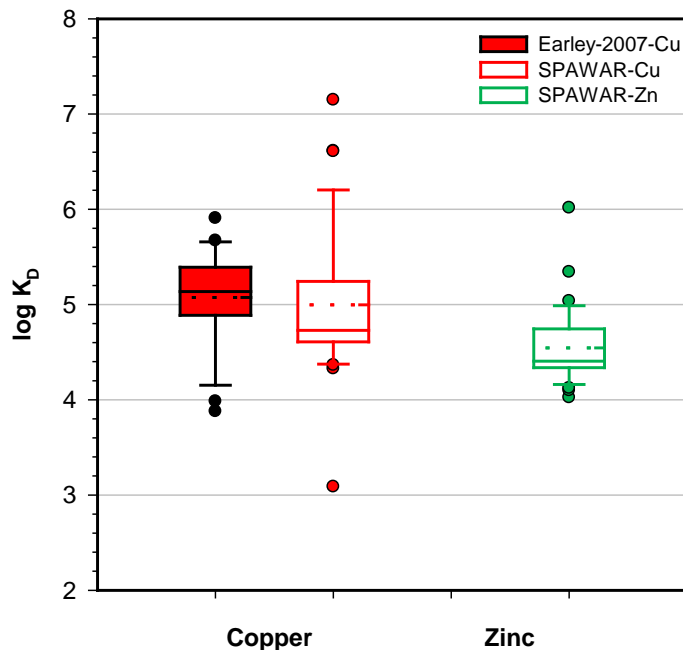


Figure 31. Summary of observed $\log K_D$ data from Earley et al. (2007) and the SPAWAR propeller wash sampling events at Pearl Harbor. The boundary of the box closest to zero indicates the 25th percentile, the solid line within the box marks the median, the dashed line within the box indicates the mean, and the boundary of the box farthest from zero indicates the 75th percentile. The error bars above and below the box indicate the 95th and 5th percentiles values, respectively. Points represent values outside of the 5th and 95th percentile (i.e. outliers), respectively. Error bars and outliers are only calculated if a minimum number of data points exist.

A comparison of model-predicted and observed $\log K_D$ values is provided for copper and zinc (Figure 32a). Similar to the San Diego Bay data, the model-predicted $\log K_D$ values for copper are generally within an order of magnitude of the observed $\log K_D$ values. WHAM7 calculations however greatly underestimate the observed $\log K_D$ values for zinc (i.e., values fell below the 1:1 line). As in the case of the San Diego Bay data, exclusion of cation competition for DOC, POC, HFO and HMO binding sites greatly improved the performance of WHAM7 in predicting $\log K_D$ values for zinc and had minimal effect on the $\log K_D$ calculations for copper (Figure 32b). These findings further support excluding Ca and Mg binding to DOC, POC, HFO and HMO when developing metal partitioning look-up tables for saline waters with WHAM7.

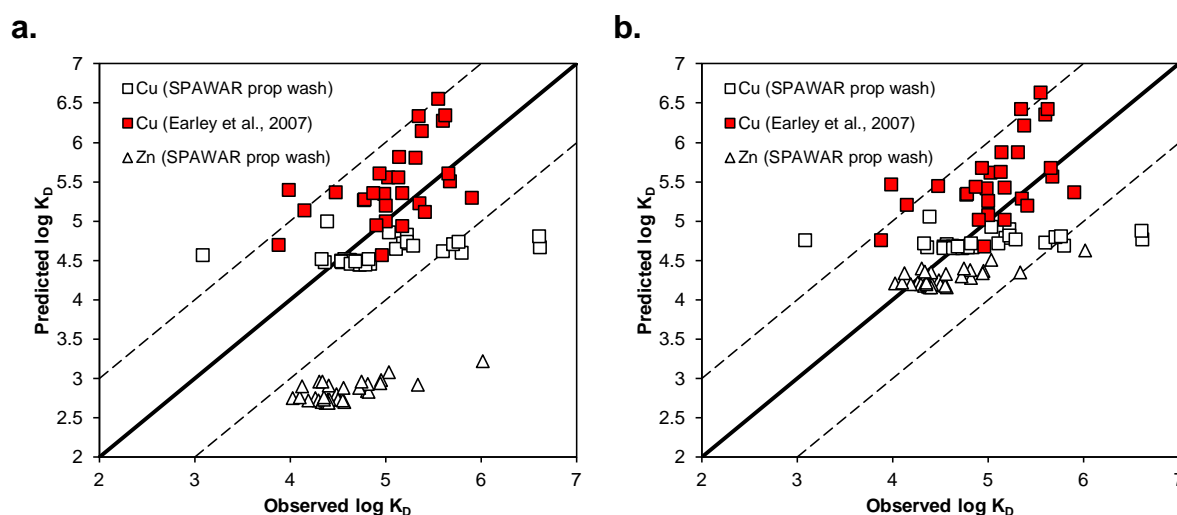


Figure 32. Pearl Harbor performance assessment plot for copper (Cu, squares) and zinc (Zn, triangles) for the Earley et al. (2007) dataset (hollow symbols) and the SPAWAR prop wash dataset (filled symbols). The analysis was made using (a) default model parameters and (b) with hardness cation (calcium and magnesium) binding to DOC, POC, HFO and HMO turned off.

Look-Up Table Development

As a first step in producing a look-up table, it is necessary to select the key determinants (state variables) of metal partitioning and select relevant ranges over which to evaluate K_D values. These are the water quality parameters that affect the extent to which metal bind to TSS and would be expected to vary significantly at the site or type of site being modeled. For WHAM7, the input parameters listed above can all potentially impact metal partitioning. However, for conditions associated with a particular site or site-type, not all of these parameters necessarily impact the K_D calculation significantly, nor do they always vary enough to warrant inclusion as a state variable. For example, the major ion composition and pH would not be expected to vary considerably in full-salinity marine water.

Once the state variables and their ranges are selected, a model input deck must be generated that considers all the various permutations of the state variables as input parameters to the speciation model. Once the model is run, the input and output values for K_D constitute the look up table for the particular site.

Application to San Diego Bay

To better illustrate the process of look up table generation, consider the following case of San Diego Bay. The salinity of San Diego Bay varies between approximately 32 and 35 practical salinity units (psu) (Chadwick et al., 2005). While this variation is generally small, it was nevertheless decided to use salinity as a state-variable since the concentration of key major ions can be related to this value through a simple end-member analysis (Di Toro et al., 2005). Table 16 below represents water quality parameters (low, average, high) for San Diego Bay compiled from recent SPAWAR propeller wash resuspension field activities and earlier San Diego Bay reports (Chadwick et al., 1999; Chadwick et al., 2005).

Table 16: Water Quality Parameters for San Diego Bay

	Total Copper, $\mu\text{g/L}$	pH	POC, mg/L	DOC, mg/L	Iron, mg/L	Salinity, psu
Value 1 (Low)	4	7.8	0.04	0.75	0.05	32
Value 2 (Ave)	10	8.2	0.25	1.5	0.40	33.5
Value 3 (High)	26	8.6	1.6	4	3.25	35

Using the three values of the six state variables in Table 16, there are 729 possible parameter combinations. Visual Basic for Applications (VBA) code, accessible within Microsoft Excel, was used to generate the WHAM7 input file with all parameter combinations. Details regarding the conversion of POC and DOC to particulate and colloidal humic and fulvic acid (i.e., the metal binding functional groups modeled in WHAM), and the conversion of iron to HFO can be found in Table A-27. The model was used to predict 729 realizations of the fraction particulate and the dimensionless distribution coefficient (K_D') that represent different water chemistries (i.e., different combinations of the input parameters). For these simulations hardness cation binding to DOC, POC, and HFO was excluded. The equation describing K_D , K_D' , and the fraction particulate (f_p) are presented in Table A-28. Tables with input values of the state variables, WHAM input values, and model-generated K_D' and fraction particulate output values are presented in Tables A-29 and A-30.

Application to Pearl Harbor

A lookup table was also generated for Pearl Harbor. Values are based on water quality parameters from the Earley et al. (2007) dataset and the SPAWAR propeller wash resuspension field activities from August 2012 (see Table 17).

Table 17: Water Quality Parameters for Pearl Harbor

	Total Copper, μg/L	pH	POC, mg/L	DOC, mg/L	Iron, mg/L	Salinity, psu
Value 1 (Low)	0.1	7.90	0.05	1	0.02	26
Value 2 (Ave)	3	8.25	0.8	2	0.2	30
Value 3 (High)	36	8.60	7	4	3	35.5

Using the same procedure as that for San Diego Bay, the model was used to predict 729 realizations of the fraction particulate and the dimensionless distribution coefficient (K_D') that represent different water chemistries (i.e., different combinations of the input parameters) for Pearl Harbor. Similar to the San Diego Bay simulations, hardness cation binding to DOC, POC, and HFO was excluded. Tables with input values of the state variables, WHAM input values, and model-generated K_D' and fraction particulate output values are presented in Tables A-31 and A-32.

Task 1c*: Predictive Capabilities in Lagrangian Modeling of Active Contaminant Transport in Complex Surface Water Environments

Task 1c: Background

The dredging and operation of harbors is a critical contributing element supporting the nation's and the world's economies. However, port activities must be managed in environmentally responsible ways. A risk assessment is required for developing an understanding of the balance of navigation objectives, environmental concerns, and costs. Environmental risk can only be determined when both exposure and effects are understood. Determining exposure involves identifying the key biological receptors (the impacted organisms), describing the course a stressor (e.g., a metal contaminant) takes from the release point to the receptor (i.e., direct, indirect, ingestion pathways), and describing the extent of the contact (e.g., dredged material plume migrating over a fish spawning site). Effects are the response of the biological receptor to the exposure, which can range from benign to acutely fatal. The predictive modeling discussed in this work describes the development and refinement of a scientifically justifiable methodology for quantifying contaminant exposure in coastal and inland water environments.

Understanding and predicting the exposure caused by contaminated sediments is most commonly accomplished through numerical modeling. However, models employing an Eulerian framework can be computationally expensive, which usually results in a limited number of scenarios examined and limited key parameters analyzed. In contrast, utilizing a Lagrangian methodology, which tracks the parcels of interest, usually allows for a more complete exploration of the system when the initial release of re-suspended sediment into the water column is well characterized. The Particle Tracking Model (PTM) has been developed specifically for the purpose of simulating the movement of multiple sediment classes (discretized as parcels of material) through complex open water flow fields (McDonald et al 2006, Lackey and McDonald 2007, Gailani et al. 2007, Lackey and Smith 2008). The numerical model combines accurate and efficient Lagrangian transport computations with effective visualization tools, making it a broadly applicable analysis tool for studies that focus on the release and dispersion of constituents throughout a surface water environment. PTM simulates the processes of particle advection, diffusion, settling, deposition, burial, and re-suspension as appropriate for each parcel at each numerical time-step. Data from both field and laboratory studies have been obtained to support the theoretical physical processes modeled.

** The numerical order of the Tasks are not followed – rather are presented in the natural progression of the research.*

The movement of dissolved water quality constituents, especially conservative ones such as salinity, can be easily mapped using PTM. The standard methodology for doing this treats the constituents as passive tracers. To a certain degree, a contaminant can be reasonably modeled as a conservative constituent, especially over short time scales. However, detailed tracing of active contaminants over the longer term is challenging for any numerical model because they are strongly affected by the partitioning of the contaminant into particulate and dissolved phases. This partitioning is important not only because it affects the contaminant pathways, but more importantly, because the toxicity of many contaminants is strongly dependent upon whether the contaminant is in a solid or dissolved state. In certain cases other processes, such as volatilization at water surface, may be important. Figure 33 shows a schematic of the contaminant partitioning processes.

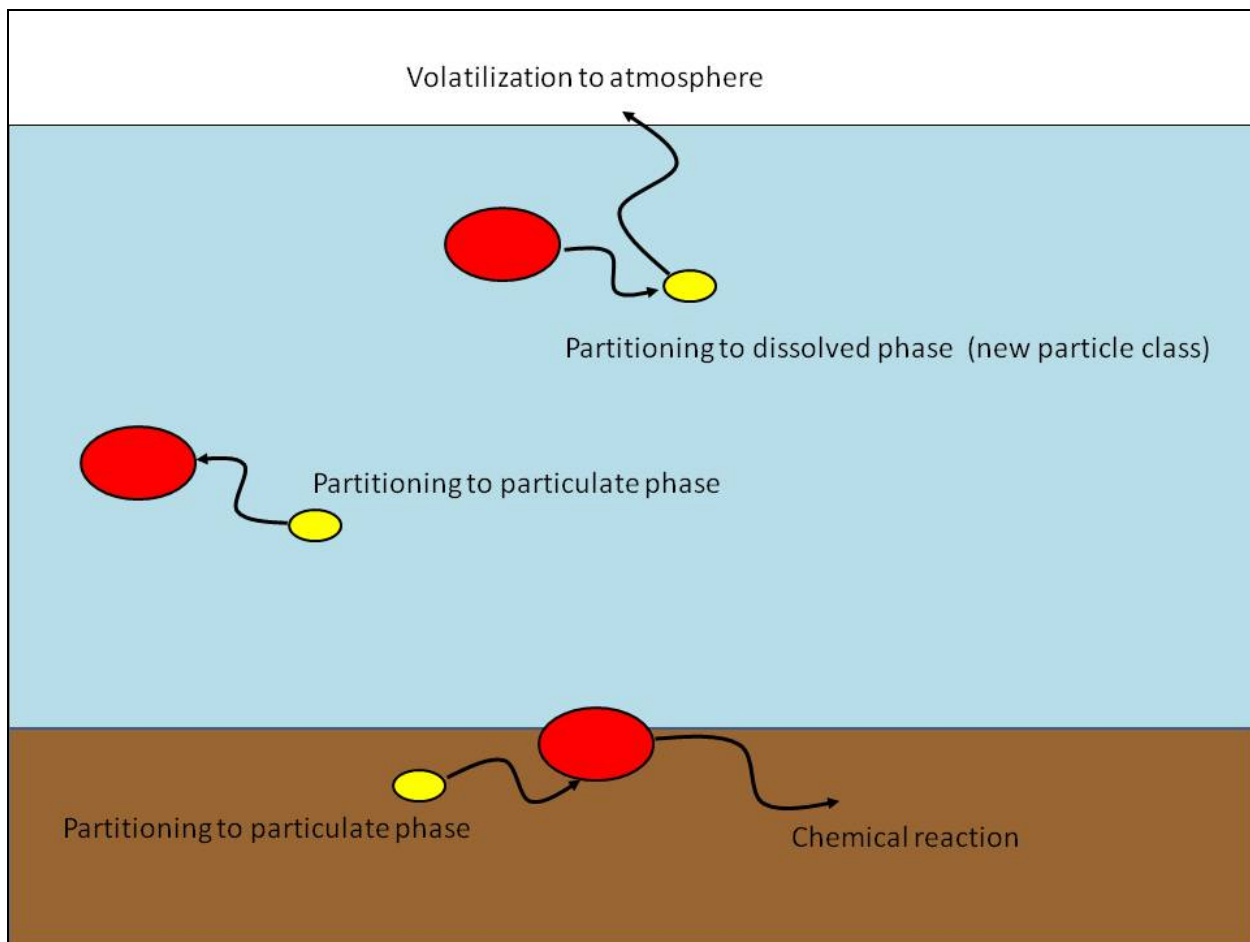


Figure 303: Schematics of contaminant partitioning between particulate (red) and dissolved (yellow) phases.

A new methodology, which is described in this report, has been developed within the PTM framework that allows for the partitioning of waterborne contaminants into solid and dissolved phases. The modeling assumes that the contaminants of concern (CoC) are initially incorporated into the bed in particulate form. As a bed disturbance releases them into the water column, PTM models their behavior by releasing large number of pairs of parcels. For each pair, one of the parcels behaves as a sediment parcel with sorbed contaminants, while the other behaves as a

neutrally buoyant parcel that contains the dissolved contaminant. Parcel positions and other state parameters are recorded at each model time step. Following a PTM model run, the number of particulate and dissolved parcels are summed within each water quality grid cell at each time step and the contaminant masses are partitioned among the parcels based upon the value of K_D , the partitioning coefficient. The method is organized into a three tiered approach with the increasing tiers representing increasingly complex methods of parameterizing the K_D term.

This report describes PTM's standard capabilities and provides details of the new methodology for calculating exposure from contaminated sediments. It then demonstrates the methodology using a case study in San Diego Bay where prop wash introduces contaminated sediments into the water column.

Task 1c: Materials and Methods

Tables 18 and 19 (lists of Symbols and Acronyms, respectively) are provided here for easy reference to assist the reader in following the discussions presented below.

Table 18: List of Symbols

Symbol	Name	Units
C or C_{tot}	contaminant concentration	mass/length ³
c_d	Dissolved contaminant concentration	mass/length ³
c_p	Particulate contaminant concentration	mass/length ³
C_{tot}	Contaminant concentration in water quality cell (i,j)	mass/length ³
Δt	time step	Time
E_t	Turbulent Diffusion Coefficient	length ² /time
F	functional representation of the parameters involved in the transport process	length/time

F_d	Dissolved fraction	mass/length ³
F_p	Particulate fraction	mass/length ³
h	Water Depth	Length
I,j	Position indices identifying the lateral position of a water quality parcel	dimensionless
K_d	Partitioning Coefficient	length ³ /mass
K_d'	Dimensionless partitioning Coefficient	dimensionless
K_{Et}	Empirical Diffusion Coefficient	dimensionless
m	Sediment concentration	mass/length ³
M_{caq}	Dissolved contaminant mass in water quality cell (I,j)	mass
M_{caqn}	Dissolved contaminant mass in dissolved parcel n'	mass
M_{cs}	Particulate contaminant mass in water quality cell (I,j)	mass
M_{csn}	Particulate contaminant mass in sediment parcel n	mass
M_{ctot}	Total contaminant mass in water quality cell (I,j)	mass
M_n	Sediment mass in sediment parcel n	mass
M_s	Sediment mass in a water quality cell (I,j)	mass

n	iteration timestep	dimensionless
N_p	Number of Particulate Parcels	dimensionless
II	Uniform Random Number	dimensionless
t	time	time
TSS	Total Suspended Solids Concentration	mass/length ³
u	vector velocity	length/time
u^*	Shear Velocity	length/time
u_D	Random diffusive transport velocity	length/time
V	Volume	length ³
x	vector position	length

Table 19: List of Acronyms

Acronym	Name
CH3D	Curvilinear-grid Hydrodynamics Three Dimensional model
CoC	Contaminant of Concern
DO	Dissolved Oxygen
DOC	Dissolved Organic Carbon

FeS	Iron Sulfide
f _{Fe}	Mass fraction of iron on the suspended sediment
foc	Fraction Organic Carbon
HFO	Hydrous Iron Oxide
MS	Metal Sulfide
PAH	Polycyclic aromatic hydrocarbons
POC	Particulate Organic Carbon
PTM	Particle Tracking Model
TSS	Total Suspended Solids
WHAM VII	Windermere Humic Aqueous Model Version 7

Description of Lagrangian Transport using PTM

PTM is designed to track the fate of constituents released from local sources (dredges, placement sites, outfalls, etc.) in complex hydrodynamic and wave environments. While the model was originally developed to map the fate of sediment introduced into the water column as a byproduct of dredging operations, it has been applied to a great variety of constituent types, both solids (debris, fish eggs, etc.) and dissolved chemical (salinity, outfall effluents, contaminants, etc.). Each local source is defined independently and may have multiple constituents. Model results are able to describe the fate of each constituent from each local source. Constituents are discretized into a large, but finite, number of parcels, each representing a tiny fraction of the entire mass of the constituent, and having the hydrodynamic properties of an individual particle. The model keeps track of the location and several additional variables (mass, fall velocity, suspension state, etc.) associated with each parcel as it time steps through a simulation.

The primary driver for the parcels in PTM is the flowfield, which is obtained as a pre-calculated hydrodynamic (and wave) model output. The hydrodynamic model is not coupled to the

sediment transport model (PTM); therefore the same hydrodynamic model outputs can be utilized for multiple PTM simulations. The external flow model requires a grid with bathymetry that covers the study area, and this same grid is also used by PTM. Additionally, PTM requires several other types of detailed input information (e.g., characteristics of the native bed, constituent data, a detailed description of the release protocols, etc.). Guidance about these model inputs are provided in McDonald et al (2006).

PTM employs both Eulerian and Lagrangian frameworks. Eulerian calculations are carried out over the entire domain and are thus dependent on the grid sizes. Eulerian calculations are mostly at sediment-water interface through bedform, bed shear and mobility, transport potential, and transport rates. In the Lagrangian framework, the waterborne constituents being modeled are represented as a finite number of discrete parcels that are tracked as they are transported by the flow. Like other Lagrangian particle trackers, PTM transport is in the reference frame of the particle, ultimately solving a classic system of equations:

$$\frac{d\vec{\mathbf{x}}}{dt} = \vec{\mathbf{u}} \quad (1)$$

In this system, \mathbf{x} is the particle position vector $\mathbf{x}=(x,y,z)$ and \mathbf{u} is the flow field velocity vector $\mathbf{u}=(u,v,w)$. Numerically this system of equations can be discretely solved as:

$$\mathbf{x}^{n+1} = \mathbf{x}^n + \Delta t \vec{\mathbf{u}}^n \quad (2)$$

Where n is the iteration number and Δt is the timestep. For sediment transport performed utilizing PTM, the equation becomes more complex:

$$\mathbf{x}^{n+1} = \mathbf{x}^n + \Delta t \mathbf{F}^n \quad (3)$$

where F is a function of the flow field velocity, diffusion, settling, and multiple other sediment transport processes (McDonald et al 2006). Integration of particles forward in time is performed using a Runge-Kutta scheme.

Particles deviate from the flow trajectory (the F function in Equation 3) primarily due to the forces of gravity and diffusion. PTM estimates diffusion through a turbulent diffusion coefficient, E_t , defined as:

$$E_t = K_{E_t} h u_*^n \quad (4)$$

Here, K_{E_t} is an empirical coefficient which relates E_t to water depth, h , and shear velocity, u_* . Thus, at each time step, the random diffusive transport velocity, u_D , is determined from:

$$u_D = 2(\Pi - 0.5) \sqrt{\frac{6E_t}{\Delta t}} \quad (5)$$

Here, Π is a uniform random number between 0 and 1. See (McDonald et al, 2006) for a more detailed discussion of these processes.

New PTM Capabilities for Modeling Contaminated Sediments

Modeling the fate of active contaminated sediments requires a few modifications to the normal PTM process. In PTM, a mass of sediment that is released from a bed is discretized into a large number of parcels, with each parcel representing a mass of sediment but having the hydrodynamic characteristics of an individual sediment grain. To model contaminated sediments the procedure involves releasing paired parcels, rather than individual parcels. The first parcel of each pair is the sediment parcel and contains a mass of the re-suspended bed sediment with the attached particulate contaminants. This parcel has a fall velocity equivalent to that of an individual sediment grain (or floc). The second parcel in the pair is the dissolved parcel. Being neutrally buoyant and independently subject to diffusion, its location will be expected to diverge from that of the first parcel over time. It is assumed that when the sediment is initially released from the bed, all the contaminant mass is in particulate form and zero contaminant mass is initially assigned to dissolved parcel of the pair.

The other main modification to the standard PTM procedure is that a second grid (referred to as the water quality grid) needs to be set up within the study area. This second grid is normally at a much finer horizontal resolution than the hydrodynamic grid. The second grid is two-dimensional with only one vertical grid cell. Additionally, a second time step (the water quality time step) may also be set up. This time step may be longer than the model run time step, or, for convenience, the same time step may be used for both.

For each water quality time step, each water quality grid cell is examined to determine the number of sediment parcels and the number of dissolved parcels within it. The contaminants are re-partitioned within the parcels based upon the value of the partitioning coefficient, K_D . Locally (within each water quality grid cell) it is assumed that equilibration of the contaminant between dissolved and particulate phases occurs instantaneously. Since each dissolved parcel starts with no contaminant mass, for the first time step, contaminant mass must flow from the sediment parcels to the dissolved parcels. However, for later water quality time steps contaminant mass can flow in either direction between dissolved and particulate phases. In the current scheme, it is assumed that no volatilization occurs, so locally contaminant mass is conserved. However, over time, sediment parcels can return to the bed and possibly become buried, taking their contaminant mass with them. Being neutrally buoyant, the suspended parcels remain within the water column. Special rules are set up to deal with cases where a water quality grid cell contains parcels of one type but none of the other. These involve partitioning with the nearest neighbor parcel of the missing type. Once the contaminants are re-partitioned in each of the water quality grid cells, PTM moves the parcels during the next model run time steps, until the end of a water quality time step is reached, and then re-partitioning of the contaminants occurs again.

The transport and fate of contaminants is tightly linked to their partitioning into particulate and dissolved phases. Mathematically, the total contaminant concentration, c , is separated into dissolved, c_d , and particulate, c_p , components. These components are assumed to represent fixed fractions of the total concentration through dissolved, F_d , and particulate, F_p , fractions, respectively. F_d and F_p must sum to one. The fractions are related to the suspended sediment concentration, m , through the partitioning coefficient, K_D :

$$F_d = \frac{1}{1 + K_D m} \quad (6)$$

$$F_p = \frac{K_D m}{1 + K_D m} \quad (7)$$

K_D has dimensions of volume per unit mass. Its dimensionless counterpart, K_D' , is equal to the partition coefficient times by the suspended sediment concentration. The partitioning coefficient relates the dissolved (c_d) constituent concentration to the particulate (c_p) constituent concentration as:

$$c_p = K_D' c_d \quad (8)$$

While the particulates can be removed or enter the water body through settling and resuspension, the dissolved contaminants remain in suspension. The possible alteration of dissolved constituents can happen through volatilization to air from the water surface but volatilization is not applicable for CoCs being considered (e.g., Cu, Ni, Zn). For the time period of concern in the example given below, we assume negligible volatilization so that mass is conserved between the dissolved and particulate phases. At every water quality time step, fractions of dissolved (F_d) and particulate (F_p) contaminants are calculated as functions of water column sediment concentration, m , using equations (6) and (7).

At the time of initial sediment release into the water column, the particulate contaminant mass is set proportional to the sediment mass. Once this initial condition is set, the mechanics of the contaminant partitioning between particulate and dissolved phases within each water quality cell at each water quality time step are iterated below.

Partitioning steps:

1. Determine the lateral (i,j) locations of all the particulate and dissolved parcels (note that for this application, the water quality grid is two-dimensional)
2. Update mass of particulate and dissolved contaminant at the cell (i,j).
 - a. Identify N_P particulate parcels in a cell(i,j) of volume V
 - (1) Sum of sediment mass : $M_s = \sum_1^{N_P} M_n$
 - (2) Sum of metal species mass in particulate form : $M_{cs} = \sum_1^{N_P} M_{csn}$
 - b. Identify N_D dissolved parcels in a cell(i,j) of volume V
 - (1) Sum of metal species mass in aqueous form : $M_{cdq} = \sum_1^{N_D} M_{cdqn}$
 - c. Total mass of metal species : $M_{tot} = M_{cs} + M_{cdq}$
3. Calculate sediment concentration and assign particulate concentration as a portion of sediment concentration.
 - a. Sediment concentration : $m = \frac{M_s}{V}$
 - b. $C_{tot} = \frac{M_{tot}}{V}$
4. Calculate fractions (equations (6) and (7))
5. Redistribute total contaminant into particulate and dissolved as:
 - a. $C_d = F_d C_{tot}$
 - b. $C_p = F_p C_{tot}$

6. The concentrations are converted to mass and divided up evenly by number of parcels in the grid cell, making a parcel associated with a particular mass of either particulates or dissolved metals.

- a. $M_{cp} = \frac{C_p \cdot V}{N_p}$

- b. $M_{cd} = \frac{C_d \cdot V}{N_D}$

A three tiered approach is used to calculate the important partitioning parameter, K_D , with increasing tier levels representing increasingly complex methodologies for parameterizing the term. There are benefits to each method based on computational efficiency and on the availability of data.

Tier 1 Partitioning

The Tier 1 methodology is the most straightforward. A constant value of K_D is used. The value is based upon typical or average values obtained from similar aqueous environments. It is expected to sometimes be the only realistic option when more detailed descriptions of the water chemistry are not available.

For the Case Study presented below, a Tier 1 K_D value of $10^{3.5}$ L/kg was used, based on a mean metal partition ($\log K_D$) for Cu in a sediment/pore water system (Allison and Allison 2005). This value applies to the conditions in San Diego Bay at the study site when the contaminant of concern (CoC) is copper.

Tier 2 Partitioning

To obtain K_D values using this methodology, the WHAM VII water chemistry model (Tipping et al. 2011) was used to develop a series of metal partition coefficients (K_{DS}) for the various combinations of pH, hardness (salinity), DOC, POC, hydrous iron oxides (HFO) and the total metal concentration shown in Table 20.

Additionally, fractional particulate values for copper in marine systems were also derived as a function of pH, salinity, DOC, POC, HFO and the total metal concentration. A multi-dimensional variable interpolation scheme was developed to select an appropriate K_D' value from the tabulated values based on the six state variables (pH, hardness (or salinity), DOC, POC, HFO and total metal concentration).

For the Case Study presented in tasks 3a and 3c, constant values for salinity, pH, and DOC were used which apply at the study site in San Diego Bay. POC and iron concentrations are determined from m times the f_{oc} and the f_{Fe} (mass fraction of iron on the suspended sediment), respectively. Values for m and the CoC (copper) are available in each water quality cell at each water quality time step because they have been derived through the PTM modeling. This provides the input values for all the state variables in the multivariate interpolation scheme so that a K_D value can be calculated for each cell for each timestep.

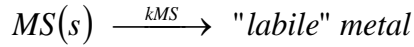
Table 20: Model Input and Output

STATE VARIABLES FOR MODEL INPUT							MODEL OUTPUT	
Total Cu		pH	POC	DOC	Particulate Iron	Salinity	logK _d ' = log(K _d x TSS)	Fract. Part.
(ug/L)	(mol/L)							
4	6.295E-08	8.2	0.04	1.5	0.05	33.5	-1.26	0.052
4	6.295E-08	8.2	0.04	1.5	0.4	33.5	-0.88	0.117
4	6.295E-08	8.2	0.04	1.5	3.25	33.5	-0.16	0.408
4	6.295E-08	8.2	0.25	1.5	0.05	33.5	-0.55	0.219
4	6.295E-08	8.2	0.25	1.5	0.4	33.5	-0.45	0.262
4	6.295E-08	8.2	0.25	1.5	3.25	33.5	-0.05	0.474
4	6.295E-08	8.2	1.6	1.5	0.05	33.5	0.25	0.639
4	6.295E-08	8.2	1.6	1.5	0.4	33.5	0.26	0.647
4	6.295E-08	8.2	1.6	1.5	3.25	33.5	0.37	0.701
10	1.57E-07	8.2	0.04	1.5	0.05	33.5	-1.23	0.056
10	1.57E-07	8.2	0.04	1.5	0.4	33.5	-0.76	0.148

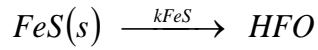
10	1.57E-07	8.2	0.04	1.5	3.25	33.5	-0.05	0.471
10	1.57E-07	8.2	0.25	1.5	0.05	33.5	-0.55	0.220
10	1.57E-07	8.2	0.25	1.5	0.4	33.5	-0.41	0.279
10	1.57E-07	8.2	0.25	1.5	3.25	33.5	0.03	0.520
10	1.57E-07	8.2	1.6	1.5	0.05	33.5	0.24	0.634
10	1.57E-07	8.2	1.6	1.5	0.4	33.5	0.26	0.644
10	1.57E-07	8.2	1.6	1.5	3.25	33.5	0.38	0.707
26	4.09E-07	8.2	0.04	1.5	0.05	33.5	-1.22	0.056
26	4.09E-07	8.2	0.04	1.5	0.4	33.5	-0.64	0.186
26	4.09E-07	8.2	0.04	1.5	3.25	33.5	0.11	0.561
26	4.09E-07	8.2	0.25	1.5	0.05	33.5	-0.59	0.203
26	4.09E-07	8.2	0.25	1.5	0.4	33.5	-0.37	0.297
26	4.09E-07	8.2	0.25	1.5	3.25	33.5	0.16	0.592
26	4.09E-07	8.2	1.6	1.5	0.05	33.5	0.23	0.629
26	4.09E-07	8.2	1.6	1.5	0.4	33.5	0.26	0.645
26	4.09E-07	8.2	1.6	1.5	3.25	33.5	0.43	0.728

Tier 3 Partitioning

The Tier 3 analysis expands upon the Tier 2 analysis and incorporates metal sulfide oxidation kinetics in PTM. This tier best reflects the scenario where anoxic sediments are resuspended into the water column. In this case, a large portion of the metal in sediment is present as metal sulfide (MS(s)). Since metal sulfides are known to oxidize slowly, the transformation of MS(s) to “labile” metal prop-wash resuspension events is described by a kinetic reaction.



where k_{MS} is the apparent first-order rate coefficient for MS(s) oxidation and is a function of the second-order MS(s) oxidation rate coefficient times the dissolved oxygen concentration (see Chapter 3 of the report for details). Similar to the metal, a portion of the iron in sediment is present as iron sulfide (FeS(s)). FeS(s) is also considered to be oxidized kinetically ultimately to hydrous iron oxides (HFO) during resuspension.



where k_{FeS} is the apparent first-order rate coefficient for FeS(s) oxidation and is a function of the second-order FeS(s) oxidation rate coefficient times the dissolved oxygen concentration. The corresponding first-order reactions for MS(s) and FeS(s) oxidation are solved as follows:

$$\frac{dC}{dt} = -kC \quad (10)$$

Thus the solution becomes

$$C = C_0 \exp(-kt) \quad (11)$$

The details of this methodology are further described in Chapter 3 of this report.

The partitioning of “labile” metal between dissolved and particulate phases is described as a function of six state parameters (pH, hardness, DOC, POC, HFO and total metal concentration). The methodology proceeds in the same way as for Tier 2 by using the multivariate interpolation scheme to derive a K_D value for a particular water quality cell at a particular water quality time step.

Task 3a and 3c: Verification Testing

Transport of Contaminants Due to Prop Wash in San Diego Bay

Task 3a and 3c: Background

Data from a field study conducted at San Diego Bay in April of 2012 were used as a proof of concept of the PTM modeling capabilities described above. Contaminant results are presented based upon all three of the Tier methodologies used to calculate the partitioning term.

San Diego Bay (Figure 34) is a crescent shaped bay, 43 km² in area, with an average depth of 8.5 m measured from mean sea level. The bay is approximately 23 km long and 1-5 km wide. The Bay contains both commercial and U.S. Navy port facilities.

Currents in San Diego Bay are predominantly produced by tides. Maximum tidal range in spring tides exceeds 2 m, whereas mean tidal range is about 0.85 m. Typical tidal current speeds range between 30-50 cm/s near the inlet and 10-20 cm/s in the southern region of the bay. Westerly afternoon winds occur throughout the year and are about 5 m/s (~10 knots); evening and early morning easterly winds occur primarily in winter and are less than 5 m/s. Because of the mild magnitudes and limited fetch areas, winds have only minor effects on currents and transport in the bay. Tides in San Diego Bay are mixed diurnal and semi-diurnal types. Water level and tidal currents in San Diego Bay have been investigated with both field and modeling studies (Richardson and Schmalz, 2012) (Wang, et al., 1998).

Task 3a and 3c: Materials and Methods

Tug-induced resuspension conditions were generated in San Diego Bay for monitoring. The objective of the field work component was the collection of discrete seawater samples, representative of background and conditions within the re-suspended sediment plume generated by a tug-boat propeller. These samples were analyzed in the laboratory for quantification of the load of metal and organic CoC associated with a suite of sediment-size fractions.

Tracking of metal and suspended solid concentrations were completed by sampling the plume generated by a tug boat. This tracking was done on a neap tide in order to have enough time to take a significant number samples on the plume. The plume was tracked by a boat equipped with a pump fast enough to fill up a 22-liter carboy in a couple of minutes. Samples were pumped from about one meter (1 m or 3 ft) below the water surface, and from mid-depth (~5 m or 15 ft). Samples from bottom waters were avoided as the sampling pump could induce resuspension from bottom sediments, affecting the concentrations in the plume.

Background samples of sediment and water were collected prior to the resuspension event. A C-14 Tractor tug-boat was used in San Diego Bay. The vessel has a 360°-rotation twin-ducted propeller, located at the bottom of the boat. The tug-boat is moored adjacent and pointing into a pier wall. The starting time for the resuspension event is predetermined based on tide times. Once the time is achieved, the tug-boat operates the engines at the predetermined time and power, or rpm, sufficient to generate a visible surface plume of re-suspended sediments. Once

the tug-boat engine stops, then the sampling boat started tracking and sampling the plume for about 2 hrs. A diagram of the resuspension event procedure, including a schematic of the mapping is shown in Figure 35.

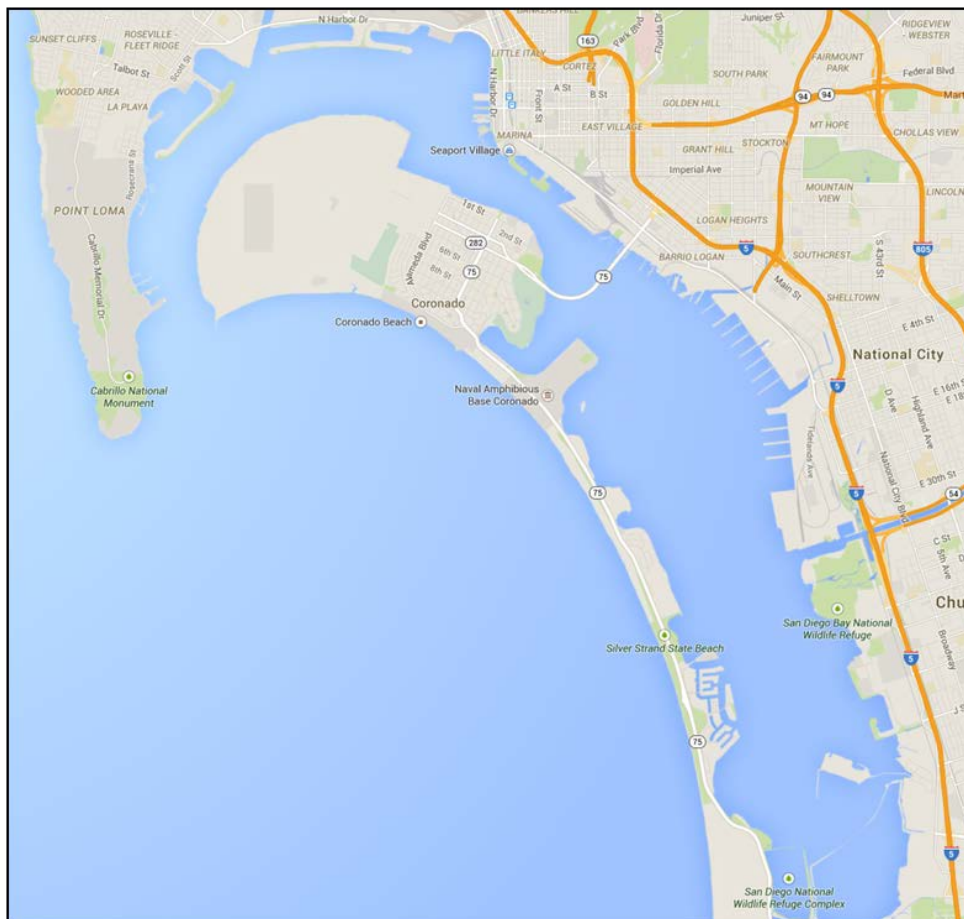


Figure 34: San Diego Bay

Water column sampling of the sediment plumes induced by the C-14 tugboat propellers was conducted on April 4, 2012 (Figure 36). The tugboat parked with the bow against the pier wall between Pier 4 and Pier 5 at 1:45 pm. At 2:00 pm, the tugboat started its propeller running at 180 rpm which was increased to 260 rpm (close to maximum power) at 2:05 pm and then stopped at 2:11 pm. During and after the running of the propellers, sediment plumes were visible both from the ECOS sampling boat and from the deck of the USS Bob Hope, which was parked in an adjacent pier. The ECOS sampling boat started to collect water samples by chasing after the plume, following directions from the observer on the deck of Bob Hope. The first sample was collected at 2:14 pm, when samples of both the surface water (3 ft below surface) and mid-depth water (15 ft below surface) were collected. Sampling continued until 3:28 pm when the last water samples of surface and mid-depth layer were collected. These water samples were analyzed for three (clay, silt, and sand) particle size classes and eight metals (Cr, Ni, Cu, Zn, As, Ag, Cd, and Pb) in both dissolved and particle-bound phases. In addition, PAH in these water samples were also analyzed.

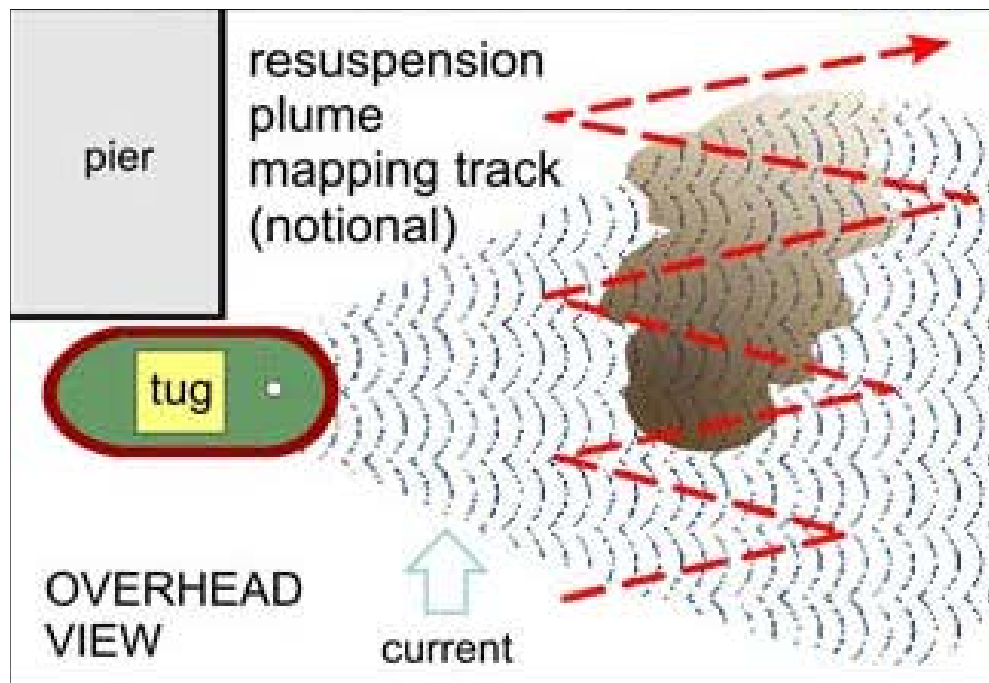


Figure 315: Schematic of tug plume monitoring



Figure 36: Tug, sampling boat, and plume in San Diego Bay

Fractionation is done by filtering through sieves, meshes or filters of the indicated pore-size. Each carboy is agitated manually following the same pattern, and a 1 L sample is collected in a graduated cylinder as soon as possible using the spigot. This aliquot is then filtered through a clean, pre-weighed (i.e., tared) 60µm mesh. Enough aliquots are filtered (about 5 L) in order to accumulate a measurable mass of sand on the mesh. The filtered sample is then used for filtration/quantification in the other two smaller pore-size filters, filtering enough sample volume to accumulate a measurable amount of sediment in each phase. All the filters are tared and the mass of retained sediment is quantified after drying. Subsamples of 125 mL filtrated seawater are collected for each fraction and acidified to $\text{pH} \leq 2.0$ with quartz-still nitric acid (Q-HNO_3) for metal quantification by Inductively Couple Plasma with detection by Mass Spectrometry (ICP-MS). Alternatively, 1 L samples are collected from selected samples in amber-glass bottles for quantification of organic contaminants. Figure 37 depicts a flowchart of laboratory processing and analysis of aforementioned samples.

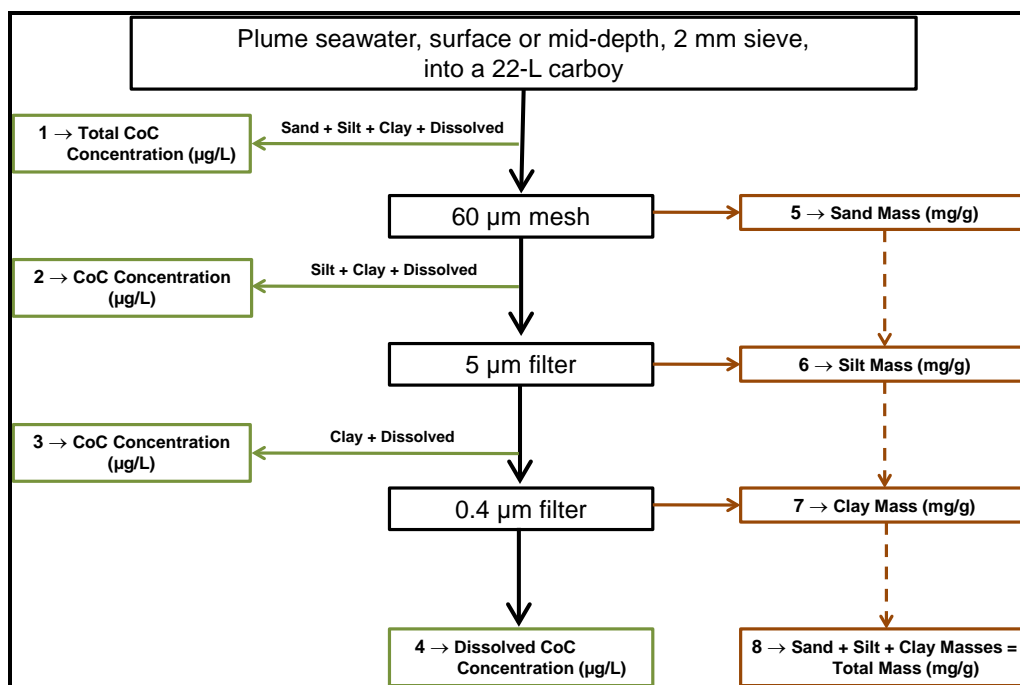


Figure 327: Flowchart of laboratory processing and analysis of the field samples for determination of CoC (i.e., metals and organic contaminants) concentrations in the total, sand, silt, clay and dissolved fractions. Information in the middle represents the filtration sequence, information to the left are concentrations measured in the filtrated seawater, and information to the right are masses retained by the respective filter.

PTM Bathymetry and Hydrodynamics Inputs

A CH3D model (Curvilinear-grid Hydrodynamics Three Dimensional model) was used to generate the San Diego Bay hydrodynamic inputs needed for PTM. CH3D is a boundary-fitted, finite difference, Z-coordinate, hydrodynamic model developed at the U.S. Army Corps of Engineers Waterways Experiment Station (Johnson et al., 1991). The 3D general purpose model is

intended for simulating flows in rivers, lakes, and coastal areas. The model solves the three-dimensional transport equations and is based upon the Boussinesq approximation and the hydrostatic assumption.

The hydrodynamic grid contained 70 by 199 rows in horizontal plane (Figure 38) with up to fifteen 2.5 m thick vertical layers, depending upon the depth. The highest resolution grid cells were placed at the study site near Piers 4 and 5 where the prop wash events occurred. The model simulation time period was 7 days between 4/2/2012 00:00 and 4/8/2012 23:00, including model spin-up time. For PTM modeling input, water level and 3-dimensional velocity data at each grid center were saved for the time span of 4/3/2012 00:00 – 4/8/2012 23:00.

PTM Sediment Resuspension Source Term

One key input parameter for the PTM model testing was the rate and duration for the bed sediment introduction into the water column (the resuspension mass rate) by prop wash from the tugboat propellers. Utilizing a propeller wash model based on Maynard's Formulae at Full Thrust (150 rpm) for 600 seconds (14:01:00-14:11:42 and subtracting 42 seconds for cold start and ending of the tugboat), an initial sediment suspension curve was generated.

This resuspension mass was introduced into the water column in the two CH3D hydrodynamic model grid cells shown in Figure 39, with half going to each over the time period (14:01:00 to 14:11:42). The sediment was uniformly distributed throughout the depth of the water column. The sediment size class was assumed to be a medium silt (20 microns) for this test case with a settling velocity calculated by the model (see MacDonald et al, 2006).

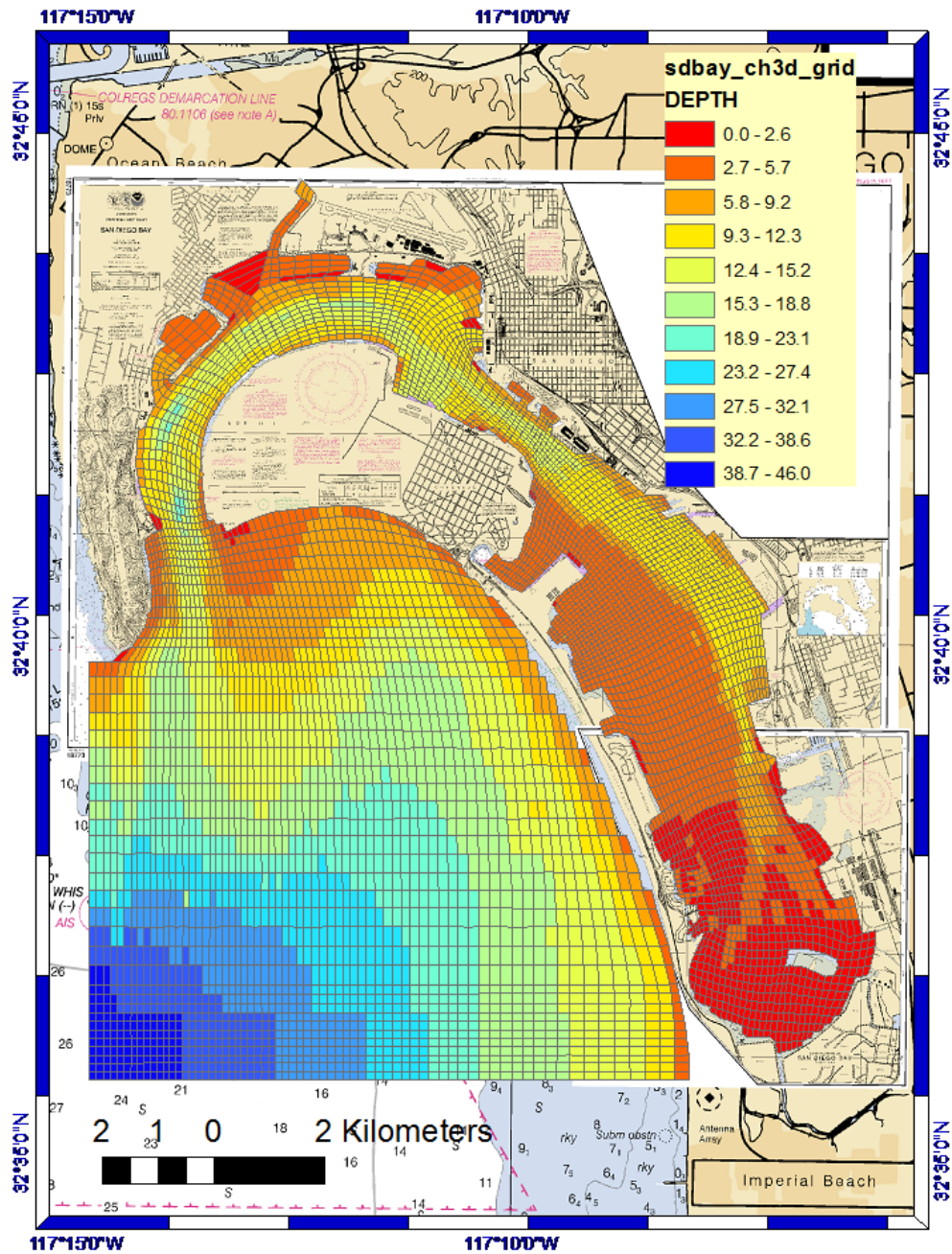


Figure 38: CH3D hydrodynamic model grid bathymetry.

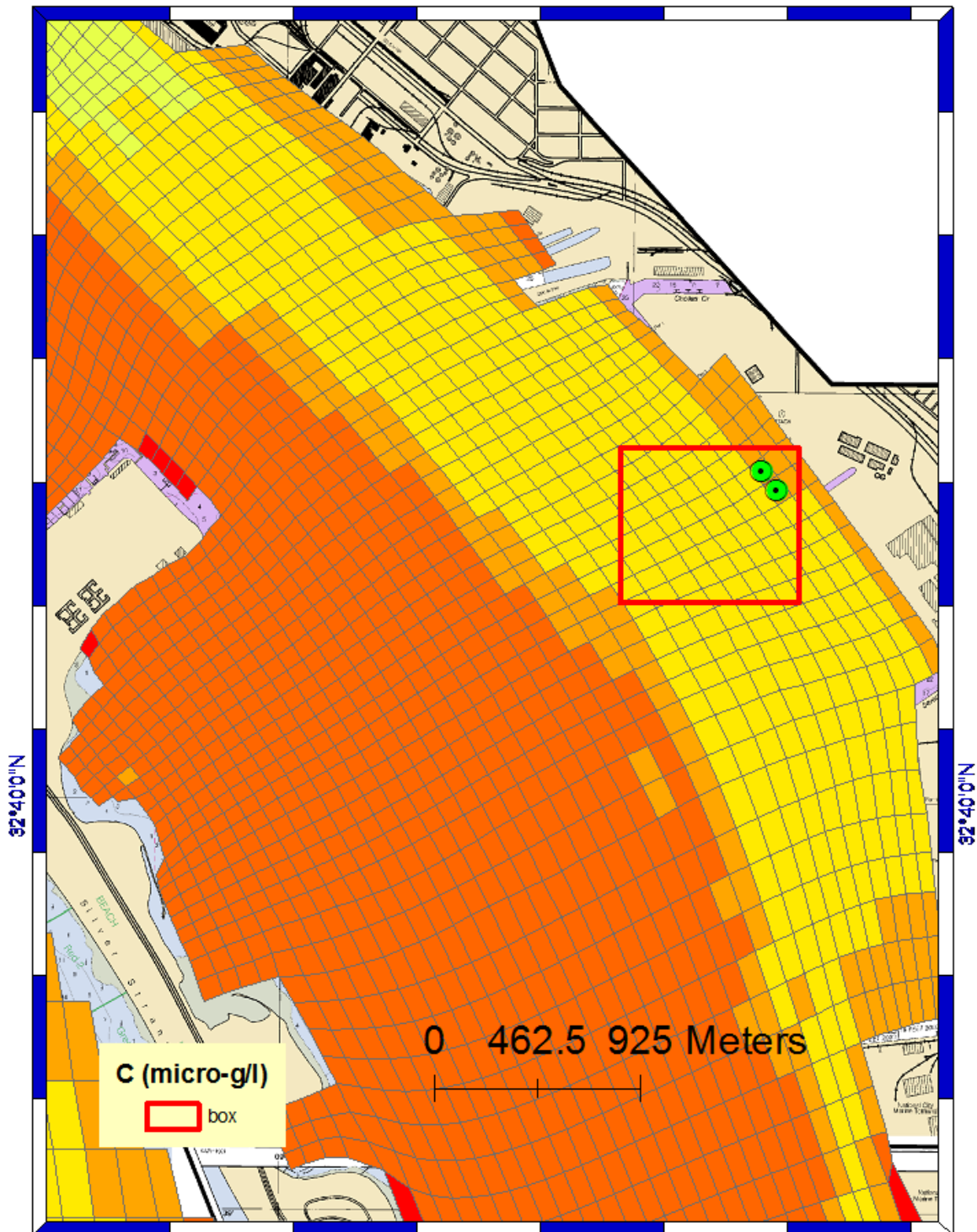


Figure 339: The location of the prop wash source terms are shown by the green circles with black centers. The red rectangle shows the location of the water quality grid.

PTM Simulation Details

A PTM simulation for re-suspended sediment in San Diego Bay was performed for 4 days (4/4/2012-4/8/2012). Figure 40 shows the tides during the simulation time period. The sediment source was introduced into the water column over a 600 second period at the beginning of the simulation. The four day model run time period was enough time for substantial particulate and contaminant transport to occur (e.g. settling of the sediment out of the water column and movement of contaminant between particulate and dissolved phases).

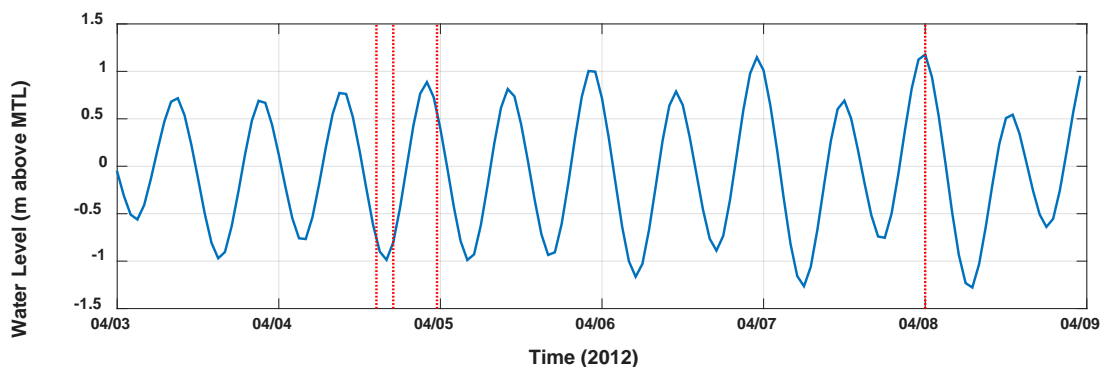


Figure 40: Tides during the simulation. The first red line represents the initiation of prop wash at 4/4/2012 14:00. The second red line represents the end of prop wash. Two following lines (3rd and 4th) represent the time references in Figure 37c and 37e.

PTM was run in full 3D mode. Model output included particle location, mass, and grainsize characterization. A 10 second time step was used as both the model run time step and as the water quality time step. A total of 4800 kg of sediments was released at the two prop wash sites contained in 48,000 sediment parcels (approximately 0.1 kg of sediment per sediment parcel). With an equal number of dissolved parcels released, a total of 96,000 parcels were tracked during the model simulation. Contaminants with a concentration of 203 mg Cu per kg of sediment were also added to the sediment parcels at the time of initial release.

A water quality grid was established as shown in Figure 38 having 800 by 700 horizontal grid cells, each with a volume of 1 m² (horizontal) times the water depth. At each water quality grid cell, the contaminant mass of both the sediment and the dissolved parcels were calculated and converted to concentration based on volume of the cell.

For the Tier 1 analysis, a constant K_D value of $10^{3.5}$ L/kg was used. For Tier 2 and 3 calculations, the salinity, pH, and DOC were assumed to have the constant values of $S = 33.5$ ppt, $pH = 8.2$, and $DOC = 1.5$ mg/L. For iron, a fixed fraction value was used based on the San Diego Bay data of 0.0201 mg Fe / mg TSS. For POC, the following relationship that was developed based on site-specific POC and TSS measurements in San Diego Bay was used (see Chapter 3 for details):

$$POC = [0.063 + (TSS - 0.246) \times 0.02] \quad (12)$$

These values were entered into the multi-dimensional variable interpolation scheme discussed in the methods section to obtain an appropriate K_D value in each water quality cell at each water quality timestep.

For the Tier 3 calculations, we introduced 202 mg of CuS and 1 mg of labile-Cu per kg sediment. We also introduced 20,000 mg of FeS and 100 mg of HFO per kg of sediment. We set $k_{FeS}=1.25/\text{Hr}$. For CuS reaction we used a range of decay rates, $k_{CuS}=0.005/\text{Hr}$ - $k_{CuS}=0.05/\text{Hr}$. These iron and copper values were used to define the terms used in the multivariate analysis described in the Methods section above, which was used to obtain appropriate K_D values in each water quality cell at each water quality timestep.

Task 3a and 3c: Results

Particulate Transport

PTM parcel pathway results are presented in Figure 41. Dissolved contaminant parcels are shown in red and parcels representing contaminant in the particulate phase are shown in blue. As dissolved and particulate parcels are released at the initial point, the hydrodynamic flow conditions transport the resuspended sediment away from the piers and then back towards the initial release point. The particulate parcels begin to settle out of the water column fairly quickly after the initial release. Within a day lateral mixing allows the discrete release from the two different locations to condense into one cloud. Soon all of the fine sediment has settled completely out of the water column and only the dissolved phase parcels are transported with the flow.

These qualitative results which represent the general transport pathways are the same for all three approaches (Tier 1-3). These results are qualitative because while they show the transport pathways of the different types of parcels, the contaminant amount associated with each parcel may differ dependent on the approach (Tier 1-3) of determining the K_D value. The quantitative differences between the three approaches are shown in subsequent plots for contaminant mass and maximum contaminant concentrations.

Figure 42 shows the time series of total mass of sediment in both deposited and suspended states. This plot also verifies mass conservation between deposition and suspension as the total mass of sediment remains constant. Initially all of the sediment is in suspension but within 36 hours of the simulation almost all the sediment has deposited. This is supported by Figure 43 which shows a time series of the maximum TSS (g/L). This is the maximum value of TSS throughout the area at a point any time. Initially the sediment is introduced at locations shown in Figure 38a. The largest values of TSS are seen at this point. Over time, the particles are transported by flow, causing the diffuse spreading of sediment (Figure 38e) and most of the sediment has deposited within 36 hours of release. Therefore the maximum TSS has decreased significantly.

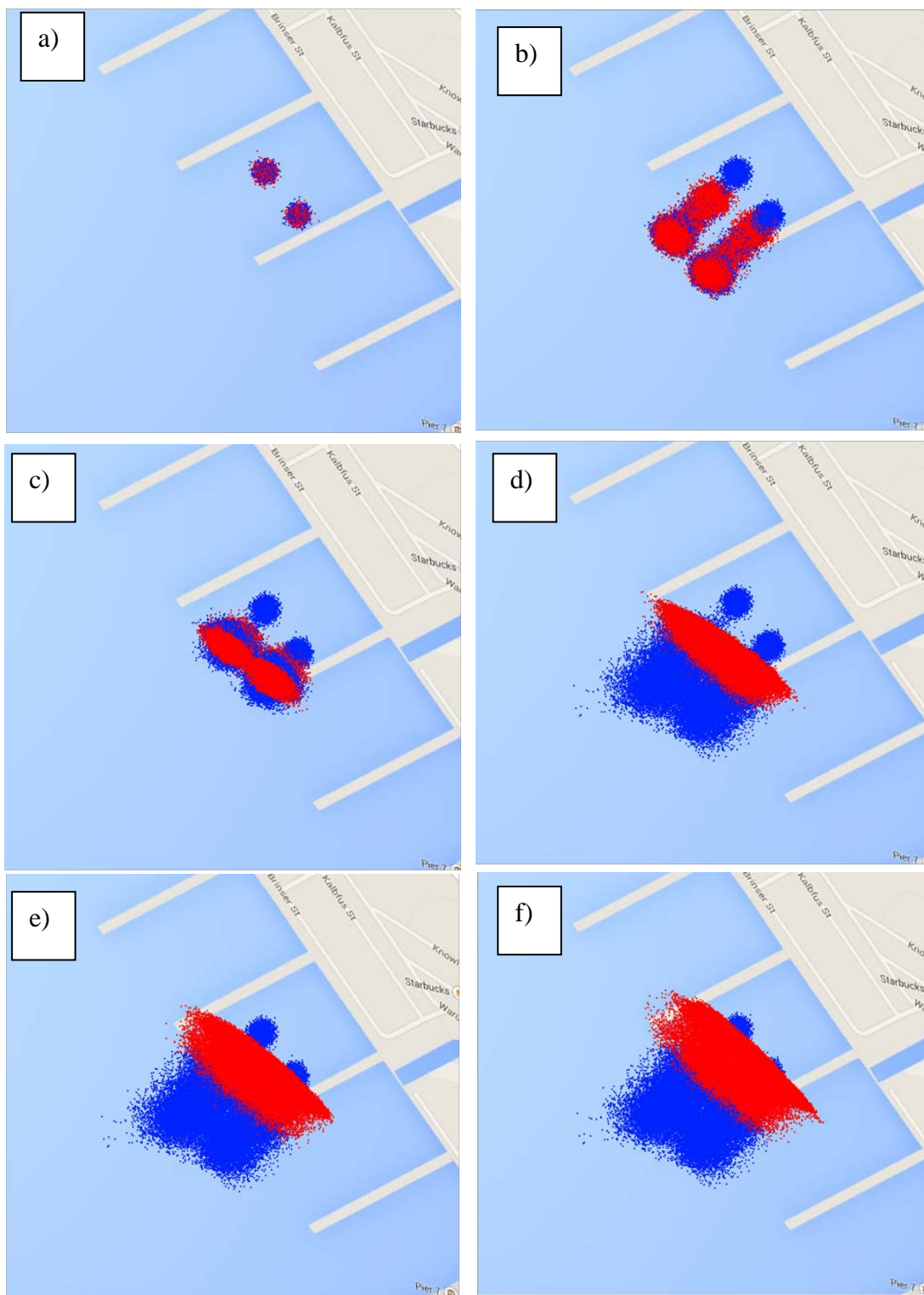


Figure 41: Parcel positions at 4/4 2pm, 4/4 4pm, 4/5 12am, 4/6 12am, 4/7 12am and 4/8 12am. Red parcels are dissolved contaminant positions and blue represents particulate parcels.

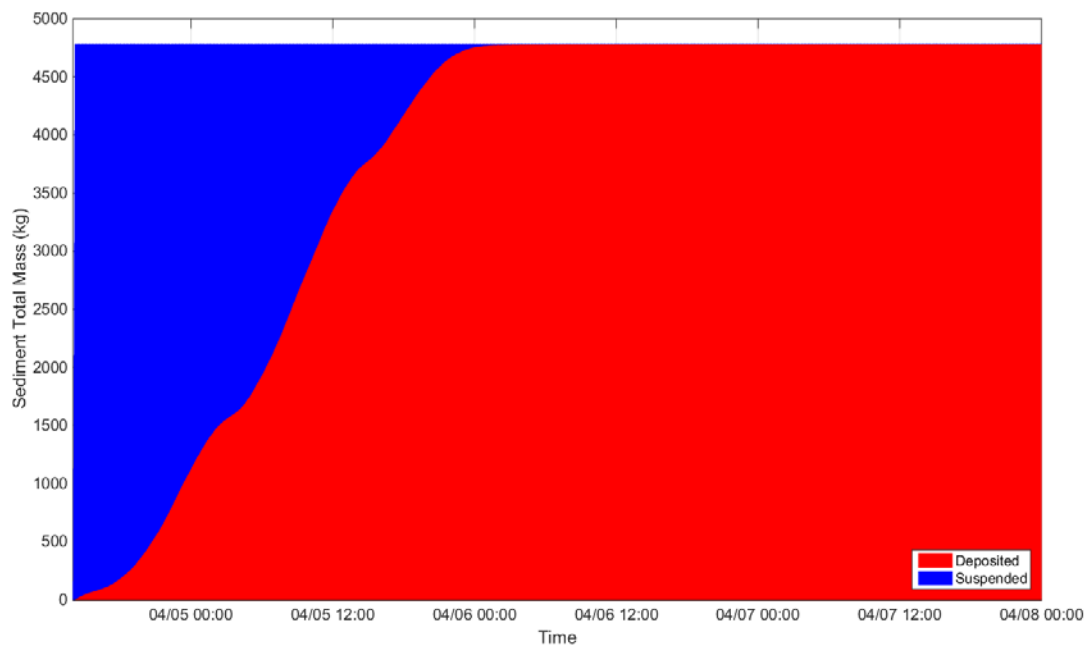


Figure 42: Time series of total sediment mass: deposited (red) and suspended (blue)

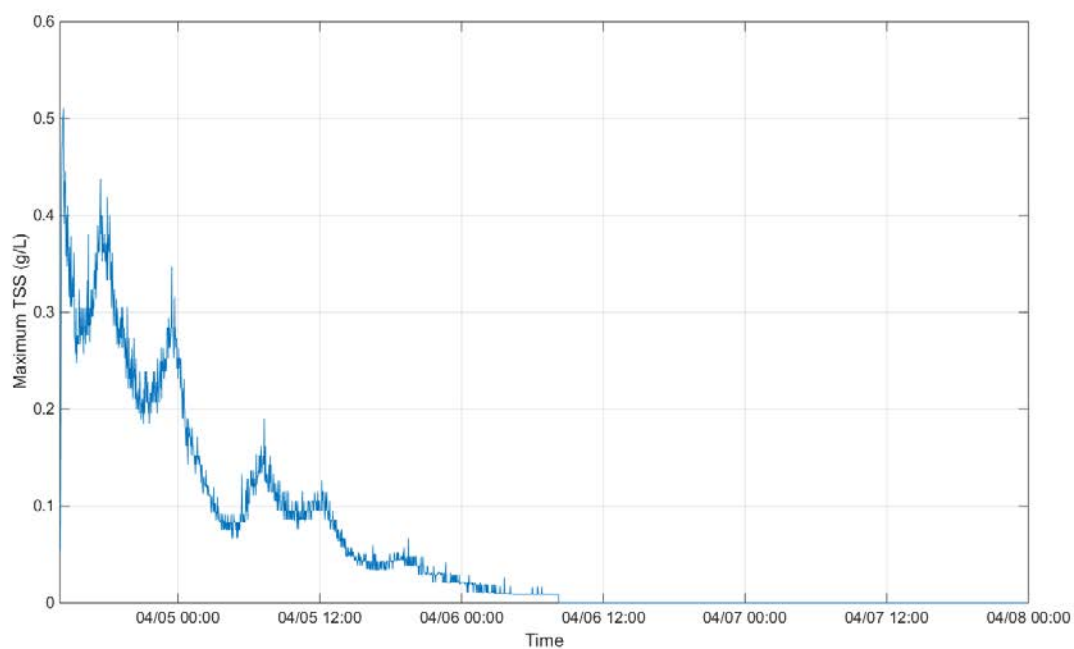


Figure 43: Maximum TSS

Contaminant Concentration

For Tier 1 and 2 methods, Cu (contaminant) mass is described as suspended in particulate form, deposited in particulate form, or dissolved (see Figure 44). Dissolved contaminants are always in suspension. Both methods follow the same trends. As seen in Figure 44, at the beginning of the simulation all contaminants are introduced into the water column in the suspended particulate form. However, some of the particulate contaminants quickly partition into the dissolved phase. Soon the particulate phase Cu begins to settle and deposit on the bed, so the amount of Cu mass shown in the red region steadily increases. The area in blue, which is the suspended contaminant, continues to decrease until there is none left. By the end of the simulations, all of the Cu is either in particulate form at the bed or in dissolved form in the water column. While the overall trends are the same for the two methods, the Tier 1 and Tier 2 calculated results differ in the percentages of contaminants in each form. The Tier 1 model, which is based on a K_D value that was selected from the literature, predicts approximately 0.4 kg of Cu in the particulate phase by the end of the simulation. The Tier 2 model, which is based on a computed K_D using WHAM VII, predicts 0.2 kg of Cu in the particulate phase.

The Tier 3 method is a more complex approach and acknowledges that Cu is initially in the form of CuS, which remains in particulate phase. CuS must transition to labile Cu before it can eventually become dissolved. An oxidation rate is used to describe how fast that transitioning occurs. Two oxidation rates were considered in this test case: 0.005/hr and 0.05/hr. In Figure 45, the time series of contaminant mass is color coded for three forms. CuS in its particulate form is shown in red. The labile-Cu is shown in blue and the dissolved Cu in green. Unlike Figure 44, the particulate forms of Cu (CuS(s) and labile particulate Cu) are not designated into deposited and suspended Cu. However by the end of the simulation, because all of the sediment is deposited, it can be deduced that all of the CuS is in sediment deposited on the bed. The overall trends between the two plots are similar but the 0.005/hr decay rate results in less than 10 percent dissolved Cu, while the 0.05/hr decay rate results in approximately 40 percent dissolved Cu.

A time series of maximum concentration for the dissolved phase is shown in Figure 46. The blue line represents Tier 1, the red line represents Tier 2, and the yellow and purple lines represent Tier3 with oxidation rates 0.005/hr and 0.05/hr respectively. Once again, the overall trends of the time series are the same. The initial maximum contaminant concentration in the dissolved phase is approximately 9 $\mu\text{g/L}$ for Tier 1 and 25 $\mu\text{g/L}$ for Tier 2 in which instantaneous partitioning is allowed while the initial maximum concentration is close to zero for Tier 3 in which labile Cu is very small at time of release (1 mg per kg of sediments). The subsequent patterns of peaks and troughs show the influence of the tide. A trend of overall decrease in the concentration value represents the diffusion and transport of the parcels away from the initial source location. Resuspension of deposited material leads to peaks in concentration after initial release. However, after about 36 hours of release, dissolved parcels are so scattered within a large volume of water body that the maximum concentration reaches nearly zero. The noise in the maximum concentration is caused by the discrete computation algorithm. Tier 2 appears to predict the largest amount of dissolved Cu after release by prop wash but becomes diluted within 36 hours. Different assumptions in the Tier 2 calculation may lead to different results. Tier 1 is very similar to Tier 2. Tier 3 predicts lower dissolved Cu concentrations during the first 36 hours before dilution. All Tier 3 computations result in nearly zero concentration of dissolved

Cu after about 36 hours. This is the result of the slow kinetics of CuS(s) oxidation. As shown in Figure 46, an apparent first-order CuS oxidation rate coefficient of 0.05/hr produced results similar to the Tier 2 model within 24 hours of the prop wash event. The slower apparent first-order CuS oxidation rate coefficient of 0.005/hr however resulted in much lower concentrations of dissolved Cu.

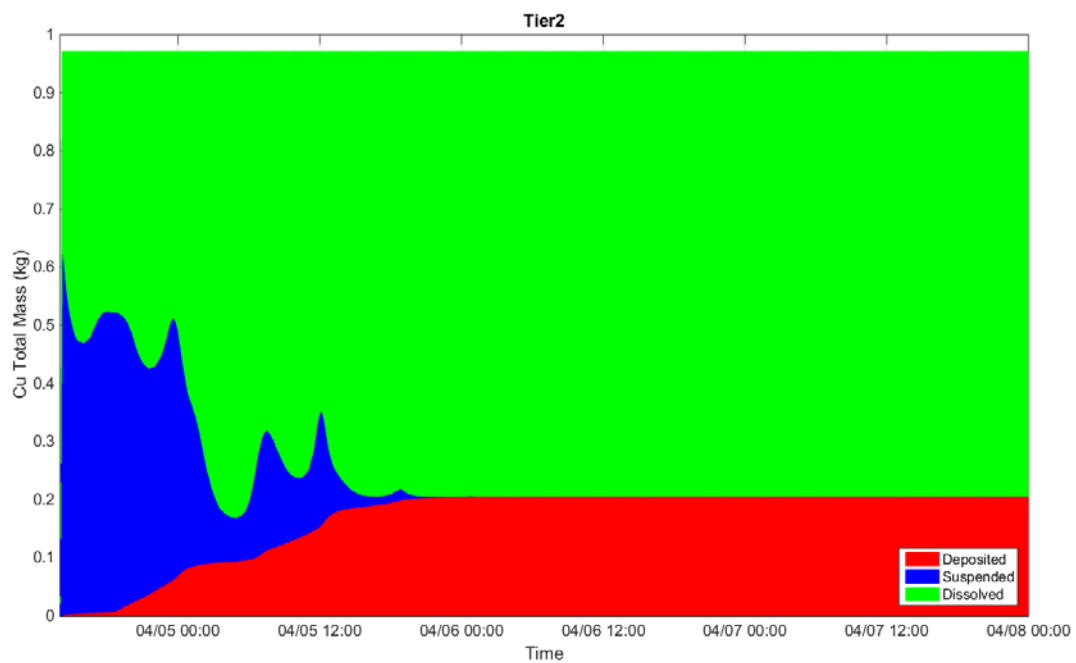
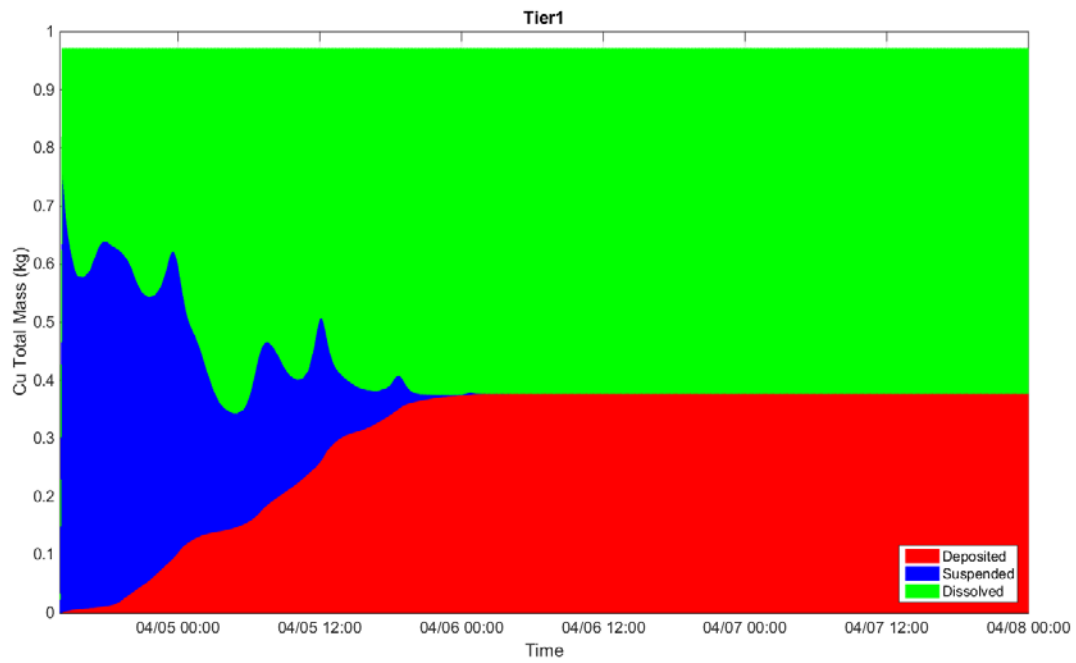


Figure 344: Time series of particulate and dissolved Cu mass for Tier 1 and Tier 2 computations.

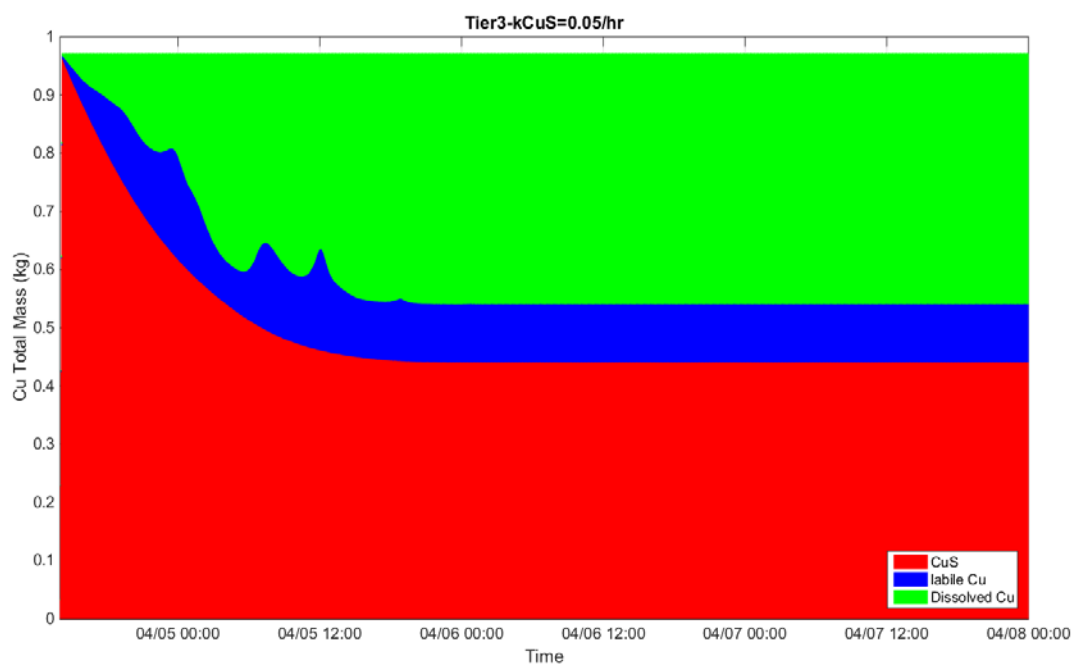
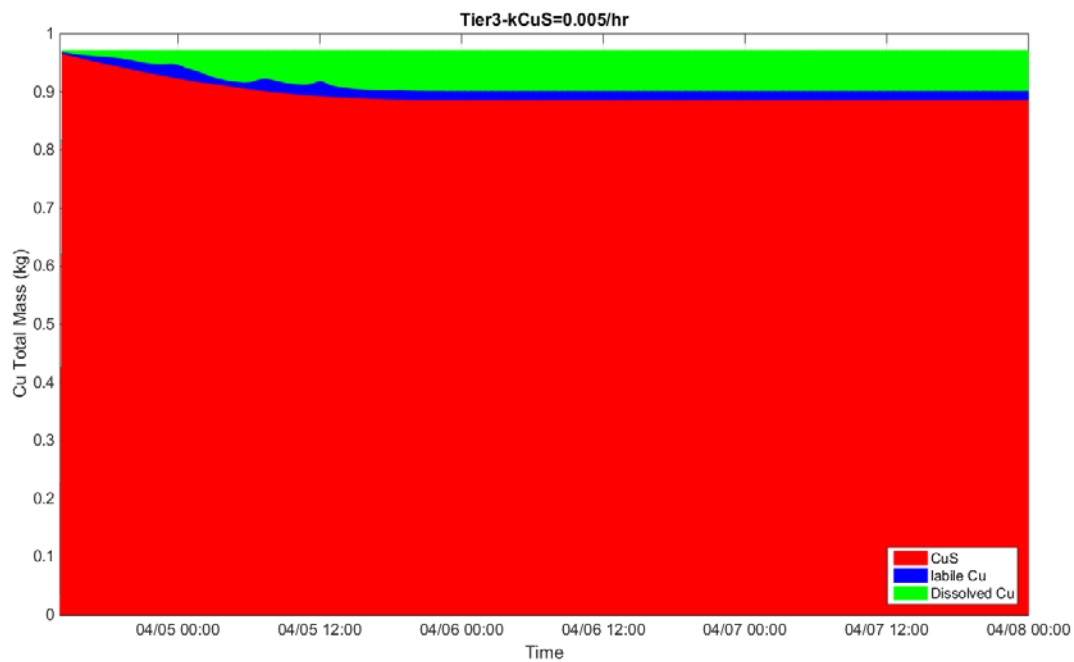


Figure 355: Time series of particulate mass (CuS – red and labile Cu-blue) and dissolved mass (green) for Tier 3 with two different decay rates.

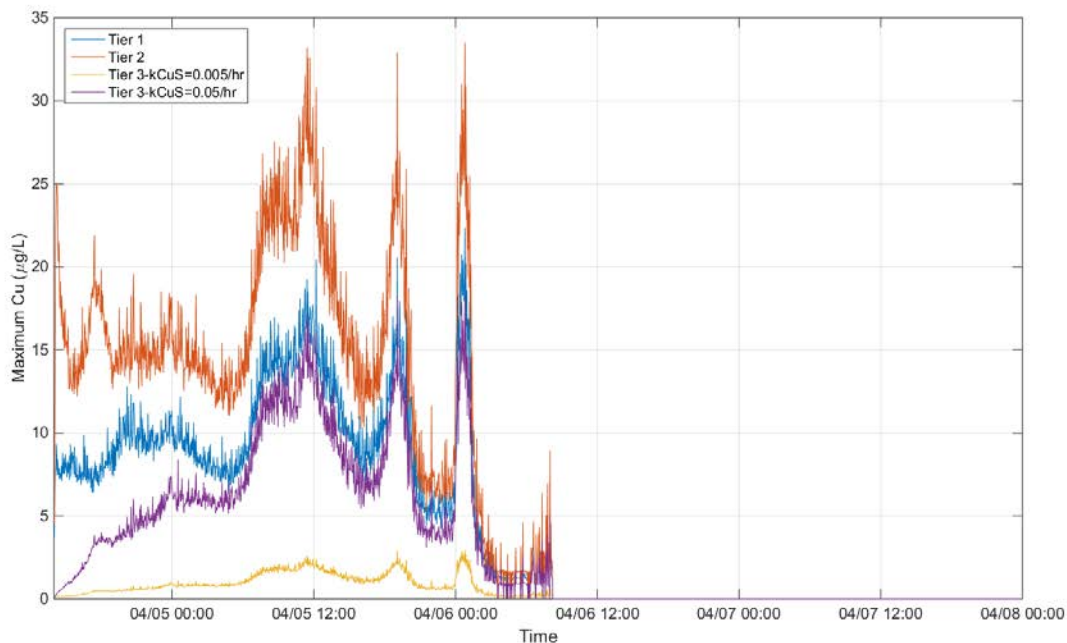


Figure 366: Time series of maximum concentration for dissolved phase contaminant

Task 3a and 3c: Case Study Conclusions

Simulations were performed to determine the amount of contaminant (Copper) released from sediment during resuspension due to prop wash. Within the simulation period, the resuspended sediment deposited rapidly with almost all of the particulate contaminant being retained within 1 km of the original release location. This limited dispersal of resuspended sediment was in large part due to the nature of the confined release point (i.e., being near shore and between two piers).

Of the simulations presented, Tier 1 and Tier 2 model results are considered to be representative of resuspension of oxic sediments. For this scenario, particulate metals in sediment are primarily sorbed to POC and HFO. Upon resuspension into the water column, sorbed metal quickly redistributed between the dissolved and particulate phases. This redistribution was described in the Tier 1 model using a constant K_D value that was selected based on a literature survey of observed partition coefficients for Cu in sediments (Allison and Allison 2005). Results of the Tier 1 model simulation showed that 60 percent of the particulate Cu ultimately partitioned in the dissolved phase. In the Tier 2 model simulation, the redistribution of metal between the dissolved and particulate phases was described by a more refined metal partitioning computation that continuously calculated K_D as a function of six state variables (pH, salinity, DOC, POC, HFO and the total metal concentration). Assigned values of the six state variables were based on site-specific information from San Diego Bay. Three of the state variables (POC, HFO and the total metal concentration) were also allowed to vary in time and space to simulate changing conditions occurring during and after the prop-wash event. The Tier 2 model simulation was therefore considered to be more representative of metal release that would be associated with

resuspension of oxic sediments in San Diego Bay. Results of this simulation showed that 75 percent of the particulate Cu ultimately partitioned in the dissolved phase.

In contrast to the Tier 1 and 2 model runs, the Tier 3 model results are considered to be more representative of resuspension of anoxic sediment. For anoxic sediment, metals such as Cu are expected to be present primarily as CuS(s), which are known to oxidize slowly in the presence of dissolved oxygen. The oxidation of CuS(s) to labile Cu was therefore modeled as kinetic process. The labile Cu was considered to partition between the dissolved and particulate phases following the Tier 2 modeling approach. For Tier 3 simulations, a range of CuS(s) oxidation rates were considered based on previous model evaluations of laboratory oxidation studies. For the faster oxidation rate of the 0.05/hr, approximately 40 percent of the particulate Cu ended up in the dissolved phase. For the slower oxidation rate of 0.005/hr, less than 10 percent of the particulate Cu ended up in the dissolved phase. The results of this modeling exercise indicate that the dynamics of transitioning from CuS to labile Cu is critical in quantifying the dissolved Cu concentrations following the resuspension of anoxic sediments.

To assess overall performance of the model, simulation results described above were compared to dissolved Cu measurements that were taken during the first hour following the San Diego prop-wash event. Results showed that the Tier 2 (oxic sediment) and Tier 3 (anoxic sediment) model results bracketed the dissolved Cu measurements which ranged from 2.5 to 17.5 $\mu\text{g/L}$. The model results therefore provided a good predictor for the upper and lower bound of Cu bioavailability in San Diego Bay following the prop-wash event. A more exact prediction of metal release from the San Diego Bay prop-wash study could not be made because information on relative amounts of oxic and anoxic sediments that were resuspended by the prop-wash event was not available. Since oxic conditions in San Diego Bay and in other harbors are generally limited to the top few millimeters of sediment, a more likely scenario is that a larger proportion of sediments resuspended during prop-wash events would be represented by anoxic conditions. However, this may not be the case in active shipping channels and pier areas where sediment resuspension is occurring on a more regular basis. In addition to metal partitioning and metal sulfide oxidation rates, another key factor that need to be considered in modeling metal release and bioavailability following prop-wash events is the relative amounts of oxic and anoxic sediments that are resuspended into the overlying waters.

Conclusions and Implications for Future Research/Implementation

Thus far we can conclude that sediment resuspension has variable effects on metal release over time. We observed lower survival rates of test organisms in resuspended sediments than in bedded sediments, as a general trend across sediment types and resuspension events. Although metal release during resuspension may have variable trends, it invariably has negative impacts on aquatic organisms.

The laboratory and TICKET modeling work that was performed as part of this project has provided us with a much clearer understanding of metal partitioning and metal sulfide oxidation kinetics that control bioavailability and ultimately toxicity effects associated with propeller-wash events. Based on model results of the laboratory data, a simplified version of the TICKET model was developed and successfully incorporated in the Particle Tracking Model. The resulting model, TICKET-PTM, provided a robust modeling approach for evaluating the combined effects of transport, metal partitioning and oxidation kinetics on metal release and bioavailability following a pilot field prop-wash event in San Diego Bay. Based on San Diego Bay model case study, TICKET-PTM was shown to meet the overall goal of the modeling efforts; i.e., to develop a modeling tool for assessing metal release and metal bioavailability following prop-wash events.

In applying TICKET-PTM to prop-wash events at other DoD sites, additional data collection will be required for assigning model inputs. These will include: (i) the hydrodynamic flow field of the site (which can be computed using the CH3D model), (ii) the chemical characterization of the overlying water (including pH, hardness or salinity, DOC and background metal concentrations), (iii) the amount of sediment expected to be resuspended by prop-wash, (iv) the chemical characterization of the resuspended sediment (including the relative amounts of oxic and anoxic sediment in the resuspended material, the total metal concentration, and the iron and organic carbon content of the resuspended sediment), and (v) an estimate of the settling velocity of the resuspended sediment.

In addition to site-specific data collection that will be required for TICKET-PTM applications to other sites, the following recommendations are made for future research and implementation:

1. Further studies should be performed to determine the chemical characterization of sediments in shipping channels and pier areas. Efforts should focus on field evaluations to determine the relative amounts of oxic and anoxic sediments that are likely to be resuspended during prop-wash events, the total metal concentrations, and the iron and organic carbon content of sediments. This information is critical in defining initial conditions for model simulations.
2. Since metal sulfide oxidation kinetics play an important role in determining metal release and metal bioavailability following prop-wash events, additional studies of metal sulfide oxidation kinetics should be performed. This work should focus on laboratory oxidation chamber studies for metal sulfide oxidation kinetics of sediments resuspended into marine waters. As part of this effort, attention should be given to scenarios where subsequent oxidation of elemental sulfur to sulfate (and an associated release of acid) may occur.

3. Additional pilot field tests should be performed to better define the extent of metal release during prop-wash events. As part of the study design, protocols for on-board oxidation studies of resuspended sediment should be developed and should be used to supplement sample collection from the prop-wash plume. In addition, sample handling procedures that have been used in previous prop-wash field studies should also be re-evaluated to ensure that field measurements are representative of in-situ dissolved metal concentrations and are not biased by continued oxidation of resuspended sediment during prolonged holding times.
4. Since only limited testing of TICKET-PTM was performed as part of this project, additional testing of the model should be performed using a variety of field conditions that are likely to be encountered at DoD sites.
5. No significant acute toxicity was observed from laboratory and *in situ* resuspension events; however, laboratory testing suggests there is a potential for chronic toxicity to be occurring at DoD sites from resuspended contaminated particles settling to the sediment surface. This increases the exposure to epibenthic macroinvertebrates, such as amphipods. Future research should investigate whether this phenomenon is ecologically significant.

This work has helped improve fundamental understanding of the behavior and ecological impacts of resuspended sediments that contain elevated levels of priority metals (zinc, copper, and lead) and oxy-anions (arsenic). This advances DOD's ability to manage these priority contaminants by contributing detailed, fundamental, and general knowledge of the processes that control their stability, mobility, and bioavailability in sediments. Additionally, this work has been performed in cooperation with the USACE who are primarily responsible for national guidance on dredging operations and is actively involved in sediment and contaminant management in harbors and waterways. Results will be transitioned through publication of peer-reviewed journal articles, technical reports, technical symposia, and short course training. It is anticipated that this work will lay the foundation for technical guidance for use in dredging, site risk assessments and feasibility studies for possible remediation efforts.

Literature Cited

Allison, J.D., Allison, T.L., 2005. Partitioning Coefficients for metals in surface water, soil, and waste. U.S. Environmental Protection Agency, Office of Research and Development, Washington DC.

Allison J.D., Brown D.S., Kevin J. (1991). MINTEQA2/PRODEFA2, a geochemical assessment model for environmental systems: Version 3.0 user's manual (p. 117). Athens, GA: Environmental Research Laboratory, Office of Research and Development, US Environmental Protection Agency.

Buchman, M. F. 1999. NOAA Screening Quick Reference Tables. NOAA HAZMAT Report 99-1. Seattle, WA. Coastal Protection and Restoration Division, National Oceanic and Atmospheric Administration. 12 pages.

Burton E.D., Bush R.T., Sullivan L.A. (2006). Acid-Volatile Sulfide Oxidation in Coastal Flood Plain Drains: Iron–Sulfur Cycling and Effects on Water Quality. *Environ Sci Technol* 40 (4), 1217-1222.

Burton E.D., Bush R.T., Sullivan L.A., Hocking R.K., Mitchell D.R.G., Johnston S.G., Fitzpatrick R.W., Raven M., McClure S., Jang L.Y. (2009). Iron-monosulfide oxidation in natural sediments: Resolving microbially mediated S transformations using XANES, electron microscopy, and selective extractions. *Environ Sci Technol* 43 (9), 3128-3134.

Burton Jr, G.A., Rosen, G., Chadwick, D.B., Greenberg, M.S., Taulbee, W.K., Lotufo, G.R., Reible, D.D. (2012). A sediment ecotoxicity assessment platform for in situ measures of chemistry, bioaccumulation and toxicity. Part 1: System description and proof of concept. *Environmental Pollution* 162, 449-456.

Canavan RW, Van Cappellen P, Zwolsman JJG, Van den Berg GA, Slomp CP. (2007). Geochemistry of trace metals in a fresh water sediment: field results and diagenetic modeling. *Sci Total Environ* 381(1), 263-279.

Carbonaro RF, Mahony JD, Walter AD, Halper EB, Di Toro D M. (2005). Experimental and modeling investigation of metal release from metal-spiked sediments. *Environ Toxicol Chem* 24(12), 3007-3019.

Chadwick, B., Leather, J., Richter, K., Apitz, S., Lapota, D., Duckworth, D., Katz, C., Kirtay, V., Davidson, B., Patterson, A., Wang, P., Curtis, S., Key, G., Steinert, S., Rosen, G., Caballero, M., Groves, J., Koon, G., Valkiers, A., Myers-Schulte, K., Stallard, M., Clawson, S., Montee, R.S., Sutton, D., Skinner, L., Germano, J., Cheng, R. (1999). Sediment Quality Characterization Naval Station San Diego. SPAWAR Systems Center San Diego, San Diego, California.

Chadwick, D.B., Rivera-Duarte, I., Carlson, A., Rosen, G. (2005). Determining the Fate and Ecological Effects of Copper and Zinc Loading in Estuarine Environments: A Multi-Disciplinary Program. SPAWAR Systems Center San Diego, San Diego, California.

Choi JH, Park SS, Jaffé PR. (2006). Simulating the dynamics of sulfur species and zinc in wetland sediments. *Ecologl Model* 199(3), 315-323.

Church, T.M., Scudlark, J.R. (1998). Trace metals in estuaries: A Delaware Bay synthesis, in: Allen, H.E., Garrison, A.W., Luther, G.W. (Eds.), *Metals in Surface Waters*. Ann Arbor Press, Chelsea, Mich.

Culberson, C.H. (1988). Delaware Bay Database (Version 1.03). Sea Grant College Program, University of Delaware. Newark, DE, USA.

Di Toro DM, Mahony JD, HansenDJ, Scott KJ, Hicks MB, Mayr SM Redmond MS. (1990). Toxicity of cadmium in sediments: The role of acid volatile sulfide. *Environ Toxicol Chem* 9: 1487–1502.

Di Toro DM, Mahony JD, Hansen DJ, Scott KJ, Carlson AR, Ankley GT. (1992). Acid volatile sulfide predicts the acute toxicity of cadmium and nickel in sediments. *Environ Sci Technol* 26 (1), 96-101.

Di Toro, D.M., McGrath, J.A., Hansen, D.J., Berry, W.J., Paquin, P.R., Mathew, R., Wu, K.B., Santore, R.C. (2005). Predicting sediment metal toxicity using a sediment biotic ligand model: Methodology and initial application. *Environ. Toxicol. Chem.* 24, 2410-2427.

Dzombak D.A., Morel, F.M.M. (1990). *Surface complexation modeling: hydrous ferric oxide*. John Wiley & Sons. New York, NY.

Eggleton J, Thomas KV. (2004). A review of factors affecting the release and bioavailability of contaminants during sediment disturbance events. *Environ Internat* 30(7), 973-980.

Earley, P.J., Rosen, G., Rivera-Duarte, I., Gauthier, R.D., Arias-Thode, Y., Thompson, J., Swope, B., 2007. *A Comprehensive Copper Compliance Strategy: Implementing Regulatory Guidance at Pearl Harbor Naval Shipyard & Intermediate Maintenance Facility*. Space Naval Warfare (SPAWAR) Systems Center San Diego, CA.

Farley K.J., Rader K.J. Miller B.E. (2008). Tableau Input Coupled Kinetic Equilibrium Transport (TICKET) Model. *Environ Sci Technol* 42 (3), 838-844.

Farley K.J., Carbonaro R.F., Fanelli C.J., Costanzo R., Rader K.J., Di Toro D.M. (2011). TICKET-UWM: A coupled kinetic, equilibrium, and transport screening model for metals in lakes. *Environ Toxicol Chem* 30: 1278-1287.

Fetters K.J. (2013). Investigating toxicological effects of short-term resuspension of metal-contaminated freshwater and marine sediments (Doctoral dissertation, University of Michigan).

Gailani, J.Z., Lackey, T.C., and Smith, J (2007). “Application of the Particle Tracking Model to predict far-field fate of sediment suspended by nearshore dredging and placement at Brunswick,

Georgia.” Proceedings XVIII World Dredging Congress 2007, WEDA, Lake Buena Vista, Florida, USA.

Hammerschmidt, C.R. and W.F. Fitzgerald. 2008. Sediment-water exchange of methylmercury determined from shipboard benthic flux chambers. *Marine Chemistry*. 109: 86-97.

Hong Y.S., Kinney K.A., Reible D.D. (2011). Acid volatile sulfides oxidation and metals (Mn, Zn) release upon sediment resuspension: Laboratory experiment and model development. *Environ Toxicol Chem* 30: 564–575.

Jensen DL, Boddum JK, Tjell JC, Christensen TH. (2002). The solubility of rhodochrosite (MnCO_3) and siderite (FeCO_3) in anaerobic aquatic environments. *Appl Geochem* 17(4), 503-511.

Johnson, B.H., Kim, K.W., Heath, R.E., Hsieh, B.B., and Butler, H.L. 1993. “Validation of A three- Dimensional Hydrodynamic Model of Chesapeake Bay,” *Journal of Hydraulic Engineering*, Am. Soc. Civil Eng. 119(1), 2-20.

Lackey, T.C. and MacDonald, N.J. (2007). "The Particle Tracking Model Description and Processes" Proceedings XVIII World Dredging Congress 2007, WEDA, Lake Buena Vista, Florida, USA.

Lackey, T.C. and Smith, S. J (2008) “Application of the Particle Tracking Model To Predict the fate of Dredged Suspended Sediment at the Willamette River” Proceedings Western Dredging Association Twenty-Eighth Annual Technical Conference, St. Louis, MO.,USA.

Luther GW. (1990). The frontier-molecular-orbital theory approach in geochemical processes. IN: *Aquatic Chemical Kinetics: Reaction Rates of Processes in Natural Waters*. Environmental Science and Technology Series. John Wiley & Sons, New York. 1990. p 173-198.

MacDonald, N.J., Davies, M.H., Zundel, A.K., Howlett, J.D., Demirbilek, Z., Gailani, J.Z., Lackey, T.C., and Smith, S.J. 2006. "PTM: Particle Tracking Model Report 1: Model Theory, Implementation, and Example Applications" Technical Report TR-06-02, U.S. Army Corps of Engineers, Engineer Research and Development Center, Vicksburg, Mississippi, USA.

Milero FJ. (1985). The effect of ionic interactions on the oxidation of metals in natural waters. *Geochimica et Cosmochimica Acta*. 49 (2), 547–553.

Millero FJ, Sotolongo S, Izaguirre M. (1987). The oxidation kinetics of Fe(II) in seawater. *Geochimica et Cosmochimica Acta*. 51 (4), 793–801.

Norwood, W., Borgmann U, Dixon D. 2006. Saturation models of arsenic, cobalt, chromium, and manganese bioaccumulation by *Hyaella azteca*. *Environmental Pollution* 143:519-528.

Peng, J. (2004). Integrated geochemical and hydrodynamic modeling of San Diego Bay, California. University of Southern California, Ann Arbor, pp. 230-230 p.

Rader, K.J. (2009). Assessing the transport, fate, and effects of metals and metalloids in surface water and sediment. University of Delaware, United States -- Delaware, p. 371.

Richardson, P.H. and Schmalz, R.A. 2012. NOS Historical Circulation Survey, Data Restoration: Casco Bay (1979), Los Angeles and Long Beach (1983), San Diego (1983) and Miami (1985). CSDL Informal Technical Note No. 13, NOAA.

Robinson, S.E., N.A. Capper, and S.J. Klaine. 2010. The effects of continuous and pulsed exposures of suspended clay on the survival, growth, and reproduction of *Daphnia magna*. *Environmental Toxicology and Chemistry*. 29(1): 168-175.

Saulnier, I. and A. Mucci. 2000. Trace metal remobilization following the resuspension of estuarine sediments: Saguenay Fjord, Canada. 15(2): 191-210.

Singer PC, Stumm W. (1970). The solubility of ferrous iron in carbonate-bearing waters. J Amer Water Works Assoc 62 (3), 198-202.

Smith, M.E., L.E. Herrin, W.T. Thoeny, J.M. Lazorchak, S. Brewer-Swartz. 1997. A reformulated, reconstituted water for testing the freshwater amphipod *Hyalella azteca*. *Environmental Toxicology and Chemistry* 16: 1229-1233.

Stumm W, Lee GF. (1961) Oxygenation of Ferrous Iron. *Indus Engr Chem* 53 (2), 143-146.

Stumm W. (1992). Chemistry of the solid-water interface: Processes at the mineral-water and particle-water interface in natural systems. John Wiley Sons. New York, NY.

Sullivan LA, Bush RT, McConchie DM. (2000). A modified chromium-reducible sulfur method for reduced inorganic sulfur: optimum reaction time for acid sulfate soil. *Soil Research*, 38(3), 729-734.

Tengberg, A. Stahl, H., Gust, H., Muller, V., Arning, U., Andersson, H., and Hall, POJ. 2004. Intercalibration of benthic flux chambers I. Accuracy of flux measurements and influence of hydrodynamics. *Progress in Oceanography*. 60(1). 1-28.

Tipping E., Lofts S., Sonke J.E. (2011). Humic ion-binding model VII: A revised parameterization of cation-binding by humic substances. *Environ Chem* 8:225–235.

Tipping, E., Lofts, S., Sonke, J.E. (2011). Humic Ion-Binding Model VII: a revised parameterisation of cation-binding by humic substances. *Environmental Chemistry* 8, 225-235.

Turner, A. (1996). Trace-metal partitioning in estuaries: importance of salinity and particle concentration. *Marine Chemistry* 54, 27-39

Thomsen, L. and G. Gust. 2000. Sediment erosion thresholds and characteristics of resuspended aggregates on the western European continental margin. *Deep Sea Research Part I: Oceanographic Research Papers*. 47(10): 1881-1897.

U.S. Environmental Protection Agency. 1991. Analytical method for determination of acid volatile sulfide in sediment. Washington, D.C.

U.S. Environmental Protection Agency. 2002. Methods for measuring the acute toxicity of effluents and receiving waters to freshwater and marine organisms, 5th ed. EPA-821-R-02-014. Washington, D.C.

U.S. Environmental Protection Agency. 2005. Procedures for the derivation of equilibrium partitioning sediment benchmarks (ESBs) for the protection of benthic organisms: metal mixtures (cadmium, Cu, lead, nickel, silver, and Zn). Washington, D.C.

Vanthuyne M, Maes A. (2006). Metal speciation in sulphidic sediments: A new method based on oxidation kinetics modelling in the presence of EDTA. *Science of the total environment*, 367(1), 405-417.

Wang, P. F., Cheng, R. T., Richter, K., Gross, E. S., Sutton, D., and Gartner, J. W. (1998). "Modeling Tidal Hydrodynamics of San Diego Bay, California." *J. Amer. Water Res. Assoc.*, 34 (5), 1123-1140.

Wang F, Tessier A. (2009). Zero-valent sulfur and metal speciation in sediment porewaters of freshwater lakes. *Environ Sci Technol* 43(19), 7252-7257.

Wehrli B, Sulzberger B, Stumm W. (1989). Redox processes catalyzed by hydrous oxide surfaces. *Chemical Geology*. 78 (3–4), 167–179. doi:10.1016/0009-2541(89)90056-9

Wehrli B. (1990). Redox reactions of metal ions at mineral surfaces. IN: *Aquatic Chemical Kinetics: Reaction Rates of Processes in Natural Waters*. Environmental Science and Technology Series. John Wiley & Sons, New York. 1990. p 311-336.

Wilkin RT, Rogers DA. (2010). Nickel sulfide formation at low temperature: initial precipitates, solubility and transformation products. *Environ Chem* 7(6), 514-523.

Appendix A

Supporting Data

Table A-1. Physiochemical data from 4-hour continuous resuspensions, including: pH, DO (mg/L), and Conductivity (μ S).

Resuspension	Averages			Standard Deviations		
	pH	DO	Conductivity	pH	DO	Conductivity
Duck Lake						
Initial	7.40	6.99	830.00	0.04	0.05	1.00
1hr	7.28	6.51	827.67	0.08	0.10	0.58
2hr	7.27	6.78	828.33	0.03	0.05	0.58
3hr	7.26	6.98	828.33	0.02	0.17	1.53
4hr	7.28	7.18	827.33	0.01	0.07	1.15
Idaho						
Initial	6.90	6.37	792.33	0.02	0.32	6.51
1hr	6.75	6.05	808.00	0.01	0.04	3.61
2hr	6.76	6.40	816.00	0.00	0.08	2.00
3hr	6.79	6.93	807.33	0.02	0.04	1.53
4hr	6.84	7.05	796.67	0.04	0.06	4.16
Lake DePue						
Initial	7.66	7.93	813.00	0.02	0.07	8.49
1hr	7.58	7.66	814.00	0.04	0.10	xxx
2hr	7.59	7.66	805.67	0.04	0.11	2.08
3hr	7.58	7.74	800.33	0.05	0.03	3.06
4hr	7.59	7.88	802.00	0.04	0.12	9.90
Portsmouth						
Initial	7.97	7.81	574.33	0.04	0.29	18.34
1hr	8.02	5.89	678.67	0.05	0.25	6.35
2hr	8.00	5.95	672.67	0.05	0.47	8.50
3hr	7.98	5.94	666.67	0.04	0.38	6.66
4hr	7.95	6.20	663.33	0.06	0.39	12.66
San Diego						
Initial	7.95	7.59	648.00	0.01	0.33	9.17
1hr	7.89	7.46	759.00	0.05	0.31	2.00
2hr	7.88	7.52	740.00	0.05	0.19	6.24
3hr	7.88	7.65	743.33	0.05	0.20	6.51
4hr	7.87	7.70	734.00	0.05	0.14	2.65

Table A-2. Dissolved metal concentration (ug/L) of water column during the 4-hour continuous resuspensions of 3 replicate SeFEC chambers.

Resuspension	Cu	Zn	Co	Fe	Mn
Duck Lake					
1hr	11.00	10.00	9.00	9.67	59.00
1hr	12.00	4.00	8.00	15.67	19.00
1hr	14.00	2.00	7.00	12.00	10.00
2hr	6.00	0.00	14.00	14.33	41.33
2hr	14.00	-1.00	12.00	12.67	14.33
2hr	13.00	2.00	12.00	8.67	15.33
3hr	16.00	2.00	12.00	11.00	7.33
3hr	13.00	-3.00	15.00	3.00	7.33
3hr	15.00	3.00	6.00	12.33	38.67
4hr	11.00	2.00	12.00	14.67	6.67
4hr	6.00	-1.00	13.00	3.67	5.33
4hr	20.00	5.00	8.00	6.00	4.67
San Diego					
1hr	10.00	4.00	14.00	6.33	3.33
1hr	6.00	0.00	15.00	0.67	2.67
1hr	18.00	0.00	8.00	35.33	1.67
2hr	13.00	0.00	7.00	6.33	1.33
2hr	19.00	1.00	9.00	20.33	1.33
2hr	11.00	-4.00	14.00	7.67	0.67
3hr	12.00	6.00	7.00	12.00	1.00
3hr	20.00	2.00	14.00	22.67	1.33
3hr	18.00	0.00	10.00	15.33	0.33
4hr	18.00	7.00	8.00	8.67	1.33
4hr	17.00	6.00	5.00	11.67	1.00
4hr	25.00	0.00	8.00	7.67	0.67
Idaho					
1hr	23.00	24.00	33.00	38.33	610.00
1hr	12.00	6.00	28.00	8.00	640.33
1hr	17.00	0.00	29.00	29.00	638.33
2hr	20.00	8.00	33.00	25.67	595.33
2hr	10.00	3.00	32.00	21.33	609.33
2hr	6.00	4.00	32.00	27.00	617.33
3hr	13.00	6.00	32.00	24.33	576.00
3hr	24.00	0.00	39.00	32.00	576.00
3hr	7.00	7.00	26.00	24.67	573.33

4hr	18.00	10.00	30.00	21.00	551.33
4hr	12.00	4.00	30.00	23.00	575.67
4hr	23.00	3.00	27.00	26.00	587.33
Resuspension	Cu	Zn	Co	Fe	Mn
Portsmouth					
1hr	5.77	47.49	-----	23.92	8.78
1hr	5.63	53.55	-----	24.86	7.78
1hr	7.72	41.17	-----	24.45	8.24
2hr	4.77	52.69	-----	19.73	8.46
2hr	4.62	52.18	-----	21.47	7.24
2hr	31.77	67.73	-----	25.23	8.30
3hr	16.85	67.95	-----	20.86	8.56
3hr	4.62	49.94	-----	21.11	7.37
3hr	7.32	51.22	-----	20.92	7.37
4hr	3.80	56.22	-----	18.83	8.36
4hr	5.05	58.12	-----	21.84	7.74
4hr	6.29	42.04	-----	19.33	7.10
Lake DePue*					
1hr	-1.08	69.85	-----	7.99	128.68
1hr	0.90	94.58	-----	23.50	104.47
1hr	0.70	65.81	-----	6.95	103.75
2hr	1.03	54.30	-----	27.02	114.13
2hr	5.05	143.36	-----	58.14	105.06
2hr	1.95	81.22	-----	26.99	113.73
3hr	0.05	53.55	-----	19.56	118.71
3hr	5.32	144.85	-----	47.56	106.80
3hr	3.25	114.27	-----	42.85	124.89
4hr	-0.38	101.86	-----	11.36	125.80
4hr	0.91	149.77	-----	22.32	108.50
4hr	2.92	120.93	-----	21.24	129.65

*Lake DePue resuspensions were performed 3 at separate events, with 3 replicates each, for a total of 9 SeFEC resuspensions. Above values are averages of the 3 replicate resuspensions from each of the three resuspension events.

Table A-3. Physicochemical data for 16-hour multiple resuspensions (control and three treatments). Hours 1, 5, 9 & 13 are after 1-hour resuspension. Hours 4, 8, 12, 16 are after 3-hour settling period.

	pH				DO (mg/L)				Conductivity (µS)			
	Control	1	2	3	Control	1	2	3	Control 1	1	2	3
Duck Lake												
Initial	7.23	7.52	7.56	7.49	6.09	5.97	5.98	5.98	751	829	833	833
Hour 1	7.19	7.34	7.31	7.37	6.15	6.30	6.13	6.13	755	819	818	818
Hour 4	7.20	7.37	7.36	7.41	6.20	6.24	6.04	6.04	757	821	817	817
Hour 5	7.24	7.44	7.48	7.49	6.19	6.91	6.48	6.48	762	819	823	823
Hour 8	7.22	7.38	7.45	7.50	6.22	6.91	6.50	6.50	759	817	831	831
Hour 9	7.29	7.47	7.49	7.54	6.28	7.14	7.02	7.02	754	818	829	829
Hour 12	7.28	7.36	7.37	7.43	6.30	6.90	6.80	6.80	750	818	828	828
Hour 13	7.25	7.43	7.62	7.63	6.42	7.30	7.32	7.32	752	819	831	831
Hour 16	7.24	7.45	7.61	7.60	6.45	6.88	6.90	6.90	754	812	813	813
Lake DePue												
Initial	7.23	7.32	7.36	7.39	6.09	6.01	5.90	6.02	751	821	823	820
Hour 1	7.19	7.34	7.31	7.37	6.15	6.58	5.82	5.81	755	846	847	851
Hour 4	7.20	7.37	7.36	7.41	6.20	6.39	5.82	6.01	757	860	833	859
Hour 5	7.24	7.44	7.48	7.49	6.19	6.88	6.31	6.89	762	862	850	861
Hour 8	7.22	7.38	7.45	7.50	6.22	6.68	7.18	6.80	759	864	866	866
Hour 9	7.29	7.47	7.49	7.54	6.28	6.80	7.24	7.30	754	866	865	866
Hour 12	7.28	7.36	7.37	7.43	6.30	6.89	7.01	7.09	750	865	866	866
Hour 13	7.25	7.43	7.62	7.63	6.42	6.94	7.99	7.24	752	869	864	866
Hour 16	7.24	7.45	7.61	7.60	6.45	6.65	7.81	7.98	754	861	860	860

Table A-4. Dissolved metal concentration (ug/L) of water column during the 16-hour multiple resuspensions of 3 replicate SeFEC chambers.

Resuspension Event		Cu	Co	Zn	Fe	Mn
Duck Lake						
Hour 1	1-resusp	0.26	6.23	16.23	9.47	35.12
Hour 1	1-resusp	-1.13	8.74	4.23	10.44	43.51
Hour 1	1-resusp	1.16	12.82	2.43	9.57	35.29
Hour 4	1-settle	0.54	8.71	1.11	5.71	48.70
Hour 4	1-settle	1.72	10.08	1.45	6.87	65.92
Hour 4	1-settle	-0.22	5.50	0.30	3.96	45.13
Hour 5	2-resusp	1.24	10.00	47.77	7.10	5.03
Hour 5	2-resusp	0.73	5.94	0.37	7.46	6.31
Hour 5	2-resusp	0.25	6.00	3.51	9.04	5.83
Hour 8	2-settle	-0.69	4.36	-0.94	4.68	5.37
Hour 8	2-settle	3.50	12.87	4.20	7.96	6.75
Hour 8	2-settle	-0.74	13.47	-1.64	3.58	5.91
Hour 9	3-resusp	1.05	10.90	50.75	12.42	2.99
Hour 9	3-resusp	0.09	12.33	6.71	9.44	3.48
Hour 9	3-resusp	1.60	4.93	8.76	7.22	3.55
Hour 12	3-settle	-0.75	6.77	4.34	6.36	3.76
Hour 12	3-settle	3.07	13.91	1.62	6.89	4.22
Hour 12	3-settle	2.21	5.45	9.20	5.54	3.37
Hour 13	4-ressup	2.18	2.83	44.94	26.28	2.87
Hour 13	4-ressup	2.44	10.61	9.17	28.66	3.34
Hour 13	4-ressup	2.25	11.17	11.71	173.80	4.39
Hour 16	4-settle	-0.20	5.23	-0.11	2.39	2.87
Hour 16	4-settle	-1.73	12.59	-0.04	4.44	2.80
Hour 16	4-settle	-0.56	10.41	8.51	4.55	2.85
Idaho						
Hour 1	1-resusp	6.15	28.88	17.42	66.54	709.40
Hour 1	1-resusp	2.07	42.35	2.56	39.70	703.23
Hour 1	1-resusp	4.53	36.03	3.27	48.36	705.20
Hour 4	1-settle	2.71	30.68	3.96	14.10	712.73
Hour 4	1-settle	5.12	30.78	-0.91	13.03	711.13
Hour 4	1-settle	13.20	33.53	8.57	252.00	718.73
Hour 5	2-resusp	9.04	22.25	84.33	109.80	323.63
Hour 5	2-resusp	6.41	25.81	7.51	28.08	307.97
Hour 5	2-resusp	10.26	19.40	3.27	12.64	303.87
Hour 8	2-settle	10.81	14.67	2.52	16.11	317.33

Hour 8	2-settle	13.01	25.33	3.65	28.06	301.87
Hour 8	2-settle	12.68	23.09	0.54	10.40	291.30
Hour 9	3-resusp	13.09	17.15	78.66	77.68	144.03
Resuspension Event		Cu	Co	Zn	Fe	Mn
Hour 9	3-resusp	11.20	17.67	11.85	28.58	135.47
Hour 9	3-resusp	8.82	17.18	5.11	13.52	150.60
Hour 12	3-settle	11.04	26.09	5.81	7.26	140.23
Hour 12	3-settle	17.21	18.39	2.98	183.30	136.87
Hour 12	3-settle	10.68	18.24	2.05	15.10	158.20
Hour 13	4-ressup	9.91	15.26	60.96	62.28	56.41
Hour 13	4-ressup	2.80	7.85	0.92	16.55	47.65
Hour 13	4-ressup	2.33	15.13	-0.68	24.13	60.99
Hour 16	4-settle	8.42	18.70	7.68	7.65	62.39
Hour 16	4-settle	1.67	14.41	-2.77	9.85	49.26
Hour 16	4-settle	3.62	8.84	-2.60	6.44	69.13

Lake DePue

Hour 1	1-resusp	4.19	14.83	154.25	10.26	189.17
Hour 1	1-resusp	3.72	13.29	174.45	12.14	180.80
Hour 1	1-resusp	4.17	16.96	173.55	13.45	186.23
Hour 4	1-settle	3.21	15.00	243.35	5.52	192.40
Hour 4	1-settle	41.43	17.33	697.65	450.40	201.50
Hour 4	1-settle	2.41	9.39	258.05	7.93	183.13
Hour 5	2-resusp	12.47	17.47	317.80	156.70	113.30
Hour 5	2-resusp	1.07	8.76	211.90	13.31	105.30
Hour 5	2-resusp	2.99	12.06	227.25	25.58	113.23
Hour 8	2-settle	4.71	18.32	250.95	5.82	109.93
Hour 8	2-settle	1.32	16.28	230.60	7.97	96.17
Hour 8	2-settle	11.86	7.87	343.85	122.63	104.23
Hour 9	3-resusp	7.79	15.90	255.50	111.13	49.36
Hour 9	3-resusp	2.63	9.69	191.50	16.42	49.84
Hour 9	3-resusp	0.49	13.87	206.40	3.40	61.19
Hour 12	3-settle	2.39	10.67	271.00	15.59	61.74
Hour 12	3-settle	1.64	7.43	269.60	6.22	60.86
Hour 12	3-settle	4.20	10.26	262.45	6.32	63.48
Hour 13	4-ressup	9.47	10.92	267.65	129.57	36.73
Hour 13	4-ressup	3.15	13.88	169.40	17.27	31.35
Hour 13	4-ressup	2.74	12.91	143.55	11.22	31.95
Hour 16	4-settle	2.69	8.78	219.20	11.86	35.03
Hour 16	4-settle	2.51	1.69	189.05	4.70	30.40
Hour 16	4-settle	1.29	4.26	166.80	3.42	31.95

Table A-5. *D. magna* reproduction (number of neonates) produced over 10 day chronic exposure experiment for each of eight replicates.

Beaker	Duck Lake	San Diego	Idaho	Lake DePue	Control Chamber	Control Beaker
1	19	21	30	24	27	11
2	22	27	0	16	0	12
3	19	24	28	0	0	12
4	21	22	0	0	21	0
5	16	24	21	24	29	0
6	15	0	26	25	34	0
7	24	0	25	18	0	0
8	23	23	13	17	30	0
Average	19.88	17.63	17.88	15.50	17.63	4.38
St. Dev	3.23	11.02	12.18	10.17	15.03	6.05

Table A-6. *H. azteca* and *D. magna* survival (out of 10 individuals for each species per chamber) in 4-hour and 16-hour SeFEC resuspension exposures.

Exposure	Sediment	<u>Survival</u>		<u>Average Percent Survival</u>	
		<i>D. magna</i>	<i>H. azteca</i>	<i>Daphnia</i>	<i>Hyaella</i>
16-hour	Idaho	6	6		
16-hour	Idaho	5	8		
16-hour	Idaho	5	7	0.53	0.70
16-hour	Lake DePue	5	9		
16-hour	Lake DePue	5	8		
16-hour	Lake DePue	6	10	0.53	0.90
16-hour	Duck Lake	9	10		
16-hour	Duck Lake	7	10		
16-hour	Duck Lake	10	10	0.87	1.00
16-hour	Control	9	10		
16-hour	Control	10	10		
16-hour	Control	9	9	0.93	0.97
4-hour	San Diego	10	9		
4-hour	San Diego	6	8		
4-hour	San Diego	9	9	0.83	0.87
4-hour	Idaho	5	6		
4-hour	Idaho	9	9		
4-hour	Idaho	5	7	0.63	0.73
4-hour	Duck Lake	8	9		
4-hour	Duck Lake	10	10		
4-hour	Duck Lake	10	10	0.93	0.97
4-hour	Lake DePue	6	9		
4-hour	Lake DePue	8	10		
4-hour	Lake DePue	7	10	0.70	0.97
4-hour	Control	10	10		
4-hour	Control	10	10		
4-hour	Control	9	10	0.97	1.00

Table A-7. *H. azteca* and *D. magna* survival (out of 10 individuals for each species per beaker) in bedded sediments exposures.

Exposure	Sediment	<u>Survival</u>		<u>Average Percent Survival</u>	
		<i>D. magna</i>	<i>H. azteca</i>	<i>D. magna</i>	<i>H. azteca</i>
Beaker 1	Duck Lake	8	9		
Beaker 2	Duck Lake	10	9		
Beaker 3	Duck Lake	9	10		
Beaker 4	Duck Lake	10	9		
Beaker 5	Duck Lake	8	9		
Beaker 6	Duck Lake	6	8		
Beaker 7	Duck Lake	10	10		
Beaker 8	Duck Lake	9	8	0.88	0.90
Beaker 1	San Diego	0	9		
Beaker 2	San Diego	3	9		
Beaker 3	San Diego	2	8		
Beaker 4	San Diego	6	8		
Beaker 5	San Diego	6	7		
Beaker 6	San Diego	7	6		
Beaker 7	San Diego	6	7		
Beaker 8	San Diego	7	7	0.46	0.76
Beaker 1	Idaho	8	7		
Beaker 2	Idaho	10	6		
Beaker 3	Idaho	8	9		
Beaker 4	Idaho	8	7		
Beaker 5	Idaho	10	6		
Beaker 6	Idaho	7	8		
Beaker 7	Idaho	5	10		
Beaker 8	Idaho	9	7	0.81	0.75
Beaker 1	Lake DePue	6	0		
Beaker 2	Lake DePue	7	0		
Beaker 3	Lake DePue	7	0		
Beaker 4	Lake DePue	0	0		
Beaker 5	Lake DePue	8	0		
Beaker 6	Lake DePue	7	0		
Beaker 7	Lake DePue	8	0		
Beaker 8	Lake DePue	6	0	0.61	0.00
Beaker 1	Control	10	10		
Beaker 2	Control	10	10		
Beaker 3	Control	10	10		
Beaker 4	Control	10	10		
Beaker 5	Control	10	10		
Beaker 6	Control	9	10		
Beaker 7	Control	10	10		
Beaker 8	Control	10	10	0.99	1.00

Table A-8. Previous Sediment Oxidation Studies Reported in the Literature

	Sediment Source	Resuspension Mixture	Study Duration	Metals	Results
Hirst and Aston (1983) 22 citations	Mersey Estuary (UK)	~0.5 g/L of sediment in seawater	70 hrs	Fe, Mn, Cu, Zn	Rapid oxidation of Fe and Mn was accompanied by minimal release of Cu and Zn to the dissolved phase
Calmano et al. (1993) 393 citations	Hamburg Harbour (DE)	75 g/L of sediment in distilled water	35 days	Cd, Cu, Pb, Zn	During oxidation, pH of sediment suspension decreased (to below 4) with significant release of Cd, Zn to the aqueous phase; a re-distribution of all metals from the sulfidic fraction to easily and moderately reducible fractions also occurred during oxidation
Calmano et al. (1994) 50 citations	Hamburg Harbour (DE)	~17 g/L of sediment in constant, near-neutral pH water	26 days	Cd, Cu, Pb, Zn	Under near-neutral pH conditions, metals were released from sediment during oxidation; a portion of the released metals were subsequently sorbed to organic matter and to freshly-precipitated Fe- and Mn-oxyhydroxide
Zhuang et al. (1994) 78 citations	Susquehanna River, Maryland fish pond, Newark River	25-314 g/L of sediment in soft water	30 days	Cd	Rapid decrease in AVS with concomitant increases in Fe- and Mn-oxyhydroxides; after aeration, ~50% Cd in dissolved phase; remainder associated with Fe- and Mn-oxyhydroxides
Peterson et al. (1997) 112 citations	Elbe River (DE)	1 g/L of sediment in artificial seawater	15 days	Cd, Cu, Zn	Release of sediment-bound metal was small during the first 2-4 days; up to 2% of the sediment-bound metal was released over longer times
Simpson et al. (1998) 247 citations	Cook River (AU)	~10 g/L of sediment in seawater and freshwater	8 hrs	Fe, Mn, Cd, Cu, Pb, Zn	Rapid decrease in AVS was attributed to the oxidation of Fe-monosulfide phases; CdS, CuS, PbS and ZnS were found to oxidize more slowly

Saulnier and Mucci (2000)	Saguenay Fjord (CA)	~35 g/L of sediment in filtered seawater	83 days	As, Fe, Mn	Releases of As, Fe to the aqueous phase were correlated to the AVS content of the suspended sediment; release of Mn appeared to be related to the dissolution of a Mn carbonate or Mn-Ca carbonate solid; subsequent sorption of As on freshly-precipitated Fe- and Mn-oxyhydroxides was noted
Simpson et al. (2000)	Kings Bay on Parramatta River; Iron Cove; Cooks River (AU)	~10 g/L of sediment in seawater	24 hrs	Pb, Zn	Rapid decrease in AVS was observed; no indication of AVS stability by high Pb and Zn concentrations in sediments suggesting that a large portion of these metals were present in nonsulfide phases
Carrol et al. (2002)	Seaplane Lagoon, Alameda Naval Air Station	Sedimente resuspended in seawater in well-mixed, flow-through reactors	90 days	Cd, Cr, Cu, Fe, Mn, Ni, Pb	CdS and ZnS were found to be highly reactive in seawater; dissolved Cd and Zn concentrations however were limited by sorption to oxides
Caetano et al. (2003)	Tagus Estuary (PT)	~60 g/L of sediment in estuarine water	4 hrs	Cd, Cu, Fe, Mn, Pb	Small releases of Cd, Cu and Pb occurred during oxidation; almost all of the Cu and Pb were subsequently sorbed onto freshly-precipitated Fe-oxyhydroxide; more than 50% of the released Cd however remained in the dissolved phase
Caille et al. (2003)	Scarpe Canal Douai, France	23 g/L of sediment in deionized water	76 days	Al, Cu, Fe, Hg, Pb, Zn	During the early stages of aeration, metals were released into the aqueous phase; subsequent sorption decreased dissolved metal concentrations

Cappuyns and Swennen (2005)	Grote Beek and Grote Laak (BE)	80 g/L of sediment in distilled water	96 hrs	As, Cd, Fe, Zn	For Grote Beek sediment, Cd, Zn releases were significant after 48 hours when the pH decreased; As and Zn appeared to sorb onto freshly-precipitated HFO; For Grote Laak sediment, metal releases were small as pH increased and then remained relatively constant
Burton et al. (2006)	Tweed River (AU)	~50 g/L of sediment in drainwater	14 days	Fe, Mn, Ni, Zn	AVS oxidation occurred rapidly, produced elemental sulfur [$S_8^0(s)$], iron oxyhydroxide [$FeOOH(s)$] without significant acidification or metal release; severe acidification ($pH < 4$) and metal release occurred after 2-3 days as $S_8^0(s)$ began to oxidize to SO_4
Vanthuyne and Maes (2006)	River Schijn, Canal Gent-Terneuzen, Zuid-Willemsvaart and Docks of Brussels (BE)	~12.5 g/L of sediment in 0.02 M $NaNO_3$ water with 0.02 M EDTA and fixed $pH = 8$	12-24 hrs	Cd, Cu, Fe, Mn, Pb, Zn	Oxidation of sediment in a background solution containing excess EDTA permitted metals to be fractionated into a “quickly-oxidizable” fraction (e.g., associated with FeS minerals) and a “slowly-oxidizable” fraction (representing discrete metal sulfide phases)
Maddock et al. (2007)	River Iguacu, Canal de Sao Francisco, Sepetiba Bay (BR)	25 g/L of sediment in estuarine water	??	Cd, Mn, Zn	Release of Cd, Mn, Zn occurred after 5 hrs and coincided with a decrease in pH (to less than 5) that was attributed to the complete oxidation of sulfide to sulfate; in a sediment heavily-polluted with Zn, AVS oxidation was slower
Burton et al. (2009)	Clarence River (AU)	12.6 g/L of sediment in 0.1 M NaCl	21 days		Abiotic oxidation of mackinawite [$FeS(s)$] occurred rapidly, producing elemental sulfur [$S_8^0(s)$] without significant acidification; severe acidification ($pH < 4$) occurred after 2-3 days due to microbially-mediated oxidation of $S_8^0(s)$ to SO_4

Hong et al. (2011)	Anacostia River (US)	~75 g/L of sediment in artificial river water	14 days	Fe, Mn, Zn	AVS was rapidly oxidized to elemental sulfur [S ₈ ⁰ (s)]; after 10 hrs, a slow oxidation of S ₈ ⁰ (s) to SO ₄ was accompanied by a decrease in pH and an increase dissolved Mn, Zn concentrations
Shipley et al. (2011)	Trepangier Bayou (US)	4-40 g/L of sediment in either 0.01 M NaCl or artificial river water	7 days	As, Cd, Co, Cu, Ni, Pb, Zn	After 1-2 days, significant amounts of Cd, Co, Mn, Ni, Zn were released to the aqueous phase as pH decreased

References

- Burton ED, Bush RT, Sullivan LA. (2006). Acid-volatile sulfide oxidation in coastal flood plain drains: iron-sulfur cycling and effects on water quality. *Environ Sci Technol* 40(4), 1217-1222.
- Burton ED, Bush RT, Sullivan LA, Hocking RK, Mitchell DR, Johnston SG, Fitzpatrick RW, Raven M, McClure S, Jang LY. (2009). Iron-monosulfide oxidation in natural sediments: resolving microbially mediated S transformations using XANES, electron microscopy, and selective extractions. *Environ Sci Technol* 43(9), 3128-3134.
- Caetano M, Madureira MJ, Vale C. (2003). Metal remobilisation during resuspension of anoxic contaminated sediment: short-term laboratory study. *Water Air Soil Poll* 143(1-4), 23-40.
- Caille N, Tiffreau C, Leyval C, Morel JL. (2003). Solubility of metals in an anoxic sediment during prolonged aeration. *Sci Total Environ* 301(1), 239-250.
- Calmano W, Hong J, Förstner U. (1993). Binding and mobilization of heavy metals in contaminated sediments affected by pH and redox potential. In ER Christensen ... (eds.) *Contaminated aquatic sediments: Proceedings of the First International Specialized Conference*, held in Milwaukee, WI, June 1993, pp. 223-35.
- Calmano W, Förstner U, Hong J. (1994). Mobilization and scavenging of heavy metals following resuspension of anoxic sediments from the Elbe River. In CN Alpers ... (eds.) *Environmental geochemistry of sulfide oxidation, developed from a symposium*, Washington, DC, August 1992, Washington, DC 1994, pp. 298-321.
- Cappuyns V, Swennen R. (2005). Kinetics of element release during combined oxidation and pH stat leaching of anoxic river sediments. *Applied Geochemistry*, 20(6), 1169-1179.
- Carroll S, O'Day PA, Esser B, Randall S. (2002). Speciation and fate of trace metals in estuarine sediments under reduced and oxidized conditions, Seaplane Lagoon, Alameda Naval Air Station(USA). *Geochemical Transactions*, 3(10), 81.
- Hirst JM, Aston SR. (1983). Behaviour of copper, zinc, iron and manganese during experimental resuspension and reoxidation of polluted anoxic sediments. *Estuarine, Coastal and Shelf Science*, 16(5), 549-558.
- Hong YS, Kinney KA, Reible DD. (2011). Acid volatile sulfides oxidation and metals (Mn, Zn) release upon sediment resuspension: Laboratory experiment and model development. *Environmental toxicology and chemistry*, 30(3), 564-575.
- Maddock JEL, Carvalho MF, Santelli RE, Machado W. (2007). Contaminant metal behaviour during re-suspension of sulphidic estuarine sediments. *Water, Air, and Soil Pollution*, 181(1-4), 193-200.
- Petersen W, Willer E, Willamowski C. (1997). Remobilization of trace elements from polluted anoxic sediments after resuspension in oxic water. *Water, Air, and Soil Pollution*, 99(1-4), 515-522.
- Saulnier I, Mucci A. (2000). Trace metal remobilization following the resuspension of estuarine sediments: Saguenay Fjord, Canada. *Applied Geochemistry*, 15(2), 191-210.

Shipley HJ, Gao Y, Kan AT, Tomson MB. (2011). Mobilization of trace metals and inorganic compounds during resuspension of anoxic sediments from Trepangier Bayou, Louisiana. *Journal of environmental quality*, 40(2), 484-491.

Simpson SL, Apte SC, Batley GE. (1998). Effect of short-term resuspension events on trace metal speciation in polluted anoxic sediments. *Environmental Science & Technology*, 32(5), 620-625.

Simpson SL, Apte SC, Batley GE. (2000). Effect of short-term resuspension events on the oxidation of cadmium, lead, and zinc sulfide phases in anoxic estuarine sediments. *Environmental science & technology*, 34(21), 4533-4537.

Vanthuyne M, Maes A. (2006). Metal speciation in sulphidic sediments: A new method based on oxidation kinetics modelling in the presence of EDTA. *Science of the total environment*, 367(1), 405-417.

Zhuang Y, Allen HE, Fu G. (1994). Effect of aeration of sediment on cadmium binding. *Environmental toxicology and chemistry*, 13(5), 717-724.

Table A-9. Chemical Characterization of Bedded Sediment, Porewater and Resuspension Water for the Clarence River Sediment Oxidation Study (Burton et al. 2009).

	<u>Sediment</u>	<u>Pore Water</u>	<u>Resusp. Water</u>
pH		7.3	
Eh(mV)		62	
SO ₄ (mmol/L)		0.75	
Fe ²⁺ (mmol/L)		0.55	
Sum S(-II) (mmol/L)		<0.002	
AVS (umol/g)	1031		
S(0) (umol/g)	60		
FeS ₂ as S(umol/g as S)	109		
Total S(umol/g)	1453		
Total Fe(umol/g)	3950		
Total C (%)	8.14%		
Na ⁺ (mmol/L) ^b		100	100
Cl ⁻ (mmol/L) ^b		100	100
Water content (% w/w)	88%		
Bulk density (g/mL)	1.04		
Porosity ^c		0.915	
Particle density (g/mL) ^d	1.47		
Solids Conc. [g/L(bulk)] ^e	124.8		
Solids Conc. [g/L(pore water)] ^f	136.4		
Volume (L) ^g	0.5	0.458	4.5

^a Data from Table S1 in Burton et al. 2009 Supporting Information or found within the paper.

^b Since Na⁺ and Cl⁻ pore water concentrations were not reported, their values were assumed to be equal to their respective concentrations in the resuspension water.

^c Porosity (ϕ) is calculated from the water content (WC), the bulk density (ρ_{bulk}) and the density of water (ρ_w) as: $\phi = WC \times (\rho_{bulk} / \rho_w)$ where $\rho_w = 1.0$ g/mL.

^d Sediment density (ρ_{sed}) is calculated from the bulk density (ρ_{bulk}), the porosity (ϕ), and the density of water (ρ_w) as: $\rho_{sed} = (\rho_{bulk} - \phi \rho_w) / (1 - \phi)$

^e Solids concentration, [m_{sed}(bulk)], in g/L(bulk) is calculated from the porosity (ϕ) and the sediment density (ρ_{sed}) as: $m_{sed}(bulk) = \phi \rho_{sed}$

^f Solids concentration, [m_{sed}(pw)], in g/L(pore water) is calculated from the solids concentration in g/L(bulk) [m_{sed}(bulk)] and the porosity (ϕ) as: $m_{sed}(pw) = m_{sed}(bulk) / \phi$

^g Volume sediment in the resuspension mixture is given in terms of the wet sediment volume [V(wet sed)]. Volume of pore water [V(pw)] is calculated from the porosity (ϕ) and the volume of wet sediment as: $V(pw) = \phi V(sed)$

Table A-10. Chemical Equilibrium Model Calculation for Bedded Sediments from the Clarence River.

<u>Model Input</u>		<u>Model Calculated Values</u>					<u>Measured</u>
<u>Measured</u>		<u>Total</u>	<u>Sorbed</u>	<u>Precipitated</u>	<u>Dissolved</u>	<u>Dissolved</u>	
pH	7.3	H(+)	-1.02E+00	-1.43E-02	-1.00E+00	-4.35E-04	5.50E-04
Total Cl-	1.00E-01	Cl(-)	1.00E-01	0.00E+00	0.00E+00	1.00E-01	
Total Fe	5.32E-01	H2CO3	2.72E-01	0.00E+00	2.71E-01	4.68E-04	
Total Na	1.00E-01	Fe(2+)	4.25E-01	1.29E-02	4.12E-01	5.50E-04	
Total S(0)	8.18E-03	Fe(3+)	1.06E-01	0.00E+00	1.06E-01	2.99E-09	
Total dis. SO4(2-)	7.50E-04	Na(+)	1.00E-01	0.00E+00	0.00E+00	1.00E-01	
Total Sulfide	1.41E-01	S(0)	2.09E-07	0.00E+00	0.00E+00	2.09E-07	
		SO4(2-)	4.28E-03	3.53E-03	0.00E+00	7.50E-04	
		HS(-)	1.41E-01	0.00E+00	1.41E-01	1.21E-07	
<u>Assumed Values</u>		<u>Precipitated Solids</u>					
% Fe(II)	80%			FeS(s)	1.41E-01		
%Fe(III)	20%			FeCO3(s)	2.72E-01		
P(CO2)	1.11E-03			FeOOH(s)	1.06E-01		
				S8(s)	8.18E-03		

Table A-11. Initial Conditions Computed for Clarence River Sediment Resuspension Mixture.

Model Input ^a				Model Calculated Values					Measured	
	<u>Sed-PW</u>	<u>Resusp Water</u>	<u>Mixture</u>		<u>Total</u>	<u>Sorbed</u>	<u>Precip- itated.</u>	<u>Dissolved</u>	<u>Dissolved</u>	
<u>Equilibrium Phases</u>				<u>Equilibrium Phases</u>					7.39	
Total H(+)	-8.78E-01		-8.10E-02	H(+)	-8.10E-02	-1.54E-03	-7.92E-02	-3.10E-04		
Total Cl(-)	1.00E-01	1.00E-01	1.00E-01	Cl(-)	1.00E-01	0.00E+00	0.00E+00	1.00E-01		
Total H2CO3	2.73E-01	1.00E-05	2.52E-02	H2CO3	2.52E-02	0.00E+00	2.49E-02	3.16E-04		
Total Fe(2+)	2.85E-01		2.63E-02	Fe(2+)	2.63E-02	1.09E-03	2.49E-02	3.29E-04		
Total Fe(3+)	1.06E-01		9.82E-03	Fe(3+)	9.82E-03	0.00E+00	9.82E-03	1.57E-09		
Total Na(+)	1.00E-01	1.00E-01	1.00E-01	Na(+)	1.00E-01	0.00E+00	0.00E+00	1.00E-01		
Total S(0)	2.09E-07		1.93E-08	S(0)	1.93E-08	0.00E+00	0.00E+00	1.93E-08		
Total SO4(2-)	3.45E-03		3.19E-04	SO4(2-)	3.19E-04	8.91E-05	0.00E+00	2.30E-04		
Total HS(-)	1.16E-07		1.07E-08	HS(-)	1.07E-08	0.00E+00	1.79E-21	1.07E-08		
				<u>Precipitated Solids</u>						
				FeCO3(s) 2.49E-02						
				FeOOH(s) 9.82E-03						
				<u>Other Calculated Values</u>						
				pH 7.65						
				log{H2CO3} -4.94						
<u>Non-equilibrium Phases</u>				<u>Non-equilibrium Phases</u>						
FeS(s)	1.41E-01		1.30E-02	FeS(s)	1.30E-02					
S8(0) as S	8.18E-03		7.55E-04	S8(0) as S	7.55E-04					
<u>Volume in Mixture</u>										
Volume (L)	0.458	4.500	4.958							

Table A-12. Chemical Characterization of Bedded Sediment, Porewater and Resuspension Water for the Tweed River Sediment Oxidation Study (Burton et al. 2006).^a

	<u>Sediment</u> ($\mu\text{g g}^{-1}$)	<u>Pore Water</u> (mg L^{-1})	<u>Drain- water</u> (mg L^{-1})	<u>Molecular Weight</u>
SO ₄		452	202	96
Cl		4160	37	35.5
HCO ₃		208	0	61
Na		2301	41.9	23
K		62.5	4.65	39.1
Ca		85.3	14.3	40.1
Mg		281	17.9	24.3
Fe(II)		82	0	55.8
Fe(III)		0	1.48	55.8
Fe(Total)	98,600	82	1.48	55.8
Al	31,500	0.556	9.2	27
Mn	192	0.39	0.69	54.9
Ni	15.2	0.009	0.041	58.7
Zn	77	0.015	0.176	65.4
pH		6.21	3.26	
Eh(mV)		-151	515	
Org C (% w/w)	4.70%			12
Inorg C (% w/w)	1.50%			12
AVS ($\mu\text{mol/g}$)	220			
Pyrite-S ($\mu\text{mol/g}$)	36.4			
Element S ($\mu\text{mol/g}$)	113			
Alkalinity ($\mu\text{mol/g}$)	854			
Water content (% w/w)	70%			
Bulk density (g/mL)	1.22			
Porosity ^b		0.854		
Particle density (g/mL) ^c	2.51			
Solids Conc. [g/L(bulk)] ^d	366			
Solids Conc. [g/L(pore water)] ^e	428.6			
Volume (mL) ^f		280	2000	

^a Data from Tables 1 and 2 in Burton et al. 2006.

^b See Footnote c in Table A-2

^c See Footnote d in Table A-2

^d See Footnote e in Table A-2

^e See Footnote f in Table A-2

^f Volume pore water was calculated from the porosity (ϕ), the bulk density (ρ_{bulk}), and the weight of wet sediment added to resuspension mixture ($W_{\text{wet sed}}$) as: $V(pw) = (\phi / \rho_{\text{bulk}}) \times W_{\text{wet sed}}$ where $W_{\text{wet sed}}$ is given as 400 grams.

Table A-13. Chemical Equilibrium Model Calculation for Bedded Sediments from the Tweed River.

Model Input		Model Calculated Values					Measured
	<u>Measured</u>		<u>Total</u>	<u>Sorbed</u>	<u>Precipitated</u>	<u>Dissolved</u>	<u>Dissolved</u>
pH	6.2	H(+)	-3.47E+00	1.79E-02	-3.49E+00	-2.45E-03	-3.41E-03 ^a
Total Al(3+)	5.00E-01	Al(3+)	5.00E-01	0.00E+00	5.00E-01	8.89E-06	2.06E-05
Total Ca(2+)	2.13E-03	Ca(2+)	2.13E-03	7.62E-06	3.18E-22	2.12E-03	2.13E-03
Total Cl-	1.17E-01	Cl(-)	1.17E-01	0.00E+00	0.00E+00	1.17E-01	1.17E-01
Total Fe	7.59E-01	H2CO3	1.72E-02	0.00E+00	1.24E-02	4.80E-03	
Total K(+)	1.60E-03	Fe(2+)	1.37E-01	3.06E-02	1.05E-01	1.45E-03	1.47E-03
Total Mg(2+)	1.16E-02	Fe(3+)	6.22E-01	0.00E+00	6.22E-01	3.23E-08	
Total Mn(2+)	1.51E-03	K(+)	1.60E-03	0.00E+00	0.00E+00	1.60E-03	1.60E-03
Total Na(+)	1.00E-03	Mg(2+)	1.16E-02	0.00E+00	5.11E-23	1.16E-02	1.00E-02
Total Ni(2+)	1.11E-04	Mn(2+)	1.51E-03	4.74E-06	1.49E-03	7.87E-06	7.10E-06
Total S(0)	4.84E-02	Na(+)	1.00E-01	0.00E+00	0.00E+00	1.00E-01	1.00E-01
Total dis. SO42-	4.71E-03	Ni(2+)	1.11E-04	6.54E-09	1.11E-04	1.36E-09	1.53E-07
Total HS(-)	9.43E-02	S(0)	2.09E-07	0.00E+00	0.00E+00	2.09E-07	
Total Zn(2+)	5.05E-04	SO4(2-)	3.36E-02	2.89E-02	0.00E+00	4.71E-03	4.71E-03
		HS(-)	9.43E-02	0.00E+00	9.43E-02	2.82E-06	
		Zn(2+)	5.05E-04	9.93E-08	5.05E-04	1.02E-08	2.29E-07
	<u>Assumed</u>			<u>Precipitated Solids</u>			
% Fe(II)	19%	Al(OH)3(s)		5.00E-01	MnCO3(s)	1.49E-03	
% Fe(III)	81%	FeS(s)		9.37E-02	NiS(s)	1.11E-04	
P(CO2)	7.5E-02	FeCO3(s)		1.09E-02	ZnS(s)	5.05E-04	
		FeOOH(s)		6.22E-01	S8(0) as S	4.84E-02	
^a Computed concentration of Total Dissolved H(+) in the dissolved phase was compared to the measured acidity (i.e., the negative alkalinity), where the measured acidity is given as: $Total\ H(+) = -1 \times HCO_3\ (mg / L) / 61000$							

Table A-14. Initial Conditions Computed for Tweed River Sediment Resuspension Mixture.

Model Input ^a				Model Calculated Values					Measured _b
	<u>Sed-PW</u>	<u>Drain-water</u>	<u>Mixture</u>		<u>Total</u>	<u>Sorbed</u>	<u>Precipitated</u>	<u>Dissolved</u>	<u>Dissolved</u>
<u>Equilibrium Phases</u>				<u>Equilibrium Phases</u>					
Total H(+)	-3.38E+00	0.00E+00	-4.15E-01	H(+)	-4.15E-01	1.08E-03	-4.15E-01	-9.10E-04	-4.97E-04 ^c
Total Al(3+)	5.00E-01	3.41E-04	6.17E-02	Al(3+)	6.17E-02	0.00E+00	6.17E-02	7.72E-06	7.00E-06
Total Ca(2+)	2.13E-03	3.57E-04	5.74E-04	Ca(2+)	5.74E-04	2.98E-07	4.94E-23	5.74E-04	4.36E-04
Total Cl(-)	1.17E-01	1.04E-03	1.53E-02	Cl(-)	1.53E-02	0.00E+00	0.00E+00	1.53E-02	1.13E-02
Total H ₂ CO ₃	1.72E-02	0.00E+00	2.11E-03	H ₂ CO ₃	2.11E-03	0.00E+00	1.84E-04	1.93E-03	
Total Fe(2+)	4.29E-02	0.00E+00	5.27E-03	Fe(2+)	5.27E-03	4.06E-03	1.36E-20	1.21E-03	2.92E-04
Total Fe(3+)	6.22E-01	2.65E-05	7.64E-02	Fe(3+)	7.64E-02	0.00E+00	7.64E-02	2.89E-08	
Total K(+)	1.60E-03	1.19E-04	3.01E-04	K(+)	3.01E-04	0.00E+00	0.00E+00	3.01E-04	4.09E-04
Total Mg(2+)	1.16E-02	7.37E-04	2.07E-03	Mg(2+)	2.07E-03	0.00E+00	1.15E-24	2.07E-03	1.88E-03
Total Mn(2+)	1.51E-03	1.26E-05	1.96E-04	Mn(2+)	1.96E-04	1.09E-06	1.84E-04	1.10E-05	6.08E-06
Total Na(+)	1.00E-01	1.82E-03	1.39E-02	Na(+)	1.39E-02	0.00E+00	0.00E+00	1.39E-02	1.41E-02
Total Ni(2+)	7.90E-09	6.98E-07	6.14E-07	Ni(2+)	6.14E-07	1.28E-07	3.33E-07	1.53E-07	8.52E-08
Total S(0)	2.09E-07		2.57E-08	S(0)	2.57E-08	0.00E+00	0.00E+00	2.57E-08	
Total SO ₄ (2-)	3.36E-02	2.10E-03	5.98E-03	SO ₄ (2-)	5.98E-03	3.99E-03	0.00E+00	1.98E-03	2.49E-03
Total HS(-)	2.82E-06		3.47E-07	HS(-)	3.47E-07	0.00E+00	3.33E-07	1.39E-08	
Total Zn(2+)	1.10E-07	2.69E-06	2.37E-06	Zn(2+)	2.37E-06	1.75E-06	9.78E-20	6.19E-07	1.30E-06
				<u>Precipitated Solids</u>					
				Al(OH) ₃ (s)					6.17E-02
				FeOOH(s)					7.64E-02
				MnCO ₃ (s)					1.84E-04
				<u>Other Calculated Values</u>					
				pH					6.21
				log{H ₂ CO ₃ }					-2.98
									6.21

<u>Non-equilibrium Phases</u>				<u>Non-equilibrium Phases</u>		
FeS(s)	9.37E-02		1.15E-02	FeS(s)	1.15E-02	
NiS(s)	1.11E-04		1.36E-05	NiS(s)	1.36E-05	
ZnS(s)	5.05E-04		6.20E-05	ZnS(s)	6.20E-05	
S8(0) as S	4.84E-02		5.95E-03	S8(0) as S	5.95E-03	
<u>Volume in Mixture</u>						
Volume (L)	0.280	2.000	2.280			
<p>^a Model input values were calculated from model output for the sediment-pore water chemistry (Table A-6) and the reported chemistry of the resuspension water (Table A-5) mixed according to the respective volumes.</p> <p>^b Measured values were taken at 20 minutes after the sediment resuspension experiment began.</p> <p>^c Computed concentration of Total Dissolved H(+) in the dissolved phase was compared to the measured acidity (i.e., the negative alkalinity), where the measured acidity is given as: $Total\ H(+) = -1 \times HCO_3\ (mg / L) / 61000$</p>						

Table A-15. Chemical Characterization of Bedded Sediment, Porewater and Resuspension Water for the Anacostia River Sediment Oxidation Study (Hong et al. 2011).^a

	<u>Sediment</u> ($\mu\text{g g}^{-1}$)	<u>Porewater</u> (mM)	<u>Resusp. water</u> (mg L^{-1})	<u>Molecular</u> <u>Weight</u>
SO4		0.00063		96
Cl		0.272	97.2	35.5
HCO3		0.7		61
Na		2.3	52.9	23
K		0.051	2	39.1
Ca	11,200	0.291	2	40.1
Mg	1,950	0.129	6.6	24.3
Fe(II) ^b	3,050	0.049		55.8
Fe(III) ^b	20,850			55.8
Fe(Total)	53,420			55.8
Al	12,330			27
Mn	240			54.9
Zn	700			65.4
pH		--		
Org C (% w/w)	7.00%			12
Inorg C (% w/w)	1.05%			12
AVS ($\mu\text{mol/g}$)	54.03			
Water content (% w/w)	53.4%			
Particle density (g/mL) ^c	2.50			
Porosity ^d		0.741		
Bulk density (g/mL) ^e	1.39			
Solids Conc. [g/L(bulk)] ^f	646.9			
Solids Conc. [g/L(pore water)] ^g	872.7			
Vol (mL) ^h		267	2800	

^a Data from Table S3 and information in text (Hong et al. 2011).

^b Fe(II) and Fe(III) concentrations are based on oxalate extractable Fe(2+) and Fe(3+).

^c Sediment particle density was assumed to be equal to 2.5 g/mL .

^d Porosity (ϕ) is calculated from the water content (WC), the sediment dry density (ρ_{sed}) and the density of water (ρ_w) as:
$$\phi = \frac{WC \cdot \rho_{\text{sed}}}{(\rho_{\text{sed}} - \rho_w) \cdot WC + \rho_w} \quad \text{where } \rho_w = 1.0 \text{ g/mL.}$$

^e Sediment bulk density (ρ_{bulk}) is calculated from the sediment dry density (ρ_{sed}), the porosity (ϕ), and the density of water (ρ_w) as:
$$\rho_{\text{bulk}} = \phi \cdot \rho_w + (1 - \phi) \cdot \rho_{\text{sed}}$$

^f See Footnote e in Table A-2

^g See Footnote f in Table A-2

^h Volume pore water was calculated from the water content (WC), the water density (ρ_w), and the weight of wet sediment added to sediment resuspension mixture ($W_{\text{wet sed}}$) as:
$$V(pw) = (WC / \rho_w) \times W_{\text{wet sed}}$$
 where $W_{\text{wet sed}}$ is given as 500 grams.

Table A-16. Initial Conditions Computed for Anacostia River Sediment Resuspension Mixture.

Model Input ^a					Model Calculated Values					Measured
	<u>Sed-PW</u>	<u>Porewater</u>	<u>Resusp.</u> <u>water</u>	<u>Mixture</u>		<u>Total</u>	<u>Sorbed</u>	<u>Precipi-</u> <u>tated</u>	<u>Dissolved</u>	<u>Dissolved</u>
<u>Equilibrium Phases</u>					<u>Equilibrium Phases</u>					
pH				6.1	H(+)	-3.09E-01	4.12E-03	-3.12E-01	-8.58E-04	
Total Al(3+)	3.99E-01			3.47E-02	Al(3+)	3.47E-02	0.00E+00	3.47E-02	9.07E-06	
Total Ca(2+)	2.44E-01	2.91E-04	4.99E-05	2.13E-02	Ca(2+)	2.13E-02	7.19E-05	1.08E-21	2.12E-02	2.96E-04
Total Cl(-)		2.72E-04	2.74E-03	2.52E-03	Cl(-)	2.52E-03	0.00E+00	0.00E+00	2.52E-03	
Total Fe(2+) ^b	2.29E-03	4.90E-05		2.04E-04	H2CO3	2.15E-03	0.00E+00	3.00E-04	1.85E-03	
Total Fe(3+)	7.95E-01			6.92E-02	Fe(2+)	2.04E-04	1.90E-04	3.52E-23	1.37E-05	1.38E-05
Total K(+)		5.12E-05	5.12E-05	5.12E-05	Fe(3+)	6.92E-02	0.00E+00	6.92E-02	3.89E-08	
Total Mg(2+)	7.00E-02	1.29E-04	2.72E-04	6.36E-03	K(+)	5.12E-05	0.00E+00	0.00E+00	5.12E-05	
Total Mn(2+)	3.81E-03			3.32E-04	Mg(2+)	6.36E-03	0.00E+00	3.62E-23	6.36E-03	1.47E-04
Total Na(+)		2.30E-03	2.30E-03	2.30E-03	Mn(2+)	3.32E-04	1.11E-05	3.00E-04	2.10E-05	9.29E-06
Total S(0)				0.00E+00	Na(+)	2.30E-03	0.00E+00	0.00E+00	2.30E-03	
Dis. SO4(2-)		6.30E-07		9.00E-05	S(0)	2.09E-07	0.00E+00	0.00E+00	2.09E-07	
Total HS(-)				0.00E+00	SO4(2-)	1.03E-03	9.43E-04	0.00E+00	9.00E-05	
Total Zn(2+)				0.00E+00	HS(-)	1.00E-10	0.00E+00	3.59E-27	1.00E-10	
					Zn(2+)	1.00E-10	9.30E-11	4.21E-28	6.97E-12	
				<u>Assumed^c</u>				<u>Precipitated Solids</u>		
			% Fe(II)	4.8%				Al(OH)3(s)	3.47E-02	
			%Fe(III)	95.2%				FeOOH(s)	6.92E-02	
			P(CO2)	3.2E-2				MnCO3(s)	3.00E-04	
								<u>Other Calculated Values</u>		
								log{H2CO3}	-2.99	
								HCO3-	6.94E-04	6.90E-04 ^e
<u>Non-equilibrium Phases^d</u>					<u>Non-equilibrium Phases</u>					

FeS(s)	3.78E-02		3.29E-03	FeS(s)	3.29E-03	
ZnS(s)	9.34E-03		8.13E-04	ZnS(s)	8.13E-04	
S8(0) as S	---		---	S8(0) as S	---	
<u>Volume in Mixture</u>						
Volume (L)	0.267	0.267	2.8	3.067		

^a Total chemical concentrations were calculated from measured sediment, pore water and resuspension water chemistry (Table A-8).
^b For chemical equilibrium model calculations, Total Fe(2+) = % Fe(II) * Total Fe - FeS(s) ; Total HS(-) and Total Zn were set equal to negligible concentrations (i.e., 10⁻⁹ M).
^c Assumed values for P(CO2) and percent of total Fe as Fe(2+) and Fe(3+) were checked by comparing equilibrium model calculations for alkalinity and dissolved Fe(2+) to initial measurements for alkalinity and dissolved Fe(2+) in the sediment resuspension mixture.
^d Non-equilibrium solid phases were calculated as follows: ZnS(s) was set equal to the Total Zn concentration. FeS(s) was set equal to the Total AVS concentration minus the ZnS(s) concentration.
^e Measured concentration of HCO₃⁻ in the resuspension mixture was calculated from: $HCO_3^- = HCO_3 (mg / L) / 61000$

Table A-17. Chemical Characterization of Bedded Sediment, Porewater and Resuspension Water for the Portsmouth Naval Station (MS03) Sediment Oxidation Study (Fetters 2013).^a

	<u>Sediment</u> ($\mu\text{g g}^{-1}$)	<u>Pore Water</u> (mg L^{-1})	<u>Resusp.</u> <u>water</u> ^b (mg L^{-1})	<u>Molecular</u> <u>Weight</u>
SO ₄		2,402 ^c	2,402	96
Cl		17,142 ^c	17,142	35.5
HCO ₃		126 ^c	126	61
Na		9,539 ^c	9,539	23
K		353 ^c	353	39.1
Ca		365 ^c	365	40.1
Mg		1,14 ^c	1,143	24.3
Fe(II)		14		55.8
Fe(III)				55.8
Fe(Total)	39,600 (5,540) ^d	14		55.8
Mn	332 (39) ^d	0.351		54.9
Cu	575 (52) ^d	ND		63.5
Ni	69 (20) ^d	0.022		58.7
Zn	533 (293) ^d	0.028		65.4
pH		7.05		
Dissolved Oxygen (mg/L)		1.04		32
Dissolved Organic Carbon (mg/L)		103		12
Org C (% w/w)	1.60%			12
AVS ($\mu\text{mol/g}$)	20			
TRIS ($\mu\text{mol/g}$) ^e	117			
Pyrite ($\mu\text{mol/g}$) ^f	48.5			
Porosity ^g		0.80		
Particle density (g/mL) ^h	2.50			
Solids Conc. [g/L(bulk)] ⁱ	500			
Solids Conc. [g/L(pore water)] ^j	625			
Volume (L) ^k		0.2	249.8	

^a Data from Tables 1, 2, SI-2 in Fetters 2013.

^b Chemical composition of resuspension water is based on chemical composition of seawater (reported in Stumm and Morgan 1981) adjusted to 31 ppt salinity)

^c Concentration of major cations and anions in porewater is assumed to be equal to concentrations in the resuspension water.

^d Measured concentrations of metals in sediments are given as total recoverable metal with concentrations of simultaneously extracted metal (SEM) given in parentheses.

^e TRIS represents total reduced inorganic sulfur concentration.

^f Estimate of pyrite in sediment is given as: $FeS_2(s) = (TRIS - AVS)/2$

^g A porosity of 0.80 was assumed.

^h A particle density of 2.5 g/mL was assumed.

ⁱ Solids concentration, $[m_{sed}(bulk)]$, in g/L(bulk) is calculated from the porosity (ϕ) and the sediment particle density (ρ_{sed}) as: $m_{sed}(bulk) = \phi \rho_{sed}$

^j Solids concentration, $[m_{sed}(pw)]$, in g/L(pore water) is calculated from the solids concentration in g/L(bulk) $[m_{sed}(bulk)]$ and the porosity (ϕ) as: $m_{sed}(pw) = m_{sed}(bulk)/\phi$

^k Volume of the porewater and the resuspension water were set to result in a suspended solids concentration of 0.5 g/L.

Table A-18. Chemical Characterization of Bedded Sediment, Porewater and Resuspension Water for the Portsmouth Naval Station (MS04) Sediment Oxidation Study (Fetters 2013).^a

	<u>Sediment</u> ($\mu\text{g g}^{-1}$)	<u>Pore Water</u> (mg L^{-1})	<u>Resusp.</u> <u>water</u> ^b (mg L^{-1})	<u>Molecular</u> <u>Weight</u>
SO ₄		2,402 ^c	2,402	96
Cl		17,142 ^c	17,142	35.5
HCO ₃		126 ^c	126	61
Na		9,539 ^c	9,539	23
K		353 ^c	353	39.1
Ca		365 ^c	365	40.1
Mg		1,14 ^c	1,143	24.3
Fe(II)		14		55.8
Fe(III)				55.8
Fe(Total)	24,900 (5,478) ^d	14		55.8
Mn	289 (32) ^d	0.103		54.9
Cu	364 (55) ^d	ND		63.5
Ni	48 (12.5) ^d	0.018		58.7
Zn	223 (145) ^d	0.040		65.4
pH		7.08		
Dissolved Oxygen (mg/L)		0.81		32
Dissolved Organic Carbon (mg/L)		98		12
Org C (% w/w)	2.00%			12
AVS ($\mu\text{mol/g}$)	9			
TRIS ($\mu\text{mol/g}$) ^e	98			
Pyrite ($\mu\text{mol/g}$) ^f	44.5			
Porosity ^g		0.80		
Particle density (g/mL) ^h	2.50			
Solids Conc. [g/L(bulk)] ⁱ	500			
Solids Conc. [g/L(pore water)] ^j	625			
Volume (L) ^k		0.2	249.8	

^a Data from Tables 1, 2, SI-2 in Fetters 2013.

^b Chemical composition of resuspension water is based on chemical composition of seawater (reported in Stumm and Morgan 1981) adjusted to 31 ppt salinity)

^c Concentration of major cations and anions in porewater is assumed to be equal to concentrations in the resuspension water.

^d Measured concentrations of metals in sediments are given as total recoverable metal with concentrations of simultaneously extracted metal (SEM) given in parentheses.

^e TRIS represents total reduced inorganic sulfur concentration.

^f Estimate of pyrite in sediment is given as: $FeS_2(s) = (TRIS - AVS)/2$

^g A porosity of 0.80 was assumed.

^h A particle density of 2.5 g/mL was assumed.

ⁱ Solids concentration, $[m_{sed}(bulk)]$, in g/L(bulk) is calculated from the porosity (ϕ) and the sediment particle density (ρ_{sed}) as: $m_{sed}(bulk) = \phi \rho_{sed}$

^j Solids concentration, $[m_{sed}(pw)]$, in g/L(pore water) is calculated from the solids concentration in g/L(bulk) $[m_{sed}(bulk)]$ and the porosity (ϕ) as: $m_{sed}(pw) = m_{sed}(bulk)/\phi$

^k Volume of the porewater and the resuspension water were set to result in a suspended solids concentration of 0.5 g/L.

Table A-19. Chemical Equilibrium Model Calculation for Bedded Sediments from the Portsmouth Naval Station (MS03) Using Total Recoverable Iron and Total Recoverable Metal Concentrations.

Model Input		Model Calculated Values					Measured
	<u>Measured</u>		<u>Total</u>	<u>Sorbed</u>	<u>Precipitated</u>	<u>Dissolved</u>	<u>Dissolved</u>
pH	7.05	H(+)	-1.03E+00	-1.49E-02	-1.01E+00	-3.35E-03	
Total Ca(2+)	9.10E-03	Ca(2+)	9.10E-03	7.99E-05	2.04E-20	9.02E-03	
Total Cl-	4.83E-01	Cl(-)	4.83E-01	0.00E+00	0.00E+00	4.83E-01	
Total Cu	5.66E-03	H2CO3	1.94E-01	0.00E+00	1.90E-01	3.70E-03	
Total Fe	4.13E-01	Cu(2+)	5.66E-03	1.18E-18	5.66E-03	7.20E-17	
Total K(+)	9.04E-03	Fe(2+)	2.07E-01	1.89E-02	1.87E-01	2.53E-04	2.52E-04
Total Mg(2+)	4.70E-02	Fe(3+)	2.07E-01	0.00E+00	2.07E-01	5.18E-09	
Total Mn(2+)	3.79E-03	K(+)	9.04E-03	0.00E+00	0.00E+00	9.04E-03	
Total Na(+)	4.15E-01	Mg(2+)	4.70E-02	0.00E+00	6.18E-29	4.70E-02	
Total Ni(2+)	7.35E-04	Mn(2+)	3.79E-03	2.86E-06	3.78E-03	1.47E-06	6.39E-06
Total S(0)	--	Na(+)	4.15E-01	0.00E+00	0.00E+00	4.15E-01	
Total dis. SO42-	2.50E-02	Ni(2+)	7.35E-04	4.06E-09	7.35E-04	2.64E-10	3.75E-07
Total HS(-)	1.25E-02	S(0)	2.09E-07	0.00E+00	0.00E+00	2.09E-07	
Total Zn(2+)	5.09E-03	SO4(2-)	3.19E-02	6.89E-03	0.00E+00	2.50E-02	
		HS(-)	1.25E-02	0.00E+00	1.25E-02	9.06E-07	
		Zn(2+)	5.09E-03	6.09E-08	5.09E-03	4.82E-09	4.28E-07
	<u>Assumed</u>			<u>Precipitated Solids</u>			
% Fe(II)	50%		FeS(s)	1.01E-03	MnCO3(s)	3.78E-03	
%Fe(III)	50%		FeCO3(s)	1.86E-01	NiS(s)	7.35E-04	
P(CO2)	1.02E-02		FeOOH(s)	2.07E-01	ZnS(s)	5.09E-03	
			CuS(s)	5.66E-03	CaCO3(s)	2.04E-20	

Table A-20. Chemical Equilibrium Model Calculation for Bedded Sediments from the Portsmouth Naval Station (MS04) Using Total Recoverable Iron and Total Recoverable Metal Concentrations.

Model Input		Model Calculated Values					Measured
	<u>Measured</u>		<u>Total</u>	<u>Sorbed</u>	<u>Precipitated</u>	<u>Dissolved</u>	<u>Dissolved</u>
pH	7.08	H(+)	-6.30E-01	-9.89E-03	-6.17E-01	-3.17E-03	
Total Ca(2+)	9.10E-03	Ca(2+)	9.10E-03	4.92E-05	2.16E-20	9.05E-03	
Total Cl-	4.83E-01	Cl(-)	4.83E-01	0.00E+00	0.00E+00	4.83E-01	
Total Cu	3.58E-03	H2CO3	1.21E-01	0.00E+00	1.17E-01	3.48E-03	
Total Fe	2.51E-01	Cu(2+)	3.58E-03	1.05E-14	3.58E-03	0.00E+00	
Total K(+)	9.04E-03	Fe(2+)	1.26E-01	1.14E-02	1.14E-01	2.50E-04	2.50E-04
Total Mg(2+)	4.70E-02	Fe(3+)	1.26E-01	0.00E+00	1.26E-01	4.87E-09	
Total Mn(2+)	3.29E-03	K(+)	9.04E-03	0.00E+00	0.00E+00	9.04E-03	
Total Na(+)	4.15E-01	Mg(2+)	4.70E-02	0.00E+00	6.39E-29	4.70E-02	
Total Ni(2+)	5.11E-04	Mn(2+)	3.29E-03	1.73E-06	3.29E-03	1.45E-06	1.88E-06
Total S(0)	--	Na(+)	4.15E-01	0.00E+00	0.00E+00	4.15E-01	
Total dis. SO42-	2.50E-02	Ni(2+)	5.11E-04	3.61E-05	4.71E-04	3.82E-06	3.07E-07
Total HS(-)	5.63E-03	S(0)	2.09E-07	0.00E+00	0.00E+00	2.09E-07	
Total Zn(2+)	2.13E-03	SO4(2-)	2.92E-02	4.20E-03	0.00E+00	2.50E-02	
		HS(-)	5.63E-03	0.00E+00	5.62E-03	5.57E-11	
		Zn(2+)	2.13E-03	5.41E-04	1.57E-03	2.02E-05	6.12E-07
	<u>Assumed</u>			<u>Precipitated Solids</u>			
% Fe(II)	50%	FeS(s)		6.79E-25	MnCO3(s)	3.29E-03	
%Fe(III)	50%	FeCO3(s)		1.14E-01	NiS(s)	4.71E-04	
P(CO2)	1.06E-02	FeOOH(s)		1.26E-01	ZnS(s)	1.57E-03	
		CuS(s)		3.58E-03	CaCO3(s)	2.16E-20	

Table A-21. Initial Conditions Computed for Portsmouth Naval Station (MS03) Sediment Resuspension Mixture. Based on Total Recoverable Iron and Total Recoverable Metal Concentrations.

Model Input ^a				Model Calculated Values					Measure d
	<u>Sed-PW</u>	<u>Resusp. water</u>	<u>Mixture</u>		<u>Total</u>	<u>Sorbed</u>	<u>Precipi- tated</u>	<u>Dissolved</u>	<u>Dissolved</u>
<u>Equilibrium Phases</u>				<u>Equilibrium Phases</u>					
Total H(+)	-1.02E+00	-2.07E-03	-2.88E-03	H(+)	-2.88E-03	-1.85E-05	-8.59E-04	-2.00E-03	
Total Ca(2+)	9.10E-03	9.04E-03	9.04E-03	Ca(2+)	9.04E-03	1.31E-07	1.80E-04	8.86E-03	
Total Cl(-)	4.83E-01	4.83E-01	4.83E-01	Cl(-)	4.83E-01	0.00E+00	0.00E+00	4.83E-01	
Total H2CO3	1.94E-01	2.08E-03	2.23E-03	H2CO3	2.23E-03	0.00E+00	1.82E-04	2.05E-03	
Total Cu(2+)	7.29E-17	0.00E+00	5.83E-20	Cu(2+)	5.83E-20	5.28E-20	8.23E-22	4.71E-21	6.30E-08
Total Fe(2+)	2.06E-01	0.00E+00	1.64E-04	Fe(2+)	1.64E-04	1.81E-05	6.90E-20	1.46E-04	< 1.81E-07
Total Fe(3+)	2.07E-01	0.00E+00	1.65E-04	Fe(3+)	1.65E-04	0.00E+00	1.65E-04	2.28E-09	
Total K(+)	9.04E-03	9.04E-03	9.04E-03	K(+)	9.04E-03	0.00E+00	0.00E+00	9.04E-03	
Total Mg(2+)	4.70E-02	4.70E-02	4.70E-02	Mg(2+)	4.70E-02	0.00E+00	1.39E-28	4.70E-02	
Total Mn(2+)	3.79E-03	0.00E+00	3.03E-06	Mn(2+)	3.03E-06	3.12E-09	2.05E-06	9.71E-07	1.28E-07
Total Na(+)	4.15E-01	4.15E-01	4.15E-01	Na(+)	4.15E-01	0.00E+00	0.00E+00	4.15E-01	
Total Ni(2+)	4.32E-09	0.00E+00	3.46E-12	Ni(2+)	3.46E-12	8.73E-14	3.68E-25	3.37E-12	
Total S(0)	2.09E-07		1.67E-10	S(0)	1.67E-10	0.00E+00	0.00E+00	1.67E-10	
Total SO4(2-)	3.19E-02	2.50E-02	2.50E-02	SO4(2-)	2.50E-02	5.02E-06	0.00E+00	2.50E-02	
Total HS(-)	9.06E-07		7.25E-10	HS(-)	7.25E-10	0.00E+00	8.41E-22	7.25E-10	
Total Zn(2+)	6.57E-08	0.00E+00	5.26E-11	Zn(2+)	5.26E-11	3.43E-12	9.67E-25	4.91E-11	< 5.38E-8
				<u>Precipitated Solids</u>					
				FeCO3(s)			6.90E-20		
				FeOOH(s)			1.65E-04		
				MnCO3(s)			2.05E-06		
				CaCO3(s)			1.80E-04		

				<u>Other Calculated Values</u>		
				pH		7.46
				log{H2CO3}		-4.07
<u>Non-equilibrium Phases</u>				<u>Non-equilibrium Phases</u>		
FeS(s)	1.01E-03		8.08E-07	FeS(s)	8.08E-07	
CuS(s)	5.66E-03		4.53E-06	CuS(s)	4.53E-06	
NiS(s)	7.35E-04		5.88E-07	NiS(s)	5.88E-07	
ZnS(s)	5.09E-03		4.08E-06	ZnS(s)	4.08E-06	
<u>Volume in Mixture</u>						
Volume (L) ^b	0.2	249.8	250.0			
^a Model input values were calculated from model output for the sediment-pore water chemistry (Table A-12) and the reported chemistry of the resuspension water (Table A-10) mixed according to the respective volumes.						
^b Volumes were assumed to yield a suspended sediment concentration of 500 mg/L in the resuspension mixture.						

Table A-22. Initial Conditions Computed for Portsmouth Naval Station (MS04) Sediment Resuspension Mixture. Based on Total Recoverable Iron and Total Recoverable Metal Concentrations.

Model Input ^a				Model Calculated Values					Measure d
	<u>Sed-PW</u>	<u>Resusp. water</u>	<u>Mixture</u>		<u>Total</u>	<u>Sorbed</u>	<u>Precipi- tated</u>	<u>Dissolved</u>	<u>Dissolved</u>
<u>Equilibrium Phases</u>				<u>Equilibrium Phases</u>					
Total H(+)	-6.24E-01	-2.07E-03	-2.57E-03	H(+)	-2.57E-03	-9.81E-06	-5.58E-04	-2.00E-03	
Total Ca(2+)	9.10E-03	9.04E-03	9.04E-03	Ca(2+)	9.04E-03	1.14E-07	1.27E-04	8.91E-03	
Total Cl(-)	4.83E-01	4.83E-01	4.83E-01	Cl(-)	4.83E-01	0.00E+00	0.00E+00	4.83E-01	
Total H2CO3	1.21E-01	2.08E-03	2.17E-03	H2CO3	2.17E-03	0.00E+00	1.28E-04	2.04E-03	
Total Cu(2+)	1.05E-14	0.00E+00	8.41E-18	Cu(2+)	8.41E-18	7.62E-18	7.79E-24	7.85E-19	< 4.20E-08
Total Fe(2+)	1.26E-01	0.00E+00	1.00E-04	Fe(2+)	1.00E-04	9.71E-06	1.16E-20	9.07E-05	< 1.81E-07
Total Fe(3+)	1.26E-01	0.00E+00	1.00E-04	Fe(3+)	1.00E-04	0.00E+00	1.00E-04	2.29E-09	
Total K(+)	9.04E-03	9.04E-03	9.04E-03	K(+)	9.04E-03	0.00E+00	0.00E+00	9.04E-03	
Total Mg(2+)	4.70E-02	4.70E-02	4.70E-02	Mg(2+)	4.70E-02	0.00E+00	1.39E-28	4.70E-02	
Total Mn(2+)	3.29E-03	0.00E+00	2.63E-06	Mn(2+)	2.63E-06	2.73E-09	1.65E-06	9.77E-07	1.28E-07
Total Na(+)	4.15E-01	4.15E-01	4.15E-01	Na(+)	4.15E-01	0.00E+00	0.00E+00	4.15E-01	
Total Ni(2+)	3.99E-05	0.00E+00	3.19E-08	Ni(2+)	3.19E-08	7.01E-10	2.09E-25	3.12E-08	
Total S(0)	2.09E-07		1.67E-10	S(0)	1.67E-10	0.00E+00	0.00E+00	1.67E-10	
Total SO4(2-)	2.92E-02	2.50E-02	2.50E-02	SO4(2-)	2.50E-02	2.81E-06	0.00E+00	2.50E-02	
Total HS(-)	5.57E-11		4.45E-14	HS(-)	4.45E-14	0.00E+00	8.51E-24	4.45E-14	
Total Zn(2+)	5.61E-04	0.00E+00	4.49E-07	Zn(2+)	4.49E-07	2.57E-08	5.09E-25	4.23E-07	3.06E-07
				<u>Precipitated Solids</u>					
						FeCO3(s)	1.16E-20		
						FeOOH(s)	1.00E-04		
						MnCO3(s)	1.65E-06		
						CaCO3(s)	1.27E-04		

				<u>Other Calculated Values</u>		
				pH		7.46
				log{H2CO3}		-4.07
<u>Non-equilibrium Phases</u>				<u>Non-equilibrium Phases</u>		
FeS(s)	6.79E-25		5.43E-28	FeS(s)	5.43E-28	
CuS(s)	3.58E-03		2.87E-06	CuS(s)	2.87E-06	
NiS(s)	4.71E-04		3.77E-07	NiS(s)	3.77E-07	
ZnS(s)	1.57E-03		1.26E-06	ZnS(s)	1.26E-06	
<u>Volume in Mixture</u>						
Volume (L) ^b	0.2	249.8	250.0			
^a Model input values were calculated from model output for the sediment-pore water chemistry (Table A-13) and the reported chemistry of the resuspension water (Table A-11) mixed according to the respective volumes.						
^b Volumes were assumed to yield a suspended sediment concentration of 500 mg/L in the resuspension mixture.						

Table A-22. Chemical Equilibrium Model Calculation for Bedded Sediments from the Portsmouth Naval Station (MS03) Using Simultaneously Extracted Iron and Simultaneously Extracted Metal (SEM) Concentrations.

Model Input		Model Calculated Values					Measured
	<u>Measured</u>		<u>Total</u>	<u>Sorbed</u>	<u>Precipitated</u>	<u>Dissolved</u>	<u>Dissolved</u>
pH	7.05	H(+)	-1.50E-01	-2.23E-03	-1.45E-01	-3.35E-03	
Total Ca(2+)	9.10E-03	Ca(2+)	9.10E-03	1.21E-05	2.09E-20	9.09E-03	
Total Cl-	4.83E-01	Cl(-)	4.83E-01	0.00E+00	0.00E+00	4.83E-01	
Total Cu	5.09E-04	H2CO3	2.31E-02	0.00E+00	1.94E-02	3.70E-03	
Total Fe	6.21E-02	Cu(2+)	5.09E-04	1.77E-19	5.09E-04	7.16E-17	
Total K(+)	9.04E-03	Fe(2+)	3.10E-02	2.84E-03	2.80E-02	2.53E-04	2.52E-04
Total Mg(2+)	4.70E-02	Fe(3+)	3.10E-02	0.00E+00	3.10E-02	5.18E-09	
Total Mn(2+)	4.60E-04	K(+)	9.04E-03	0.00E+00	0.00E+00	9.04E-03	
Total Na(+)	4.15E-01	Mg(2+)	4.70E-02	0.00E+00	6.23E-29	4.70E-02	
Total Ni(2+)	2.13E-04	Mn(2+)	4.60E-04	4.30E-07	4.58E-04	1.47E-06	6.39E-06
Total S(0)	--	Na(+)	4.15E-01	0.00E+00	0.00E+00	4.15E-01	
Total dis. SO42-	2.50E-02	Ni(2+)	2.13E-04	6.10E-10	2.13E-04	2.64E-10	3.75E-07
Total HS(-)	1.25E-02	S(0)	2.09E-07	0.00E+00	0.00E+00	2.09E-07	
Total Zn(2+)	2.80E-03	SO4(2-)	2.61E-02	1.04E-03	0.00E+00	2.50E-02	
		HS(-)	1.25E-02	0.00E+00	1.25E-02	9.06E-07	
		Zn(2+)	2.80E-03	9.15E-09	2.80E-03	4.82E-09	4.28E-07
	<u>Assumed</u>			<u>Precipitated Solids</u>			
% Fe(II)	50%	FeS(s)		8.97E-03	MnCO3(s)	4.58E-04	
%Fe(III)	50%	FeCO3(s)		1.90E-02	NiS(s)	2.13E-04	
P(CO2)	1.20E-02	FeOOH(s)		3.10E-02	ZnS(s)	2.80E-03	
		CuS(s)		5.09E-04	CaCO3(s)	2.09E-20	

Table A-24. Chemical Equilibrium Model Calculation for Bedded Sediments from the Portsmouth Naval Station (MS04) Using Simultaneously Extracted Iron and Simultaneously Extracted Metal (SEM) Concentrations.

Model Input		Model Calculated Values					Measured
	<u>Measured</u>		<u>Total</u>	<u>Sorbed</u>	<u>Precipitated</u>	<u>Dissolved</u>	<u>Dissolved</u>
pH	7.08	H(+)	-8.38E-02	-1.29E-03	-7.94E-02	-3.14E-03	
Total Ca(2+)	9.10E-03	Ca(2+)	9.10E-03	6.79E-06	2.13E-20	9.10E-03	
Total Cl-	4.83E-01	Cl(-)	4.83E-01	0.00E+00	0.00E+00	4.83E-01	
Total Cu	5.37E-04	H2CO3	1.52E-02	0.00E+00	1.17E-02	3.45E-03	
Total Fe	3.35E-02	Cu(2+)	5.37E-04	9.88E-20	5.37E-04	5.88E-17	
Total K(+)	9.04E-03	Fe(2+)	1.68E-02	1.58E-03	1.49E-02	2.52E-04	2.50E-04
Total Mg(2+)	4.70E-02	Fe(3+)	1.68E-02	0.00E+00	1.68E-02	4.87E-09	
Total Mn(2+)	3.64E-04	K(+)	9.04E-03	0.00E+00	0.00E+00	9.04E-03	
Total Na(+)	4.15E-01	Mg(2+)	4.70E-02	0.00E+00	6.30E-29	4.70E-02	
Total Ni(2+)	1.33E-04	Mn(2+)	3.64E-04	2.39E-07	3.62E-04	1.46E-06	1.88E-06
Total S(0)	--	Na(+)	4.15E-01	0.00E+00	0.00E+00	4.15E-01	
Total dis. SO42-	2.50E-02	Ni(2+)	1.33E-04	3.39E-10	1.33E-04	2.62E-10	3.07E-07
Total HS(-)	5.63E-03	S(0)	2.09E-07	0.00E+00	0.00E+00	2.09E-07	
Total Zn(2+)	1.39E-03	SO4(2-)	2.56E-02	5.58E-04	0.00E+00	2.50E-02	
		HS(-)	5.62E-03	0.00E+00	5.62E-03	8.26E-07	
		Zn(2+)	1.39E-03	5.09E-09	1.39E-03	4.59E-09	6.12E-07
	<u>Assumed</u>			<u>Precipitated Solids</u>			
% Fe(II)	50%		FeS(s)	3.57E-03	MnCO3(s)	3.62E-04	
%Fe(III)	50%		FeCO3(s)	1.14E-02	NiS(s)	1.33E-04	
P(CO2)	1.05E-02		FeOOH(s)	1.68E-02	ZnS(s)	1.39E-03	
			CuS(s)	5.37E-04	CaCO3(s)	2.13E-20	

Table A-25. Initial Conditions Computed for Portsmouth Naval Station (MS03) Sediment Resuspension Mixture. Based on Simultaneously Extracted Iron and Simultaneously Extracted Metal SEM) Concentrations.

Model Input ^a				Model Calculated Values					Measure d
	<u>Sed-PW</u>	<u>Resusp. water</u>	<u>Mixture</u>		<u>Total</u>	<u>Sorbed</u>	<u>Precipi- tated</u>	<u>Dissolved</u>	<u>Dissolved</u>
<u>Equilibrium Phases</u>				<u>Equilibrium Phases</u>					
Total H(+)	-1.38E-01	-2.07E-03	-2.18E-03	H(+)	-2.18E-03	-9.28E-07	-1.82E-04	-1.99E-03	
Total Ca(2+)	9.10E-03	9.04E-03	9.04E-03	Ca(2+)	9.04E-03	7.52E-08	5.37E-05	8.98E-03	
Total Cl(-)	4.83E-01	4.83E-01	4.83E-01	Cl(-)	4.83E-01	0.00E+00	0.00E+00	4.83E-01	
Total H2CO3	2.31E-02	2.08E-03	2.09E-03	H2CO3	2.09E-03	0.00E+00	5.37E-05	2.04E-03	
Total Cu(2+)	7.18E-17	0.00E+00	5.74E-20	Cu(2+)	5.74E-20	4.85E-20	1.38E-21	7.51E-21	6.30E-08
Total Fe(2+)	2.21E-02	0.00E+00	1.77E-05	Fe(2+)	1.77E-05	1.21E-06	1.07E-21	1.65E-05	< 1.81E-07
Total Fe(3+)	3.10E-02	0.00E+00	2.48E-05	Fe(3+)	2.48E-05	0.00E+00	2.48E-05	2.30E-09	
Total K(+)	9.04E-03	9.04E-03	9.04E-03	K(+)	9.04E-03	0.00E+00	0.00E+00	9.04E-03	
Total Mg(2+)	4.70E-02	4.70E-02	4.70E-02	Mg(2+)	4.70E-02	0.00E+00	1.37E-28	4.70E-02	
Total Mn(2+)	4.60E-04	0.00E+00	3.68E-07	Mn(2+)	3.68E-07	7.19E-10	5.95E-21	3.67E-07	1.28E-07
Total Na(+)	4.15E-01	4.15E-01	4.15E-01	Na(+)	4.15E-01	0.00E+00	0.00E+00	4.15E-01	
Total Ni(2+)	8.74E-10	0.00E+00	6.99E-13	Ni(2+)	6.99E-13	1.06E-14	7.44E-26	6.88E-13	
Total S(0)	2.09E-07		1.67E-10	S(0)	1.67E-10	0.00E+00	0.00E+00	1.67E-10	
Total SO4(2-)	2.61E-02	2.50E-02	2.50E-02	SO4(2-)	2.50E-02	4.74E-07	0.00E+00	2.50E-02	
Total HS(-)	9.06E-07		7.25E-10	HS(-)	7.25E-10	0.00E+00	1.38E-21	7.25E-10	
Total Zn(2+)	1.40E-08	0.00E+00	1.12E-11	Zn(2+)	1.12E-11	4.51E-13	2.09E-25	1.07E-11	< 5.38E-8
				<u>Precipitated Solids</u>					
					FeCO3(s)	1.07E-21			
					FeOOH(s)	2.48E-05			
					MnCO3(s)	5.95E-21			
					CaCO3(s)	5.37E-05			

				<u>Other Calculated Values</u>		
				pH		7.46
				log{H2CO3}		-4.06
<u>Non-equilibrium Phases</u>				<u>Non-equilibrium Phases</u>		
FeS(s)	8.97E-03		7.18E-06	FeS(s)	7.18E-06	
CuS(s)	5.09E-04		4.07E-07	CuS(s)	4.07E-07	
NiS(s)	2.13E-04		1.71E-07	NiS(s)	1.71E-07	
ZnS(s)	2.80E-03		2.24E-06	ZnS(s)	2.24E-06	
<u>Volume in Mixture</u>						
Volume (L) ^b	0.2	249.8	250.0			
^a Model input values were calculated from model output for the sediment-pore water chemistry (Table A-16) and the reported chemistry of the resuspension water (Table A-10) mixed according to the respective volumes.						
^b Volumes were assumed to yield a suspended sediment concentration of 500 mg/L in the resuspension mixture.						

Table A-26. Initial Conditions Computed for Portsmouth Naval Station (MS04) Sediment Resuspension Mixture. Based on Simultaneously Extracted Iron and Simultaneously Extracted Metal (SEM) Concentrations.

Model Input ^a				Model Calculated Values					Measure d
	<u>Sed-PW</u>	<u>Resusp. water</u>	<u>Mixture</u>		<u>Total</u>	<u>Sorbed</u>	<u>Precipi- tated</u>	<u>Dissolved</u>	<u>Dissolved</u>
<u>Equilibrium Phases</u>				<u>Equilibrium Phases</u>					
Total H(+)	-7.82E-02	-2.07E-03	-2.13E-03	H(+)	-2.13E-03	-2.86E-07	-1.35E-04	-1.99E-03	
Total Ca(2+)	9.10E-03	9.04E-03	9.04E-03	Ca(2+)	9.04E-03	4.86E-08	4.75E-05	8.99E-03	
Total Cl(-)	4.83E-01	4.83E-01	4.83E-01	Cl(-)	4.83E-01	0.00E+00	0.00E+00	4.83E-01	
Total H2CO3	1.52E-02	2.08E-03	2.09E-03	H2CO3	2.09E-03	0.00E+00	4.75E-05	2.04E-03	
Total Cu(2+)	5.89E-17	0.00E+00	4.71E-20	Cu(2+)	4.71E-20	3.69E-20	1.47E-21	8.76E-21	< 4.20E-08
Total Fe(2+)	1.32E-02	0.00E+00	1.06E-05	Fe(2+)	1.06E-05	4.92E-07	6.30E-22	1.01E-05	< 1.81E-07
Total Fe(3+)	1.68E-02	0.00E+00	1.34E-05	Fe(3+)	1.34E-05	0.00E+00	1.34E-05	2.30E-09	
Total K(+)	9.04E-03	9.04E-03	9.04E-03	K(+)	9.04E-03	0.00E+00	0.00E+00	9.04E-03	
Total Mg(2+)	4.70E-02	4.70E-02	4.70E-02	Mg(2+)	4.70E-02	0.00E+00	1.37E-28	4.70E-02	
Total Mn(2+)	3.64E-04	0.00E+00	2.91E-07	Mn(2+)	2.91E-07	3.82E-10	4.18E-21	2.91E-07	1.28E-07
Total Na(+)	4.15E-01	4.15E-01	4.15E-01	Na(+)	4.15E-01	0.00E+00	0.00E+00	4.15E-01	
Total Ni(2+)	6.01E-10	0.00E+00	4.81E-13	Ni(2+)	4.81E-13	4.85E-15	4.69E-26	4.76E-13	
Total S(0)	2.09E-07		1.67E-10	S(0)	1.67E-10	0.00E+00	0.00E+00	1.67E-10	
Total SO4(2-)	2.56E-02	2.50E-02	2.50E-02	SO4(2-)	2.50E-02	2.32E-07	0.00E+00	2.50E-02	
Total HS(-)	8.26E-07		6.61E-10	HS(-)	6.61E-10	0.00E+00	1.48E-21	6.61E-10	
Total Zn(2+)	9.68E-09	0.00E+00	7.74E-12	Zn(2+)	7.74E-12	2.11E-13	1.34E-25	7.53E-12	3.06E-07
				<u>Precipitated Solids</u>					
					FeCO3(s)	6.29E-22			
					FeOOH(s)	1.34E-05			
					MnCO3(s)	4.18E-21			
					CaCO3(s)	4.75E-05			

				<u>Other Calculated Values</u>			
				pH		7.46	
				log{H2CO3}		-4.06	
<u>Non-equilibrium Phases</u>				<u>Non-equilibrium Phases</u>			
FeS(s)	3.57E-03		2.85E-06	FeS(s)	2.85E-06		
CuS(s)	5.37E-04		4.30E-07	CuS(s)	4.30E-07		
NiS(s)	1.33E-04		1.07E-07	NiS(s)	1.07E-07		
ZnS(s)	1.39E-03		1.11E-06	ZnS(s)	1.11E-06		
<u>Volume in Mixture</u>							
Volume (L) ^b	0.2	249.8	250.0				

^a Model input values were calculated from model output for the sediment-pore water chemistry (Table A-17) and the reported chemistry of the resuspension water (Table A-11) mixed according to the respective volumes.

^b Volumes were assumed to yield a suspended sediment concentration of 500 mg/L in the resuspension mixture.

Table A-27: Formulas Used to Specify Input Concentrations of Metal Binding Phases in WHAM

Particulate and Colloidal Humic and Fulvic Acid

The generalized formulas describing the conversion from particulate organic carbon (POC) and dissolved organic carbon (DOC) (in units of g OC/L) to particulate humic acid (HA_p) / particulate fulvic acid (FA_p) and dissolved HA (HA_d) / dissolved FA (FA_d) (all in units g HA/L or g FA/L) are:

$$HA_p = \frac{[POC]}{f_{OC,p}} f_{act,p} (1 - f_{FA,p}) \quad (1)$$

$$FA_p = \frac{[POC]}{f_{OC,p}} f_{act,p} f_{FA,p} \quad (2)$$

$$HA_d = \frac{[DOC]}{f_{OC,d}} f_{act,d} (1 - f_{FA,d}) \quad (3)$$

$$FA_d = \frac{[DOC]}{f_{OC,d}} f_{act,d} f_{FA,d} \quad (4)$$

where

$f_{OC,p}$ =	fraction of particulate organic matter (POM) that is POC {g POC / g POM}
$f_{OC,d}$ =	fraction of dissolved organic matter (DOM) that is DOC {g DOC / g DOM}
$f_{act,p}$ =	fraction of POM that is active for proton/metal binding {g POM _{active} / g POM}
$f_{act,d}$ =	fraction of DOM that is active for proton/metal binding {g DOM _{active} / g DOM}
$f_{FA,p}$ =	fraction of active POM that is FA {g FA _p / g POM _{active} }
$f_{FA,d}$ =	fraction of active DOM that is FA {g FA _p / g DOM _{active} }

The WHAM7 simulations for Delaware Bay, San Diego Bay and the look-up table development, the following values were used:

$f_{OC,p}$ =	0.5
$f_{OC,d}$ =	0.5
$f_{act,p}$ =	1
$f_{act,d}$ =	0.68
$f_{FA,p}$ =	0.5
$f_{FA,d}$ =	1

Particulate Hydrous Iron Oxide

To estimate metal binding to HFO, the WHAM model requires specification of the mass concentration (e.g., g/L) of particulate HFO (denoted “FeOx” in WHAM). Typical particulate iron measurements have units of mg Fe/L. To convert the particulate iron concentration in mg Fe/L to particulate HFO in g/L the following equation is used:

$$\text{HFO} = \text{Fe} \times \left(\frac{1 \text{ g}}{1000 \text{ mg}} \right) \times f_{\text{HFO}} \times \left(\frac{1 \text{ mol Fe}}{55.845 \text{ mg Fe}} \right) \times \left(\frac{90 \text{ g HFO}}{1 \text{ mol Fe}} \right) \quad (5)$$

where Fe is the particulate iron concentration measured in a water sample in mass units (mg/L)
 f_{HFO} is the fraction of the total iron in suspended particulate material that is HFO (g/g)

The final conversion from moles of Fe to grams HFO is taken from Dzombak and Morel (1990). Research indicates that approximately 40% of the particulate Fe in suspended particulate.

Table A-28: Formulas Used to Calculate Partitioning Relationships

Partitioning Relationships

Assuming porosity very close to 1

$$K_D = \frac{r}{C_{dis}} \left\{ \frac{M_{partMe}/M_{solid}}{M_{disMe}/L_{water}^3} \right\} = \left\{ \frac{L_{water}^3}{M_{solid}} \right\}$$

$$C_{part} = r \cdot TSS \left\{ \frac{M_{partCu}}{L_{water}^3} \right\}$$

$$K_D = \frac{C_{part}}{C_{dis} \cdot TSS}$$

$$K_D' = K_D \cdot TSS = \frac{C_{part}}{C_{dis}}$$

$$f_{part} = \frac{C_{part}}{C_{dis} + C_{part}} = \frac{K_D'}{1 + K_D'}$$

Note: "Me" in the above stands for "metal"

**Table 29: Input and Output from San Diego Bay Look-Up Table Development
State Variable for Model Input**

STATE VARIABLES FOR MODEL INPUT						
Input Number	Total Cu (mol/L)	pH	POC (mg/L)	DOC (mg/L)	Particulate Iron (mg Fe/L)	Salinity (psu)
1	6.29E-08	7.8	0.04	0.75	0.05	32
2	6.29E-08	7.8	0.04	0.75	0.05	33.5
3	6.29E-08	7.8	0.04	0.75	0.05	35
4	6.29E-08	7.8	0.04	0.75	0.4	32
5	6.29E-08	7.8	0.04	0.75	0.4	33.5
6	6.29E-08	7.8	0.04	0.75	0.4	35
7	6.29E-08	7.8	0.04	0.75	3.25	32
8	6.29E-08	7.8	0.04	0.75	3.25	33.5
9	6.29E-08	7.8	0.04	0.75	3.25	35
10	6.29E-08	7.8	0.04	1.5	0.05	32
11	6.29E-08	7.8	0.04	1.5	0.05	33.5
12	6.29E-08	7.8	0.04	1.5	0.05	35
13	6.29E-08	7.8	0.04	1.5	0.4	32
14	6.29E-08	7.8	0.04	1.5	0.4	33.5
15	6.29E-08	7.8	0.04	1.5	0.4	35
16	6.29E-08	7.8	0.04	1.5	3.25	32
17	6.29E-08	7.8	0.04	1.5	3.25	33.5
18	6.29E-08	7.8	0.04	1.5	3.25	35
19	6.29E-08	7.8	0.04	4	0.05	32
20	6.29E-08	7.8	0.04	4	0.05	33.5
21	6.29E-08	7.8	0.04	4	0.05	35
22	6.29E-08	7.8	0.04	4	0.4	32
23	6.29E-08	7.8	0.04	4	0.4	33.5
24	6.29E-08	7.8	0.04	4	0.4	35
25	6.29E-08	7.8	0.04	4	3.25	32
26	6.29E-08	7.8	0.04	4	3.25	33.5
27	6.29E-08	7.8	0.04	4	3.25	35
28	6.29E-08	7.8	0.25	0.75	0.05	32
29	6.29E-08	7.8	0.25	0.75	0.05	33.5
30	6.29E-08	7.8	0.25	0.75	0.05	35
31	6.29E-08	7.8	0.25	0.75	0.4	32
32	6.29E-08	7.8	0.25	0.75	0.4	33.5
33	6.29E-08	7.8	0.25	0.75	0.4	35
34	6.29E-08	7.8	0.25	0.75	3.25	32
35	6.29E-08	7.8	0.25	0.75	3.25	33.5
36	6.29E-08	7.8	0.25	0.75	3.25	35
37	6.29E-08	7.8	0.25	1.5	0.05	32
38	6.29E-08	7.8	0.25	1.5	0.05	33.5
39	6.29E-08	7.8	0.25	1.5	0.05	35
40	6.29E-08	7.8	0.25	1.5	0.4	32
41	6.29E-08	7.8	0.25	1.5	0.4	33.5
42	6.29E-08	7.8	0.25	1.5	0.4	35
43	6.29E-08	7.8	0.25	1.5	3.25	32
44	6.29E-08	7.8	0.25	1.5	3.25	33.5
45	6.29E-08	7.8	0.25	1.5	3.25	35
46	6.29E-08	7.8	0.25	4	0.05	32
47	6.29E-08	7.8	0.25	4	0.05	33.5
48	6.29E-08	7.8	0.25	4	0.05	35
49	6.29E-08	7.8	0.25	4	0.4	32
50	6.29E-08	7.8	0.25	4	0.4	33.5

STATE VARIABLES FOR MODEL INPUT						
Input Number	Total Cu (mol/L)	pH	POC (mg/L)	DOC (mg/L)	Particulate Iron (mg Fe/L)	Salinity (psu)
51	6.29E-08	7.8	0.25	4	0.4	35
52	6.29E-08	7.8	0.25	4	3.25	32
53	6.29E-08	7.8	0.25	4	3.25	33.5
54	6.29E-08	7.8	0.25	4	3.25	35
55	6.29E-08	7.8	1.6	0.75	0.05	32
56	6.29E-08	7.8	1.6	0.75	0.05	33.5
57	6.29E-08	7.8	1.6	0.75	0.05	35
58	6.29E-08	7.8	1.6	0.75	0.4	32
59	6.29E-08	7.8	1.6	0.75	0.4	33.5
60	6.29E-08	7.8	1.6	0.75	0.4	35
61	6.29E-08	7.8	1.6	0.75	3.25	32
62	6.29E-08	7.8	1.6	0.75	3.25	33.5
63	6.29E-08	7.8	1.6	0.75	3.25	35
64	6.29E-08	7.8	1.6	1.5	0.05	32
65	6.29E-08	7.8	1.6	1.5	0.05	33.5
66	6.29E-08	7.8	1.6	1.5	0.05	35
67	6.29E-08	7.8	1.6	1.5	0.4	32
68	6.29E-08	7.8	1.6	1.5	0.4	33.5
69	6.29E-08	7.8	1.6	1.5	0.4	35
70	6.29E-08	7.8	1.6	1.5	3.25	32
71	6.29E-08	7.8	1.6	1.5	3.25	33.5
72	6.29E-08	7.8	1.6	1.5	3.25	35
73	6.29E-08	7.8	1.6	4	0.05	32
74	6.29E-08	7.8	1.6	4	0.05	33.5
75	6.29E-08	7.8	1.6	4	0.05	35
76	6.29E-08	7.8	1.6	4	0.4	32
77	6.29E-08	7.8	1.6	4	0.4	33.5
78	6.29E-08	7.8	1.6	4	0.4	35
79	6.29E-08	7.8	1.6	4	3.25	32
80	6.29E-08	7.8	1.6	4	3.25	33.5
81	6.29E-08	7.8	1.6	4	3.25	35
82	6.29E-08	8.2	0.04	0.75	0.05	32
83	6.29E-08	8.2	0.04	0.75	0.05	33.5
84	6.29E-08	8.2	0.04	0.75	0.05	35
85	6.29E-08	8.2	0.04	0.75	0.4	32
86	6.29E-08	8.2	0.04	0.75	0.4	33.5
87	6.29E-08	8.2	0.04	0.75	0.4	35
88	6.29E-08	8.2	0.04	0.75	3.25	32
89	6.29E-08	8.2	0.04	0.75	3.25	33.5
90	6.29E-08	8.2	0.04	0.75	3.25	35
91	6.29E-08	8.2	0.04	1.5	0.05	32
92	6.29E-08	8.2	0.04	1.5	0.05	33.5
93	6.29E-08	8.2	0.04	1.5	0.05	35
94	6.29E-08	8.2	0.04	1.5	0.4	32
95	6.29E-08	8.2	0.04	1.5	0.4	33.5
96	6.29E-08	8.2	0.04	1.5	0.4	35
97	6.29E-08	8.2	0.04	1.5	3.25	32
98	6.29E-08	8.2	0.04	1.5	3.25	33.5
99	6.29E-08	8.2	0.04	1.5	3.25	35
100	6.29E-08	8.2	0.04	4	0.05	32

STATE VARIABLES FOR MODEL INPUT						
Input Number	Total Cu (mol/L)	pH	POC (mg/L)	DOC (mg/L)	Particulate Iron (mg Fe/L)	Salinity (psu)
101	6.29E-08	8.2	0.04	4	0.05	33.5
102	6.29E-08	8.2	0.04	4	0.05	35
103	6.29E-08	8.2	0.04	4	0.4	32
104	6.29E-08	8.2	0.04	4	0.4	33.5
105	6.29E-08	8.2	0.04	4	0.4	35
106	6.29E-08	8.2	0.04	4	3.25	32
107	6.29E-08	8.2	0.04	4	3.25	33.5
108	6.29E-08	8.2	0.04	4	3.25	35
109	6.29E-08	8.2	0.25	0.75	0.05	32
110	6.29E-08	8.2	0.25	0.75	0.05	33.5
111	6.29E-08	8.2	0.25	0.75	0.05	35
112	6.29E-08	8.2	0.25	0.75	0.4	32
113	6.29E-08	8.2	0.25	0.75	0.4	33.5
114	6.29E-08	8.2	0.25	0.75	0.4	35
115	6.29E-08	8.2	0.25	0.75	3.25	32
116	6.29E-08	8.2	0.25	0.75	3.25	33.5
117	6.29E-08	8.2	0.25	0.75	3.25	35
118	6.29E-08	8.2	0.25	1.5	0.05	32
119	6.29E-08	8.2	0.25	1.5	0.05	33.5
120	6.29E-08	8.2	0.25	1.5	0.05	35
121	6.29E-08	8.2	0.25	1.5	0.4	32
122	6.29E-08	8.2	0.25	1.5	0.4	33.5
123	6.29E-08	8.2	0.25	1.5	0.4	35
124	6.29E-08	8.2	0.25	1.5	3.25	32
125	6.29E-08	8.2	0.25	1.5	3.25	33.5
126	6.29E-08	8.2	0.25	1.5	3.25	35
127	6.29E-08	8.2	0.25	4	0.05	32
128	6.29E-08	8.2	0.25	4	0.05	33.5
129	6.29E-08	8.2	0.25	4	0.05	35
130	6.29E-08	8.2	0.25	4	0.4	32
131	6.29E-08	8.2	0.25	4	0.4	33.5
132	6.29E-08	8.2	0.25	4	0.4	35
133	6.29E-08	8.2	0.25	4	3.25	32
134	6.29E-08	8.2	0.25	4	3.25	33.5
135	6.29E-08	8.2	0.25	4	3.25	35
136	6.29E-08	8.2	1.6	0.75	0.05	32
137	6.29E-08	8.2	1.6	0.75	0.05	33.5
138	6.29E-08	8.2	1.6	0.75	0.05	35
139	6.29E-08	8.2	1.6	0.75	0.4	32
140	6.29E-08	8.2	1.6	0.75	0.4	33.5
141	6.29E-08	8.2	1.6	0.75	0.4	35
142	6.29E-08	8.2	1.6	0.75	3.25	32
143	6.29E-08	8.2	1.6	0.75	3.25	33.5
144	6.29E-08	8.2	1.6	0.75	3.25	35
145	6.29E-08	8.2	1.6	1.5	0.05	32
146	6.29E-08	8.2	1.6	1.5	0.05	33.5
147	6.29E-08	8.2	1.6	1.5	0.05	35
148	6.29E-08	8.2	1.6	1.5	0.4	32
149	6.29E-08	8.2	1.6	1.5	0.4	33.5
150	6.29E-08	8.2	1.6	1.5	0.4	35

STATE VARIABLES FOR MODEL INPUT						
Input Number	Total Cu (mol/L)	pH	POC (mg/L)	DOC (mg/L)	Particulate Iron (mg Fe/L)	Salinity (psu)
151	6.29E-08	8.2	1.6	1.5	3.25	32
152	6.29E-08	8.2	1.6	1.5	3.25	33.5
153	6.29E-08	8.2	1.6	1.5	3.25	35
154	6.29E-08	8.2	1.6	4	0.05	32
155	6.29E-08	8.2	1.6	4	0.05	33.5
156	6.29E-08	8.2	1.6	4	0.05	35
157	6.29E-08	8.2	1.6	4	0.4	32
158	6.29E-08	8.2	1.6	4	0.4	33.5
159	6.29E-08	8.2	1.6	4	0.4	35
160	6.29E-08	8.2	1.6	4	3.25	32
161	6.29E-08	8.2	1.6	4	3.25	33.5
162	6.29E-08	8.2	1.6	4	3.25	35
163	6.29E-08	8.6	0.04	0.75	0.05	32
164	6.29E-08	8.6	0.04	0.75	0.05	33.5
165	6.29E-08	8.6	0.04	0.75	0.05	35
166	6.29E-08	8.6	0.04	0.75	0.4	32
167	6.29E-08	8.6	0.04	0.75	0.4	33.5
168	6.29E-08	8.6	0.04	0.75	0.4	35
169	6.29E-08	8.6	0.04	0.75	3.25	32
170	6.29E-08	8.6	0.04	0.75	3.25	33.5
171	6.29E-08	8.6	0.04	0.75	3.25	35
172	6.29E-08	8.6	0.04	1.5	0.05	32
173	6.29E-08	8.6	0.04	1.5	0.05	33.5
174	6.29E-08	8.6	0.04	1.5	0.05	35
175	6.29E-08	8.6	0.04	1.5	0.4	32
176	6.29E-08	8.6	0.04	1.5	0.4	33.5
177	6.29E-08	8.6	0.04	1.5	0.4	35
178	6.29E-08	8.6	0.04	1.5	3.25	32
179	6.29E-08	8.6	0.04	1.5	3.25	33.5
180	6.29E-08	8.6	0.04	1.5	3.25	35
181	6.29E-08	8.6	0.04	4	0.05	32
182	6.29E-08	8.6	0.04	4	0.05	33.5
183	6.29E-08	8.6	0.04	4	0.05	35
184	6.29E-08	8.6	0.04	4	0.4	32
185	6.29E-08	8.6	0.04	4	0.4	33.5
186	6.29E-08	8.6	0.04	4	0.4	35
187	6.29E-08	8.6	0.04	4	3.25	32
188	6.29E-08	8.6	0.04	4	3.25	33.5
189	6.29E-08	8.6	0.04	4	3.25	35
190	6.29E-08	8.6	0.25	0.75	0.05	32
191	6.29E-08	8.6	0.25	0.75	0.05	33.5
192	6.29E-08	8.6	0.25	0.75	0.05	35
193	6.29E-08	8.6	0.25	0.75	0.4	32
194	6.29E-08	8.6	0.25	0.75	0.4	33.5
195	6.29E-08	8.6	0.25	0.75	0.4	35
196	6.29E-08	8.6	0.25	0.75	3.25	32
197	6.29E-08	8.6	0.25	0.75	3.25	33.5
198	6.29E-08	8.6	0.25	0.75	3.25	35
199	6.29E-08	8.6	0.25	1.5	0.05	32
200	6.29E-08	8.6	0.25	1.5	0.05	33.5

STATE VARIABLES FOR MODEL INPUT						
Input Number	Total Cu (mol/L)	pH	POC (mg/L)	DOC (mg/L)	Particulate Iron (mg Fe/L)	Salinity (psu)
201	6.29E-08	8.6	0.25	1.5	0.05	35
202	6.29E-08	8.6	0.25	1.5	0.4	32
203	6.29E-08	8.6	0.25	1.5	0.4	33.5
204	6.29E-08	8.6	0.25	1.5	0.4	35
205	6.29E-08	8.6	0.25	1.5	3.25	32
206	6.29E-08	8.6	0.25	1.5	3.25	33.5
207	6.29E-08	8.6	0.25	1.5	3.25	35
208	6.29E-08	8.6	0.25	4	0.05	32
209	6.29E-08	8.6	0.25	4	0.05	33.5
210	6.29E-08	8.6	0.25	4	0.05	35
211	6.29E-08	8.6	0.25	4	0.4	32
212	6.29E-08	8.6	0.25	4	0.4	33.5
213	6.29E-08	8.6	0.25	4	0.4	35
214	6.29E-08	8.6	0.25	4	3.25	32
215	6.29E-08	8.6	0.25	4	3.25	33.5
216	6.29E-08	8.6	0.25	4	3.25	35
217	6.29E-08	8.6	1.6	0.75	0.05	32
218	6.29E-08	8.6	1.6	0.75	0.05	33.5
219	6.29E-08	8.6	1.6	0.75	0.05	35
220	6.29E-08	8.6	1.6	0.75	0.4	32
221	6.29E-08	8.6	1.6	0.75	0.4	33.5
222	6.29E-08	8.6	1.6	0.75	0.4	35
223	6.29E-08	8.6	1.6	0.75	3.25	32
224	6.29E-08	8.6	1.6	0.75	3.25	33.5
225	6.29E-08	8.6	1.6	0.75	3.25	35
226	6.29E-08	8.6	1.6	1.5	0.05	32
227	6.29E-08	8.6	1.6	1.5	0.05	33.5
228	6.29E-08	8.6	1.6	1.5	0.05	35
229	6.29E-08	8.6	1.6	1.5	0.4	32
230	6.29E-08	8.6	1.6	1.5	0.4	33.5
231	6.29E-08	8.6	1.6	1.5	0.4	35
232	6.29E-08	8.6	1.6	1.5	3.25	32
233	6.29E-08	8.6	1.6	1.5	3.25	33.5
234	6.29E-08	8.6	1.6	1.5	3.25	35
235	6.29E-08	8.6	1.6	4	0.05	32
236	6.29E-08	8.6	1.6	4	0.05	33.5
237	6.29E-08	8.6	1.6	4	0.05	35
238	6.29E-08	8.6	1.6	4	0.4	32
239	6.29E-08	8.6	1.6	4	0.4	33.5
240	6.29E-08	8.6	1.6	4	0.4	35
241	6.29E-08	8.6	1.6	4	3.25	32
242	6.29E-08	8.6	1.6	4	3.25	33.5
243	6.29E-08	8.6	1.6	4	3.25	35
244	1.57E-07	7.8	0.04	0.75	0.05	32
245	1.57E-07	7.8	0.04	0.75	0.05	33.5
246	1.57E-07	7.8	0.04	0.75	0.05	35
247	1.57E-07	7.8	0.04	0.75	0.4	32
248	1.57E-07	7.8	0.04	0.75	0.4	33.5
249	1.57E-07	7.8	0.04	0.75	0.4	35
250	1.57E-07	7.8	0.04	0.75	3.25	32

STATE VARIABLES FOR MODEL INPUT						
Input Number	Total Cu (mol/L)	pH	POC (mg/L)	DOC (mg/L)	Particulate Iron (mg Fe/L)	Salinity (psu)
251	1.57E-07	7.8	0.04	0.75	3.25	33.5
252	1.57E-07	7.8	0.04	0.75	3.25	35
253	1.57E-07	7.8	0.04	1.5	0.05	32
254	1.57E-07	7.8	0.04	1.5	0.05	33.5
255	1.57E-07	7.8	0.04	1.5	0.05	35
256	1.57E-07	7.8	0.04	1.5	0.4	32
257	1.57E-07	7.8	0.04	1.5	0.4	33.5
258	1.57E-07	7.8	0.04	1.5	0.4	35
259	1.57E-07	7.8	0.04	1.5	3.25	32
260	1.57E-07	7.8	0.04	1.5	3.25	33.5
261	1.57E-07	7.8	0.04	1.5	3.25	35
262	1.57E-07	7.8	0.04	4	0.05	32
263	1.57E-07	7.8	0.04	4	0.05	33.5
264	1.57E-07	7.8	0.04	4	0.05	35
265	1.57E-07	7.8	0.04	4	0.4	32
266	1.57E-07	7.8	0.04	4	0.4	33.5
267	1.57E-07	7.8	0.04	4	0.4	35
268	1.57E-07	7.8	0.04	4	3.25	32
269	1.57E-07	7.8	0.04	4	3.25	33.5
270	1.57E-07	7.8	0.04	4	3.25	35
271	1.57E-07	7.8	0.25	0.75	0.05	32
272	1.57E-07	7.8	0.25	0.75	0.05	33.5
273	1.57E-07	7.8	0.25	0.75	0.05	35
274	1.57E-07	7.8	0.25	0.75	0.4	32
275	1.57E-07	7.8	0.25	0.75	0.4	33.5
276	1.57E-07	7.8	0.25	0.75	0.4	35
277	1.57E-07	7.8	0.25	0.75	3.25	32
278	1.57E-07	7.8	0.25	0.75	3.25	33.5
279	1.57E-07	7.8	0.25	0.75	3.25	35
280	1.57E-07	7.8	0.25	1.5	0.05	32
281	1.57E-07	7.8	0.25	1.5	0.05	33.5
282	1.57E-07	7.8	0.25	1.5	0.05	35
283	1.57E-07	7.8	0.25	1.5	0.4	32
284	1.57E-07	7.8	0.25	1.5	0.4	33.5
285	1.57E-07	7.8	0.25	1.5	0.4	35
286	1.57E-07	7.8	0.25	1.5	3.25	32
287	1.57E-07	7.8	0.25	1.5	3.25	33.5
288	1.57E-07	7.8	0.25	1.5	3.25	35
289	1.57E-07	7.8	0.25	4	0.05	32
290	1.57E-07	7.8	0.25	4	0.05	33.5
291	1.57E-07	7.8	0.25	4	0.05	35
292	1.57E-07	7.8	0.25	4	0.4	32
293	1.57E-07	7.8	0.25	4	0.4	33.5
294	1.57E-07	7.8	0.25	4	0.4	35
295	1.57E-07	7.8	0.25	4	3.25	32
296	1.57E-07	7.8	0.25	4	3.25	33.5
297	1.57E-07	7.8	0.25	4	3.25	35
298	1.57E-07	7.8	1.6	0.75	0.05	32
299	1.57E-07	7.8	1.6	0.75	0.05	33.5
300	1.57E-07	7.8	1.6	0.75	0.05	35

STATE VARIABLES FOR MODEL INPUT						
Input Number	Total Cu (mol/L)	pH	POC (mg/L)	DOC (mg/L)	Particulate Iron (mg Fe/L)	Salinity (psu)
301	1.57E-07	7.8	1.6	0.75	0.4	32
302	1.57E-07	7.8	1.6	0.75	0.4	33.5
303	1.57E-07	7.8	1.6	0.75	0.4	35
304	1.57E-07	7.8	1.6	0.75	3.25	32
305	1.57E-07	7.8	1.6	0.75	3.25	33.5
306	1.57E-07	7.8	1.6	0.75	3.25	35
307	1.57E-07	7.8	1.6	1.5	0.05	32
308	1.57E-07	7.8	1.6	1.5	0.05	33.5
309	1.57E-07	7.8	1.6	1.5	0.05	35
310	1.57E-07	7.8	1.6	1.5	0.4	32
311	1.57E-07	7.8	1.6	1.5	0.4	33.5
312	1.57E-07	7.8	1.6	1.5	0.4	35
313	1.57E-07	7.8	1.6	1.5	3.25	32
314	1.57E-07	7.8	1.6	1.5	3.25	33.5
315	1.57E-07	7.8	1.6	1.5	3.25	35
316	1.57E-07	7.8	1.6	4	0.05	32
317	1.57E-07	7.8	1.6	4	0.05	33.5
318	1.57E-07	7.8	1.6	4	0.05	35
319	1.57E-07	7.8	1.6	4	0.4	32
320	1.57E-07	7.8	1.6	4	0.4	33.5
321	1.57E-07	7.8	1.6	4	0.4	35
322	1.57E-07	7.8	1.6	4	3.25	32
323	1.57E-07	7.8	1.6	4	3.25	33.5
324	1.57E-07	7.8	1.6	4	3.25	35
325	1.57E-07	8.2	0.04	0.75	0.05	32
326	1.57E-07	8.2	0.04	0.75	0.05	33.5
327	1.57E-07	8.2	0.04	0.75	0.05	35
328	1.57E-07	8.2	0.04	0.75	0.4	32
329	1.57E-07	8.2	0.04	0.75	0.4	33.5
330	1.57E-07	8.2	0.04	0.75	0.4	35
331	1.57E-07	8.2	0.04	0.75	3.25	32
332	1.57E-07	8.2	0.04	0.75	3.25	33.5
333	1.57E-07	8.2	0.04	0.75	3.25	35
334	1.57E-07	8.2	0.04	1.5	0.05	32
335	1.57E-07	8.2	0.04	1.5	0.05	33.5
336	1.57E-07	8.2	0.04	1.5	0.05	35
337	1.57E-07	8.2	0.04	1.5	0.4	32
338	1.57E-07	8.2	0.04	1.5	0.4	33.5
339	1.57E-07	8.2	0.04	1.5	0.4	35
340	1.57E-07	8.2	0.04	1.5	3.25	32
341	1.57E-07	8.2	0.04	1.5	3.25	33.5
342	1.57E-07	8.2	0.04	1.5	3.25	35
343	1.57E-07	8.2	0.04	4	0.05	32
344	1.57E-07	8.2	0.04	4	0.05	33.5
345	1.57E-07	8.2	0.04	4	0.05	35
346	1.57E-07	8.2	0.04	4	0.4	32
347	1.57E-07	8.2	0.04	4	0.4	33.5
348	1.57E-07	8.2	0.04	4	0.4	35
349	1.57E-07	8.2	0.04	4	3.25	32
350	1.57E-07	8.2	0.04	4	3.25	33.5

STATE VARIABLES FOR MODEL INPUT						
Input Number	Total Cu (mol/L)	pH	POC (mg/L)	DOC (mg/L)	Particulate Iron (mg Fe/L)	Salinity (psu)
351	1.57E-07	8.2	0.04	4	3.25	35
352	1.57E-07	8.2	0.25	0.75	0.05	32
353	1.57E-07	8.2	0.25	0.75	0.05	33.5
354	1.57E-07	8.2	0.25	0.75	0.05	35
355	1.57E-07	8.2	0.25	0.75	0.4	32
356	1.57E-07	8.2	0.25	0.75	0.4	33.5
357	1.57E-07	8.2	0.25	0.75	0.4	35
358	1.57E-07	8.2	0.25	0.75	3.25	32
359	1.57E-07	8.2	0.25	0.75	3.25	33.5
360	1.57E-07	8.2	0.25	0.75	3.25	35
361	1.57E-07	8.2	0.25	1.5	0.05	32
362	1.57E-07	8.2	0.25	1.5	0.05	33.5
363	1.57E-07	8.2	0.25	1.5	0.05	35
364	1.57E-07	8.2	0.25	1.5	0.4	32
365	1.57E-07	8.2	0.25	1.5	0.4	33.5
366	1.57E-07	8.2	0.25	1.5	0.4	35
367	1.57E-07	8.2	0.25	1.5	3.25	32
368	1.57E-07	8.2	0.25	1.5	3.25	33.5
369	1.57E-07	8.2	0.25	1.5	3.25	35
370	1.57E-07	8.2	0.25	4	0.05	32
371	1.57E-07	8.2	0.25	4	0.05	33.5
372	1.57E-07	8.2	0.25	4	0.05	35
373	1.57E-07	8.2	0.25	4	0.4	32
374	1.57E-07	8.2	0.25	4	0.4	33.5
375	1.57E-07	8.2	0.25	4	0.4	35
376	1.57E-07	8.2	0.25	4	3.25	32
377	1.57E-07	8.2	0.25	4	3.25	33.5
378	1.57E-07	8.2	0.25	4	3.25	35
379	1.57E-07	8.2	1.6	0.75	0.05	32
380	1.57E-07	8.2	1.6	0.75	0.05	33.5
381	1.57E-07	8.2	1.6	0.75	0.05	35
382	1.57E-07	8.2	1.6	0.75	0.4	32
383	1.57E-07	8.2	1.6	0.75	0.4	33.5
384	1.57E-07	8.2	1.6	0.75	0.4	35
385	1.57E-07	8.2	1.6	0.75	3.25	32
386	1.57E-07	8.2	1.6	0.75	3.25	33.5
387	1.57E-07	8.2	1.6	0.75	3.25	35
388	1.57E-07	8.2	1.6	1.5	0.05	32
389	1.57E-07	8.2	1.6	1.5	0.05	33.5
390	1.57E-07	8.2	1.6	1.5	0.05	35
391	1.57E-07	8.2	1.6	1.5	0.4	32
392	1.57E-07	8.2	1.6	1.5	0.4	33.5
393	1.57E-07	8.2	1.6	1.5	0.4	35
394	1.57E-07	8.2	1.6	1.5	3.25	32
395	1.57E-07	8.2	1.6	1.5	3.25	33.5
396	1.57E-07	8.2	1.6	1.5	3.25	35
397	1.57E-07	8.2	1.6	4	0.05	32
398	1.57E-07	8.2	1.6	4	0.05	33.5
399	1.57E-07	8.2	1.6	4	0.05	35
400	1.57E-07	8.2	1.6	4	0.4	32

STATE VARIABLES FOR MODEL INPUT						
Input Number	Total Cu (mol/L)	pH	POC (mg/L)	DOC (mg/L)	Particulate Iron (mg Fe/L)	Salinity (psu)
401	1.57E-07	8.2	1.6	4	0.4	33.5
402	1.57E-07	8.2	1.6	4	0.4	35
403	1.57E-07	8.2	1.6	4	3.25	32
404	1.57E-07	8.2	1.6	4	3.25	33.5
405	1.57E-07	8.2	1.6	4	3.25	35
406	1.57E-07	8.6	0.04	0.75	0.05	32
407	1.57E-07	8.6	0.04	0.75	0.05	33.5
408	1.57E-07	8.6	0.04	0.75	0.05	35
409	1.57E-07	8.6	0.04	0.75	0.4	32
410	1.57E-07	8.6	0.04	0.75	0.4	33.5
411	1.57E-07	8.6	0.04	0.75	0.4	35
412	1.57E-07	8.6	0.04	0.75	3.25	32
413	1.57E-07	8.6	0.04	0.75	3.25	33.5
414	1.57E-07	8.6	0.04	0.75	3.25	35
415	1.57E-07	8.6	0.04	1.5	0.05	32
416	1.57E-07	8.6	0.04	1.5	0.05	33.5
417	1.57E-07	8.6	0.04	1.5	0.05	35
418	1.57E-07	8.6	0.04	1.5	0.4	32
419	1.57E-07	8.6	0.04	1.5	0.4	33.5
420	1.57E-07	8.6	0.04	1.5	0.4	35
421	1.57E-07	8.6	0.04	1.5	3.25	32
422	1.57E-07	8.6	0.04	1.5	3.25	33.5
423	1.57E-07	8.6	0.04	1.5	3.25	35
424	1.57E-07	8.6	0.04	4	0.05	32
425	1.57E-07	8.6	0.04	4	0.05	33.5
426	1.57E-07	8.6	0.04	4	0.05	35
427	1.57E-07	8.6	0.04	4	0.4	32
428	1.57E-07	8.6	0.04	4	0.4	33.5
429	1.57E-07	8.6	0.04	4	0.4	35
430	1.57E-07	8.6	0.04	4	3.25	32
431	1.57E-07	8.6	0.04	4	3.25	33.5
432	1.57E-07	8.6	0.04	4	3.25	35
433	1.57E-07	8.6	0.25	0.75	0.05	32
434	1.57E-07	8.6	0.25	0.75	0.05	33.5
435	1.57E-07	8.6	0.25	0.75	0.05	35
436	1.57E-07	8.6	0.25	0.75	0.4	32
437	1.57E-07	8.6	0.25	0.75	0.4	33.5
438	1.57E-07	8.6	0.25	0.75	0.4	35
439	1.57E-07	8.6	0.25	0.75	3.25	32
440	1.57E-07	8.6	0.25	0.75	3.25	33.5
441	1.57E-07	8.6	0.25	0.75	3.25	35
442	1.57E-07	8.6	0.25	1.5	0.05	32
443	1.57E-07	8.6	0.25	1.5	0.05	33.5
444	1.57E-07	8.6	0.25	1.5	0.05	35
445	1.57E-07	8.6	0.25	1.5	0.4	32
446	1.57E-07	8.6	0.25	1.5	0.4	33.5
447	1.57E-07	8.6	0.25	1.5	0.4	35
448	1.57E-07	8.6	0.25	1.5	3.25	32
449	1.57E-07	8.6	0.25	1.5	3.25	33.5
450	1.57E-07	8.6	0.25	1.5	3.25	35

STATE VARIABLES FOR MODEL INPUT						
Input Number	Total Cu (mol/L)	pH	POC (mg/L)	DOC (mg/L)	Particulate Iron (mg Fe/L)	Salinity (psu)
451	1.57E-07	8.6	0.25	4	0.05	32
452	1.57E-07	8.6	0.25	4	0.05	33.5
453	1.57E-07	8.6	0.25	4	0.05	35
454	1.57E-07	8.6	0.25	4	0.4	32
455	1.57E-07	8.6	0.25	4	0.4	33.5
456	1.57E-07	8.6	0.25	4	0.4	35
457	1.57E-07	8.6	0.25	4	3.25	32
458	1.57E-07	8.6	0.25	4	3.25	33.5
459	1.57E-07	8.6	0.25	4	3.25	35
460	1.57E-07	8.6	1.6	0.75	0.05	32
461	1.57E-07	8.6	1.6	0.75	0.05	33.5
462	1.57E-07	8.6	1.6	0.75	0.05	35
463	1.57E-07	8.6	1.6	0.75	0.4	32
464	1.57E-07	8.6	1.6	0.75	0.4	33.5
465	1.57E-07	8.6	1.6	0.75	0.4	35
466	1.57E-07	8.6	1.6	0.75	3.25	32
467	1.57E-07	8.6	1.6	0.75	3.25	33.5
468	1.57E-07	8.6	1.6	0.75	3.25	35
469	1.57E-07	8.6	1.6	1.5	0.05	32
470	1.57E-07	8.6	1.6	1.5	0.05	33.5
471	1.57E-07	8.6	1.6	1.5	0.05	35
472	1.57E-07	8.6	1.6	1.5	0.4	32
473	1.57E-07	8.6	1.6	1.5	0.4	33.5
474	1.57E-07	8.6	1.6	1.5	0.4	35
475	1.57E-07	8.6	1.6	1.5	3.25	32
476	1.57E-07	8.6	1.6	1.5	3.25	33.5
477	1.57E-07	8.6	1.6	1.5	3.25	35
478	1.57E-07	8.6	1.6	4	0.05	32
479	1.57E-07	8.6	1.6	4	0.05	33.5
480	1.57E-07	8.6	1.6	4	0.05	35
481	1.57E-07	8.6	1.6	4	0.4	32
482	1.57E-07	8.6	1.6	4	0.4	33.5
483	1.57E-07	8.6	1.6	4	0.4	35
484	1.57E-07	8.6	1.6	4	3.25	32
485	1.57E-07	8.6	1.6	4	3.25	33.5
486	1.57E-07	8.6	1.6	4	3.25	35
487	4.09E-07	7.8	0.04	0.75	0.05	32
488	4.09E-07	7.8	0.04	0.75	0.05	33.5
489	4.09E-07	7.8	0.04	0.75	0.05	35
490	4.09E-07	7.8	0.04	0.75	0.4	32
491	4.09E-07	7.8	0.04	0.75	0.4	33.5
492	4.09E-07	7.8	0.04	0.75	0.4	35
493	4.09E-07	7.8	0.04	0.75	3.25	32
494	4.09E-07	7.8	0.04	0.75	3.25	33.5
495	4.09E-07	7.8	0.04	0.75	3.25	35
496	4.09E-07	7.8	0.04	1.5	0.05	32
497	4.09E-07	7.8	0.04	1.5	0.05	33.5
498	4.09E-07	7.8	0.04	1.5	0.05	35
499	4.09E-07	7.8	0.04	1.5	0.4	32
500	4.09E-07	7.8	0.04	1.5	0.4	33.5

STATE VARIABLES FOR MODEL INPUT						
Input Number	Total Cu (mol/L)	pH	POC (mg/L)	DOC (mg/L)	Particulate Iron (mg Fe/L)	Salinity (psu)
501	4.09E-07	7.8	0.04	1.5	0.4	35
502	4.09E-07	7.8	0.04	1.5	3.25	32
503	4.09E-07	7.8	0.04	1.5	3.25	33.5
504	4.09E-07	7.8	0.04	1.5	3.25	35
505	4.09E-07	7.8	0.04	4	0.05	32
506	4.09E-07	7.8	0.04	4	0.05	33.5
507	4.09E-07	7.8	0.04	4	0.05	35
508	4.09E-07	7.8	0.04	4	0.4	32
509	4.09E-07	7.8	0.04	4	0.4	33.5
510	4.09E-07	7.8	0.04	4	0.4	35
511	4.09E-07	7.8	0.04	4	3.25	32
512	4.09E-07	7.8	0.04	4	3.25	33.5
513	4.09E-07	7.8	0.04	4	3.25	35
514	4.09E-07	7.8	0.25	0.75	0.05	32
515	4.09E-07	7.8	0.25	0.75	0.05	33.5
516	4.09E-07	7.8	0.25	0.75	0.05	35
517	4.09E-07	7.8	0.25	0.75	0.4	32
518	4.09E-07	7.8	0.25	0.75	0.4	33.5
519	4.09E-07	7.8	0.25	0.75	0.4	35
520	4.09E-07	7.8	0.25	0.75	3.25	32
521	4.09E-07	7.8	0.25	0.75	3.25	33.5
522	4.09E-07	7.8	0.25	0.75	3.25	35
523	4.09E-07	7.8	0.25	1.5	0.05	32
524	4.09E-07	7.8	0.25	1.5	0.05	33.5
525	4.09E-07	7.8	0.25	1.5	0.05	35
526	4.09E-07	7.8	0.25	1.5	0.4	32
527	4.09E-07	7.8	0.25	1.5	0.4	33.5
528	4.09E-07	7.8	0.25	1.5	0.4	35
529	4.09E-07	7.8	0.25	1.5	3.25	32
530	4.09E-07	7.8	0.25	1.5	3.25	33.5
531	4.09E-07	7.8	0.25	1.5	3.25	35
532	4.09E-07	7.8	0.25	4	0.05	32
533	4.09E-07	7.8	0.25	4	0.05	33.5
534	4.09E-07	7.8	0.25	4	0.05	35
535	4.09E-07	7.8	0.25	4	0.4	32
536	4.09E-07	7.8	0.25	4	0.4	33.5
537	4.09E-07	7.8	0.25	4	0.4	35
538	4.09E-07	7.8	0.25	4	3.25	32
539	4.09E-07	7.8	0.25	4	3.25	33.5
540	4.09E-07	7.8	0.25	4	3.25	35
541	4.09E-07	7.8	1.6	0.75	0.05	32
542	4.09E-07	7.8	1.6	0.75	0.05	33.5
543	4.09E-07	7.8	1.6	0.75	0.05	35
544	4.09E-07	7.8	1.6	0.75	0.4	32
545	4.09E-07	7.8	1.6	0.75	0.4	33.5
546	4.09E-07	7.8	1.6	0.75	0.4	35
547	4.09E-07	7.8	1.6	0.75	3.25	32
548	4.09E-07	7.8	1.6	0.75	3.25	33.5
549	4.09E-07	7.8	1.6	0.75	3.25	35
550	4.09E-07	7.8	1.6	1.5	0.05	32

STATE VARIABLES FOR MODEL INPUT						
Input Number	Total Cu (mol/L)	pH	POC (mg/L)	DOC (mg/L)	Particulate Iron (mg Fe/L)	Salinity (psu)
551	4.09E-07	7.8	1.6	1.5	0.05	33.5
552	4.09E-07	7.8	1.6	1.5	0.05	35
553	4.09E-07	7.8	1.6	1.5	0.4	32
554	4.09E-07	7.8	1.6	1.5	0.4	33.5
555	4.09E-07	7.8	1.6	1.5	0.4	35
556	4.09E-07	7.8	1.6	1.5	3.25	32
557	4.09E-07	7.8	1.6	1.5	3.25	33.5
558	4.09E-07	7.8	1.6	1.5	3.25	35
559	4.09E-07	7.8	1.6	4	0.05	32
560	4.09E-07	7.8	1.6	4	0.05	33.5
561	4.09E-07	7.8	1.6	4	0.05	35
562	4.09E-07	7.8	1.6	4	0.4	32
563	4.09E-07	7.8	1.6	4	0.4	33.5
564	4.09E-07	7.8	1.6	4	0.4	35
565	4.09E-07	7.8	1.6	4	3.25	32
566	4.09E-07	7.8	1.6	4	3.25	33.5
567	4.09E-07	7.8	1.6	4	3.25	35
568	4.09E-07	8.2	0.04	0.75	0.05	32
569	4.09E-07	8.2	0.04	0.75	0.05	33.5
570	4.09E-07	8.2	0.04	0.75	0.05	35
571	4.09E-07	8.2	0.04	0.75	0.4	32
572	4.09E-07	8.2	0.04	0.75	0.4	33.5
573	4.09E-07	8.2	0.04	0.75	0.4	35
574	4.09E-07	8.2	0.04	0.75	3.25	32
575	4.09E-07	8.2	0.04	0.75	3.25	33.5
576	4.09E-07	8.2	0.04	0.75	3.25	35
577	4.09E-07	8.2	0.04	1.5	0.05	32
578	4.09E-07	8.2	0.04	1.5	0.05	33.5
579	4.09E-07	8.2	0.04	1.5	0.05	35
580	4.09E-07	8.2	0.04	1.5	0.4	32
581	4.09E-07	8.2	0.04	1.5	0.4	33.5
582	4.09E-07	8.2	0.04	1.5	0.4	35
583	4.09E-07	8.2	0.04	1.5	3.25	32
584	4.09E-07	8.2	0.04	1.5	3.25	33.5
585	4.09E-07	8.2	0.04	1.5	3.25	35
586	4.09E-07	8.2	0.04	4	0.05	32
587	4.09E-07	8.2	0.04	4	0.05	33.5
588	4.09E-07	8.2	0.04	4	0.05	35
589	4.09E-07	8.2	0.04	4	0.4	32
590	4.09E-07	8.2	0.04	4	0.4	33.5
591	4.09E-07	8.2	0.04	4	0.4	35
592	4.09E-07	8.2	0.04	4	3.25	32
593	4.09E-07	8.2	0.04	4	3.25	33.5
594	4.09E-07	8.2	0.04	4	3.25	35
595	4.09E-07	8.2	0.25	0.75	0.05	32
596	4.09E-07	8.2	0.25	0.75	0.05	33.5
597	4.09E-07	8.2	0.25	0.75	0.05	35
598	4.09E-07	8.2	0.25	0.75	0.4	32
599	4.09E-07	8.2	0.25	0.75	0.4	33.5
600	4.09E-07	8.2	0.25	0.75	0.4	35

STATE VARIABLES FOR MODEL INPUT						
Input Number	Total Cu (mol/L)	pH	POC (mg/L)	DOC (mg/L)	Particulate Iron (mg Fe/L)	Salinity (psu)
601	4.09E-07	8.2	0.25	0.75	3.25	32
602	4.09E-07	8.2	0.25	0.75	3.25	33.5
603	4.09E-07	8.2	0.25	0.75	3.25	35
604	4.09E-07	8.2	0.25	1.5	0.05	32
605	4.09E-07	8.2	0.25	1.5	0.05	33.5
606	4.09E-07	8.2	0.25	1.5	0.05	35
607	4.09E-07	8.2	0.25	1.5	0.4	32
608	4.09E-07	8.2	0.25	1.5	0.4	33.5
609	4.09E-07	8.2	0.25	1.5	0.4	35
610	4.09E-07	8.2	0.25	1.5	3.25	32
611	4.09E-07	8.2	0.25	1.5	3.25	33.5
612	4.09E-07	8.2	0.25	1.5	3.25	35
613	4.09E-07	8.2	0.25	4	0.05	32
614	4.09E-07	8.2	0.25	4	0.05	33.5
615	4.09E-07	8.2	0.25	4	0.05	35
616	4.09E-07	8.2	0.25	4	0.4	32
617	4.09E-07	8.2	0.25	4	0.4	33.5
618	4.09E-07	8.2	0.25	4	0.4	35
619	4.09E-07	8.2	0.25	4	3.25	32
620	4.09E-07	8.2	0.25	4	3.25	33.5
621	4.09E-07	8.2	0.25	4	3.25	35
622	4.09E-07	8.2	1.6	0.75	0.05	32
623	4.09E-07	8.2	1.6	0.75	0.05	33.5
624	4.09E-07	8.2	1.6	0.75	0.05	35
625	4.09E-07	8.2	1.6	0.75	0.4	32
626	4.09E-07	8.2	1.6	0.75	0.4	33.5
627	4.09E-07	8.2	1.6	0.75	0.4	35
628	4.09E-07	8.2	1.6	0.75	3.25	32
629	4.09E-07	8.2	1.6	0.75	3.25	33.5
630	4.09E-07	8.2	1.6	0.75	3.25	35
631	4.09E-07	8.2	1.6	1.5	0.05	32
632	4.09E-07	8.2	1.6	1.5	0.05	33.5
633	4.09E-07	8.2	1.6	1.5	0.05	35
634	4.09E-07	8.2	1.6	1.5	0.4	32
635	4.09E-07	8.2	1.6	1.5	0.4	33.5
636	4.09E-07	8.2	1.6	1.5	0.4	35
637	4.09E-07	8.2	1.6	1.5	3.25	32
638	4.09E-07	8.2	1.6	1.5	3.25	33.5
639	4.09E-07	8.2	1.6	1.5	3.25	35
640	4.09E-07	8.2	1.6	4	0.05	32
641	4.09E-07	8.2	1.6	4	0.05	33.5
642	4.09E-07	8.2	1.6	4	0.05	35
643	4.09E-07	8.2	1.6	4	0.4	32
644	4.09E-07	8.2	1.6	4	0.4	33.5
645	4.09E-07	8.2	1.6	4	0.4	35
646	4.09E-07	8.2	1.6	4	3.25	32
647	4.09E-07	8.2	1.6	4	3.25	33.5
648	4.09E-07	8.2	1.6	4	3.25	35
649	4.09E-07	8.6	0.04	0.75	0.05	32
650	4.09E-07	8.6	0.04	0.75	0.05	33.5

STATE VARIABLES FOR MODEL INPUT						
Input Number	Total Cu (mol/L)	pH	POC (mg/L)	DOC (mg/L)	Particulate Iron (mg Fe/L)	Salinity (psu)
651	4.09E-07	8.6	0.04	0.75	0.05	35
652	4.09E-07	8.6	0.04	0.75	0.4	32
653	4.09E-07	8.6	0.04	0.75	0.4	33.5
654	4.09E-07	8.6	0.04	0.75	0.4	35
655	4.09E-07	8.6	0.04	0.75	3.25	32
656	4.09E-07	8.6	0.04	0.75	3.25	33.5
657	4.09E-07	8.6	0.04	0.75	3.25	35
658	4.09E-07	8.6	0.04	1.5	0.05	32
659	4.09E-07	8.6	0.04	1.5	0.05	33.5
660	4.09E-07	8.6	0.04	1.5	0.05	35
661	4.09E-07	8.6	0.04	1.5	0.4	32
662	4.09E-07	8.6	0.04	1.5	0.4	33.5
663	4.09E-07	8.6	0.04	1.5	0.4	35
664	4.09E-07	8.6	0.04	1.5	3.25	32
665	4.09E-07	8.6	0.04	1.5	3.25	33.5
666	4.09E-07	8.6	0.04	1.5	3.25	35
667	4.09E-07	8.6	0.04	4	0.05	32
668	4.09E-07	8.6	0.04	4	0.05	33.5
669	4.09E-07	8.6	0.04	4	0.05	35
670	4.09E-07	8.6	0.04	4	0.4	32
671	4.09E-07	8.6	0.04	4	0.4	33.5
672	4.09E-07	8.6	0.04	4	0.4	35
673	4.09E-07	8.6	0.04	4	3.25	32
674	4.09E-07	8.6	0.04	4	3.25	33.5
675	4.09E-07	8.6	0.04	4	3.25	35
676	4.09E-07	8.6	0.25	0.75	0.05	32
677	4.09E-07	8.6	0.25	0.75	0.05	33.5
678	4.09E-07	8.6	0.25	0.75	0.05	35
679	4.09E-07	8.6	0.25	0.75	0.4	32
680	4.09E-07	8.6	0.25	0.75	0.4	33.5
681	4.09E-07	8.6	0.25	0.75	0.4	35
682	4.09E-07	8.6	0.25	0.75	3.25	32
683	4.09E-07	8.6	0.25	0.75	3.25	33.5
684	4.09E-07	8.6	0.25	0.75	3.25	35
685	4.09E-07	8.6	0.25	1.5	0.05	32
686	4.09E-07	8.6	0.25	1.5	0.05	33.5
687	4.09E-07	8.6	0.25	1.5	0.05	35
688	4.09E-07	8.6	0.25	1.5	0.4	32
689	4.09E-07	8.6	0.25	1.5	0.4	33.5
690	4.09E-07	8.6	0.25	1.5	0.4	35
691	4.09E-07	8.6	0.25	1.5	3.25	32
692	4.09E-07	8.6	0.25	1.5	3.25	33.5
693	4.09E-07	8.6	0.25	1.5	3.25	35
694	4.09E-07	8.6	0.25	4	0.05	32
695	4.09E-07	8.6	0.25	4	0.05	33.5
696	4.09E-07	8.6	0.25	4	0.05	35
697	4.09E-07	8.6	0.25	4	0.4	32
698	4.09E-07	8.6	0.25	4	0.4	33.5
699	4.09E-07	8.6	0.25	4	0.4	35
700	4.09E-07	8.6	0.25	4	3.25	32

STATE VARIABLES FOR MODEL INPUT						
Input Number	Total Cu (mol/L)	pH	POC (mg/L)	DOC (mg/L)	Particulate Iron (mg Fe/L)	Salinity (psu)
701	4.09E-07	8.6	0.25	4	3.25	33.5
702	4.09E-07	8.6	0.25	4	3.25	35
703	4.09E-07	8.6	1.6	0.75	0.05	32
704	4.09E-07	8.6	1.6	0.75	0.05	33.5
705	4.09E-07	8.6	1.6	0.75	0.05	35
706	4.09E-07	8.6	1.6	0.75	0.4	32
707	4.09E-07	8.6	1.6	0.75	0.4	33.5
708	4.09E-07	8.6	1.6	0.75	0.4	35
709	4.09E-07	8.6	1.6	0.75	3.25	32
710	4.09E-07	8.6	1.6	0.75	3.25	33.5
711	4.09E-07	8.6	1.6	0.75	3.25	35
712	4.09E-07	8.6	1.6	1.5	0.05	32
713	4.09E-07	8.6	1.6	1.5	0.05	33.5
714	4.09E-07	8.6	1.6	1.5	0.05	35
715	4.09E-07	8.6	1.6	1.5	0.4	32
716	4.09E-07	8.6	1.6	1.5	0.4	33.5
717	4.09E-07	8.6	1.6	1.5	0.4	35
718	4.09E-07	8.6	1.6	1.5	3.25	32
719	4.09E-07	8.6	1.6	1.5	3.25	33.5
720	4.09E-07	8.6	1.6	1.5	3.25	35
721	4.09E-07	8.6	1.6	4	0.05	32
722	4.09E-07	8.6	1.6	4	0.05	33.5
723	4.09E-07	8.6	1.6	4	0.05	35
724	4.09E-07	8.6	1.6	4	0.4	32
725	4.09E-07	8.6	1.6	4	0.4	33.5
726	4.09E-07	8.6	1.6	4	0.4	35
727	4.09E-07	8.6	1.6	4	3.25	32
728	4.09E-07	8.6	1.6	4	3.25	33.5
729	4.09E-07	8.6	1.6	4	3.25	35

WHAM7 INPUT																				WHAM7 OUTPUT	
Descriptio n	S P	Temp	pC O2	p H	Part HA (g/L)	Part FA (g/L)	Part FeOx (g/L)	Coll HA (g/L)	Coll FA (g/L)	Na (M)	Mg (M)	{Al3+ (M)}	K (M)	Ca (M)	{Fe3+ (M)}	Tot Cu (M)	Cl (M)	SO4 (M)	CO3 (M)	logKD' = log(KD x TSS) (dimensionless)	Fract. Part. (dimensionless)
1	1	298.	---	7	4.000E-	4.000E-	3.223E-	0.000E+0	1.020E-	4.279E-	4.865E-	1.259E-	9.328E-	9.354E-	3.221E-	6.295E-	4.983E-	2.579E-	2.250E-	-1.00	0.091
2	1	298.	---	7	4.000E-	4.000E-	3.223E-	0.000E+0	1.020E-	4.480E-	5.093E-	1.259E-	9.764E-	9.777E-	3.221E-	6.295E-	5.216E-	2.699E-	2.315E-	-1.00	0.091
3	1	298.	---	7	4.000E-	4.000E-	3.223E-	0.000E+0	1.020E-	4.680E-	5.320E-	1.259E-	1.020E-	1.020E-	3.221E-	6.295E-	5.450E-	2.820E-	2.380E-	-1.00	0.090
4	1	298.	---	7	4.000E-	4.000E-	2.579E-	0.000E+0	1.020E-	4.279E-	4.865E-	1.259E-	9.328E-	9.354E-	3.221E-	6.295E-	4.983E-	2.579E-	2.250E-	-0.62	0.193
5	1	298.	---	7	4.000E-	4.000E-	2.579E-	0.000E+0	1.020E-	4.480E-	5.093E-	1.259E-	9.764E-	9.777E-	3.221E-	6.295E-	5.216E-	2.699E-	2.315E-	-0.62	0.193
6	1	298.	---	7	4.000E-	4.000E-	2.579E-	0.000E+0	1.020E-	4.680E-	5.320E-	1.259E-	1.020E-	1.020E-	3.221E-	6.295E-	5.450E-	2.820E-	2.380E-	-0.62	0.193
7	1	298.	---	7	4.000E-	4.000E-	2.095E-	0.000E+0	1.020E-	4.279E-	4.865E-	1.259E-	9.328E-	9.354E-	3.221E-	6.295E-	4.983E-	2.579E-	2.250E-	0.07	0.541
8	1	298.	---	7	4.000E-	4.000E-	2.095E-	0.000E+0	1.020E-	4.480E-	5.093E-	1.259E-	9.764E-	9.777E-	3.221E-	6.295E-	5.216E-	2.699E-	2.315E-	0.07	0.541
9	1	298.	---	7	4.000E-	4.000E-	2.095E-	0.000E+0	1.020E-	4.680E-	5.320E-	1.259E-	1.020E-	1.020E-	3.221E-	6.295E-	5.450E-	2.820E-	2.380E-	0.07	0.540
10	1	298.	---	7	4.000E-	4.000E-	3.223E-	0.000E+0	2.040E-	4.279E-	4.865E-	1.259E-	9.328E-	9.354E-	3.221E-	6.295E-	4.983E-	2.579E-	2.250E-	-1.27	0.050
11	1	298.	---	7	4.000E-	4.000E-	3.223E-	0.000E+0	2.040E-	4.480E-	5.093E-	1.259E-	9.764E-	9.777E-	3.221E-	6.295E-	5.216E-	2.699E-	2.315E-	-1.28	0.050
12	1	298.	---	7	4.000E-	4.000E-	3.223E-	0.000E+0	2.040E-	4.680E-	5.320E-	1.259E-	1.020E-	1.020E-	3.221E-	6.295E-	5.450E-	2.820E-	2.380E-	-1.28	0.050
13	1	298.	---	7	4.000E-	4.000E-	2.579E-	0.000E+0	2.040E-	4.279E-	4.865E-	1.259E-	9.328E-	9.354E-	3.221E-	6.295E-	4.983E-	2.579E-	2.250E-	-0.94	0.103
14	1	298.	---	7	4.000E-	4.000E-	2.579E-	0.000E+0	2.040E-	4.480E-	5.093E-	1.259E-	9.764E-	9.777E-	3.221E-	6.295E-	5.216E-	2.699E-	2.315E-	-0.94	0.103
15	1	298.	---	7	4.000E-	4.000E-	2.579E-	0.000E+0	2.040E-	4.680E-	5.320E-	1.259E-	1.020E-	1.020E-	3.221E-	6.295E-	5.450E-	2.820E-	2.380E-	-0.94	0.103
16	1	298.	---	7	4.000E-	4.000E-	2.095E-	0.000E+0	2.040E-	4.279E-	4.865E-	1.259E-	9.328E-	9.354E-	3.221E-	6.295E-	4.983E-	2.579E-	2.250E-	-0.24	0.365
17	1	298.	---	7	4.000E-	4.000E-	2.095E-	0.000E+0	2.040E-	4.480E-	5.093E-	1.259E-	9.764E-	9.777E-	3.221E-	6.295E-	5.216E-	2.699E-	2.315E-	-0.24	0.365
18	1	298.	---	7	4.000E-																

63	1	298.	---	7	1.600E-	1.600E-	2.095E-	0.000E+0	1.020E-	4.680E-	5.320E-	1.259E-	1.020E-	1.020E-	3.221E-	6.295E-	5.450E-	2.820E-	2.380E-	0.66	0.819
----	---	------	-----	---	---------	---------	---------	----------	---------	---------	---------	---------	---------	---------	---------	---------	---------	---------	---------	------	-------

WHAM7 INPUT																				WHAM7 OUTPUT	
Description	SPM (g/L)	Temp (K)	pCO2 (atm)	pH	Part HA (g/L)	Part FA (g/L)	Part FeOx (g/L)	Coll HA (g/L)	Coll FA (g/L)	Na (M)	Mg (M)	{Al3+} (M)	K (M)	Ca (M)	{Fe3+} (M)	Tot Cu (M)	Cl (M)	SO4 (M)	CO3 (M)	logK' = log(Ko x TSS) (dimensionless)	Fract. Part. (dimensionless)
190	1000	298.15	---	8.6	2.500E-04	2.500E-04	3.223E-05	0.000E+00	1.020E-03	4.279E-01	4.865E-02	5.012E-18	9.328E-03	9.354E-03	3.281E-21	6.295E-08	4.983E-01	2.579E-02	2.250E-03	-0.27	0.351
191	1000	298.15	---	8.6	2.500E-04	2.500E-04	3.223E-05	0.000E+00	1.020E-03	4.480E-01	5.093E-02	5.012E-18	9.764E-03	9.777E-03	3.281E-21	6.295E-08	5.216E-01	2.699E-02	2.315E-03	-0.27	0.350
192	1000	298.15	---	8.6	2.500E-04	2.500E-04	3.223E-05	0.000E+00	1.020E-03	4.680E-01	5.320E-02	5.012E-18	1.020E-02	1.020E-02	3.281E-21	6.295E-08	5.450E-01	2.820E-02	2.380E-03	-0.27	0.350
193	1000	298.15	---	8.6	2.500E-04	2.500E-04	2.579E-04	0.000E+00	1.020E-03	4.279E-01	4.865E-02	5.012E-18	9.328E-03	9.354E-03	3.281E-21	6.295E-08	4.983E-01	2.579E-02	2.250E-03	-0.13	0.428
194	1000	298.15	---	8.6	2.500E-04	2.500E-04	2.579E-04	0.000E+00	1.020E-03	4.480E-01	5.093E-02	5.012E-18	9.764E-03	9.777E-03	3.281E-21	6.295E-08	5.216E-01	2.699E-02	2.315E-03	-0.13	0.428
195	1000	298.15	---	8.6	2.500E-04	2.500E-04	2.579E-04	0.000E+00	1.020E-03	4.680E-01	5.320E-02	5.012E-18	1.020E-02	1.020E-02	3.281E-21	6.295E-08	5.450E-01	2.820E-02	2.380E-03	-0.13	0.428
196	1000	298.15	---	8.6	2.500E-04	2.500E-04	2.095E-03	0.000E+00	1.020E-03	4.279E-01	4.865E-02	5.012E-18	9.328E-03	9.354E-03	3.281E-21	6.295E-08	4.983E-01	2.579E-02	2.250E-03	0.33	0.681
197	1000	298.15	---	8.6	2.500E-04	2.500E-04	2.095E-03	0.000E+00	1.020E-03	4.480E-01	5.093E-02	5.012E-18	9.764E-03	9.777E-03	3.281E-21	6.295E-08	5.216E-01	2.699E-02	2.315E-03	0.33	0.682
198	1000	298.15	---	8.6	2.500E-04	2.500E-04	2.095E-03	0.000E+00	1.020E-03	4.680E-01	5.320E-02	5.012E-18	1.020E-02	1.020E-02	3.281E-21	6.295E-08	5.450E-01	2.820E-02	2.380E-03	0.33	0.683
199	1000	298.15	---	8.6	2.500E-04	2.500E-04	3.223E-05	0.000E+00	2.040E-03	4.279E-01	4.865E-02	5.012E-18	9.328E-03	9.354E-03	3.281E-21	6.295E-08	4.983E-01	2.579E-02	2.250E-03	-0.57	0.213
200	1000	298.15	---	8.6	2.500E-04	2.500E-04	3.223E-05	0.000E+00	2.040E-03	4.480E-01	5.093E-02	5.012E-18	9.764E-03	9.777E-03	3.281E-21	6.295E-08	5.216E-01	2.699E-02	2.315E-03	-0.57	0.213
201	1000	298.15	---	8.6	2.500E-04	2.500E-04	3.223E-05	0.000E+00	2.040E-03	4.680E-01	5.320E-02	5.012E-18	1.020E-02	1.020E-02	3.281E-21	6.295E-08	5.450E-01	2.820E-02	2.380E-03	-0.57	0.212
202	1000	298.15	---	8.6	2.500E-04	2.500E-04	2.579E-04	0.000E+00	2.040E-03	4.279E-01	4.865E-02	5.012E-18	9.328E-03	9.354E-03	3.281E-21	6.295E-08	4.983E-01	2.579E-02	2.250E-03	-0.44	0.266
203	1000	298.15	---	8.6	2.500E-04	2.500E-04	2.579E-04	0.000E+00	2.040E-03	4.480E-01	5.093E-02	5.012E-18	9.764E-03	9.777E-03	3.281E-21	6.295E-08	5.216E-01	2.699E-02	2.315E-03	-0.44	0.266
204	1000	298.15	---	8.6	2.500E-04	2.500E-04	2.579E-04	0.000E+00	2.040E-03	4.680E-01	5.320E-02	5.012E-18	1.020E-02	1.020E-02	3.281E-21	6.295E-08	5.450E-01	2.820E-02	2.380E-03	-0.44	0.266
205	1000	298.15	---	8.6	2.500E-04	2.500E-04	2.095E-03	0.000E+00	2.040E-03	4.279E-01	4.865E-02	5.012E-18	9.328E-03	9.354E-03	3.281E-21	6.295E-08	4.983E-01	2.579E-02	2.250E-03	0.01	0.508
206	1000	298.15	---	8.6	2.500E-04	2.500E-04	2.095E-03	0.000E+00	2.040E-03	4.480E-01	5.093E-02	5.012E-18	9.764E-03	9.777E-03	3.281E-21	6.295E-08	5.216E-01	2.699E-02	2.315E-03	0.02	0.509
207	1000	298.15	---	8.6	2.500E-04	2.500E-04	2.095E-03	0.000E+00	2.040E-03	4.680E-01	5.320E-02	5.012E-18	1.020E-02	1.020E-02	3.281E-21	6.295E-08	5.450E-01	2.820E-02	2.380E-03	0.02	0.510
208	1000	298.15	---	8.6	2.500E-04	2.500E-04	3.223E-05	0.000E+00	5.440E-03	4.279E-01	4.865E-02	5.012E-18	9.328E-03	9.354E-03	3.281E-21	6.295E-08	4.983E-01	2.579E-02	2.250E-03	-0.98	0.094
209	1000	298.15	---	8.6	2.500E-04	2.500E-04	3.223E-05	0.000E+00	5.440E-03	4.480E-01	5.093E-02	5.012E-18	9.764E-03	9.777E-03	3.281E-21	6.295E-08	5.216E-01	2.699E-02	2.315E-03	-0.98	0.094
210	1000	298.15	---	8.6	2.500E-04	2.500E-04	3.223E-05	0.000E+00	5.440E-03	4.680E-01	5.320E-02	5.012E-18	1.020E-02	1.020E-02	3.281E-21	6.295E-08	5.450E-01	2.820E-02	2.380E-03	-0.98	0.094
211	1000	298.15	---	8.6	2.500E-04	2.500E-04	2.579E-04	0.000E+00	5.440E-03	4.279E-01	4.865E-02	5.012E-18	9.328E-03	9.354E-03	3.281E-21	6.295E-08	4.983E-01	2.579E-02	2.250E-03	-0.88	0.117
212	1000	298.15	---	8.6	2.500E-04	2.500E-04	2.579E-04	0.000E+00	5.440E-03	4.480E-01	5.093E-02	5.012E-18	9.764E-03	9.777E-03	3.281E-21	6.295E-08	5.216E-01	2.699E-02	2.315E-03	-0.88	0.117
213	1000	298.15	---	8.6	2.500E-04	2.500E-04	2.579E-04	0.000E+00	5.440E-03	4.680E-01	5.320E-02	5.012E-18	1.020E-02	1.020E-02	3.281E-21	6.295E-08	5.450E-01	2.820E-02	2.380E-03	-0.88	0.117
214	1000	298.15	---	8.6	2.500E-04	2.500E-04	2.095E-03	0.000E+00	5.440E-03	4.279E-01	4.865E-02	5.012E-18	9.328E-03	9.354E-03	3.281E-21	6.295E-08	4.983E-01	2.579E-02	2.250E-03	-0.44	0.265
215	1000	298.15	---	8.6	2.500E-04	2.500E-04	2.095E-03	0.000E+00	5.440E-03	4.480E-01	5.093E-02	5.012E-18	9.764E-03	9.777E-03	3.281E-21	6.295E-08	5.216E-01	2.699E-02	2.315E-03	-0.44	0.266
216	1000	298.15	---	8.6	2.500E-04	2.500E-04	2.095E-03	0.000E+00	5.440E-03	4.680E-01	5.320E-02	5.012E-18	1.020E-02	1.020E-02	3.281E-21	6.295E-08	5.450E-01	2.820E-02	2.380E-03	-0.44	0.267
217	1000	298.15	---	8.6	1.600E-03	1.600E-03	3.223E-05	0.000E+00	1.020E-03	4.279E-01	4.865E-02	5.012E-18	9.328E-03	9.354E-03	3.281E-21	6.295E-08	4.983E-01	2.579E-02	2.250E-03	0.52	0.769
218	1000	298.15	---	8.6	1.600E-03	1.600E-03	3.223E-05	0.000E+00	1.020E-03	4.480E-01	5.093E-02	5.012E-18	9.764E-03	9.777E-03	3.281E-21	6.295E-08	5.216E-01	2.699E-02	2.315E-03	0.52	0.769
219	1000	298.15	---	8.6	1.600E-03	1.600E-03	3.223E-05	0.000E+00	1.020E-03	4.680E-01	5.320E-02	5.012E-18	1.020E-02	1.020E-02	3.281E-21	6.295E-08	5.450E-01	2.820E-02	2.380E-03	0.52	0.769
220	1000	298.15	---	8.6	1.600E-03	1.600E-03	2.579E-04	0.000E+00	1.020E-03	4.279E-01	4.865E-02	5.012E-18	9.328E-03	9.354E-03	3.281E-21	6.295E-08	4.983E-01	2.579E-02	2.250E-03	0.54	0.778
221	1000	298.15	---	8.6	1.600E-03	1.600E-03	2.579E-04	0.000E+00	1.020E-03	4.480E-01	5.093E-02	5.012E-18	9.764E-03	9.777E-03	3.281E-21	6.295E-08	5.216E-01	2.699E-02	2.315E-03	0.54	0.778
222	1000	298.15	---	8.6	1.600E-03	1.600E-03	2.579E-04	0.000E+00	1.020E-03	4.680E-01	5.320E-02	5.012E-18	1.020E-02	1.020E-02	3.281E-21	6.295E-08	5.450E-01	2.820E-02	2.380E-03	0.54	0.777
223	1000	298.15	---	8.6	1.600E-03	1.600E-03	2.095E-03	0.000E+00	1.020E-03	4.279E-01	4.865E-02	5.012E-18	9.328E-03	9.354E-03	3.281E-21	6.295E-08	4.983E-01	2.579E-02	2.250E-03	0.68	0.827
224	1000	298.15	---	8.6	1.600E-03	1.600E-03	2.095E-03	0.000E+00	1.020E-03	4.480E-01	5.093E-02	5.012E-18	9.764E-03	9.777E-03	3.281E-21	6.295E-08	5.216E-01	2.699E-02	2.315E-03	0.68	0.827
225	1000	298.15	---	8.6	1.600E-03	1.600E-03	2.095E-03	0.000E+00	1.020E-03	4.680E-01	5.320E-02	5.012E-18	1.020E-02	1.020E-02	3.281E-21	6.295E-08	5.450E-01	2.820E-02	2.380E-03	0.68	0.827
226	1000	298.15	---	8.6	1.600E-03	1.600E-03	3.223E-05	0.000E+00	2.040E-03	4.279E-01	4.865E-02	5.012E-18	9.328E-03	9.354E-03	3.281E-21	6.295E-08	4.983E-01	2.579E-02	2.250E-03	0.23	0.629
227	1000	298.15	---	8.6	1.600E-03	1.600E-03	3.223E-05	0.000E+00	2.040E-03	4.480E-01	5.093E-02	5.012E-18	9.764E-03	9.777E-03	3.281E-21	6.295E-08	5.216E-01	2.699E-02	2.315E-03	0.23	0.629
228	1000	298.15	---	8.6	1.600E-03	1.600E-03	3.223E-05	0.000E+00	2.040E-03	4.680E-01	5.320E-02	5.012E-18	1.020E-02	1.020E-02	3.281E-21	6.295E-08	5.450E-01	2.820E-02	2.380E-03	0.23	0.629
229	1000	298.15	---	8.6	1.600E-03	1.600E-03	2.579E-04	0.000E+00	2.040E-03	4.279E-01	4.865E-02	5.012E-18	9.328E-03	9.354E-03	3.281E-21	6.295E-08	4.983E-01	2.579E-02	2.250E-03	0.25	0.640
230	1000	298.15	---	8.6	1.600E-03	1.600E-03	2.579E-04	0.000E+00	2.040E-03	4.480E-01	5.093E-02	5.012E-18	9.764E-03	9.777E-03	3.281E-21	6.295E-08	5.216E-01	2.699E-02	2.315E-03	0.25	0.640
231	1000	298.15	---	8.6	1.600E-03	1.600E-03	2.579E-04	0.000E+00	2.040E-03	4.680E-01	5.320E-02	5.012E-18	1.020E-02	1.020E-02	3.281E-21	6.295E-08	5.450E-01	2.820E-02	2.380E-03	0.25	0.640
232	1000	298.15	---	8.6	1.600E-03	1.600E-03	2.095E-03	0.000E+00	2.040E-03	4.279E-01	4.865E-02	5.012E-18	9.328E-03	9.354E-03	3.281E-21	6.295E-08	4.983E-01	2.579E-02	2.250E-03	0.38	0.706
233	1000	298.15	---	8.6	1.600E-03	1.600E-03	2.095E-03	0.000E+00	2.040E-03	4.480E-01	5.093E-02	5.012E-18	9.764E-03	9.777E-03	3.281E-21	6.295E-08	5.216E-01	2.699E-02	2.315E-03	0.38	0.707
234	1000	298.15	---	8.6																	

165

169

Table 31: Input and Output Pearl Harbor Look-Up Table Development
State Variable for Model Input

STATE VARIABLES FOR MODEL INPUT						
Input Number	Total Cu (mol/L)	pH	POC (mg/L)	DOC (mg/L)	Particulate Iron (mg Fe/L)	Salinity (psu)
1	1.57E-09	7.90	0.05	1	0.02	26
2	1.57E-09	7.90	0.05	1	0.02	30
3	1.57E-09	7.90	0.05	1	0.02	35.5
4	1.57E-09	7.90	0.05	1	0.2	26
5	1.57E-09	7.90	0.05	1	0.2	30
6	1.57E-09	7.90	0.05	1	0.2	35.5
7	1.57E-09	7.90	0.05	1	3	26
8	1.57E-09	7.90	0.05	1	3	30
9	1.57E-09	7.90	0.05	1	3	35.5
10	1.57E-09	7.90	0.05	2	0.02	26
11	1.57E-09	7.90	0.05	2	0.02	30
12	1.57E-09	7.90	0.05	2	0.02	35.5
13	1.57E-09	7.90	0.05	2	0.2	26
14	1.57E-09	7.90	0.05	2	0.2	30
15	1.57E-09	7.90	0.05	2	0.2	35.5
16	1.57E-09	7.90	0.05	2	3	26
17	1.57E-09	7.90	0.05	2	3	30
18	1.57E-09	7.90	0.05	2	3	35.5
19	1.57E-09	7.90	0.05	4	0.02	26
20	1.57E-09	7.90	0.05	4	0.02	30
21	1.57E-09	7.90	0.05	4	0.02	35.5
22	1.57E-09	7.90	0.05	4	0.2	26
23	1.57E-09	7.90	0.05	4	0.2	30
24	1.57E-09	7.90	0.05	4	0.2	35.5
25	1.57E-09	7.90	0.05	4	3	26
26	1.57E-09	7.90	0.05	4	3	30
27	1.57E-09	7.90	0.05	4	3	35.5
28	1.57E-09	7.90	0.8	1	0.02	26
29	1.57E-09	7.90	0.8	1	0.02	30
30	1.57E-09	7.90	0.8	1	0.02	35.5
31	1.57E-09	7.90	0.8	1	0.2	26
32	1.57E-09	7.90	0.8	1	0.2	30
33	1.57E-09	7.90	0.8	1	0.2	35.5
34	1.57E-09	7.90	0.8	1	3	26
35	1.57E-09	7.90	0.8	1	3	30
36	1.57E-09	7.90	0.8	1	3	35.5
37	1.57E-09	7.90	0.8	2	0.02	26
38	1.57E-09	7.90	0.8	2	0.02	30
39	1.57E-09	7.90	0.8	2	0.02	35.5
40	1.57E-09	7.90	0.8	2	0.2	26
41	1.57E-09	7.90	0.8	2	0.2	30
42	1.57E-09	7.90	0.8	2	0.2	35.5
43	1.57E-09	7.90	0.8	2	3	26
44	1.57E-09	7.90	0.8	2	3	30
45	1.57E-09	7.90	0.8	2	3	35.5
46	1.57E-09	7.90	0.8	4	0.02	26
47	1.57E-09	7.90	0.8	4	0.02	30
48	1.57E-09	7.90	0.8	4	0.02	35.5
49	1.57E-09	7.90	0.8	4	0.2	26
50	1.57E-09	7.90	0.8	4	0.2	30

STATE VARIABLES FOR MODEL INPUT						
Input Number	Total Cu (mol/L)	pH	POC (mg/L)	DOC (mg/L)	Particulate Iron (mg Fe/L)	Salinity (psu)
51	1.57E-09	7.90	0.8	4	0.2	35.5
52	1.57E-09	7.90	0.8	4	3	26
53	1.57E-09	7.90	0.8	4	3	30
54	1.57E-09	7.90	0.8	4	3	35.5
55	1.57E-09	7.90	7	1	0.02	26
56	1.57E-09	7.90	7	1	0.02	30
57	1.57E-09	7.90	7	1	0.02	35.5
58	1.57E-09	7.90	7	1	0.2	26
59	1.57E-09	7.90	7	1	0.2	30
60	1.57E-09	7.90	7	1	0.2	35.5
61	1.57E-09	7.90	7	1	3	26
62	1.57E-09	7.90	7	1	3	30
63	1.57E-09	7.90	7	1	3	35.5
64	1.57E-09	7.90	7	2	0.02	26
65	1.57E-09	7.90	7	2	0.02	30
66	1.57E-09	7.90	7	2	0.02	35.5
67	1.57E-09	7.90	7	2	0.2	26
68	1.57E-09	7.90	7	2	0.2	30
69	1.57E-09	7.90	7	2	0.2	35.5
70	1.57E-09	7.90	7	2	3	26
71	1.57E-09	7.90	7	2	3	30
72	1.57E-09	7.90	7	2	3	35.5
73	1.57E-09	7.90	7	4	0.02	26
74	1.57E-09	7.90	7	4	0.02	30
75	1.57E-09	7.90	7	4	0.02	35.5
76	1.57E-09	7.90	7	4	0.2	26
77	1.57E-09	7.90	7	4	0.2	30
78	1.57E-09	7.90	7	4	0.2	35.5
79	1.57E-09	7.90	7	4	3	26
80	1.57E-09	7.90	7	4	3	30
81	1.57E-09	7.90	7	4	3	35.5
82	1.57E-09	8.25	0.05	1	0.02	26
83	1.57E-09	8.25	0.05	1	0.02	30
84	1.57E-09	8.25	0.05	1	0.02	35.5
85	1.57E-09	8.25	0.05	1	0.2	26
86	1.57E-09	8.25	0.05	1	0.2	30
87	1.57E-09	8.25	0.05	1	0.2	35.5
88	1.57E-09	8.25	0.05	1	3	26
89	1.57E-09	8.25	0.05	1	3	30
90	1.57E-09	8.25	0.05	1	3	35.5
91	1.57E-09	8.25	0.05	2	0.02	26
92	1.57E-09	8.25	0.05	2	0.02	30
93	1.57E-09	8.25	0.05	2	0.02	35.5
94	1.57E-09	8.25	0.05	2	0.2	26
95	1.57E-09	8.25	0.05	2	0.2	30
96	1.57E-09	8.25	0.05	2	0.2	35.5
97	1.57E-09	8.25	0.05	2	3	26
98	1.57E-09	8.25	0.05	2	3	30
99	1.57E-09	8.25	0.05	2	3	35.5
100	1.57E-09	8.25	0.05	4	0.02	26

STATE VARIABLES FOR MODEL INPUT						
Input Number	Total Cu (mol/L)	pH	POC (mg/L)	DOC (mg/L)	Particulate Iron (mg Fe/L)	Salinity (psu)
101	1.57E-09	8.25	0.05	4	0.02	30
102	1.57E-09	8.25	0.05	4	0.02	35.5
103	1.57E-09	8.25	0.05	4	0.2	26
104	1.57E-09	8.25	0.05	4	0.2	30
105	1.57E-09	8.25	0.05	4	0.2	35.5
106	1.57E-09	8.25	0.05	4	3	26
107	1.57E-09	8.25	0.05	4	3	30
108	1.57E-09	8.25	0.05	4	3	35.5
109	1.57E-09	8.25	0.8	1	0.02	26
110	1.57E-09	8.25	0.8	1	0.02	30
111	1.57E-09	8.25	0.8	1	0.02	35.5
112	1.57E-09	8.25	0.8	1	0.2	26
113	1.57E-09	8.25	0.8	1	0.2	30
114	1.57E-09	8.25	0.8	1	0.2	35.5
115	1.57E-09	8.25	0.8	1	3	26
116	1.57E-09	8.25	0.8	1	3	30
117	1.57E-09	8.25	0.8	1	3	35.5
118	1.57E-09	8.25	0.8	2	0.02	26
119	1.57E-09	8.25	0.8	2	0.02	30
120	1.57E-09	8.25	0.8	2	0.02	35.5
121	1.57E-09	8.25	0.8	2	0.2	26
122	1.57E-09	8.25	0.8	2	0.2	30
123	1.57E-09	8.25	0.8	2	0.2	35.5
124	1.57E-09	8.25	0.8	2	3	26
125	1.57E-09	8.25	0.8	2	3	30
126	1.57E-09	8.25	0.8	2	3	35.5
127	1.57E-09	8.25	0.8	4	0.02	26
128	1.57E-09	8.25	0.8	4	0.02	30
129	1.57E-09	8.25	0.8	4	0.02	35.5
130	1.57E-09	8.25	0.8	4	0.2	26
131	1.57E-09	8.25	0.8	4	0.2	30
132	1.57E-09	8.25	0.8	4	0.2	35.5
133	1.57E-09	8.25	0.8	4	3	26
134	1.57E-09	8.25	0.8	4	3	30
135	1.57E-09	8.25	0.8	4	3	35.5
136	1.57E-09	8.25	7	1	0.02	26
137	1.57E-09	8.25	7	1	0.02	30
138	1.57E-09	8.25	7	1	0.02	35.5
139	1.57E-09	8.25	7	1	0.2	26
140	1.57E-09	8.25	7	1	0.2	30
141	1.57E-09	8.25	7	1	0.2	35.5
142	1.57E-09	8.25	7	1	3	26
143	1.57E-09	8.25	7	1	3	30
144	1.57E-09	8.25	7	1	3	35.5
145	1.57E-09	8.25	7	2	0.02	26
146	1.57E-09	8.25	7	2	0.02	30
147	1.57E-09	8.25	7	2	0.02	35.5
148	1.57E-09	8.25	7	2	0.2	26
149	1.57E-09	8.25	7	2	0.2	30
150	1.57E-09	8.25	7	2	0.2	35.5

STATE VARIABLES FOR MODEL INPUT						
Input Number	Total Cu (mol/L)	pH	POC (mg/L)	DOC (mg/L)	Particulate Iron (mg Fe/L)	Salinity (psu)
151	1.57E-09	8.25	7	2	3	26
152	1.57E-09	8.25	7	2	3	30
153	1.57E-09	8.25	7	2	3	35.5
154	1.57E-09	8.25	7	4	0.02	26
155	1.57E-09	8.25	7	4	0.02	30
156	1.57E-09	8.25	7	4	0.02	35.5
157	1.57E-09	8.25	7	4	0.2	26
158	1.57E-09	8.25	7	4	0.2	30
159	1.57E-09	8.25	7	4	0.2	35.5
160	1.57E-09	8.25	7	4	3	26
161	1.57E-09	8.25	7	4	3	30
162	1.57E-09	8.25	7	4	3	35.5
163	1.57E-09	8.60	0.05	1	0.02	26
164	1.57E-09	8.60	0.05	1	0.02	30
165	1.57E-09	8.60	0.05	1	0.02	35.5
166	1.57E-09	8.60	0.05	1	0.2	26
167	1.57E-09	8.60	0.05	1	0.2	30
168	1.57E-09	8.60	0.05	1	0.2	35.5
169	1.57E-09	8.60	0.05	1	3	26
170	1.57E-09	8.60	0.05	1	3	30
171	1.57E-09	8.60	0.05	1	3	35.5
172	1.57E-09	8.60	0.05	2	0.02	26
173	1.57E-09	8.60	0.05	2	0.02	30
174	1.57E-09	8.60	0.05	2	0.02	35.5
175	1.57E-09	8.60	0.05	2	0.2	26
176	1.57E-09	8.60	0.05	2	0.2	30
177	1.57E-09	8.60	0.05	2	0.2	35.5
178	1.57E-09	8.60	0.05	2	3	26
179	1.57E-09	8.60	0.05	2	3	30
180	1.57E-09	8.60	0.05	2	3	35.5
181	1.57E-09	8.60	0.05	4	0.02	26
182	1.57E-09	8.60	0.05	4	0.02	30
183	1.57E-09	8.60	0.05	4	0.02	35.5
184	1.57E-09	8.60	0.05	4	0.2	26
185	1.57E-09	8.60	0.05	4	0.2	30
186	1.57E-09	8.60	0.05	4	0.2	35.5
187	1.57E-09	8.60	0.05	4	3	26
188	1.57E-09	8.60	0.05	4	3	30
189	1.57E-09	8.60	0.05	4	3	35.5
190	1.57E-09	8.60	0.8	1	0.02	26
191	1.57E-09	8.60	0.8	1	0.02	30
192	1.57E-09	8.60	0.8	1	0.02	35.5
193	1.57E-09	8.60	0.8	1	0.2	26
194	1.57E-09	8.60	0.8	1	0.2	30
195	1.57E-09	8.60	0.8	1	0.2	35.5
196	1.57E-09	8.60	0.8	1	3	26
197	1.57E-09	8.60	0.8	1	3	30
198	1.57E-09	8.60	0.8	1	3	35.5
199	1.57E-09	8.60	0.8	2	0.02	26
200	1.57E-09	8.60	0.8	2	0.02	30

STATE VARIABLES FOR MODEL INPUT						
Input Number	Total Cu (mol/L)	pH	POC (mg/L)	DOC (mg/L)	Particulate Iron (mg Fe/L)	Salinity (psu)
201	1.57E-09	8.60	0.8	2	0.02	35.5
202	1.57E-09	8.60	0.8	2	0.2	26
203	1.57E-09	8.60	0.8	2	0.2	30
204	1.57E-09	8.60	0.8	2	0.2	35.5
205	1.57E-09	8.60	0.8	2	3	26
206	1.57E-09	8.60	0.8	2	3	30
207	1.57E-09	8.60	0.8	2	3	35.5
208	1.57E-09	8.60	0.8	4	0.02	26
209	1.57E-09	8.60	0.8	4	0.02	30
210	1.57E-09	8.60	0.8	4	0.02	35.5
211	1.57E-09	8.60	0.8	4	0.2	26
212	1.57E-09	8.60	0.8	4	0.2	30
213	1.57E-09	8.60	0.8	4	0.2	35.5
214	1.57E-09	8.60	0.8	4	3	26
215	1.57E-09	8.60	0.8	4	3	30
216	1.57E-09	8.60	0.8	4	3	35.5
217	1.57E-09	8.60	7	1	0.02	26
218	1.57E-09	8.60	7	1	0.02	30
219	1.57E-09	8.60	7	1	0.02	35.5
220	1.57E-09	8.60	7	1	0.2	26
221	1.57E-09	8.60	7	1	0.2	30
222	1.57E-09	8.60	7	1	0.2	35.5
223	1.57E-09	8.60	7	1	3	26
224	1.57E-09	8.60	7	1	3	30
225	1.57E-09	8.60	7	1	3	35.5
226	1.57E-09	8.60	7	2	0.02	26
227	1.57E-09	8.60	7	2	0.02	30
228	1.57E-09	8.60	7	2	0.02	35.5
229	1.57E-09	8.60	7	2	0.2	26
230	1.57E-09	8.60	7	2	0.2	30
231	1.57E-09	8.60	7	2	0.2	35.5
232	1.57E-09	8.60	7	2	3	26
233	1.57E-09	8.60	7	2	3	30
234	1.57E-09	8.60	7	2	3	35.5
235	1.57E-09	8.60	7	4	0.02	26
236	1.57E-09	8.60	7	4	0.02	30
237	1.57E-09	8.60	7	4	0.02	35.5
238	1.57E-09	8.60	7	4	0.2	26
239	1.57E-09	8.60	7	4	0.2	30
240	1.57E-09	8.60	7	4	0.2	35.5
241	1.57E-09	8.60	7	4	3	26
242	1.57E-09	8.60	7	4	3	30
243	1.57E-09	8.60	7	4	3	35.5
244	4.72E-08	7.90	0.05	1	0.02	26
245	4.72E-08	7.90	0.05	1	0.02	30
246	4.72E-08	7.90	0.05	1	0.02	35.5
247	4.72E-08	7.90	0.05	1	0.2	26
248	4.72E-08	7.90	0.05	1	0.2	30
249	4.72E-08	7.90	0.05	1	0.2	35.5
250	4.72E-08	7.90	0.05	1	3	26

STATE VARIABLES FOR MODEL INPUT						
Input Number	Total Cu (mol/L)	pH	POC (mg/L)	DOC (mg/L)	Particulate Iron (mg Fe/L)	Salinity (psu)
251	4.72E-08	7.90	0.05	1	3	30
252	4.72E-08	7.90	0.05	1	3	35.5
253	4.72E-08	7.90	0.05	2	0.02	26
254	4.72E-08	7.90	0.05	2	0.02	30
255	4.72E-08	7.90	0.05	2	0.02	35.5
256	4.72E-08	7.90	0.05	2	0.2	26
257	4.72E-08	7.90	0.05	2	0.2	30
258	4.72E-08	7.90	0.05	2	0.2	35.5
259	4.72E-08	7.90	0.05	2	3	26
260	4.72E-08	7.90	0.05	2	3	30
261	4.72E-08	7.90	0.05	2	3	35.5
262	4.72E-08	7.90	0.05	4	0.02	26
263	4.72E-08	7.90	0.05	4	0.02	30
264	4.72E-08	7.90	0.05	4	0.02	35.5
265	4.72E-08	7.90	0.05	4	0.2	26
266	4.72E-08	7.90	0.05	4	0.2	30
267	4.72E-08	7.90	0.05	4	0.2	35.5
268	4.72E-08	7.90	0.05	4	3	26
269	4.72E-08	7.90	0.05	4	3	30
270	4.72E-08	7.90	0.05	4	3	35.5
271	4.72E-08	7.90	0.8	1	0.02	26
272	4.72E-08	7.90	0.8	1	0.02	30
273	4.72E-08	7.90	0.8	1	0.02	35.5
274	4.72E-08	7.90	0.8	1	0.2	26
275	4.72E-08	7.90	0.8	1	0.2	30
276	4.72E-08	7.90	0.8	1	0.2	35.5
277	4.72E-08	7.90	0.8	1	3	26
278	4.72E-08	7.90	0.8	1	3	30
279	4.72E-08	7.90	0.8	1	3	35.5
280	4.72E-08	7.90	0.8	2	0.02	26
281	4.72E-08	7.90	0.8	2	0.02	30
282	4.72E-08	7.90	0.8	2	0.02	35.5
283	4.72E-08	7.90	0.8	2	0.2	26
284	4.72E-08	7.90	0.8	2	0.2	30
285	4.72E-08	7.90	0.8	2	0.2	35.5
286	4.72E-08	7.90	0.8	2	3	26
287	4.72E-08	7.90	0.8	2	3	30
288	4.72E-08	7.90	0.8	2	3	35.5
289	4.72E-08	7.90	0.8	4	0.02	26
290	4.72E-08	7.90	0.8	4	0.02	30
291	4.72E-08	7.90	0.8	4	0.02	35.5
292	4.72E-08	7.90	0.8	4	0.2	26
293	4.72E-08	7.90	0.8	4	0.2	30
294	4.72E-08	7.90	0.8	4	0.2	35.5
295	4.72E-08	7.90	0.8	4	3	26
296	4.72E-08	7.90	0.8	4	3	30
297	4.72E-08	7.90	0.8	4	3	35.5
298	4.72E-08	7.90	7	1	0.02	26
299	4.72E-08	7.90	7	1	0.02	30
300	4.72E-08	7.90	7	1	0.02	35.5

STATE VARIABLES FOR MODEL INPUT						
Input Number	Total Cu (mol/L)	pH	POC (mg/L)	DOC (mg/L)	Particulate Iron (mg Fe/L)	Salinity (psu)
301	4.72E-08	7.90	7	1	0.2	26
302	4.72E-08	7.90	7	1	0.2	30
303	4.72E-08	7.90	7	1	0.2	35.5
304	4.72E-08	7.90	7	1	3	26
305	4.72E-08	7.90	7	1	3	30
306	4.72E-08	7.90	7	1	3	35.5
307	4.72E-08	7.90	7	2	0.02	26
308	4.72E-08	7.90	7	2	0.02	30
309	4.72E-08	7.90	7	2	0.02	35.5
310	4.72E-08	7.90	7	2	0.2	26
311	4.72E-08	7.90	7	2	0.2	30
312	4.72E-08	7.90	7	2	0.2	35.5
313	4.72E-08	7.90	7	2	3	26
314	4.72E-08	7.90	7	2	3	30
315	4.72E-08	7.90	7	2	3	35.5
316	4.72E-08	7.90	7	4	0.02	26
317	4.72E-08	7.90	7	4	0.02	30
318	4.72E-08	7.90	7	4	0.02	35.5
319	4.72E-08	7.90	7	4	0.2	26
320	4.72E-08	7.90	7	4	0.2	30
321	4.72E-08	7.90	7	4	0.2	35.5
322	4.72E-08	7.90	7	4	3	26
323	4.72E-08	7.90	7	4	3	30
324	4.72E-08	7.90	7	4	3	35.5
325	4.72E-08	8.25	0.05	1	0.02	26
326	4.72E-08	8.25	0.05	1	0.02	30
327	4.72E-08	8.25	0.05	1	0.02	35.5
328	4.72E-08	8.25	0.05	1	0.2	26
329	4.72E-08	8.25	0.05	1	0.2	30
330	4.72E-08	8.25	0.05	1	0.2	35.5
331	4.72E-08	8.25	0.05	1	3	26
332	4.72E-08	8.25	0.05	1	3	30
333	4.72E-08	8.25	0.05	1	3	35.5
334	4.72E-08	8.25	0.05	2	0.02	26
335	4.72E-08	8.25	0.05	2	0.02	30
336	4.72E-08	8.25	0.05	2	0.02	35.5
337	4.72E-08	8.25	0.05	2	0.2	26
338	4.72E-08	8.25	0.05	2	0.2	30
339	4.72E-08	8.25	0.05	2	0.2	35.5
340	4.72E-08	8.25	0.05	2	3	26
341	4.72E-08	8.25	0.05	2	3	30
342	4.72E-08	8.25	0.05	2	3	35.5
343	4.72E-08	8.25	0.05	4	0.02	26
344	4.72E-08	8.25	0.05	4	0.02	30
345	4.72E-08	8.25	0.05	4	0.02	35.5
346	4.72E-08	8.25	0.05	4	0.2	26
347	4.72E-08	8.25	0.05	4	0.2	30
348	4.72E-08	8.25	0.05	4	0.2	35.5
349	4.72E-08	8.25	0.05	4	3	26
350	4.72E-08	8.25	0.05	4	3	30

STATE VARIABLES FOR MODEL INPUT						
Input Number	Total Cu (mol/L)	pH	POC (mg/L)	DOC (mg/L)	Particulate Iron (mg Fe/L)	Salinity (psu)
351	4.72E-08	8.25	0.05	4	3	35.5
352	4.72E-08	8.25	0.8	1	0.02	26
353	4.72E-08	8.25	0.8	1	0.02	30
354	4.72E-08	8.25	0.8	1	0.02	35.5
355	4.72E-08	8.25	0.8	1	0.2	26
356	4.72E-08	8.25	0.8	1	0.2	30
357	4.72E-08	8.25	0.8	1	0.2	35.5
358	4.72E-08	8.25	0.8	1	3	26
359	4.72E-08	8.25	0.8	1	3	30
360	4.72E-08	8.25	0.8	1	3	35.5
361	4.72E-08	8.25	0.8	2	0.02	26
362	4.72E-08	8.25	0.8	2	0.02	30
363	4.72E-08	8.25	0.8	2	0.02	35.5
364	4.72E-08	8.25	0.8	2	0.2	26
365	4.72E-08	8.25	0.8	2	0.2	30
366	4.72E-08	8.25	0.8	2	0.2	35.5
367	4.72E-08	8.25	0.8	2	3	26
368	4.72E-08	8.25	0.8	2	3	30
369	4.72E-08	8.25	0.8	2	3	35.5
370	4.72E-08	8.25	0.8	4	0.02	26
371	4.72E-08	8.25	0.8	4	0.02	30
372	4.72E-08	8.25	0.8	4	0.02	35.5
373	4.72E-08	8.25	0.8	4	0.2	26
374	4.72E-08	8.25	0.8	4	0.2	30
375	4.72E-08	8.25	0.8	4	0.2	35.5
376	4.72E-08	8.25	0.8	4	3	26
377	4.72E-08	8.25	0.8	4	3	30
378	4.72E-08	8.25	0.8	4	3	35.5
379	4.72E-08	8.25	7	1	0.02	26
380	4.72E-08	8.25	7	1	0.02	30
381	4.72E-08	8.25	7	1	0.02	35.5
382	4.72E-08	8.25	7	1	0.2	26
383	4.72E-08	8.25	7	1	0.2	30
384	4.72E-08	8.25	7	1	0.2	35.5
385	4.72E-08	8.25	7	1	3	26
386	4.72E-08	8.25	7	1	3	30
387	4.72E-08	8.25	7	1	3	35.5
388	4.72E-08	8.25	7	2	0.02	26
389	4.72E-08	8.25	7	2	0.02	30
390	4.72E-08	8.25	7	2	0.02	35.5
391	4.72E-08	8.25	7	2	0.2	26
392	4.72E-08	8.25	7	2	0.2	30
393	4.72E-08	8.25	7	2	0.2	35.5
394	4.72E-08	8.25	7	2	3	26
395	4.72E-08	8.25	7	2	3	30
396	4.72E-08	8.25	7	2	3	35.5
397	4.72E-08	8.25	7	4	0.02	26
398	4.72E-08	8.25	7	4	0.02	30
399	4.72E-08	8.25	7	4	0.02	35.5
400	4.72E-08	8.25	7	4	0.2	26

STATE VARIABLES FOR MODEL INPUT						
Input Number	Total Cu (mol/L)	pH	POC (mg/L)	DOC (mg/L)	Particulate Iron (mg Fe/L)	Salinity (psu)
401	4.72E-08	8.25	7	4	0.2	30
402	4.72E-08	8.25	7	4	0.2	35.5
403	4.72E-08	8.25	7	4	3	26
404	4.72E-08	8.25	7	4	3	30
405	4.72E-08	8.25	7	4	3	35.5
406	4.72E-08	8.60	0.05	1	0.02	26
407	4.72E-08	8.60	0.05	1	0.02	30
408	4.72E-08	8.60	0.05	1	0.02	35.5
409	4.72E-08	8.60	0.05	1	0.2	26
410	4.72E-08	8.60	0.05	1	0.2	30
411	4.72E-08	8.60	0.05	1	0.2	35.5
412	4.72E-08	8.60	0.05	1	3	26
413	4.72E-08	8.60	0.05	1	3	30
414	4.72E-08	8.60	0.05	1	3	35.5
415	4.72E-08	8.60	0.05	2	0.02	26
416	4.72E-08	8.60	0.05	2	0.02	30
417	4.72E-08	8.60	0.05	2	0.02	35.5
418	4.72E-08	8.60	0.05	2	0.2	26
419	4.72E-08	8.60	0.05	2	0.2	30
420	4.72E-08	8.60	0.05	2	0.2	35.5
421	4.72E-08	8.60	0.05	2	3	26
422	4.72E-08	8.60	0.05	2	3	30
423	4.72E-08	8.60	0.05	2	3	35.5
424	4.72E-08	8.60	0.05	4	0.02	26
425	4.72E-08	8.60	0.05	4	0.02	30
426	4.72E-08	8.60	0.05	4	0.02	35.5
427	4.72E-08	8.60	0.05	4	0.2	26
428	4.72E-08	8.60	0.05	4	0.2	30
429	4.72E-08	8.60	0.05	4	0.2	35.5
430	4.72E-08	8.60	0.05	4	3	26
431	4.72E-08	8.60	0.05	4	3	30
432	4.72E-08	8.60	0.05	4	3	35.5
433	4.72E-08	8.60	0.8	1	0.02	26
434	4.72E-08	8.60	0.8	1	0.02	30
435	4.72E-08	8.60	0.8	1	0.02	35.5
436	4.72E-08	8.60	0.8	1	0.2	26
437	4.72E-08	8.60	0.8	1	0.2	30
438	4.72E-08	8.60	0.8	1	0.2	35.5
439	4.72E-08	8.60	0.8	1	3	26
440	4.72E-08	8.60	0.8	1	3	30
441	4.72E-08	8.60	0.8	1	3	35.5
442	4.72E-08	8.60	0.8	2	0.02	26
443	4.72E-08	8.60	0.8	2	0.02	30
444	4.72E-08	8.60	0.8	2	0.02	35.5
445	4.72E-08	8.60	0.8	2	0.2	26
446	4.72E-08	8.60	0.8	2	0.2	30
447	4.72E-08	8.60	0.8	2	0.2	35.5
448	4.72E-08	8.60	0.8	2	3	26
449	4.72E-08	8.60	0.8	2	3	30
450	4.72E-08	8.60	0.8	2	3	35.5

STATE VARIABLES FOR MODEL INPUT						
Input Number	Total Cu (mol/L)	pH	POC (mg/L)	DOC (mg/L)	Particulate Iron (mg Fe/L)	Salinity (psu)
451	4.72E-08	8.60	0.8	4	0.02	26
452	4.72E-08	8.60	0.8	4	0.02	30
453	4.72E-08	8.60	0.8	4	0.02	35.5
454	4.72E-08	8.60	0.8	4	0.2	26
455	4.72E-08	8.60	0.8	4	0.2	30
456	4.72E-08	8.60	0.8	4	0.2	35.5
457	4.72E-08	8.60	0.8	4	3	26
458	4.72E-08	8.60	0.8	4	3	30
459	4.72E-08	8.60	0.8	4	3	35.5
460	4.72E-08	8.60	7	1	0.02	26
461	4.72E-08	8.60	7	1	0.02	30
462	4.72E-08	8.60	7	1	0.02	35.5
463	4.72E-08	8.60	7	1	0.2	26
464	4.72E-08	8.60	7	1	0.2	30
465	4.72E-08	8.60	7	1	0.2	35.5
466	4.72E-08	8.60	7	1	3	26
467	4.72E-08	8.60	7	1	3	30
468	4.72E-08	8.60	7	1	3	35.5
469	4.72E-08	8.60	7	2	0.02	26
470	4.72E-08	8.60	7	2	0.02	30
471	4.72E-08	8.60	7	2	0.02	35.5
472	4.72E-08	8.60	7	2	0.2	26
473	4.72E-08	8.60	7	2	0.2	30
474	4.72E-08	8.60	7	2	0.2	35.5
475	4.72E-08	8.60	7	2	3	26
476	4.72E-08	8.60	7	2	3	30
477	4.72E-08	8.60	7	2	3	35.5
478	4.72E-08	8.60	7	4	0.02	26
479	4.72E-08	8.60	7	4	0.02	30
480	4.72E-08	8.60	7	4	0.02	35.5
481	4.72E-08	8.60	7	4	0.2	26
482	4.72E-08	8.60	7	4	0.2	30
483	4.72E-08	8.60	7	4	0.2	35.5
484	4.72E-08	8.60	7	4	3	26
485	4.72E-08	8.60	7	4	3	30
486	4.72E-08	8.60	7	4	3	35.5
487	5.67E-07	7.90	0.05	1	0.02	26
488	5.67E-07	7.90	0.05	1	0.02	30
489	5.67E-07	7.90	0.05	1	0.02	35.5
490	5.67E-07	7.90	0.05	1	0.2	26
491	5.67E-07	7.90	0.05	1	0.2	30
492	5.67E-07	7.90	0.05	1	0.2	35.5
493	5.67E-07	7.90	0.05	1	3	26
494	5.67E-07	7.90	0.05	1	3	30
495	5.67E-07	7.90	0.05	1	3	35.5
496	5.67E-07	7.90	0.05	2	0.02	26
497	5.67E-07	7.90	0.05	2	0.02	30
498	5.67E-07	7.90	0.05	2	0.02	35.5
499	5.67E-07	7.90	0.05	2	0.2	26
500	5.67E-07	7.90	0.05	2	0.2	30

STATE VARIABLES FOR MODEL INPUT						
Input Number	Total Cu (mol/L)	pH	POC (mg/L)	DOC (mg/L)	Particulate Iron (mg Fe/L)	Salinity (psu)
501	5.67E-07	7.90	0.05	2	0.2	35.5
502	5.67E-07	7.90	0.05	2	3	26
503	5.67E-07	7.90	0.05	2	3	30
504	5.67E-07	7.90	0.05	2	3	35.5
505	5.67E-07	7.90	0.05	4	0.02	26
506	5.67E-07	7.90	0.05	4	0.02	30
507	5.67E-07	7.90	0.05	4	0.02	35.5
508	5.67E-07	7.90	0.05	4	0.2	26
509	5.67E-07	7.90	0.05	4	0.2	30
510	5.67E-07	7.90	0.05	4	0.2	35.5
511	5.67E-07	7.90	0.05	4	3	26
512	5.67E-07	7.90	0.05	4	3	30
513	5.67E-07	7.90	0.05	4	3	35.5
514	5.67E-07	7.90	0.8	1	0.02	26
515	5.67E-07	7.90	0.8	1	0.02	30
516	5.67E-07	7.90	0.8	1	0.02	35.5
517	5.67E-07	7.90	0.8	1	0.2	26
518	5.67E-07	7.90	0.8	1	0.2	30
519	5.67E-07	7.90	0.8	1	0.2	35.5
520	5.67E-07	7.90	0.8	1	3	26
521	5.67E-07	7.90	0.8	1	3	30
522	5.67E-07	7.90	0.8	1	3	35.5
523	5.67E-07	7.90	0.8	2	0.02	26
524	5.67E-07	7.90	0.8	2	0.02	30
525	5.67E-07	7.90	0.8	2	0.02	35.5
526	5.67E-07	7.90	0.8	2	0.2	26
527	5.67E-07	7.90	0.8	2	0.2	30
528	5.67E-07	7.90	0.8	2	0.2	35.5
529	5.67E-07	7.90	0.8	2	3	26
530	5.67E-07	7.90	0.8	2	3	30
531	5.67E-07	7.90	0.8	2	3	35.5
532	5.67E-07	7.90	0.8	4	0.02	26
533	5.67E-07	7.90	0.8	4	0.02	30
534	5.67E-07	7.90	0.8	4	0.02	35.5
535	5.67E-07	7.90	0.8	4	0.2	26
536	5.67E-07	7.90	0.8	4	0.2	30
537	5.67E-07	7.90	0.8	4	0.2	35.5
538	5.67E-07	7.90	0.8	4	3	26
539	5.67E-07	7.90	0.8	4	3	30
540	5.67E-07	7.90	0.8	4	3	35.5
541	5.67E-07	7.90	7	1	0.02	26
542	5.67E-07	7.90	7	1	0.02	30
543	5.67E-07	7.90	7	1	0.02	35.5
544	5.67E-07	7.90	7	1	0.2	26
545	5.67E-07	7.90	7	1	0.2	30
546	5.67E-07	7.90	7	1	0.2	35.5
547	5.67E-07	7.90	7	1	3	26
548	5.67E-07	7.90	7	1	3	30
549	5.67E-07	7.90	7	1	3	35.5
550	5.67E-07	7.90	7	2	0.02	26

STATE VARIABLES FOR MODEL INPUT						
Input Number	Total Cu (mol/L)	pH	POC (mg/L)	DOC (mg/L)	Particulate Iron (mg Fe/L)	Salinity (psu)
551	5.67E-07	7.90	7	2	0.02	30
552	5.67E-07	7.90	7	2	0.02	35.5
553	5.67E-07	7.90	7	2	0.2	26
554	5.67E-07	7.90	7	2	0.2	30
555	5.67E-07	7.90	7	2	0.2	35.5
556	5.67E-07	7.90	7	2	3	26
557	5.67E-07	7.90	7	2	3	30
558	5.67E-07	7.90	7	2	3	35.5
559	5.67E-07	7.90	7	4	0.02	26
560	5.67E-07	7.90	7	4	0.02	30
561	5.67E-07	7.90	7	4	0.02	35.5
562	5.67E-07	7.90	7	4	0.2	26
563	5.67E-07	7.90	7	4	0.2	30
564	5.67E-07	7.90	7	4	0.2	35.5
565	5.67E-07	7.90	7	4	3	26
566	5.67E-07	7.90	7	4	3	30
567	5.67E-07	7.90	7	4	3	35.5
568	5.67E-07	8.25	0.05	1	0.02	26
569	5.67E-07	8.25	0.05	1	0.02	30
570	5.67E-07	8.25	0.05	1	0.02	35.5
571	5.67E-07	8.25	0.05	1	0.2	26
572	5.67E-07	8.25	0.05	1	0.2	30
573	5.67E-07	8.25	0.05	1	0.2	35.5
574	5.67E-07	8.25	0.05	1	3	26
575	5.67E-07	8.25	0.05	1	3	30
576	5.67E-07	8.25	0.05	1	3	35.5
577	5.67E-07	8.25	0.05	2	0.02	26
578	5.67E-07	8.25	0.05	2	0.02	30
579	5.67E-07	8.25	0.05	2	0.02	35.5
580	5.67E-07	8.25	0.05	2	0.2	26
581	5.67E-07	8.25	0.05	2	0.2	30
582	5.67E-07	8.25	0.05	2	0.2	35.5
583	5.67E-07	8.25	0.05	2	3	26
584	5.67E-07	8.25	0.05	2	3	30
585	5.67E-07	8.25	0.05	2	3	35.5
586	5.67E-07	8.25	0.05	4	0.02	26
587	5.67E-07	8.25	0.05	4	0.02	30
588	5.67E-07	8.25	0.05	4	0.02	35.5
589	5.67E-07	8.25	0.05	4	0.2	26
590	5.67E-07	8.25	0.05	4	0.2	30
591	5.67E-07	8.25	0.05	4	0.2	35.5
592	5.67E-07	8.25	0.05	4	3	26
593	5.67E-07	8.25	0.05	4	3	30
594	5.67E-07	8.25	0.05	4	3	35.5
595	5.67E-07	8.25	0.8	1	0.02	26
596	5.67E-07	8.25	0.8	1	0.02	30
597	5.67E-07	8.25	0.8	1	0.02	35.5
598	5.67E-07	8.25	0.8	1	0.2	26
599	5.67E-07	8.25	0.8	1	0.2	30
600	5.67E-07	8.25	0.8	1	0.2	35.5

STATE VARIABLES FOR MODEL INPUT						
Input Number	Total Cu (mol/L)	pH	POC (mg/L)	DOC (mg/L)	Particulate Iron (mg Fe/L)	Salinity (psu)
601	5.67E-07	8.25	0.8	1	3	26
602	5.67E-07	8.25	0.8	1	3	30
603	5.67E-07	8.25	0.8	1	3	35.5
604	5.67E-07	8.25	0.8	2	0.02	26
605	5.67E-07	8.25	0.8	2	0.02	30
606	5.67E-07	8.25	0.8	2	0.02	35.5
607	5.67E-07	8.25	0.8	2	0.2	26
608	5.67E-07	8.25	0.8	2	0.2	30
609	5.67E-07	8.25	0.8	2	0.2	35.5
610	5.67E-07	8.25	0.8	2	3	26
611	5.67E-07	8.25	0.8	2	3	30
612	5.67E-07	8.25	0.8	2	3	35.5
613	5.67E-07	8.25	0.8	4	0.02	26
614	5.67E-07	8.25	0.8	4	0.02	30
615	5.67E-07	8.25	0.8	4	0.02	35.5
616	5.67E-07	8.25	0.8	4	0.2	26
617	5.67E-07	8.25	0.8	4	0.2	30
618	5.67E-07	8.25	0.8	4	0.2	35.5
619	5.67E-07	8.25	0.8	4	3	26
620	5.67E-07	8.25	0.8	4	3	30
621	5.67E-07	8.25	0.8	4	3	35.5
622	5.67E-07	8.25	7	1	0.02	26
623	5.67E-07	8.25	7	1	0.02	30
624	5.67E-07	8.25	7	1	0.02	35.5
625	5.67E-07	8.25	7	1	0.2	26
626	5.67E-07	8.25	7	1	0.2	30
627	5.67E-07	8.25	7	1	0.2	35.5
628	5.67E-07	8.25	7	1	3	26
629	5.67E-07	8.25	7	1	3	30
630	5.67E-07	8.25	7	1	3	35.5
631	5.67E-07	8.25	7	2	0.02	26
632	5.67E-07	8.25	7	2	0.02	30
633	5.67E-07	8.25	7	2	0.02	35.5
634	5.67E-07	8.25	7	2	0.2	26
635	5.67E-07	8.25	7	2	0.2	30
636	5.67E-07	8.25	7	2	0.2	35.5
637	5.67E-07	8.25	7	2	3	26
638	5.67E-07	8.25	7	2	3	30
639	5.67E-07	8.25	7	2	3	35.5
640	5.67E-07	8.25	7	4	0.02	26
641	5.67E-07	8.25	7	4	0.02	30
642	5.67E-07	8.25	7	4	0.02	35.5
643	5.67E-07	8.25	7	4	0.2	26
644	5.67E-07	8.25	7	4	0.2	30
645	5.67E-07	8.25	7	4	0.2	35.5
646	5.67E-07	8.25	7	4	3	26
647	5.67E-07	8.25	7	4	3	30
648	5.67E-07	8.25	7	4	3	35.5
649	5.67E-07	8.60	0.05	1	0.02	26
650	5.67E-07	8.60	0.05	1	0.02	30

STATE VARIABLES FOR MODEL INPUT						
Input Number	Total Cu (mol/L)	pH	POC (mg/L)	DOC (mg/L)	Particulate Iron (mg Fe/L)	Salinity (psu)
651	5.67E-07	8.60	0.05	1	0.02	35.5
652	5.67E-07	8.60	0.05	1	0.2	26
653	5.67E-07	8.60	0.05	1	0.2	30
654	5.67E-07	8.60	0.05	1	0.2	35.5
655	5.67E-07	8.60	0.05	1	3	26
656	5.67E-07	8.60	0.05	1	3	30
657	5.67E-07	8.60	0.05	1	3	35.5
658	5.67E-07	8.60	0.05	2	0.02	26
659	5.67E-07	8.60	0.05	2	0.02	30
660	5.67E-07	8.60	0.05	2	0.02	35.5
661	5.67E-07	8.60	0.05	2	0.2	26
662	5.67E-07	8.60	0.05	2	0.2	30
663	5.67E-07	8.60	0.05	2	0.2	35.5
664	5.67E-07	8.60	0.05	2	3	26
665	5.67E-07	8.60	0.05	2	3	30
666	5.67E-07	8.60	0.05	2	3	35.5
667	5.67E-07	8.60	0.05	4	0.02	26
668	5.67E-07	8.60	0.05	4	0.02	30
669	5.67E-07	8.60	0.05	4	0.02	35.5
670	5.67E-07	8.60	0.05	4	0.2	26
671	5.67E-07	8.60	0.05	4	0.2	30
672	5.67E-07	8.60	0.05	4	0.2	35.5
673	5.67E-07	8.60	0.05	4	3	26
674	5.67E-07	8.60	0.05	4	3	30
675	5.67E-07	8.60	0.05	4	3	35.5
676	5.67E-07	8.60	0.8	1	0.02	26
677	5.67E-07	8.60	0.8	1	0.02	30
678	5.67E-07	8.60	0.8	1	0.02	35.5
679	5.67E-07	8.60	0.8	1	0.2	26
680	5.67E-07	8.60	0.8	1	0.2	30
681	5.67E-07	8.60	0.8	1	0.2	35.5
682	5.67E-07	8.60	0.8	1	3	26
683	5.67E-07	8.60	0.8	1	3	30
684	5.67E-07	8.60	0.8	1	3	35.5
685	5.67E-07	8.60	0.8	2	0.02	26
686	5.67E-07	8.60	0.8	2	0.02	30
687	5.67E-07	8.60	0.8	2	0.02	35.5
688	5.67E-07	8.60	0.8	2	0.2	26
689	5.67E-07	8.60	0.8	2	0.2	30
690	5.67E-07	8.60	0.8	2	0.2	35.5
691	5.67E-07	8.60	0.8	2	3	26
692	5.67E-07	8.60	0.8	2	3	30
693	5.67E-07	8.60	0.8	2	3	35.5
694	5.67E-07	8.60	0.8	4	0.02	26
695	5.67E-07	8.60	0.8	4	0.02	30
696	5.67E-07	8.60	0.8	4	0.02	35.5
697	5.67E-07	8.60	0.8	4	0.2	26
698	5.67E-07	8.60	0.8	4	0.2	30
699	5.67E-07	8.60	0.8	4	0.2	35.5
700	5.67E-07	8.60	0.8	4	3	26

STATE VARIABLES FOR MODEL INPUT						
Input Number	Total Cu (mol/L)	pH	POC (mg/L)	DOC (mg/L)	Particulate Iron (mg Fe/L)	Salinity (psu)
701	5.67E-07	8.60	0.8	4	3	30
702	5.67E-07	8.60	0.8	4	3	35.5
703	5.67E-07	8.60	7	1	0.02	26
704	5.67E-07	8.60	7	1	0.02	30
705	5.67E-07	8.60	7	1	0.02	35.5
706	5.67E-07	8.60	7	1	0.2	26
707	5.67E-07	8.60	7	1	0.2	30
708	5.67E-07	8.60	7	1	0.2	35.5
709	5.67E-07	8.60	7	1	3	26
710	5.67E-07	8.60	7	1	3	30
711	5.67E-07	8.60	7	1	3	35.5
712	5.67E-07	8.60	7	2	0.02	26
713	5.67E-07	8.60	7	2	0.02	30
714	5.67E-07	8.60	7	2	0.02	35.5
715	5.67E-07	8.60	7	2	0.2	26
716	5.67E-07	8.60	7	2	0.2	30
717	5.67E-07	8.60	7	2	0.2	35.5
718	5.67E-07	8.60	7	2	3	26
719	5.67E-07	8.60	7	2	3	30
720	5.67E-07	8.60	7	2	3	35.5
721	5.67E-07	8.60	7	4	0.02	26
722	5.67E-07	8.60	7	4	0.02	30
723	5.67E-07	8.60	7	4	0.02	35.5
724	5.67E-07	8.60	7	4	0.2	26
725	5.67E-07	8.60	7	4	0.2	30
726	5.67E-07	8.60	7	4	0.2	35.5
727	5.67E-07	8.60	7	4	3	26
728	5.67E-07	8.60	7	4	3	30
729	5.67E-07	8.60	7	4	3	35.5

WHAM7 INPUT																					WHAM7 OUTPUT	
Description	SPM (g/L)	Temp (K)	pCO2 (atm)	pH	Part HA (g/L)	Part FA (g/L)	Part FeOx (g/L)	Coll HA (g/L)	Coll FA (g/L)	Na (M)	Mg (M)	{Al3+} (M)	K (M)	Ca (M)	{Fe3+} (M)	Tot Cu (M)	Cl (M)	SO4 (M)	CO3 (M)	logKo* = log(Ko x TSS) (dimensionless)	Fract. Part. (dimensionless)	
1	1000	298.15	---	7.90	5.00E-05	5.00E-05	1.29E-05	0.00E+00	1.36E-03	3.48E-01	3.96E-02	6.31E-16	7.58E-03	7.66E-03	1.82E-19	1.57E-09	4.05E-01	2.10E-02	1.99E-03	-1.01	0.089	
2	1000	298.15	---	7.90	5.00E-05	5.00E-05	1.29E-05	0.00E+00	1.36E-03	4.01E-01	4.56E-02	6.31E-16	8.75E-03	8.79E-03	1.82E-19	1.57E-09	4.67E-01	2.42E-02	2.16E-03	-1.02	0.088	
3	1000	298.15	---	7.90	5.00E-05	5.00E-05	1.29E-05	0.00E+00	1.36E-03	4.75E-01	5.40E-02	6.31E-16	1.03E-02	1.03E-02	1.82E-19	1.57E-09	5.53E-01	2.86E-02	2.40E-03	-1.02	0.087	
4	1000	298.15	---	7.90	5.00E-05	5.00E-05	1.29E-04	0.00E+00	1.36E-03	3.48E-01	3.96E-02	6.31E-16	7.58E-03	7.66E-03	1.82E-19	1.57E-09	4.05E-01	2.10E-02	1.99E-03	-0.87	0.119	
5	1000	298.15	---	7.90	5.00E-05	5.00E-05	1.29E-04	0.00E+00	1.36E-03	4.01E-01	4.56E-02	6.31E-16	8.75E-03	8.79E-03	1.82E-19	1.57E-09	4.67E-01	2.42E-02	2.16E-03	-0.87	0.118	
6	1000	298.15	---	7.90	5.00E-05	5.00E-05	1.29E-04	0.00E+00	1.36E-03	4.75E-01	5.40E-02	6.31E-16	1.03E-02	1.03E-02	1.82E-19	1.57E-09	5.53E-01	2.86E-02	2.40E-03	-0.88	0.116	
7	1000	298.15	---	7.90	5.00E-05	5.00E-05	1.93E-03	0.00E+00	1.36E-03	3.48E-01	3.96E-02	6.31E-16	7.58E-03	7.66E-03	1.82E-19	1.57E-09	4.05E-01	2.10E-02	1.99E-03	-0.14	0.418	
8	1000	298.15	---	7.90	5.00E-05	5.00E-05	1.93E-03	0.00E+00	1.36E-03	4.01E-01	4.56E-02	6.31E-16	8.75E-03	8.79E-03	1.82E-19	1.57E-09	4.67E-01	2.42E-02	2.16E-03	-0.15	0.415	
9	1000	298.15	---	7.90	5.00E-05	5.00E-05	1.93E-03	0.00E+00	1.36E-03	4.75E-01	5.40E-02	6.31E-16	1.03E-02	1.03E-02	1.82E-19	1.57E-09	5.53E-01	2.86E-02	2.40E-03	-0.16	0.411	
10	1000	298.15	---	7.90	5.00E-05	5.00E-05	1.29E-05	0.00E+00	2.72E-03	3.48E-01	3.96E-02	6.31E-16	7.58E-03	7.66E-03	1.82E-19	1.57E-09	4.05E-01	2.10E-02	1.99E-03	-1.30	0.048	
11	1000	298.15	---	7.90	5.00E-05	5.00E-05	1.29E-05	0.00E+00	2.72E-03	4.01E-01	4.56E-02	6.31E-16	8.75E-03	8.79E-03	1.82E-19	1.57E-09	4.67E-01	2.42E-02	2.16E-03	-1.31	0.047	
12	1000	298.15	---	7.90	5.00E-05	5.00E-05	1.29E-05	0.00E+00	2.72E-03	4.75E-01	5.40E-02	6.31E-16	1.03E-02	1.03E-02	1.82E-19	1.57E-09	5.53E-01	2.86E-02	2.40E-03	-1.31	0.046	
13	1000	298.15	---	7.90	5.00E-05	5.00E-05	1.29E-04	0.00E+00	2.72E-03	3.48E-01	3.96E-02	6.31E-16	7.58E-03	7.66E-03	1.82E-19	1.57E-09	4.05E-01	2.10E-02	1.99E-03	-1.16	0.065	
14	1000	298.15	---	7.90	5.00E-05	5.00E-05	1.29E-04	0.00E+00	2.72E-03	4.01E-01	4.56E-02	6.31E-16	8.75E-03	8.79E-03	1.82E-19	1.57E-09	4.67E-01	2.42E-02	2.16E-03	-1.17	0.064	
15	1000	298.15	---	7.90	5.00E-05	5.00E-05	1.29E-04	0.00E+00	2.72E-03	4.75E-01	5.40E-02	6.31E-16	1.03E-02	1.03E-02	1.82E-19	1.57E-09	5.53E-01	2.86E-02	2.40E-			

63	1000	298.15	---	7.90	7.00E-03	7.00E-03	1.93E-03	0.00E+00	1.36E-03	4.75E-01	5.40E-02	6.31E-16	1.03E-02	1.03E-02	1.82E-19	1.57E-09	5.53E-01	2.86E-02	2.40E-03	1.13	0.931
----	------	--------	-----	------	----------	----------	----------	----------	----------	----------	----------	----------	----------	----------	----------	----------	----------	----------	----------	------	-------

Task 3a and 3c Supplemental Material:

The proposed sample design for collection of background and resuspended information is shown in **Error! Reference source not found.** The metals of interest and the analytical methods used for quantification are listed below.**Error! Reference source not found.**

Table A-22. Number and type of analytical samples.

Task	Matrix	Location	Number of Sites	Analytes	Fractions
Background levels	Water	Resuspension site mid-depth	3	Metal ¹ and organic CoCs	Total and dissolved
	Sediment	Resuspension site surface sediments	3	Metal and organic CoCs	Total, sand, silt, clay
Plume levels	Water	Plume surface	Site & event dependent	Metal and organic CoCs	Total, sand, silt, clay, dissolved
	Water	Plume mid-depth	Site & event dependent	Metal and organic CoCs	Total, sand, silt, clay, dissolved

Table A-221. Metal analysis in seawater samples. Method is the “title” suggested by USEPA.

Metal	Method	Matrix	Digestion	MRL	MDL	Units
Arsenic	200.8 / 6020	Seawater	Q-HNO ₃ pH ≤2.	0.5	0.04	µg/L
Cadmium	200.8 / 6020	Seawater	Q-HNO ₃ pH ≤2.	0.02	0.002	µg/L
Chromium	200.8 / 6020	Seawater	Q-HNO ₃ pH ≤2	0.2	0.03	µg/L
Copper	200.8 / 6020	Seawater	Q-HNO ₃ pH ≤2	0.1	0.004	µg/L
Lead	200.8 / 6020	Seawater	Q-HNO ₃ pH ≤2	0.02	0.009	µg/L
Nickel	200.8 / 6020	Seawater	Q-HNO ₃ pH ≤2	0.2	0.04	µg/L
Silver	200.8 / 6020	Seawater	Q-HNO ₃ pH ≤2	0.02	0.004	µg/L
Zinc	200.8 / 6020	Seawater	Q-HNO ₃ pH ≤2	0.5	0.06	µg/L

Quality Assurance/Quality Control (QA/QC) for these quantifications is as follows. A duplicate sub-sample is obtained from a sample for each event. QA/QC for metal quantification includes calibration curves with correlation coefficients ≥0.999, blank every five samples with a concentration within ±10% of background, a standard reference material every five samples with a recovery of ±15% of certified concentration, a spiked sample per run with a recovery of ±15% of spiked concentration

Appendix B

List of Scientific/Technical Publications

Eggleston, ME. 2012. Impact of sediment resuspension events on the availability of heavy metals in freshwater sediments. *Master's Thesis*. University of Michigan, Ann Arbor, MI, USA.

Fetters, KJ. 2013. Investigation toxicology effects of short-term resuspension of metal-contaminated freshwater and marine sediments. *Master's Thesis*. University of Michigan, Ann Arbor, MI, USA.

**Appendix C: Draft Summary Report: Biological Effects Associated with Resuspension
from Propeller Wash at Navy Facilities**

Draft Summary Report

Biological Effects Associated with Resuspension from Propeller Wash at Navy Facilities

Summary

This study demonstrated a novel, practical use of *in situ* bioassay technology, in combination with laboratory bioassays, towards improved understanding of the short-term impacts of sediment resuspension events on surface water organisms. The project was a Modification to SERDP Project # ER-1746, "Predicting the Fate and Effects of Resuspended Metal Contaminated Sediments" to promote collaboration between this project and the two ESTCP projects led by PF Wang and Gunther Rosen. *In situ* bioassays provided an integrated exposure of the sediment plumes over space and time, while concurrent laboratory tests were used to characterize toxic effects from discrete samples at specific points in space and time. Controlled resuspension of contaminated sediments was conducted using the propellers from tug boats at two heavily industrialized DoD harbors, San Diego Bay and Pearl Harbor, which followed deployment of *in situ* bioassays and collection of discrete samples in the resulting plume's path. Overall, very few adverse effects were observed both *in situ* and in the laboratory at both sites, which might be expected due to the short-term nature of the plume exposure. Toxicity that was observed, however, tended to be in samples that were associated with the highest suspended solids and total metal concentrations.

Introduction

This report summarizes the purpose, technical approach, and results associated with two field studies designed to provide realistic ecotoxicological data associated with sediment resuspension induced by propeller wash in DoD harbors. The study was conducted as a modification to SERDP Project # ER-1746, "Predicting the Fate and Effects of Resuspended Metal Contaminated Sediments", and was coordinated with scheduled field efforts being conducted under ESTCP Project #ER-201031, "Evaluation of Resuspension from Dredging, Extreme Storm Events, and Propeller Wash in DoD Harbors." The study involved deployment of *in situ* bioassays, specifically SEA Rings (developed under other SERDP and ESTCP projects), during scheduled tug boat propeller wash events at Naval Base San Diego and Naval Base Pearl Harbor.

The key objective of this study was to collect appropriate ecotoxicological data to supplement the fate and transport characterization of potential contaminants associated with sediment resuspension due to propeller wash. When combined with objectives from Projects ER-1746 and ER-201031, anticipated benefits of the study include: 1) improved understanding of resuspension effects due to propeller wash and its impact on water column organisms and bedded sediment in DoD harbors; 2) predictive capabilities to assess potential re-contamination of sediment remedial sites; 3) improved understanding of the bioavailability and toxicity of contaminants associated

with resuspended sediments; and 4) better information-based decision making in managing propeller wash induced sediment resuspension, transport and re-contamination potential.

Methods

Tracking and Sampling of Sediment Plume

The sample design involved collection of water samples from, and exposure of SEA Rings to, a tug-induced sediment plume, shown conceptually in Figure 1. A tug boat was moored adjacent to the quay wall between Piers 4 and 5 at NBSD (Figure 2) and approximately 22 pilings from the end of Bravo Pier at Pearl Harbor Naval Shipyard (Figure 3). Prior to the resuspension events, background water (15 foot depth) and sediment grab samples were collected at the site of resuspension for later characterization (e.g. chemical analysis and laboratory toxicity testing). The tugs operated their engines at an rpm (power) sufficient to produce a visible plume at the surface. The survey vessels were a C-14 Tractor and a slightly smaller Tiger tug at NBSD and Pearl Harbor, respectively. Both vessels have twin ducted propellers of approximately the same size. Both propellers are at the bottom of the boat with 360 degrees of rotation, and propellers were adjusted to make the rpm about the same during the two studies at San Diego Bay and Pearl Harbor.

At NBSD, a single controlled event of approximately 10 minutes occurred, while at Pearl Harbor three shorter resuspension events occurred (two for 90 seconds each followed by a third for 5-minutes). Samples were collected for sediment and water contaminant concentrations at the surface and mid-depth via a high volume pump. A subset of the mid-depth samples were used in laboratory toxicity tests. Survey boats tracked the plume via any visible surface expression, via real-time transmissometers attached at the ends of intake hoses, via acoustic return from the onboard ADCP, and via one of the principal investigator's (Dr. Pei-Fang Wang) own expectations of plume movement, based on CH3D hydrodynamic predictions. Samples were collected by crisscrossing over the

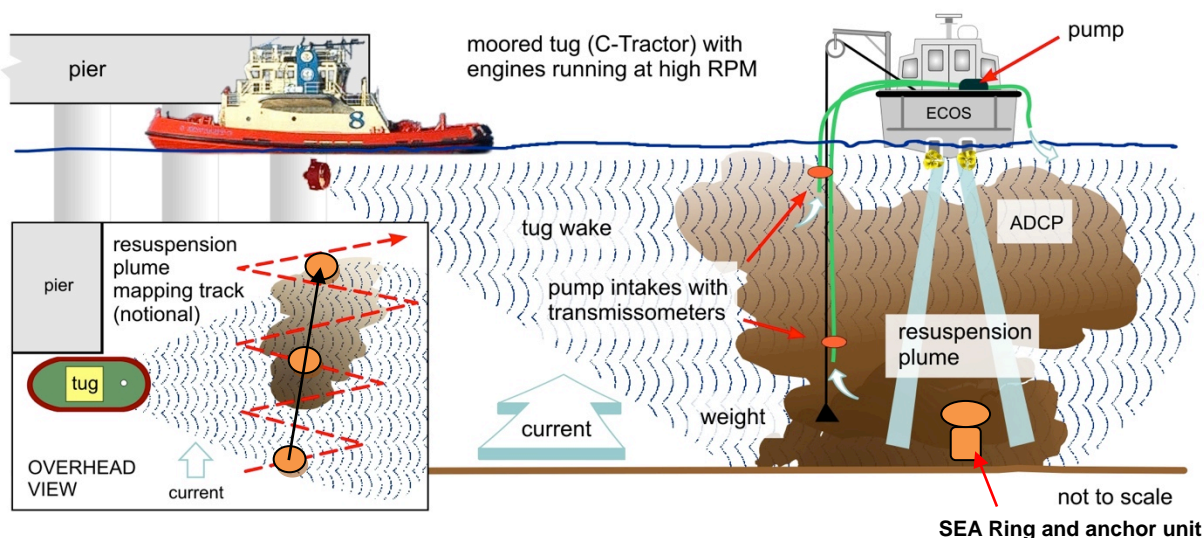


Figure 1. Sample design to collect water samples and evaluate biological effects associated with the resuspended plume.

plume, sampling at the perimeter and in the plume center. A GPS fix of the research boat position was recorded. Sampling occurred for approximately 2 hours at NBSD and approximately 3 hours at Pearl Harbor.

The tugboat, Tractor C-14, used for the San Diego study is similar to the tugboat, Tiger, for the Pearl Harbor study. Both have twin ducted propellers with about the same size. Both propellers are at the bottom of the boat with 360 degrees of rotation. The Tiger is a little bit smaller than Tractor C-14 in size. The propellers of these two tugboats were adjusted to make the rpm (power) about the same during the two studies at San Diego Bay and Pearl Harbor.



Figure 2. Sampling locations at Naval Base San Diego. The tug was positioned against the quay wall just east of SEA Ring #1. Stations 1, 2, and 6 (green circles) included SEA Rings, all other stations were where discrete samples were collected.

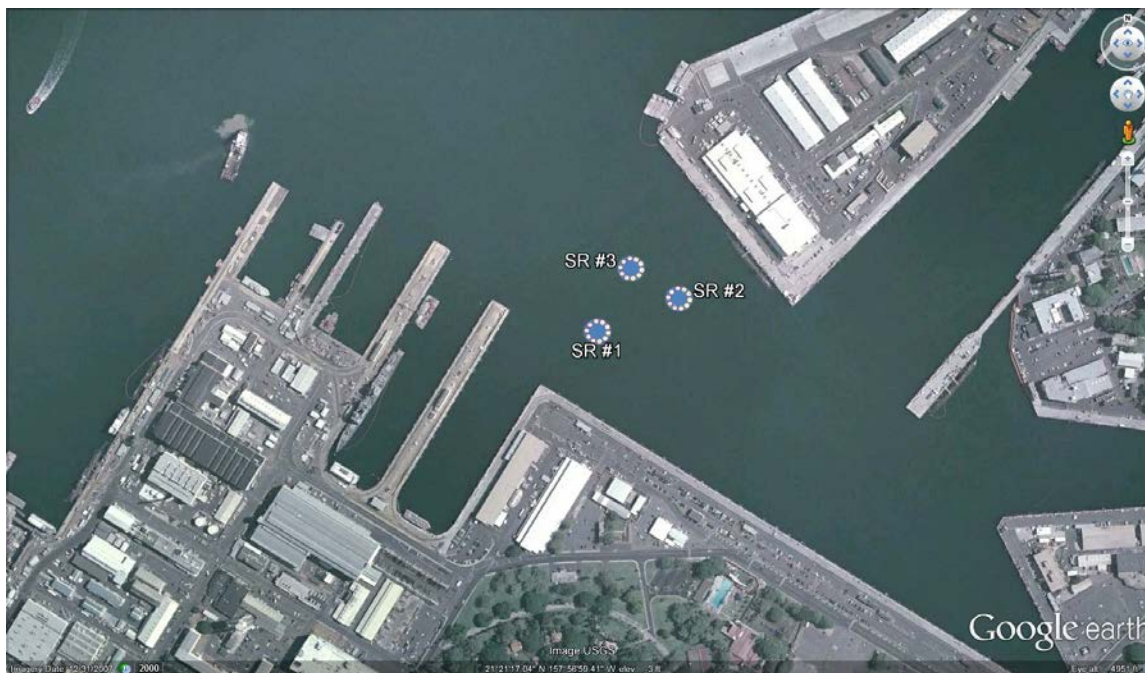


Figure 3. SEA Ring locations adjacent to Bravo Pier in Southeast Loch at Pearl Harbor, HI. The tug was positioned against the quay wall just south of SEA Ring #1.

Naval Base San Diego (NBSD) Toxicity Survey

Three SEA Rings were loaded with pre-acclimated organisms on the morning of April 4, 2012 at the SSC Pacific Bioassay lab, and transported in Chemtainers by boat to the field site. Information on the test species used, endpoints, and number of replicates exposed in each SEA Ring, and in concurrent laboratory exposures on discrete samples, is shown in Table 1 and Figure 4. Polychaetes and mysids were added directly into core tubes with 250 μm mesh screen. Sea urchin embryos (obtained from gravid adults the same morning) were added to separate 50 mL plastic drums enclosed with 25 μm mesh screen, and then inserted into the SEA Ring core tubes with 500 μm mesh screen. Temperature was monitored (range 16-17 $^{\circ}\text{C}$) during transport to the field site. SEA Rings were attached to a weighted chain anchor and sub-surface buoy system that suspended the chambers at a depth of approximately 15 feet (Figure 5). All three SEA Rings were deployed within 10 minutes of the plume event, in conjunction with the plume tracking and discrete sampling collection. SEA Rings were deployed at stations 1, 2, and 6, to maximize exposure to the plume. After the plume tracking study was complete (approximately 2 h), SEA Rings were retrieved in the same order of deployment and observed at the SSC Pac lab under laboratory conditions for the remainder of the 48-96 h exposures (species dependent).

A total of nine discrete samples collected from the plume sampling were incorporated into laboratory toxicity tests for two species (sea urchin embryo development and dinoflagellate bioluminescence). Three of the samples (stations 1, 2, and 6) were tested

Table 1. Summary of Methodology for Toxicity Tests at San Diego Bay

Survival Tests	
Polychaete	Polychaete worm (<i>Neanthes arenaceodentata</i>)
Duration/Endpoints	48-hour survival and 1 h post exposure feeding rate
Supplier	Aquatic Toxicology Support LLC in Bremerton, WA
Age class	Adult, 6 weeks old at test initiation
Date received	3/30/12
# Replicates	5 (per SEA Ring and per sample in the lab exposure)
# Organisms per replicate	10
Test method referenced	ASTM E1611 – 00 (2007), Rosen and Miller (2011)
Shrimp	Mysid shrimp (<i>Americamysis bahia</i>)
Duration/Endpoint	96-hour survival
Supplier	Aquatic Biosystems, Fort Collins, CO
Age class	Larval – 1-5 days post-hatch
Date received	3/30/12
# Replicates	4 per sample
# Organisms per replicate	5
Test method referenced	EPA Acute 2002, EPA-821-R-02-012
Development Test	
Sea Urchin	Purple Sea Urchin (<i>Strongylocentrotus purpuratus</i>)
Duration/Endpoint	96-hour embryo-larval development
Supplier	Nautilus Environmental, San Diego, CA
Age class	Gravid adults received/newly fertilized embryos tested <4 hours post-fertilization
Date received	4/2/12
# Replicates	5 (per SEA Ring and per sample in the lab exposure)
# Organisms per replicate	~ 300 embryos/ 10 mL
Test method referenced	EPA/600-R-95/136
Bioluminescence Test	
Qwiklite	Dinoflagellate (<i>Pyrocystis lunula</i>)
Duration/Endpoint	24-hr bioluminescence (light output)
Supplier	SSC Pacific Bioassay Laboratory in house culture , San Diego, CA
Age class	Culture with cell count > 5,000 cells/mL
Date cell counts	4/3/12
# Replicates	4 per sample in the lab exposure (no SEA Ring exposure)
Test method referenced	ASTM E1924-97 (2005)

Table 2. Summary of Methodology for Toxicity Tests at Pearl Harbor

Survival Tests	
Polychaete	Polychaete worm (<i>Neanthes arenaceodentata</i>)
Duration/Endpoint	96-hour survival
Supplier	Aquatic Toxicology Support LLC in Bremerton, WA
Age class	Juvenile - 18 days old at test initiation
Date received	8/24/12
# Replicates	4 (per SEA Ring and per sample in the lab exposure)
# Organisms per replicate	5
Test method referenced	ASTM E1611 – 00 (2007)
Shrimp	Pacific white shrimp (<i>Litopenaeus vannamei</i>)
Duration/Endpoint	96-hour survival
Supplier	Shrimp Improvement Systems (SIS) of Islamorada, FL
Age class	Larval – 8-9 days post-hatch
Date received	8/29/12
# Replicates	4 per sample in the lab exposure (no SEA Ring exposure)
# Organisms per replicate	5
Test method referenced	EPA Acute 2012, EPA-821-R-02-012 ^a
Urchin (larval survival)	Hawaiian collector urchin (<i>Tripneustes gratilla</i>)
Duration/Endpoint	96-hour survival
Supplier	Anuenue Fisheries Research Center
Age class	Approx. 14 days old at test initiation
Date received	8/27/12
# Replicates	3 (per SEA Ring and per sample in the lab exposure)
# Organisms per replicate	10
Test method referenced	EPA Acute 2012, EPA-821-R-02-012 ^a
Development Test	
Urchin (embryo dev)	Hawaiian collector urchin (<i>Tripneustes gratilla</i>)
Duration/Endpoint	72 or 96-hour development
Supplier	David Cunningham, Kaneohe Bay, Oahu, HI
Age class	Gravid adults received/newly fertilized embryos tested <3 hours post-fertilization
Date received	8/26/12
# Replicates	4 (per SEA Ring and per sample in the lab exposure)
# Organisms per replicate	~ 300 embryos/ 10 mL
Test method referenced	EPA/600/R-12/022 and EPA/600-R-95/136
Bioluminescence Test	
Qwiklite	Dinoflagellate (<i>Pyrocystis lunula</i>)
Duration/Endpoint	24-hr bioluminescence (light output)
Supplier	Assure Controls, Carlsbad, CA
Age class	unknown
Date received	8/27/12
# Replicates	6 per sample in the lab exposure (no SEA Ring exposure)
Test method referenced	ASTM E1924-97 (2005)

^a This is not a standard test species for this method. This testing was for research purposes and the method is referenced only as a guideline for general toxicity testing procedures.

both filtered (0.45µm) and unfiltered, while the remaining samples were tested unfiltered only.

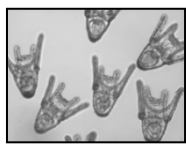
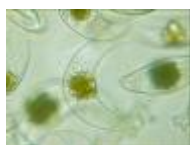


Figure 4.
Naval
Base San
Diego test
species.

From left to right, *Pyrocystis lunula* (bioluminescent dinoflagellate), *Strongylocentrotus purpuratus* (purple sea urchin larvae), *Americamysis bahia* (mysid shrimp), and *Neanthes arenaceodentata* (marine polychaete).

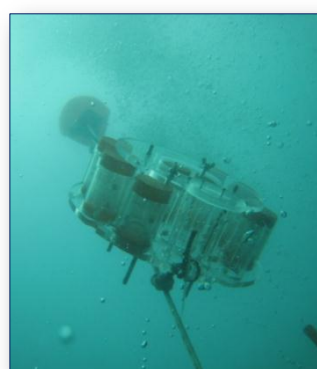


Figure 5. SEA Ring surface buoy at NBSD (left), SEA Ring generation one device used at both resuspension sites (center), and bottom view of SEA Ring suspended at mid-water depth (right).

Pearl Harbor Toxicity Survey

Three SEA Rings were loaded with pre-acclimated organisms on the morning of August 28, 2012 during transport by boat to the field site. Information on the test species used, endpoints, and number of replicates exposed in each SEA Ring, and in concurrent laboratory exposures on discrete samples, is shown in Table 2 and Figure 6. Polychaete worms were added directly into core tubes with 250 µm mesh screen. Two-week old urchin larvae, and newly fertilized urchin embryos were added to separate 50 mL plastic drums enclosed with 25 µm mesh screen, and then inserted into the SEA Ring core tubes with 500 µm mesh screen. Oyster embryos, initially included as part of the study, were of insufficient quality to use. SEA Rings were attached to a weighted chain anchor and sub-surface buoy system, and lowered to the sea floor (30-40 feet) just after the first 90 second plume event. The SEA Rings were placed approximately 75 meters (m) apart in a triangular pattern (Figure 3) within the plume at a distance of approximately 100-200 m from the tug and remained in place for the duration of the water sampling period throughout all three plume generating events (approximately 3 hours).



Figure 6. Pearl Harbor test species. From left to right, *Pyrocystis lunula* (bioluminescent dinoflagellate), *Tripneustes gratilla* (Hawaiian collector urchin), *Litopenaeus vannamei*, (Pacific white shrimp), *Neanthes arenaceodentata* (marine polychaete), and *Crassostrea gigas* (pacific oyster).

Following exposure to the plumes, the SEA Rings were removed from Pearl Harbor and immediately transported to the Hawaii Institute of Marine Biology (HIMB) at Coconut Island on the Island of Oahu, approximately 30 miles from Pearl Harbor, in 17-gallon chemtainers containing site water. Upon arrival they were placed into the marine environment (HIMB ambient water) for the duration of the 96-hour exposure. The SEA Rings were suspended off a concrete platform at the HIMB facility in a clean, well-flushed area of Kaneohe Bay. For comparison, organisms were deployed into a fourth SEA Ring (defined as the reference [REF] SEA Ring) and were exposed to the HIMB ambient water for the entire 96-hour test period. None of the organisms exposed in the SEA Rings were fed for the 96-hour period except what they could obtain through the screen of the test chambers in the natural environment.

A total of nine discrete plume samples collected from the plume sampling were incorporated into laboratory toxicity tests for several of the test species (polychaete, shrimp, sea urchin, and dinoflagellate). Most species were exposed to the raw water samples only, while the dinoflagellates were exposed to both unfiltered and filtered (10 μ m) to assess whether particulates may be a potential physical factor. Laboratory control water consisted of filtered (10 μ m) seawater collected from the intake system at the HIMB facility.

A list of sample ID numbers, time collected, and water quality measurements upon receipt at the lab is provided in Table 3. All lab tests were initiated on the same day as sample collection, with the exception of the white shrimp test which was initiated the day following sample collection. Due to complications obtaining a permit in time to import these test organisms to the island, they were not received until August 29, 2012, and were tested the same day as received. As a quality control measure, laboratory controls for each species were exposed at the HIMB. Polychaete worms were fed ground Tetramin while in holding and not again during the 96-hour exposure. Because shrimp can be cannibalistic and affect results by consuming other test organisms, they were fed *Artemia* in holding and once daily in the test chambers during the laboratory exposures. No other organisms were fed during lab exposures.

Table 3. Summary of Initial Water Quality on Discrete Plume Samples Collected at mid depth (15 ft) on Aug 28, 2012 at Bravo Pier, Southeast Loch, Pearl Harbor.

Sample ID	Time Collected	pH	D.O. (mg/L)	Temp. (°C)	Salinity (ppt)
Backgrnd1	1012	8.14	8.8	24.9	35.1
HIMB Control	-	-	-	-	-
R1	1041	8.12	9.3	25.2	35.2
13	1151	8.10	9.4	23.0	35.0
14	1153	8.13	8.8	24.1	34.8
15	1155	8.14	8.8	23.0	34.7
16	1156	8.14	9.5	23.2	34.8
17	1204	8.14	8.9	23.1	34.8
18	1211	8.14	8.5	25.2	35.0
19	1219	8.17	9.2	24.0	35.5

TSS=total suspended solids, measured gravimetrically, DOC= dissolved organic carbon, D.O.=Dissolved oxygen. R1= Plume Event #1, first mid-depth sample. Coconut Island was laboratory control water.

Table 4. Summary of Discrete Plume Samples Collected at mid depth (15 ft) on April 3, 2012 at Naval Base San Diego, CA.

Sample ID	Lat	Long	Tot Cu (µg/L)	Diss Cu (µg/L)	Tot Zn (µg/L)	Diss Zn (µg/L)	TSS (mg/L)	DOC (mg/L)
Backgrnd*	-	-	3.58	2.87	4.30	3.91	5.0	
1	32.68009	-117.12662	8.41	4.88	14.66	11.66	11.2	
2	32.67953	-117.12682	24.57	3.71	44.04	13.48	57.7	
5	32.67958	-117.12753	13.90	3.72	23.25	19.81	34.2	
6	32.67899	-117.12773	25.05	2.46	24.32	13.71	40.3	
8	32.67825	-117.12827	11.12	3.43	18.68	14.04	20.5	
10	32.67746	-117.12948	23.33	3.22	32.34	14.47	64.9	
13	32.67651	-117.12820	4.52	3.95	16.69	13.65	5.6	
17	32.67793	-117.12691	10.71	8.46	11.24	9.94	3.2	

*Average of 5 background samples collected on 3/28/12.

Bold indicates where SEA Rings were also placed for 2 hour field plume exposure.

Table 5. Summary of Discrete Plume Samples Collected at mid depth (15 ft) on Aug 28, 2012 at Bravo Pier, Southeast Loch, Pearl Harbor.

Sample ID	Lat	Long	Tot Cu (µg/L)	Diss Cu (µg/L)	Tot Zn (µg/L)	Diss Zn (µg/L)	TSS (mg/L)	DOC (mg/L)
Backgrnd			3.45	NA	2.87	NA	3	2.3
R1	21.35519	-157.94936	10.85	10.71	17.68	13.47	NA	NA
13	21.3551153	-157.949195	18.78	5.38	21.4	10.29	40	1.0
14	21.35550427	-157.948713	15.02	5.57	27.5	11.09	66	1.2
15	21.35542137	-157.9481455	24.02	5.41	43.3	10.25	242	1.2
16	21.35554073	-157.9482005	35.98	5.23	42.8	11.82	105	1.1
17	21.35562287	-157.9479435	35.51	5.50	28.8	11.02	109	1.2
18	21.35695517	-157.94902	27.00	5.94	18.5	10.18	13	1.1
19	21.35694361	-157.949975	16.22	9.22	16.8	13.80	16	1.1

R1= Plume Event #1, first mid-depth sample. NA=data not available.

Results

Data collected from the SEA Ring and laboratory toxicity tests were summarized and analyzed using one-tailed t-tests ($p < 0.05$) and are shown in Tables 6-10 and Figures 7-8. For SEA Rings, statistical comparisons were made between station locations and the corresponding reference site SEA Ring, while for the lab exposures, comparisons were made between samples and the laboratory control seawater used at each site.

San Diego Bay In Situ Exposures. For San Diego Bay, *in situ* bioassay data were successfully obtained from all three species deployed (Table 6). Survival following the 48 or 96 h full exposure (initially at site, and then in filtered seawater at the SSC bioassay lab) was very high ($\geq 86\%$) for polychaetes and mysid shrimp for the reference sites, while sea urchin larval development was also high (81.4%) at the reference site. No significant reduction in survival was observed at any site location for the polychaete or mysid, nor for normal larval development in sea urchins. Post exposure feeding rate for the polychaete, however, resulted in small, yet statistically significant ($p < 0.05$) differences between the reference site and all three test sites.

Table 6. Summary of SEA Ring toxicity data at three stations within the plume at Naval Base San Diego.

Sample ID	Polychaete % Survival		Polychaete Feeding Rate (# <i>Artemia</i> /h)		Mysid Shrimp % Survival		Sea Urchin % Normal	
	Mean	SD	Mean	SD	Mean	SD	Mean	SD
Lab Control	100	0	141	17	100	0	98.6	1.1
Travel Control	100	0	165	11	96	9	33.2	12.4
SPAWAR Ref (SR#4)	98	4	160	10	86	9	81.4	21.6
Stn #1 (SR#3)	100	0	145	23	90	10	80.9	10.0
Stn #2 (SR#2)	92	13	127	19	92	8	88.9	4.0
Stn #6 (SR#1)	98	4	140	19	94	5	82.2	6.3

San Diego Bay Discrete Samples. None of the nine discrete plume samples had an adverse effect on sea urchin larval development, whether filtered or unfiltered (Table 7). The QwikLite bioluminescence test showed statistically lower light production from *P. lunula* at stations 2, 10, and 13 in unfiltered samples, and at stations 2 and 6 in filtered samples (Table 7).

Table 7. Summary of toxicity data on discrete samples collected from the plume at Naval Base San Diego.

Sample ID	Sea Urchin % Normal				Bioluminescence Counts					
	Unfiltered		Filtered		Unfiltered			Filtered		
	Mean	SD	Mean	SD	Mean	SD	% Control	Mean	SD	% Control
Lab Control	99.0	1.4	99.0	1.4	24460*	5898	NA	24460*	5898	NA
Background	99.4	0.9	-	-	22547	2359	101.1	-	-	-
1	99.0	1.0	99.6	0.5	23143	1736	82.0	26137	5428	92.6
2	98.6	1.1	99.6	0.5	18019	2069	63.9	20379	4037	72.2
5	99.2	0.8	-	-	21532	4889	76.3	-	-	-
6	99.6	0.5	99.2	0.8	22488	2541	98.4	17819	4032	78.0
8	99.0	1.4	-	-	21588	1184	96.7	-	-	-
10	98.8	0.4	-	-	19799	2143	88.8	-	-	-
13	99.2	0.8	-	-	19881	2648	89.1	-	-	-
17	99.2	0.8	-	-	21755	5098	95.2	-	-	-
*Combined mean and standard deviations of three sets of controls. Actual statistical comparisons to site samples were made with control from same test batch.										

Pearl Harbor In Situ. For Pearl Harbor, valuable *in situ* bioassay data were obtained from one (polychaete) of the three species deployed. Reference SEA Ring survival was high (85%). None of the 96 h SEA Ring exposures resulted in statistically lower polychaete survival. Mean survival at Stn #3, however, was only 65% (Table 7).

Unfortunately, oysters received were not in gravid condition and did not yield viable embryos for use in the exposures, and the shrimp arrived on site too late (and were, therefore, only able to be used in the laboratory tests). The use of the Hawaiian collector urchin embryos in the field has never been done, to our knowledge, and we knew that use of this organism was risky in terms of likelihood for success. The collector urchin fertilization test (USEPA 2012) is widely considered problematic in laboratory tests required under many NPDES permits in the region. Although embryos were obtained and appeared to develop, few larvae were recovered from the SEA Rings. Additional discussion of the field tests species for which no data were derived is detailed in the Quality Assurance section.

Table 7. Summary of SEA Ring toxicity data at three stations within the plume at Bravo Pier, Pearl Harbor, HI.

Sample ID	Polychaete % Survival	
	Mean	SD
HIMB Reference	85	10.0
Stn #1	90	11.5
Stn #2	90	11.5
Stn #3	65	19.1

Pearl Harbor Discrete Samples. Data were generated from all four species used in the laboratory testing of discrete plume samples (Tables 9 and 10). No statistically significant reduction in survival was observed for either polychaetes or white shrimp after a combined 96 h exposure (3 hour field, followed by 93 hours at the reference site). The QwikLite test results

revealed significant adverse effects at stations 16 and 17, which also were characterized by relatively high TSS (>100 mg/L) and total copper and zinc concentrations (Table 5).

Collector urchin larvae (approximately 2 weeks old) were available from the Anuenue Fisheries Research Center on Oahu at the time of testing and were also included in a 96-hour acute survival test. This test is not part of a standard protocol but was added as an additional test of a local species at a different life stage than the embryo development test. Survival results in the lab were highly variable and there was no recovery of these larvae in SEA rings. It is likely that the reason for the poor survival and recovery is that they require heavy feeding during this life-stage. These organisms were not fed during the entire exposure, and so some organisms were deceased and decomposing at test termination. Regardless, these data are presented to show that there was survival in all samples tested. Due to the high variability, there was not enough statistical power to detect differences between any the plume samples and the lab control or Pearl Harbor background sample.

Juvenile Pacific white shrimp (*L. vannamei*) were purchased from Shrimp Improvement Systems of Islamorada, Florida. There are facilities in the Hawaiian Islands that culture Pacific white shrimp for restaurant supply; however, no juvenile organisms within the post-larval sensitive life stage were available for toxicity testing. Due to permitting complications, the shrimp were not shipped in time for the field deployment in the SEA Rings, but they were exposed in the laboratory to the plume samples on the day following sample collection.

Table 9. Summary of toxicity data on discrete samples collected from the plume at Bravo Pier, Pearl Harbor, HI. Bold values are statistically lower than the laboratory water from Hawaii Institute of Marine Biology (HIMB). ^indicates data were reported but had relatively high variability.

	Polychaete % Survival		White Shrimp % Survival		Sea urchin % Survival^	
Sample ID	Mean	SD	Mean	SD	Mean	SD
HIMB	100	0	95	10	93	12
Background	90	20	95	10	67	58
Plume #1	95	10	95	10	63	55
13	100	0	100	0	97	5.8
14	100	0	95	10	23	40
15	75	30	100	0	30	30
16	85	30	95	10	80	35
17	95	10	85	30	100	0
18	100	0	100	0	73	46
19	100	0	100	0	60	53

Table 10. Summary of QwikLite (dinoflagellate bioluminescence) toxicity results from discrete samples collected from the plume at Bravo Pier, Pearl Harbor, HI. Bold values are statistically lower than the laboratory water from Hawaii Institute of Marine Biology (HIMB).

	Bioluminescence Counts (Unfiltered)			Bioluminescence Counts (Filtered)		
Sample ID	Mean	SD	% Control	Mean	SD	% Control
HIMB	1189	359	NA	1345	286	NA
Background	979	144	82	1980	287	147
Plume #1	1298	325	109	1547	302	115
13	1032	203	87	1136	231	84
14	939	171	79	1441	191	107
15	1349	214	113	1380	131	103
16	966	114	81	727	158	54
17	763	144	64	900	102	67
18	1479	379	124	1409	218	105
19	1286	243	108	1169	387	87

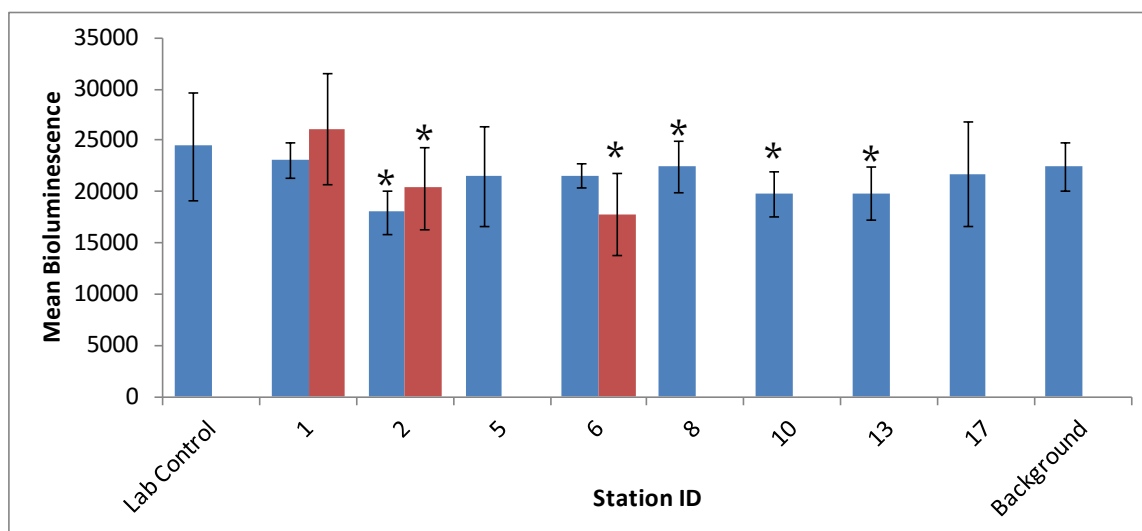


Figure 7. Qwiklite bioluminescence results (mean bioluminescence counts) after a 24-hour laboratory exposure to discrete plume samples. Test Initiation: April 5, 2012. Asterisks indicated significantly different from SSC Pacific laboratory control seawater. Blue bars= unfiltered samples; red bars= filtered (0.45 μ m) samples.

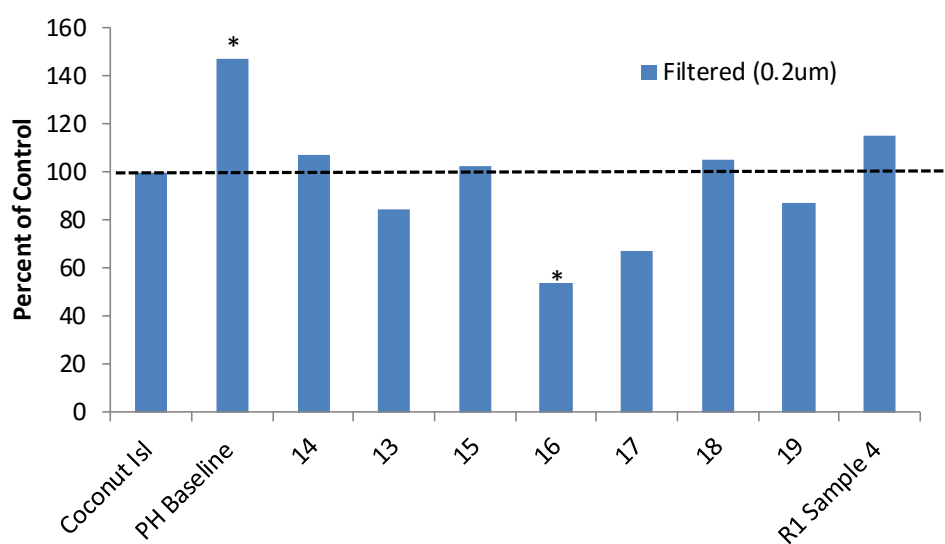
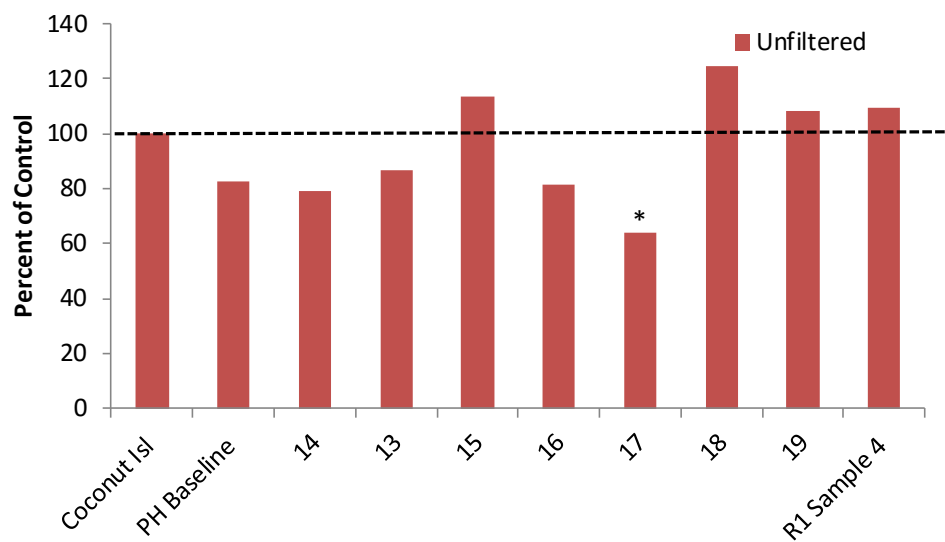


Figure 8. Qwiklite bioluminescence results (% of control) after a 24-hour laboratory exposure to discrete plume samples. Test Date: August 28, 2012. Asterisks indicated significantly different from Coconut Island (HIMB) lab control.

Quality Assurance/Quality Control

All testing involved either uncontaminated seawater controls and/or reference sites for comparison. Water quality was generally within ranges expected for each test (data not shown). When possible, copper reference toxicant tests were conducted alongside the laboratory tests with the same test organism batch. Travel controls were included in the San Diego Bay effort and were used to help interpret any field responses. A summary of the control performance and reference toxicant test results are shown in Table 11.

Table 11. Summary of laboratory control performance and copper reference toxicant tests for test species at two sites. Dashes indicated not tested.

Species/Endpoint	San Diego		Pearl Harbor	
	Control	LOEC/LC50	Control	LOEC/LC50
Polychaete Survival	100 (0)	200	100 (0)	-
Polychaete Feeding ¹	141 (17)	100	-	-
Shrimp Survival ²	100 (0)	238	95 (10)	>800
Sea Urchin Development ³	99 (1.4)	21.4	93 (4.1)	39.8
Sea Urchin Survival ⁴	-	-	93 (11.5)	-
QwikLite Bioluminescence ⁵	>5000	383	>1000	-
Oyster Development	-	-	Failed Spawn, No Data	
¹ Number <i>Artemia</i> consumed per hour.				
² <i>Americamysis bahia</i> at NBSD; <i>Litopenaeus vannamei</i> at Pearl Harbor.				
³ <i>Strongylocentrotus purpuratus</i> at NBSD; <i>Trineustes gratilla</i> at Pearl Harbor.				
⁴ Two-week old <i>T. gratilla</i> larvae.				
⁵ No minimum acceptable bioluminescence count, target of >5000 in controls.				

Naval Base San Diego. Control performance and copper reference toxicant tests for this event indicated that test performance were acceptable for all tests, with LC50/EC50 values falling within normal ranges for mysid shrimp and sea urchin larval development. Because most of the SSC Pacific laboratory data for polychaete survival are based on 96 h exposures (and not the 48 h exposure used here), the polychaete data are expressed as LOECs, as an LC50 was not obtained. The lower LOEC for the polychaete feeding rate test indicated higher sensitivity than the survival endpoint, which has been reported previously (Rosen and Miller, 2011).

Pearl Harbor. Concurrent copper reference toxicant tests were conducted for the Pacific white shrimp test and the urchin development test. Neither of these two species has been tested at the HIMB or SPAWAR labs, and therefore, there is no control chart or historical copper sensitivity data for these species; reference toxicant tests conducted were for experimental/comparison purposes only. The LC50 (lethal concentration to 50% of the organisms) value for the shrimp test was greater than the highest concentration tested (>800 µg/L copper), indicating that these organisms were not sensitive to copper at the concentrations tested. Neither polychaete nor QwikLite reference toxicant tests were performed at Pearl Harbor.

The collector urchin embryo development test was ended after 72 hours due to an apparent microbial contamination in the test chambers. Visual inspection in the microscope after 24 and 48 hours indicated that embryos were developing normally. However, upon viewing at 72 hours, the tissue of developing embryos was being consumed by microbes whose population had grown exponentially since the beginning of the test. The microbes were not visually apparent at the beginning of the test; however, they were present in large numbers in all vials of the lab exposure at 72 hours, including filtered and unfiltered samples. This indicates that they were likely present in the seawater used to create the embryo stock and may have been inadvertently inoculated into all test chambers at the beginning of the test. Coconut Island intake lab water was used to hold the adult organisms and also to make the embryo stock.

Laboratory vials and test water from the SEA Rings were quickly fixed in formalin as soon as the contamination was discovered, but many of the embryos were nothing but skeletal formations at this point. It is assumed that any abnormal embryos were completely devoured and there is no way to quantify normal vs. abnormal in this test. However, there were normally shaped skeletal structures found in all samples and SEA Ring test chambers, indicating that at least some normal development occurred in every sample.

A second embryo development test was also attempted using the Pacific oyster (*Crassostrea gigas*). A local supply of gravid adult oysters was not available at the time of testing, so oysters were purchased from Carlsbad Aquafarms in Carlsbad, CA and shipped by Fedex overnight delivery to Oahu. They were acclimated for 4 days prior to testing, but attempts to obtain gametes from the oysters using traditional spawning methods (heat and UV exposure) were not successful. The oysters were then strip spawned and gametes were combined for testing. A fertilized egg stock was prepared and initiated into the three SEA Rings deployed in the tug plumes. However, upon viewing the stock under the microscope hours later, it was discovered that none of the eggs had been fertilized and so the reference SEA Ring and lab test were not inoculated using this species. Upon retrieval of the three SEA Rings the oyster eggs were added to, it was discovered that the eggs added to the test chambers had disintegrated by the end of the exposure and therefore no data were collected for this species.

Discussion

This study demonstrated a novel, practical use of *in situ* bioassay technology, in combination with laboratory bioassays, towards improved understanding of the short-term impacts of sediment resuspension events on surface water organisms. The *in situ* bioassays utilized the first generation SEA Ring device (Burton et al. 2012, Rosen et al. 2012), which was developed under SERDP Project #ER-1550. A second generation device currently being developed and demonstrated under ESTCP Project #ER-201130 was not available at the time this study occurred. The SEA Ring deployments provided an integrated exposure of the sediment plumes over space and time, while concurrent laboratory tests were used to characterize any biological effects on discrete samples at one point in time and space.

Both *in situ* and laboratory toxicity data showed very few significant adverse effects at either site. The lack of adverse effects is corroborated by relatively low dissolved contaminant concentrations. The short exposure time in the field, by design to isolate exposure to the resuspension event only, and mesh (25-500 μm) size, on the *in situ* chambers likely minimized or

prohibited large particles (relatively high in metal concentration) from interacting with the test organisms. Unfiltered sample laboratory exposure data, however, also indicated an overall absence of effects. Therefore, any desorption of metals from sediment particles and/or ingestion of metal contaminated particles was also not biologically available or toxic.

Several of the test organisms employed in this study are known to be particularly sensitive to aqueous exposure to metals, particularly the embryo-development tests with sea urchins and bivalves, and the polychaete. However, dissolved metal concentrations did not approach published thresholds for these species.

Naval Base San Diego. At NBSD, of the five endpoints used, only the polychaete feeding rate and QwikLite (dinoflagellate bioluminescence) endpoints showed statistically significant adverse effects. In both cases, however, the reductions are moderate, and potentially not biologically meaningful. Using statistical significance and at least a 20% reduction relative to the corresponding lab control or reference SEA Ring, no polychaete samples and only two QwikLite samples (Stations 2 and 6) would be considered toxic. Interestingly, both Stations 2 and 6 were among the highest in terms of total suspended solids concentration and total metal concentrations, either which of could have contributed to the reduced light output of the dinoflagellates. PAH data (not shown) from the NBSD event were all below expected concentrations to induce short-term toxicity (maximum total priority pollutant PAH concentration of 0.29 µg/L).

Pearl Harbor. The lack of significant adverse effects in the polychaete survival in the SEA Ring is not surprising based on the relatively low exposure of metals measured. Pesticide and PCB concentrations (not shown) were below method detection limits for all discrete samples tested.

Laboratory results for the Pearl Harbor study similarly generally showed minimal toxicity. As with NBSD, the QwikLite test showed the largest effects. Stations 16 and 17 had the most light reduction, and also the highest total metal concentrations. Because station 15 had higher TSS concentrations and did not have any adverse effect, it is unlikely that interference with the QwikLite optics influenced dinoflagellate light production readings.

The Pearl Harbor event involved several species and endpoints that are not traditionally used or refined in order to ensure the study was relevant to the site. Therefore, this event involved relatively high risk, not only in terms of test performance, but also logistical challenges associated with receiving organisms of the correct life stage and quality, which were in most cases shipped from the mainland, and even as far as Florida. The various difficulties with individual tests used in Pearl Harbor are detailed in the QA/QC section of this report. Amid the challenges, much was learned about the use of these organisms in bioassays, which bodes well for potential future efforts in the Hawaiian region.

References

- ASTM E1611 – 00 (2007). Standard Guide for Conducting Sediment Toxicity Tests with Polychaetous Annelids ASTM International, West Conshohocken, PA, ASTM 2007. www.astm.org.
- ASTM E1924-97 (2005). Standard guide for conducting toxicity tests with bioluminescent dinoflagellates. Designation E1924-97. Reapproved 2004. American Society for Testing and Materials, West Conshohocken, PA. pp 1520–1530
- Burton GA Jr., Rosen G, Chadwick DB, Greenberg MS, Taulbee K, Lotufo G, Reible D, 2012. A sediment ecotoxicity assessment platform for *in situ* measures of chemistry, bioaccumulation, and toxicity. Part 1: System description and proof of concept. *Environmental Pollution* 162:449-456.
- Rosen G, Miller K, 2011. A post exposure feeding assay using the marine polychaete *Neanthes arenaceodentata* suitable for laboratory and in situ exposures. *Environmental Toxicology and Chemistry* 30:730-737.
- Rosen G, Chadwick DB, Burton GA Jr., Greenberg MS, Taulbee K, Lotufo G, Reible D, 2012. A sediment ecotoxicity assessment platform for *in situ* measures of chemistry, bioaccumulation, and toxicity. Part 2: Integrated application to a shallow estuary. *Environmental Pollution* 162:457-465.
- USEPA. 1995. Short-term methods for estimating the chronic toxicity of effluents and receiving waters to west coast marine and estuarine organisms. Office of Research and Development, Cincinnati, OH. 600-R-95/136. August 1995.
- USEPA 2002. Methods for measuring the acute toxicity of effluents and receiving waters to freshwater and marine organisms (5th edition). Office of Water, Washington DC. 821-R-02-012. October 2002.
- USEPA 2012. Tropical Collector Urchin, *Tripneustes gratilla*, Fertilization Test Method. Office of Water, Washington DC. EPA/600/R-12/022. April 2012.